# Formation, characterization and analysis of transformation products of food relevant mycotoxins

vorgelegt von
M. Sc.
Julia Keller
geb. in Berlin

von der Fakultät III – Prozesswissenschaften
der Technischen Universität Berlin
zur Erlangung des akademischen Grades

Doktor der Naturwissenschaften
—Dr. rer. nat. —

genehmigte Dissertation

Promotionsausschuss:

| | |
|---|---|
| Vorsitz: | Prof. Dr. rer. nat. Lothar W. Kroh<br>Technische Universität Berlin |
| Gutachter: | Prof. Dr. rer. nat. Hajo Haase<br>Technische Universität Berlin |
| | Dr. rer. nat. Matthias Koch<br>Bundesanstalt für Materialforschung und -prüfung |
| | Dr. rer. nat. Rudolf Schneider<br>Bundesanstalt für Materialforschung und -prüfung |

Tag der wissenschaftlichen Aussprache: 13.12.2018

Berlin 2019

This thesis was prepared from February 2015 to August 2018 at the Technische Universität Berlin (TU Berlin, Department of 'Food chemistry and toxicology', 'Institute of food technology and food chemistry') in cooperation with the 'Bundesanstalt für Materialforschung und -prüfung (BAM)', Division 'Organic trace and food analysis' under the supervision of Prof. Dr. rer. nat. Hajo Haase. The presented results were published in international and peer-reviewed journals [1-6].

**Contents**

# ABSTRACT

Besides mycotoxins found worldwide in food and feed, the occurrence of transformation products (TPs) of mycotoxins poses a further threat for food safety. Simulation methods of natural abiotic and biotic degradation processes leading to TPs have the advantage of being fast and easy. This work investigates the application of several simulation methods to mimic phase I biotransformation reactions of mycotoxins and highlights the strengths and limitations of the tested systems. Also, the instrumental analysis, structural elucidation and toxicity of new TPs is a further key element of this work.

Electrochemistry (EC) as method of choice is established for several years in pharmaceutical research. The electrochemical reactor is coupled online to a mass spectrometer and reaction products are analyzed online within minutes. Using a three-electrode flow-through cell the oxidation of zearalenone (ZEN), citrinin (CIT) and dihydroergocristine (DHEC) was achieved. Mostly hydroxylation, dealkylation, dehydrogenation and dimerization were observed. To obtain a comprehensive picture of EC coupled online to mass spectrometry (EC/MS) as reliable simulation technique, it was compared to Fenton-like reaction, UV-C irradiation, enzymatic *in vitro* assays with liver microsomes and oxidation with Ce(IV)sulfate. The combination of EC/MS and Fenton-like reaction was the most promising one leading to hydroxylated species which were also found *in vitro*, whereas Ce(IV) dimerized ZEN to several new dimeric species.

A further concern for food safety is the lack of available standards of emerging mycotoxins or their TPs. Therefore, two strategies were investigated to produce standards: the electrochemical production with the synthesis cell was implemented as well as the two-staged biosynthesis using different fungal strains. The first stage was used to produce ZEN in high quantities and in a second step the successful stereoselective synthesis of conjugates like ZEN-14-sulfate (ZEN-14-S) and two ZEN-glucosides was achieved. Besides oxidation and conjugation reactions, mycotoxins with 1,3-dicarbonyle moieties can chelate with metal ions. Using fluorescence and UV/Vis spectroscopy, aluminum complexes of CIT and OTA were characterized. The complexation altered the optical properties and in case of CIT, enhanced the fluorescence. This enhancement can be used to decrease the limit of detection when using HPLC-FLD systems in routine analysis.

The toxicity of emerging mycotoxins and TPs was assessed using the nematode *Caenorhabditis elegans* as well-established model organism, which is easy to cultivate and gives reliable toxicological data from different available biotests. CIT, ZEN and ZEN-14-S were tested on parameters like lifespan, reproduction, thermal and oxidative stress resistance as well as the metabolization *in vivo*. ZEN and ZEN-14-S were reduced to $\alpha$- and $\beta$-zearalenol (ZEL) and $\alpha/\beta$-ZEL-14-S and CIT was hydroxylated. CIT and ZEN led to a decrease of lifespan whereas ZEN-14-S had life elongation effects. All tested mycotoxin decreased significantly the reproduction. Taken together with data obtained *in vivo* and analyzed by HPLC-MS/MS, the worm can be easily used for toxicity tests for a variety of mycotoxins and their TPs.

# KURZZUSAMMENFASSUNG

Neben bereits bekannten Mykotoxinen, welche weltweit in Lebens- und Futtermitteln auffindbar sind, stellt das Vorhandensein von natürlichen Transformationsprodukten (TPs) ein weiteres Risiko für Mensch und Tier dar. Verschiedene Simulationsmodelle zur Nachahmung biotischer und abiotischer Abbauprozesse haben den Vorteil schnell und einfach durchführbar zu sein. Diese Arbeit untersucht die Anwendbarkeit diverser Simulationsmodelle auf Mykotoxine und bewertet die Stärken und Schwächen. Die instrumentelle Analyse, strukturelle Aufklärung und Toxizität neuentdeckter TPs ist ein weiteres wichtiges Element der vorliegenden Arbeit.

Die Elektrochemie als Methode der Wahl wird schon seit Jahren in der Pharmazeutik eingesetzt, um Biotransformationsreaktionen zu simulieren. Hierfür wird der elektrochemische Reaktor mit einem Massenspektrometer gekoppelt und erlaubt so die minutenschnelle Analyse von TPs. Unter Verwendung einer Durchflusszelle wurde die Oxidation von Zearalenon (ZEN), Citrinin (CIT) und Dihydroergocristin (DHEC) untersucht. Hierbei konnten als typische Reaktionen die Hydroxylierung, Dehydrogenierung, Dealkylierung und Dimerisierung der Mykotoxine festgestellt werden. Die Elektrochemie wurde ebenfalls mit alternativen Simulationstechniken verglichen. Hierzu zählt die Bestrahlung mit UV-C Licht, die Fenton-like Reaktion, *in vitro* Tests mit Lebermikrosomen und die Oxidation mit Ce(IV)Sulfat. Die Kombination aus EC und Fenton-like Reaktion führte zu den meisten Übereinstimmungen hydroxylierter Spezies, welche auch *in vitro* gefunden wurden.

Die Reaktion von ZEN mit Ce(IV) führte hingegen zu zahlreichen neuen ZEN Dimeren.

Eine weitere Problematik ist der Mangel an verfügbaren Mykotoxin Standards. Im Rahmen dieser Arbeit wurden zwei Ansätze zur Herstellung von Reinsubstanzen verfolgt. Zum einen die Verwendung der EC-Synthesezelle mit der mg-Mengen generiert werden können und die Etablierung einer zweistufigen Biosynthese mithilfe verschiedener Pilzstämme. Im ersten Schritt wurde ZEN biosynthetisch hergestellt, um dann im Weiteren zu ZEN-14-Sulfat (ZEN-14-S) und ZEN-Glucosiden umgewandelt zu werden. Neben Oxidation und Konjugation können Mykotoxine auch mit Metallionen komplexieren, wenn sie über eine 1,3-Dicarbonyl Funktionalität verfügen. Mithilfe von Fluoreszenz- und UV/Vis-Spektroskopie wurden Ochratoxin A- und CIT-Aluminium Komplexe charakterisiert. Die Komplexierung geht bei CIT mit einer starken Fluoreszenzverstärkung einher, welche optimal in die Routineanalyse miteingebunden werden kann, um die Nachweisgrenze von CIT zu verbessern.

Die Toxizität von Mykotoxinen und ihren TPs sollte mithilfe des Nematoden *Caenorhabditis elegans* untersucht werden. Dieser Modelorganismus ist überaus leicht zu handhaben und ermöglicht die Erfassung diverser toxikologisch relevanter Daten. Hierfür wurden die Auswirkungen von CIT, ZEN und ZEN-14-S auf Parameter wie Lebenslänge, Reproduktion und Stresstoleranz untersucht. *In vivo* konnte die Reduktion von ZEN zu $\alpha$- und $\beta$-Zearalenol (ZEL) und von ZEN-14-S zu ZEL-14-S mittels HPLC-MS/MS festgestellt werden, wohingegen CIT oxidiert wird. Verglichen zur Kontrollgruppe, führten CIT und ZEN zu einer Verkürzung der mittleren Lebensdauer, während ZEN-14-S diese verlängerte. Weiterhin reduzierten die drei getesteten Mykotoxine die Anzahl der Nachkommen signifikant in Abhängigkeit zur eingesetzten Konzentration. Die Kombination von Biotests und der Untersuchung von Metaboliten *in vivo* mit *C. elegans* ist noch nicht fest etabliert, kann jedoch für verschiedene Mykotoxine und deren TPs überaus sinnvoll sein.

# ABBREVIATIONS

| | |
|---|---|
| $\lambda$ | Wavelength |
| a.u. | Arbitrary units |
| ACN | Acetonitrile |
| BDD | Boron doped diamond |
| CAD | Collision gas (Instrument setting) |
| CE | Collision energy |
| CIT | Citrinin |
| cps | Count per second |
| CUR | Curtain gas (instrument setting) |
| CXP | Cell exit potential (instrument setting) |
| CYP450 | Cytochrome P450 |
| DAD | Diode array detector |
| Da | Dalton |
| DHEC | Dihydroergocristine |
| DMSO | Dimethyl sulfoxide |
| DNA | Deoxyribonucleic acid |
| DON | Deoxynivalenol |
| DP | Declustering potential (instrument setting) |
| EC | Electrochemistry |
| EC/MS | Electrochemistry/mass spectrometry |
| $EC_{50}$ | Half maximal effective concentration |
| EP | Entrance potential (instrument setting) |
| ESI | Electrospray |
| EU | European Union |
| EFSA | European Food Safety Authority |
| FLD | Fluorescence detector |
| FT-ICR | Fourier-transform ion cyclotron resonance |
| FTMS | Fourier transmission mass spectrometry |
| 5-FUdR | 5-fluorodeoxyuridine |
| GC | Glassy carbon electrode |
| GS1/GS2 | Gas $^1/_2$ (instrument setting) |
| HLM | Human liver microsomes |
| HPLC | High performance liquid chromatography |
| HRMS | High resolution mass spectrometry |
| LB | Lysogeny broth |

| | |
|---|---|
| LLE | Liquid-liquid extraction |
| LTQ | Linear trap quadrupole |
| MeOH | Methanol |
| MRM | Multiple reaction mode |
| MS | Mass spectrometry |
| MS/MS | Tandem mass spectrometry |
| *m*/*z* | Mass-to-charge ratio |
| NADPH | Nicotinamide adenine dinucleotide phosphate |
| $NH_4Ac$ | Ammonium acetate |
| NGM | Nematode growth medium |
| NMR | Nuclear magnetic resonance spectroscopy |
| OTA | Ochratoxin A |
| OH-DHEC | Hydroxylated dihydroergocristine |
| OH-CIT | Hydroxylated citrinin |
| OH-ZEN | Hydroxylated zearalenone |
| PDA | Potato dextrose agar |
| PDB | Potato dextrose broth |
| $Pd/H_2$ | Palladium-hydrogen |
| ppm | Parts per million |
| PTFE | Polytetrafluoroethylene |
| RASFF | Rapid Alert System for Food and Feed |
| RLM | Rat liver microsomes |
| ROS | Reactive oxygen species |
| SEM | Standard error of the mean |
| TP | Transformation product |
| $t_R$ | Retention time |
| UV | Ultraviolet |
| Vis | Visible |
| WHO | World Health Organization |
| ZEL | Zearalenol |
| ZEN | Zearalenone |
| ZEN-14-S | Zearalenone-14-sulfate |
| ZEN-14-G | Zearalenone-14-glucoside |
| ZEN-16-G | Zearalenone-16-glucoside |

# 1 INTRODUCTION

## 1.1 Fungi and mycotoxins

Filamentous fungi are found in every environment as major pathogenic organisms of plants and many of these fungi produce toxic compounds called mycotoxins, a diverse class of secondary metabolites [7-10]. The word mycotoxin is originated from the Greek word *mykes* for fungus and the Latin word *toxicum* for poison. These low-molecular-weight compounds enter the food chain either by contamination of the crops directly on the field or due to inadequate storage [7, 11]. Consumption of mycotoxin-containing food or feed may cause acute or more often, chronic diseases. Symptoms caused by mycotoxins are diverse like the class of mycotoxins [12, 13]. Historically, several severe mycotoxicoses have been reported, like the outbreak of ergotism in the Middle Ages as one prominent example, caused by consumption of ergot alkaloid-contaminated cereals [14]. These mycotoxins are produced by *Claviceps purpurea* fungi and caused the death of thousands of people in Europe. The modern mycotoxicology started with the Turkey X disease in the 1960s in Great Britain, which was the result of the carcinogenic aflatoxins, produced by *Aspergillus flavus*, contaminating feed for turkey, ducks and other poultry [15]. Major mycotoxin-producing and food relevant fungi are members of the genera *Aspergillus*, *Fusarium* and *Penicillium* [10]. *Penicillium* and *Aspergillus* spp. contaminate food and feed under storage when humidity and temperature are high. *Fusarium* spp. are found worldwide also in colder climate and have a wide host range, which causes the infestation of several kinds of crop plants like barley, corn and wheat on the field. Once contaminated, the removal of mycotoxins is a complex, time-consuming and a laborious process [16].

## 1.2 Investigated mycotoxins

More than 400 mycotoxins have been described to date, but only a few are found in food and feed and are regulated by the food authorities. Major mycotoxins like zearalenone, ochratoxins and patulin frequently contaminate food and animal feedstuffs. Other mycotoxins are emerging like citrinin or conjugates of mycotoxins

with glucose or sulfate originating from the xenobiotic biotransformation processes of infested plants. In the following section, mycotoxins used within this work are described.

Table 1. Molecular structures, names, chemical formulas and molar weights of the tested mycotoxins; red circled is the missing double bond, which is the only difference between DHEC and ergocristine

| **Molecular structure** | **Name, chemical formula and molar weight** |
|---|---|
| 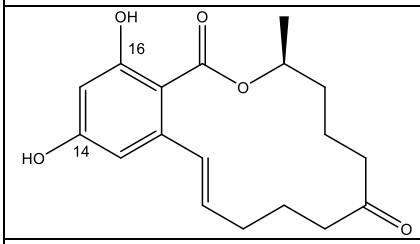 | **Zearalenone (ZEN)**<br><br>$C_{18}H_{22}O_5$<br><br>318.15 g/mol |
| 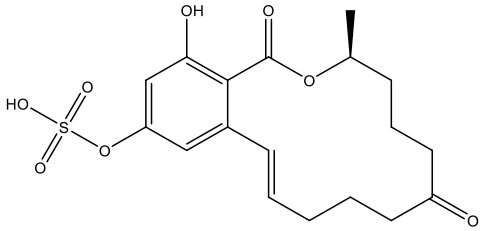 | **Zearalenone-14- *O*-β-sulfate (ZEN-14-S)**<br><br>$C_{18}H_{22}O_8S$<br><br>398.10 g/mol |
| 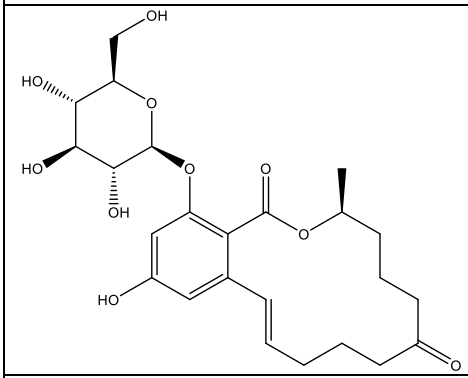 | **Zearalenone-16-*O*-β-glucoside (ZEN-16-G)**<br><br>$C_{24}H_{32}O_{10}$<br><br>480.20 g/mol |
| 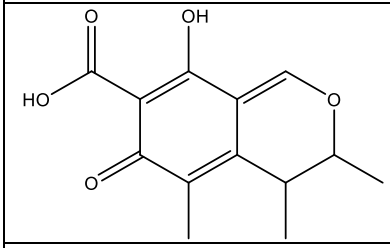 | **Citrinin (CIT)**<br><br>$C_{13}H_{14}O_5$<br><br>250.08 g/mol |
| 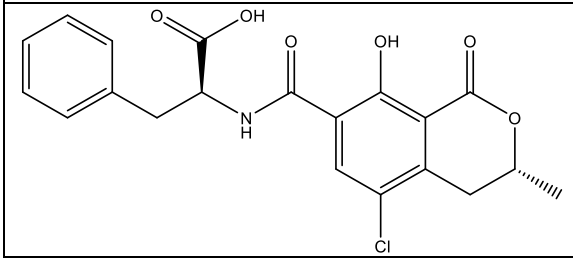 | **Ochratoxin A (OTA)**<br><br>$C_{20}H_{18}ClNO_6$<br><br>403.08 g/mol |

| | |
|---|---|
| 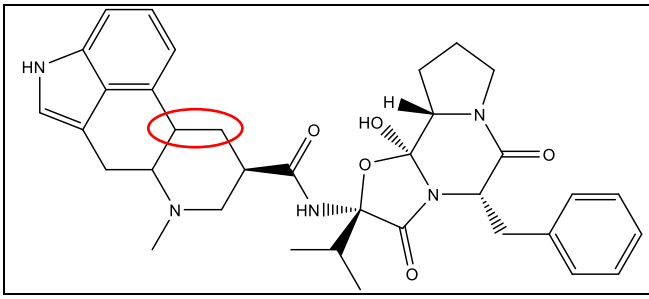 | **Dihydroergocristine (DHEC)**<br><br>$C_{35}H_{41}N_5O_5$<br><br>611.31 g/mol |

## 1.2.1 ZEARALENONE

Zearalenone (ZEN) and its reduced metabolite zearalenol are estrogenic compounds with resorcylic acid lactone structure (Table 1) and are mainly produced by *Fusarium graminearum*, *F. semitectum*, *F. culmorum* and *F. cerealis* [17]. ZEN is often co-occurring with deoxynivalenol and less often together with aflatoxins [18] and is found in important crops like corn, wheat, rice, soybeans, sorghum, spices and walnuts [19]. As mycoestrogen, it binds to the cytosolic receptor proteins and translocates a hormone-receptor complex into the nucleus of the cell, causing hyperestrogenic effects. Typical symptoms after consumption of ZEN are swelling of the uterus and vulva, infertility and atrophy of ovaries reported as in swine and cattle, but the acute toxicity is low [20-22].

ZEN is lipophilic and highly soluble in methylene chloride, alcohols, ethyl acetate and acetonitrile, but not in water. The UV absorption maxima in ethanol are at $\lambda$ = 236, 274 and 316 nm and ZEN is also fluorescent at an emission wavelength of $\lambda$ = 450 nm. Like other mycotoxins, ZEN is not degraded during storage, grinding, conservation, cooking and baking and the largest contributor to ZEN exposure is given by the consumption of grains and grain products like bread or pastries [23]. Due to its good solubility in lipids it is also found in several vegetable oils [24]. To protect consumers from ZEN, contamination maximum levels have been set in the European Union (EU) ranging from 20 µg/kg for baby food to 400 µg/kg in refined maize germ oils and a tolerable intake of ZEN would be 0.25 µg/kg of bodyweight [19].

### 1.2.2 ZEARALENONE CONJUGATES

Infected host plants and other fungi can transform ZEN into conjugated forms, which are mainly sulfate or glucose esters binding to the C14 and C16 positions, also called "masked mycotoxins"[25]. In barley, ZEN is transformed to a mixture of Zearalenone-14-*O*-β-glucoside (ZEN-14-G) and Zearalenone-16-*O*-β-glucoside (ZEN-16-G), the latter shown in Table 1 [26]. Fungi of the genera *Rhizopus* and *Thamnidium* also showed the formation of ZEN-14-G and ZEN-14,16-*O*-β-diglucoside [27, 28]. ZEN-14-S is a natural metabolite of *F. graminearum*, *Aspergillus niger* and *Rhizopus arrhizus* and shown in Table 1 [29]. Conjugated ZEN derivatives were found in a variety of food and feed such as corn and wheat products [30]. The content of conjugated forms can exceed the amount of parental mycotoxins [25]. Biotechnological processes such as fermentation of soy and tempeh products use fungi which could form conjugated ZEN species if the unfermented product contains ZEN [31]. Studies revealed that the conjugates are hydrolyzed into their parental compound by human colonic microbiota during digestion and thus the free ZEN pose a risk to the consumer [32]. This is concerning due to the lack of pure reference standards and the hampered detection of these conjugated forms during routine analysis.

### 1.2.3 CITRININ

Citrinin (CIT) is a polyketide mycotoxin with a bright yellow color produced by several *Penicillium* and *Aspergillus* spp. [33, 34]. The name is originated from *P. citrinum*, where it was purified from and described for the first time [35]. Due to its planar structure (Table 1) and double bonds, CIT possesses a natural low fluorescence at $\lambda_{Em}$=500 nm which is used for fluorescence detection. It can be found in several cereals like barley, wheat, oats, rice and corn and is often co-occurring with ochratoxin A due to poor storage conditions [33, 36]. CIT is nephrotoxic and causes like OTA kidney damage. It is toxic by multiple pathways, which include the inhibition of nucleic acid synthesis, alteration of mitochondrial function, inactivation of heat shock proteins as well as the activation of apoptosis processes [37, 38]. It also affects domestic birds and causes a reduced weight gain, watery diarrhea together with an increased water consumption [39]. Furthermore, the outbreak of the Balkan endemic nephropathy, a chronic kidney disease in southeastern Europe is probably related to the consumption of food contaminated with CIT and OTA [40]. Currently

it is not regulated by the food authorities but as an emerging mycotoxin, limits will be set in the near future. Further research concerning occurrence, toxicity and reliable analysis methods are needed as recommended by the European Food Safety authority (EFSA) [41].

### 1.2.4 OCHRATOXIN A

Ochratoxin A (OTA) is primarily produced by *Aspergillus ochraceus* and *Penicillium verrucosum* which are ubiquitously found worldwide [33, 42, 43] (Table 1). It was originally discovered in 1965 as product of *A. ochraceus* and belongs to the group of isocoumarin derivative mycotoxins together with ochratoxin B and C [44]. Like CIT, OTA is a polyketide mycotoxin and its structure consists of a dihydroisocoumarin moiety linked to a phenylalanine group and it is poorly soluble in water. Due to the structure of OTA, the mycotoxin shows strong fluorescence. OTA was found in a variety of food such as cereal crops and can also be found in nuts, coffee beans and red wine, occurring worldwide from temperate to tropical climates [34, 45]. Ochratoxin B, which lacks chlorine is less toxic than OTA and could be found together with OTA in food and feed [46]. Like CIT, OTA causes nephropathy in animals and human (Balkan endemic nephropathy) and is at least 10 times more toxic than CIT [40]. To avoid OTA contamination, harvesting and subsequent storage conditions need to be strictly controlled. Furthermore, the carry-over of OTA was observed in pigs and poultry meats, whereas the carry-over to milk in cattle is estimated to be less than 1% [47].

### 1.2.5 DIHYDROERGOCRISTINE

Dihydroergocristine (DHEC) is a semisynthetic ergot alkaloid (EA) which is used to treat age-related cognitive impairment. It is structurally similar to the EA ergocristine, but lacking the C9/C10 double bond (shown in a red circle in Table 1). The elimination of the C9/C10 double bond by catalytic hydrogenation, transforming ergotamine into dihydroergotamine and the corresponding EAs into dihydroergocristine, dihydroergocornine, dihydro-alpha-ergocryptine and dihydro-beta-ergocryptine [48]. Furthermore, DHEC can be easily produced from commercially available DHEC mesylate which is a feasible and low-priced alternative when compared to the

production from ergocristine [49]. As indole alkaloids, EAs are produced as a toxic mixture by *Claviceps* spp. in sclerotia of the fungi. *Claviceps* spp. are specialized parasites which infest grasses, corn, wheat, oats, rice and barley during cold and wet weather [50, 51]. The infestation of these plants leads to the development of dark colored mycelia mass. The latter contains a number of highly toxic fungal metabolites. Four main groups of EAs are found: the ergopeptides, the clavines, the lysergic acid and acid amides. Main EAs are ergometrine, ergotamine, ergocristine, ergosine, ergocornine and $\alpha$-ergocryptine and their derived C8 stereo isomers (-inine) [52]. While the C8-(*R*)-isomers (suffix '-ine') are highly toxic, the C8-(*S*)-isomers ('-inine') show a reduced toxicity and are biologically less or not active [53, 54]. The consumption of EA-contaminated food results in a disease called ergotism also known from the Middle Ages as St. Anthony´s fire [14]. Symptoms are burning skin, gangrene, loss of hands and feet, hallucinations and even death.

## 1.3 Metabolism and biotransformation of mycotoxins

To understand the diverse toxic effects of mycotoxins it is crucial to investigate the metabolic pathways and processes during biotransformation. The latter can be divided into phase I and phase II reactions which take place mainly in the liver of humans and animals [55]. During phase I, exogenous substances like drugs, environmental pollutants or naturally occurring toxins are functionalized by enzymes of the cytochrome P450 family (CYP450) [56]. Phase II conjugation reactions such as glucuronidation and sulfation are mediated by transferase enzymes [57]. After phase I and II, the exogenous compounds are excreted and removed from the body. The biotransformation of exogenous substances is a process of detoxification, but could also lead to metabolites possessing a higher toxicity compared to the parental compound [58].

ZEN is one of the best studied mycotoxins and its metabolization was intensively investigated in the recent years. During phase I, ZEN is reduced to $\alpha$-zearalenol ($\alpha$-ZEL) and β-ZEL [59, 60]. Both epimers were detected in fractions of liver cells derived from different animal species like swine, cattle or chicken and also *in vivo* as relevant metabolites. Involved in the reduction of ZEN are the 3$\alpha$- and 3β-hydroxysteroid dehydrogenases [59]. Further reduction of the double bond between C11 and C12 leads to $\alpha$-zearalanol ($\alpha$-ZAL) and β-ZAL, which are still used

as anabolic agents for cattle and sheep in the USA and Canada [61, 62]. Besides reduction of ZEN, also the hydroxylation was described and a various number of OH-ZEN were generated using human and rat liver microsomes [63]. Hydroxylation can take place at the aromatic ring as well as at aliphatic positions and 8-OH-ZEN was detected *in vivo* in urine of rats, which were fed with ZEN [64]. Conjugated during phase II biotransformation, ZEN can be glucoronated and these metabolites were confirmed for various animal species as well as for humans [65]. The sulfation of the 14-OH group at the aromatic ring was described using Caco-2 cells [66].
CIT is metabolized to its hydroxylated form dihydrocitrinone, which is used as typical biomarker for CIT in urine [67]. The hydroxylation of CIT led to a decrease of toxicity and is therefore, a detoxification product [38]. Beside OH-CIT, nearly no data concerning the metabolization of CIT is currently available and no phase II metabolites have been found or described.
The metabolism of OTA was investigated using liver microsomes from rat, chicken, goat, swine, cow and human and three hydroxylated metabolites of OTA at the phenylalanine moiety were found [68, 69]. In humans and chicken especially 7′-OH-OTA was detected. Main reactions are the mono-hydroxylation, dechlorination, lactone opening and conjugation with glutathione [68, 70]. Mono-hydroxylated 8′-hydroxy-DHEC was found in incubates of rat and bovine liver preparations and microsomes as well as in human plasma [71, 72].

## 1.4 Simulation techniques for metabolic reactions

The investigation of metabolic processes is often hampered due to the complexity of living organisms. *In vivo* and *in vitro* models are used to identify metabolites and metabolic pathways and models with different complexity are established and include cell cultures, laboratory animals and human subjects in clinical trials. However, these models are often laborious and expensive and matrix effects can disturb the subsequent analysis when searching for new and toxicologically relevant metabolites. Especially in mycotoxin research elucidation of metabolic pathways is crucial to understand their toxicity. As a result, innovative techniques are needed to allow a faster achievement of reliable data concerning mycotoxins and their metabolites and TPs. The following section explains the established *in vitro* models as well as new and innovative simulation techniques.

### 1.4.1 IN VITRO ASSAYS

There are several *in vitro* techniques available which are used to address numerous aspects of metabolic processes. Because the liver is the primary organ in metabolism, identification of metabolites is done mainly with liver subcellular fractions like microsomes, S9 fraction or the cytosol from a variety of rodent and non-rodent animal species and also from humans [56, 73, 74]. Microsomes contain most of the metabolically relevant CYP enzymes specific for the used species as well as other enzymes of the endoplasmic reticulum [75]. Liver microsomes are most commonly used and need the co-factor nicotinamide adenine dinucleotide phosphate (NADPH). Cryopreserved hepatocytes still possess their cellular morphology and allow investigation of phase I and phase II processes but suffer from low enzyme concentrations and loss of enzyme activity during incubation [76]. Studies revealed that S9 and hepatocytes are able to form *in vivo* metabolites with 85 to 90% success and microsomes with a success rate of 75% [77]. Even if the loss of cellular morphology, enzyme activity and the use of artificial concentrations of cofactors are drawbacks of liver subcellular fractions, they are widely used due to commercial availability and the low costs when compared to *in vivo.* Furthermore, microsomes contain most of the enzymes involved in the metabolism of drugs. In mycotoxin research subcellular fractions are well established and commonly used, as well as various cell models like Caco-2 cells from human colon adenocarcinoma, HepG2 cells from human liver carcinoma or IPEC-J2 from pigs' small intestine to name a few [78].

### 1.4.2 ELECTROCHEMISTRY

Established for several years in drug and pharmaceutical research this purely instrumental set-up allows the simulation of metabolic phase I reactions [79]. By applying positive or negative potentials, substances are oxidized or reduced. Often used are flow-through cells with a three-electrode system consisting of the working electrode, one reference electrode and the counter electrode (Table 2). The EC-reactor can be coupled with different devices such as ESI-MS, ESI-HRMS or HPLC-MS to allow fast and reliable detection of the generated products. Also possible is the offline synthesis with bulk cells (or synthesis cell) which is used to oxidize or reduce samples in mg or even g quantities to generate high amounts of transformation products. The oxidation and reduction of substances is possible without interfering matrices and

due to immediate analysis via an attached mass spectrometric device, even short living and reactive species are detectable [80-82]. The electrochemical oxidation is caused by hydroxyl radicals which are formed through a one-electron loss of water on the working electrode surface [83, 84]. The reaction spectrum is broad and includes phase I typical reactions like hydroxylation, dehydrogenation or dealkylation. Further oxidative reactions are the N-dealkylation, S- and P-oxidation, alcohol oxidation and dehalogenation. Phase II reactions can be also simulated [80, 85]. For that purpose, electrochemically oxidized or reduced TPs are trapped in a loop and mixed with biomolecules such as glucuronic acid and glutathione. The conjugated molecules are subsequently analyzed with the connected detection devices [86, 87]. Studies showed a good comparability between metabolites generated from *in vitro* assays and TPs generated electrochemically [85]. Electrochemistry in mycotoxin research was used as a pure detection method so far, but one study showed several reaction products derived from the *Alternaria* toxins AOH and AME. Hydroxylation and adduct formation with methanol was observed and the data obtained from EC/MS were compared with *in vitro* assays with human liver microsomes showing some similarities [88].

Table 2. Different electrode materials available for electrochemical measurements

| **Working electrode** | **Reference electrode** | **Counter electrode** |
|---|---|---|
| • Glassy carbon (GC)<br>• Boron doped diamond (BDD)<br>• Gold<br>• Silver<br>• Platinum | • Silver/silver chloride (Ag/AgCl)<br>• Palladium-hydrogen ($Pd/H_2$) | • Titanium<br>• Carbon-loaded PTFE |

### 1.4.3 FENTON-LIKE REACTION

The Fenton-like oxidation ($Fe^{3+}/H_2O_2$) is used to destruct harmful organic pollutants in waste water to improve the water quality [89]. When compared to Fenton-like reactions, degradation reactions caused by the Fenton reaction ($Fe^{2+}/H_2O_2$) are initially faster. For both reactions the kinetics are complex and can be described as a combined pseudo-first-order (Fenton) and a simpler pseudo-first-order (Fenton-like) [90]. The non-selective oxidation reaction of $Fe^{3+}$ and $H_2O_2$ can be also applied for the generation of TPs comparable to EC and *in vitro*. However, the iron salt functions as a catalyst and leads to the decomposition of hydrogen peroxide. The resulting

hydroxyl radicals attack the organic compounds and cause the generation of oxidation products and finally the complete destruction.

### 1.4.4 UV IRRADIATION

Light and photo-induced cleavage of chemical bonds, called photolysis, occurs in the atmosphere as well as in water and soil systems [91-93]. The direct photolysis is observed when the compound absorbs light of a certain wavelength or a range of wavelengths causing the breakage of chemical bonds [94, 95]. The indirect photolysis takes place, when a second molecule in the reaction mixture absorbs the light and is transformed into a highly reactive species like hydroxyl radicals or alkyl peroxyl radicals [95]. The radicals are then reacting with the compound of interest. Natural occurring photolytic processes can be easily simulated in the laboratory using mercury-vapor lamps or low-pressure mercury vapor lamps (mainly emit at $\lambda$=254 nm). The UV-range is divided into four groups, VUV-light (100 - 200 nm), UV-C light (200 -280 nm), UV-B light (280 - 320 nm) and UV-A light (320 nm - 400 nm). Besides the chosen wavelength and time of irradiation, the used solvent system is important for method development and UV-irradiation experiments. Like Fenton reagents UV-irradiation is often used as method to destruct harmful compounds in water but is also used to investigate reaction kinetics as well as photo-TPs [93]. Irradiation of ZEN led to the transformation from the natural trans isoform to the cis isoform [24, 96]. OTA, OTB and CIT were degraded by blue light. Here, CIT is completely degraded, whereas OTA and OTB did no longer contain phenylalanine [97]. However, other studies which are focused on TPs and not the degradation itself are scarce by now.

## 1.5 Reactions with metal ions

New TPs can be the result of oxidation or complexation reactions between mycotoxins and metal ions. Iron and copper ions are naturally present in food and are bound to plant or animal proteins. These metal ions are most likely the cause for oxidative processes and are involved in the formation of reactive oxygen species which could in turn, cause oxidative stress [98]. Several studies described metal phenol complexes with binding and redox processes. Copper ions are more efficient compared to iron

ions when it comes to the enhancement of electron transfers under neutral conditions [99]. Concerning mycotoxins, only a few studies are available by now. It was shown that OTA forms stable complexes with several alkaline earth ions which were confirmed by X-ray analysis [100, 101]. A further example is the fungal metabolite tenuazonic acid which forms complexes with $Cu^{2+}$, $Fe^{3+}$, $Ni^{2+}$, and $Mg^{2+}$ ions [102]. The mycoestrogen ZEN chelates with $Al^{3+}$ and a HPLC method with post-column derivatization was described using aluminum chloride, which led to an increased ZEN signal [103]. Chemical oxidation using aqueous $Ce^{4+}$ solutions is known for the addition of radicals to alkenes leading to carbon-carbon bonds as well as carbon-heteroatom bonds and the destruction of ZEN by $Ce^{4+}$ and $H_2SO_4$ was described [104].

## 1.6 Toxicity testing with *Caenorhabditis elegans*

To evaluate the health risks of mycotoxins and their derived TPs reliable test systems are needed. Often used are *in vitro* assays with cell lines as described in 1.4.1 and with laboratory animals in rodent and non-rodent systems. The cultivation of the nematode *Caenorhabditis elegans* is well established in genetic biology and for several years its potential as model for toxicity testing is increasingly recognized [105]. The nematodes are easy to culture and to handle and biotests including reproduction, growth or lifespan are standardized and established for several years [106, 107]. *C. elegans* can serve as a bridge between mammalian models and *in vitro* assays. There is a strong need for fast toxicity testing because of the growing number of newly discovered mycotoxins, their TPs and metabolites [108]. The fast life cycle with 4 different larval stages from L1 to L4 of *C. elegans* allows optimal conditions for toxicity tests, shown in Figure 1. Adults live for approximately three weeks and reproduce during the first five to six days of adulthood. They are fed on bacteria, mostly the *Escherichia coli* strain OP50 and can be cultivated between 15 and 25 °C. Under unfavorable conditions such as starving, crowding or to high temperature, worms undergo into a stage of stasis, called dauer larvae [109]. This stage survives up to four months and melt into L4 stage after the conditions are favorable again and makes the worm an ideal candidate for long term storage.

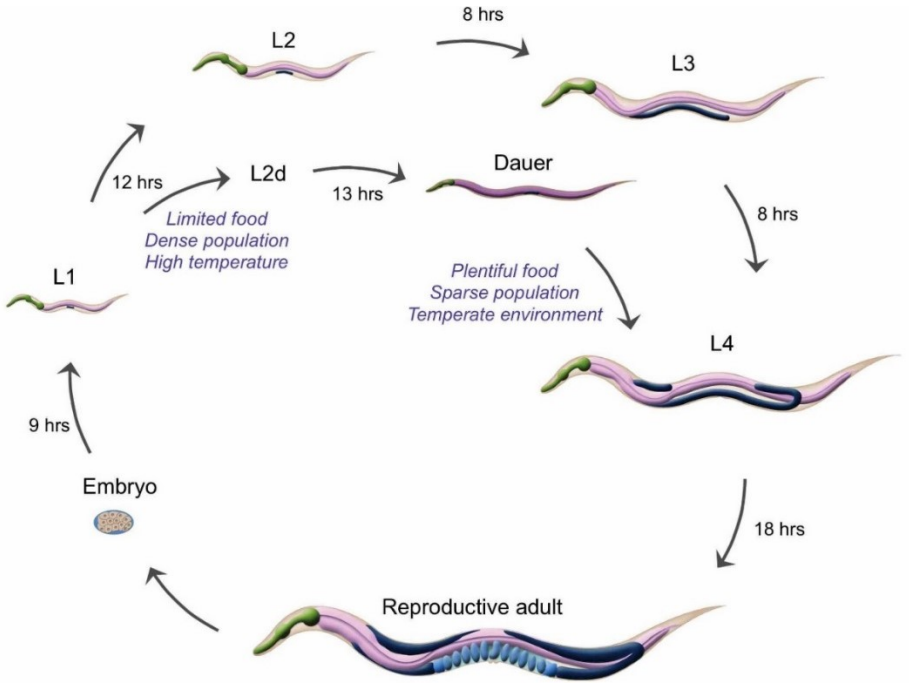


Figure 1. Lifecycle of *Caenorhabditis elegans* with dauer branch (from wormbook.org)

## 1.7 Instrumental analysis

Due to the diverse toxic effects of mycotoxins even in very low concentrations, reliable, sensitive and selective analytical procedures are needed. Besides separation and detection techniques, structural elucidation plays a significant role in the identification of new TPs of mycotoxins. The most important analytical techniques are described in the following sections.

### 1.7.1 HPLC-DAD/FLD AND HPLC-MS/MS

High performance liquid chromatography (HPLC) allows the fast separation of analyte-mixtures into their components based on their molecular structure and composition. The separation involves a stationary phase in HPLC-columns which allow the use of high pressures during analysis and a mobile phase: mostly a combined use of water and solvent systems. Depending on the chosen parameters like stationary phase, solvent system, temperature or flow rate of the mobile phase,

separation is achieved by different elution times of the analytes. Commonly used detector types are diode array detectors (DAD), fluorescence detectors (FLD) or mass spectrometric devices. The ionization of analytes by ESI (electrospray ionization) is a ´soft´ ionization method and is applicable to a wide range of different analytes, from small organic molecules to bigger molecules like proteins and polymers. The mass analysis is achieved in two steps, at first a precursor ion is selected from the sum of all present ions and supplied by the ion source. The precursor ion is fragmented by collision and the resulting fragments are detected by the second mass analyzer. By analyzing the fragments, conclusions can be drawn about the structural composition. Because of the structural diversity of mycotoxins, it can be useful to use optical as well as mass spectrometric detection.

### 1.7.2 NMR

Nuclear magnetic resonance (NMR) spectroscopy is used in analytical chemistry for quality control, evaluation of purity and the elucidation of unknown structures, and the quantification of organic compounds as primary method using reliable internal standards. Many nuclei have a natural spin and all nuclei are electrically charged. By applying an external magnetic field, an energy transfer is achieved between the base energy to a higher energy level. When the spin returns to its base level the energy is emitted and can be measured. The intramolecular magnetic field of an atom influences the resonance frequency and details of the electronic structure of a molecule and its functional groups can be drawn. The most commonly used types of NMR are proton ($^{1}$H-NMR) and carbon-13 NMR spectroscopy ($^{13}$C-NMR). This technique is non-destructive and leaves the analyte unaltered which is optimal for further measurements. Unfortunately, relatively large amounts are needed for the measurements (at least 5 mg).

## 1.8 Aims of the thesis

### 1.8.1 MAIN OBJECTIVES

As outlined in the introduction, TPs of food relevant mycotoxins could pose an additional risk to humans and animals due to unknown occurrence in food and feed and their toxicity. In order to improve the data situation this thesis follows four key aims:

1) To establish effective simulation methods to produce TPs from mycotoxins
2) To generate pure substances of TPs for structural analysis and toxicity testing
3) To assess the toxicity of mycotoxins and their TPs
4) To identify new areas of application for the discovered TPs

The key objectives will be described in more detail in the following sections.

### 1.8.2 ESTABLISHMENT OF SIMULATION TECHNIQUES TO PRODUCE TPs FROM FOOD RELEVANT MYCOTOXINS

Yet, in recent years the coupling of EC/MS gained increasing importance as promising technique for fast simulation of metabolic processes and was successfully applied for drug metabolism research. In the first place, the potential of EC/MS to predict phase I metabolites of priority mycotoxins should be compared to the results obtained from *in vitro* experiments with liver cell microsomes. To ensure a comparative overview, different established oxidation methods from other fields of research are tested as well. The Fenton-like reaction and irradiation with UV-light are used in waste water treatment as methods of choice to decompose organic molecules and should be now applied on mycotoxins. Main goal is to point out the benefits and drawbacks of EC/MS and other simulation techniques in mycotoxin research, based on selected food relevant mycotoxins.

### 1.8.3 GENERATION OF PURE SUBSTANCES OF TPS FOR STRUCTURAL ELUCIDATION AND TOXICITY TESTING

The assessment of toxicity and the occurrence of mycotoxins and their TPs in food and feed is often hampered by missing analytical standards and pure substances. Furthermore, the structural elucidation of these compounds is dependent on pure substances in sufficient quantities. Consequently, the synthesis of TPs was pursued in a first step using the established simulation techniques as well as biosynthetic approaches to obtain mg-quantities.

### 1.8.4 ASSESSMENT OF THE TOXICITY OF MYCOTOXINS

To keep up with the increasing occurrence of emerging mycotoxins and their transformation products, fast and reliable toxicity tests are needed. Toxicity testing of mycotoxins is carried out usually by performing *in vitro* assays or is evaluated using laboratory animals like mice, rats or chicken in *in vivo* studies. Settled between classical *in vitro* approaches and *in vivo* studies with higher animals are tests with the nematode *C. elegans.* This worm is widely used as a model organism in developmental biology and neurology. In mycotoxin research the methods of choice have been *in vitro* and *in vivo* approaches, so far. Besides hundreds of documented mycotoxins, numerous new ones need to be elucidated and enhance the demand for fast and reliable methods. *C. elegans* should be tested as affordable and straightforward alternative in toxicity testing of mycotoxins.

### 1.8.5 IDENTIFICATION OF NEW AREAS OF APPLICATIONS FOR MYCOTOXIN-METAL COMPLEXES

Often the toxic effects of mycotoxins are in the focus of current research, but also reliable analytical methods with high sensitivities are needed to detect even low concentrations of these diverse food contaminants. By altering the chemical properties of a mycotoxin, for example due to complex formation with metal ions, a

new approach of HPLC detection could be achieved. Thus, the specific aim is to characterize the new optical properties of the fluorescent metal complexes and to gain information about the composition of the formed mycotoxin-metal complexes.

# 2 RESULTS AND DISCUSSION

The following parts of ´Results and Discussion´ were published in international and peer-reviewed journals:

J. Keller, H. Haase, M. Koch (2017); **Electrochemical simulation of biotransformation reactions of citrinin and dihydroergocristine compared to UV irradiation and Fenton-like reaction**; *Analytical and Bioanalytical Chemistry*; 409: 4037-4045 (2017); https://doi.org/10.1007/s00216-017-0350-6

J. Keller, H. Haase, M. Koch; **Hydroxylation and dimerization of zearalenone: comparison of chemical, enzymatic and electrochemical oxidation methods**; *World Mycotoxin Journal* (2017); 10(4): 297-307; https://doi.org/10.3920/WMJ2017.2213

A. Borzekowski, T. Drewitz, J. Keller, D. Pfeifer, H.-J. Kunte, M. Koch, S. Rohn, R. Maul; **Biosynthesis and characterization of zearalenone-14-sulfate, zearalenone-14-glucoside and zearalenone-16-glucoside using common fungal strains**; *Toxins* (2018); *10*(3), 104; https://doi.org/10.3390/toxins10030104

J. Keller, A. Borzekowski, H. Haase, R. Menzel, L. Rueß, M. Koch; **Toxicity assay for citrinin, zearalenone and zearalenone-14-sulfate using the nematode *Caenorhabditis elegans* as model organism**; *Toxins* (2018); *10*(7), 284; https://doi.org/10.3390/toxins10070284

J. Keller, D. Moldenhauer, L. Byrne, H. Haase, U. Resch-Genger, M. Koch; C**omplexes of the mycotoxins citrinin and ochratoxin A with aluminum ions and their spectroscopic properties**; *Toxins (2018);* *10*(12), 538 https://doi.org/10.3390/toxins10120538

J. Keller, L. Hantschke, H. Haase, M. Koch**; Synthesis and structural identification of a biaryl ether-linked zearalenone dimer**; *Molecules* (2018), 23(10), 2624; https://doi.org/10.3390/molecules23102624

# 2.1 Electrochemical simulation of biotransformation reactions of citrinin and dihydroergocristine compared to UV irradiation and Fenton-like reaction

J. Keller, H. Haase, M. Koch*

Originally published in **Analytical and Bioanalytical Chemistry**
409: 4037-4045 (2017)
https://doi.org/10.1007/s00216-017-0350-6


J. Keller, M. Koch
*Federal Institute for Materials Research and Testing (BAM), Richard-Willstätter-Straße 11, 12489, Berlin, Germany. E-mail: Matthias.koch@bam.de*

H. Haase
*Department of Food Chemistry and Toxicology, Berlin Institute of Technology, Gustav-Meyer-Allee 25, D-13355 Berlin, Germany. E-mail: Haase@TU-Berlin.de*
* *Corresponding author*

## 2.1.1 ABSTRACT

Mycotoxins occur widely in foodstuffs and cause a variety of mold-related health risks to humans and animals. Elucidation of the metabolic fate of mycotoxins and the growing number of newly discovered mycotoxins have enhanced the demand for fast and reliable simulation methods. The viability of electrochemistry coupled with mass spectrometry (EC/ESI-MS), Fenton-like oxidation and UV irradiation for the simulation of oxidative phase I metabolism of the mycotoxins citrinin (CIT) and dihydroergocristine (DHEC) was investigated. The specific reaction products are compared with metabolites produced by human and rat liver microsomes *in vitro*. Depending on the applied potential between 0 and 2,000 mV vs. $Pd/H_2$ by using a flow-through cell, CIT and DHEC are oxidized to various products. Beside

dehydrogenation and dealkylation reactions, several hydroxylated DHEC and CIT species are produced by EC and Fenton-like reaction, separated and analyzed by HPLC-MS/MS and ESI-HRMS. Compared to reaction products from performed microsomal incubations, several mono- and dihydroxylated DHEC species were found to be similar to the reaction products of EC, Fenton-like reaction and UV-induced oxidation. Consequentially, non-microsomal efficient and economic simulation techniques can be useful in early stage metabolic studies, even if one to one simulation is not always feasible.

### 2.1.2 INTRODUCTION

Mycotoxins are secondary metabolites produced by different types of fungi belonging mainly to the *Aspergillus*, *Penicillium* and *Fusarium* genera and contaminating almost 25% of food and feed worldwide [110]. Besides huge economic losses, the ingestion of contaminated food may cause various acute and chronic diseases in humans and animals due to their diverse chemical structures [11]. To ensure the highest possible level of food safety the Rapid Alert System for Food and Feed (RASFF) was launched in 1979. The consumption of mycotoxins is almost inevitable and according to the RASFF mycotoxins are still important hazard contaminants which need to be strictly controlled [111].

Up to now several hundred mycotoxins have been identified but only 11 of them are regulated and controlled by authorities within the European Union [112]. So far, maximum levels have been set in products for human consumption for mycotoxins such as aflatoxins, zearalenone, ochratoxin A or deoxynivalenol to secure food safety for the consuming public.

To understand the toxic effects of mycotoxins in human and animal organisms it is necessary to elucidate their metabolic pathways during biotransformation which can be divided into phase I and phase II reactions. In phase I exogenous compounds like drugs or toxins are functionalized by cytochrome P450 (CYP450) isoenzymes, mainly through oxidative reactions such as hydroxylation, dehydrogenation and dealkylation [75, 113]. In phase II transferase enzymes catalyze the conjugation of the functionalized phase I metabolites with endogenous substances. During biotransformation CYP450-mediated reactions may lead to the production of highly reactive compounds like epoxides, quinones or semiquinones which easily react with electrophilic DNA or proteins causing severe damage to these structures [114]. Besides performing animal studies for metabolic elucidation of these substances and

their metabolites, biotransformation processes are investigated *in vitro* as well, using subcellular fractions such as microsomes or cytosol. In addition to these established approaches interest in new simulation methods have increased over the past years and new techniques like electrochemistry (EC) have been successfully used in drug and pharmaceutical research [73, 81]. Besides enzymes of the cytochrome P450 family and EC, the chemical oxidation with Fenton-like reactions are sufficient for the oxidation of organic compounds as well. Fenton-like reactions ($Fe^{3+}/H_2O_2$) are often used to destruct hazardous organic pollutants in waste water by non-selective oxidation [90]. Degradation of organic pollutants is also achieved by using photocatalytic techniques. Photo-degradation experiments have been performed with mycotoxins to decontaminate apple juice or red wine from mycotoxins or isomerization [24, 115, 116]. Comparative studies dealing with all of the described techniques were rare and in the case of mycotoxins such an overview is missing completely. For this reason, the food relevant mycotoxin citrinin (CIT) and the model mycotoxin dihydroergocristine (DHEC) were chosen to be investigated with regard to their oxidation products (structures shown in Figure 2). DHEC is a semi-synthetic ergot alkaloid used for age-related cognitive impairment [117]. Ergot alkaloids are classified as indole alkaloids that are produced as a toxic mixture in the sclerotia of *Claviceps* infesting especially grass and crops [118]. CIT is a nephrotoxic mycotoxin produced by several species of *Penicillium, Aspergillus* and *Monascus* and contaminates grains, cereal products and feeds [10]. Toxicity pathways of CIT, as yet, have not been clarified causing a strong need for further investigation, recently reviewed by the European Food Safety Authority (EFSA) [36]. In this study, electrochemical oxidation, Fenton-like reaction and UV irradiation were tested in a comparative study to simulate the oxidative metabolism of the mycotoxins CIT and DHEC. The obtained results present new possibilities to obtain phase I reaction products and highlight the benefits and limits of EC in mycotoxin research.

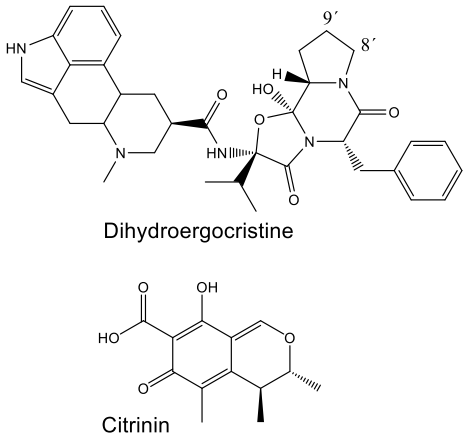


Figure 2. Structures of the investigated mycotoxins citrinin (CIT) and dihydroergocristine (DHEC)

## 2.1.3 MATERIAL AND METHODS

*Chemicals*

Citrinin (purity 98%) was purchased from *Santa Cruz Biotechnology* Inc. (Santa Cruz, CA). Dihydroergocristine was generated from dihydroergocristine mesylate (Teva Czech Industries s.r.o., Opava, Komárov, Czech Republic) by a procedure reported earlier [49]. $KH_2PO_4$ and $FeCl_3 \cdot 6\ H_2O$ were purchased from Merck (Darmstadt, Germany) and $K_2HPO_4$ from Carl Roth (Karlsruhe, Germany). NADPH tetrasodium salt was obtained from AppliChem GmbH (Darmstadt, Germany). Aqueous $H_2O_2$ (30%) was obtained from Sigma-Aldrich (Steinheim, Germany) and ultrapure water was produced by a Seralpur PRO 90 CN system (Ransbach-Baumbach, Germany). All standard chemicals were of p.a. grade, and all solvents, HPLC grade.

*Microsomal sources* Human and rat liver microsomes (HLM and RLM) were purchased from Thermo Fisher Scientific (Pittsburgh, PA, US). HLM were derived from a male gender pool of 20 donors with a protein concentration of 20 mg/mL and a CYP450 content of 170 pmol/mg protein. RLM were prepared from Sprague-Dawley male rats with a protein concentration of 20 mg/mL and a CYP450 content of 319 pmol/mg protein. The total protein content and CYP450 concentrations were provided by the manufacturer.

*Microsomal incubations*

Incubations with either HLM or RLM were carried out in a volume of 200 µL. The mixture contained 5 µmol/L mycotoxin dissolved in ACN, microsomes (1.5 mg/mL microsomal protein), 0.1 M potassium phosphate buffer, pH 7.4 and 0.1 mmol/L $MgCl_2$. The fraction of ACN in the final incubation mixture was not higher than 1%. After a preincubation of 5 minutes at 37 °C 6 mmol/L NADPH were added to the mixture to start the enzymatic reaction (incubation for 90 minutes at 37 °C, 800 rpm). In order to stop the reaction, 150 µL of ice-cold ACN were added and the sample was mixed thoroughly for 20 seconds. The incubation mixtures were centrifuged at 11,650g for 5 minutes to allow the precipitated proteins to settle on the ground. The supernatant was analyzed by HPLC-MS/MS. Control incubations were performed in duplicate for each of the tested mycotoxins without the co-factor NADPH. All other reactions were performed in triplicate.

*EC/ESI-MS*

Mass voltammograms were recorded by online coupling of an electrochemical flow through cell (µPrepCell, Antec Leyden, Zoeterwoude, Netherlands) to an electrospray ionization source of a single Quadrupole mass spectrometer (Agilent Technologies GmbH, Böblingen, Germany), shown in Figure 3. The mycotoxin solutions were passed through the cell by a SP2 - ROXY dual piston syringe pump (Antec Leyden). The EC cell was equipped with a glassy carbon (GC) or boron doped diamond (BDD) working electrode material, an auxiliary electrode (fully inert polymeric material containing conductive carbon) and a reference electrode ($Pd/H_2$). The working and auxiliary electrodes were separated by two 100-µm spacers. An electrochemical potentiostat ROXY (Antec Leyden) was used to apply a potential ramped between 0 and 2,000 mV versus $Pd/H_2$ at a scan rate of 20 mV/s (continuous scan mode). Electrochemical conditions were set up individually, as listed in Table 3.

Table 3. EC/ESI-MS parameter for electrochemical oxidation of CIT and DHEC

| Mycotoxin | *c* (µmol/L) | Solvent | Flow rate (µL/min) | Working electrode |
|---|---|---|---|---|
| **CIT** | 100 | $H_2O$:MeOH 50:50<br>20 mmol/L $NH_4Ac$ | 30 | Glassy Carbon |
| **DHEC** | 100 | $H_2O$:ACN 20:80<br>0.1% HAc | 70 | Boron Doped Diamond |

ACN: acetonitrile; MeOH: methanol; Ac: acetate

The method optimization revealed GC as more suitable for the oxidation of CIT and BDD as working electrode material for DHEC due to enhanced reproducibility and increased production yield. Each mass voltammogram was recorded at least three times to ensure the reproducibility of the measurements. Working electrodes were activated before each measurement using the from the manufacturer provided pulse cleaning program. Control measurements were performed using the solvent without analyte. The mass spectrometer was operated in positive ion mode. Ionization of the electrochemically generated reaction products was achieved with nitrogen drying gas (12 L/min, 35 psi nebulizer pressure) of 350 °C and 3,000 V on the capillary inlet. The scan range was $m/z$ = 100-700 and the threshold was set to 2,000 counts/s. For further analysis of the electrochemically generated products the direct current mode was used. Aliquots were collected offline into HPLC vials from the electrochemical cell and were used for further HPLC-MS/MS and ESI-HRMS measurements.

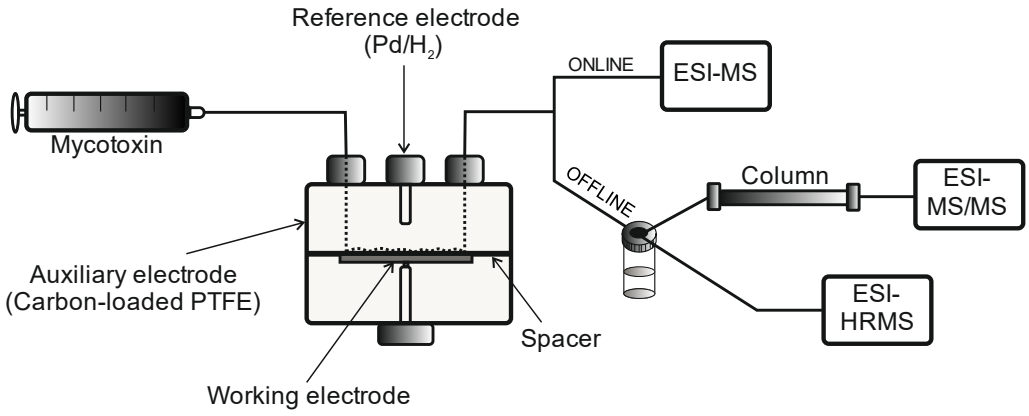


Figure 3. General setup for online EC/ESI-MS and EC offline LC/MS-MS for mycotoxin metabolism Studies

*UV irradiation*

For all UV-irradiation experiments a water-cooled UV reactor was used equipped with a 150 W medium-pressure mercury lamp (TQ 150, Heraeus Noblelight, Hanau, Germany) emitting light in the UV-C wavelength range of $\lambda$ = 200 nm to 280 nm. 100 mL of a 100 µmol/L solution of CIT ($H_2O$:MeOH 50:50 v/v) and DHEC ($H_2O$:ACN 20:80 v/v) were filled into the reactor vessel and constantly stirred with a magnetic stirrer (450 min-1). After cooling down the system to 12.5 °C the UV lamp was switched on and samples were collected at different time points (t = 2.5, 3, 5, 10, 15, 20, 30, 45, 60, 90 and 120 minutes). In case of DHEC samples were irradiated for 60 min resulting in a higher yield compared to the other time points and was used for further analysis. There was no degradation observable using CIT, but 60 min irradiation time were chosen as well to ensure comparability of the measurements.

*Fenton-like reaction*

The Fenton-like reaction ($Fe^{3+}/H_2O_2$) for each of the investigated mycotoxins was carried out in a volume of 1 mL. The mixture contained 100 µmol/L of mycotoxin dissolved in ACN, 5 µmol/L ferric (III) chloride and 100 µmol/L of $H_2O_2$. The reaction proceeded at 30°C and 800 rpm in a thermoshaker and was stopped at different time points (t = 1, 3, 5, 7, 15 and 30 minutes) by adding manganese dioxide. Shown and discussed are the results from samples incubated for 15 min due to increased yield of reaction products. For the HPLC-MS/MS analysis, samples were centrifuged (11,650g for 2 minutes) and the supernatant was used. Control samples containing CIT, DHEC and manganese dioxide were analyzed in duplicate for both mycotoxins. All other reactions were performed in triplicate.

*HPLC-MS/MS*

All products from microsomal, electrochemical, photochemical and chemical oxidation studies were analyzed by HPLC-MS/MS using an API 4000 mass spectrometer (AB Sciex, MA, USA) connected to an Agilent 1100 series HPLC (Agilent Technologies GmbH, Böblingen, Germany). The analytical column was a Gemini® NX-C18, particle size 3 µm, pore size 110 Å, 250 x 4.6 mm (Phenomenex, Torrance,

CA, USA) and the column oven was set to 40 °C. For the separation of CIT and its oxidation products a mobile phase consisting of $H_2O$ with 5 mmol/L $NH_4Ac$ and 0.05% HAc (A) and MeOH/$H_2O$ (95:5 *v*/*v*) containing 5 mmol/L $NH_4Ac$ and 0.05% HAc (B) was used. The injection volume was 5 µL. The flow rate of the mobile phase was 0.25 mL $min^{-1}$ and a gradient program was used starting at 30% mobile phase B. Within 30 min, B was raised to 100%, followed by a decrease back to 30% at minute 31. Afterwards, the column was re-equilibrated to starting conditions for 9 min. To separate DHEC and its reaction products a mobile phase consisting of $H_2O$ with 0.1% HAc (A) and ACN with 0.1% HAc (B) was used. The injection volume was 5 µL. The flow rate of the mobile phase was 0.3 mL $min^{-1}$ and an isocratic method was used with 20% mobile phase B. The MS/MS conditions used for the investigated mycotoxins and their corresponding hydroxylated forms are shown in Table 4. In the case of CIT the mass spectrometer was operated in multiple reaction monitoring (MRM) mode with negative electrospray ionization (ESI). For CIT the monitored transitions were *m*/*z* 249 → 205 and for OH-CIT *m*/*z* 265 →221 which have been carried out by performing product ion scans of *m*/*z* 249 and *m*/*z* 265. DHEC and hydroxylated DHEC were detected by using multiple ion scan with *m*/*z* 612 (DHEC), 628 (OH-DHEC) und 644 (Di-OH-DHEC) with positive electrospray ionization.

Table 4. MS/MS conditions for the mass-spectrometric detection of CIT and DHEC and their oxidation products

| **Mycotoxin** | **Ionization mode** | **$N_2$ (L)** | **Ion source gas 1 (L)** | **Ion source gas 2 (L)** | **Ion spray Voltage (V)** | **Desolvation Temp. (°C)** |
|---|---|---|---|---|---|---|
| CIT; OH-CIT | negative | 10 | 45 | 35 | -4,000 | 450 |
| DHEC; OH-and Di-OH-DHEC | positive | 14 | 40 | 30 | 5,500 | 500 |

*High-resolution mass spectrometry (HRMS)*

HRMS was performed by using a hybrid linear quadrupole ion trap (LTQ) Fourier transform ion cyclotron resonance (FT-ICR) mass spectrometer (Thermo Finnigan Corp., Bremen Germany) with a magnetic field force of 7 Tesla. Samples were diluted with MeOH containing 0.1% formic acid to obtain a final concentration of 10 µmol/L and pipette to a static nano-ESI emitter. The ion spray voltage was set to 1,500 V and the detection was achieved by a FTMS analyzer. Data were acquired in the positive

ionization mode within a range of *m*/*z* 100 to 800 and the resolving power was set to 100,000 at *m*/*z* 400. Determination of the elemental composition of individual reaction products was based on accurate masses, typically better than 5 ppm mass accuracy.

### 2.1.4 RESULTS AND DISCUSSION

The present study was dedicated to the investigation of the oxidative phase I metabolism of CIT and DHEC by performing different approaches. Emphasis was on online EC/ESI-MS as a promising technique for a fast prediction of metabolic pathways by elucidating biotransformation products.

*Electrochemical oxidation of citrinin:*

Based on the state of scientific knowledge regarding the metabolism of CIT the EC/ESI-MS data obtained in this study are of particular interest. The signal of CIT with *m*/*z* 251 decreased after applying a ramped potential in a range from 0 and 2,000 mV by simultaneous production of various oxidation products occurring as shown in Figure 4. An initial identification of the reaction products was made by HRMS measurements listed in Table 5 with the suggested modifications.

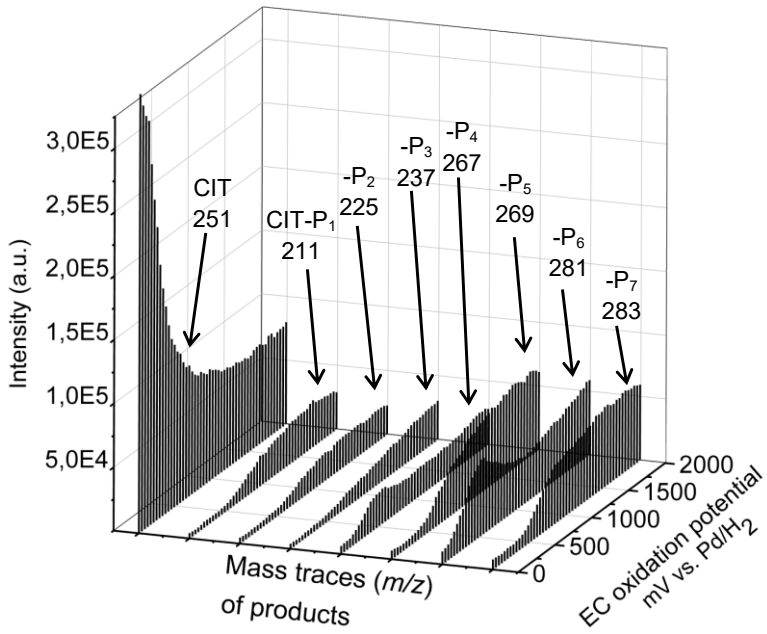


Figure 4. Mass traces (*m*/*z*) of the oxidation products of CIT in dependence of the applied oxidation potential ramped from $E_0$=0 mV to $E_1$=2000 mV with the ramping velocity of 20 mV/s

A reaction product with *m*/*z* 281 is the result of an electrochemical reaction of CIT with the solvent MeOH. In the range of 250 and 1,000 mV vs. Pd/$H_2$ a reaction product with *m*/*z* 283, indicating the mass gain of two hydrogens, was very likely generated from *m*/*z* 281. Similar electrochemical reaction products have already been described for the secondary fungi metabolites alternariol and alternariol methyl ether [88] . The fungi *Penicillium citrinum* decomposes CIT to dimethyl dicitrinin A [119], bearing two methoxy groups and demonstrates that the addition of a methoxy group achieved by EC is closely related to biochemical reactions in living systems. CIT-$P_2$ with *m*/*z* 225 resulted from the hydroxylation of CIT followed by the opening of the ring and the loss of carbon dioxide leading to the formation of citrinin H2. This reaction also occurred without the loss of carbon dioxide and led to the product CIT-$P_5$ with *m*/*z* 269 which is increasingly produced with higher potentials. It was also observed that the dealkylation of CIT led to the products with *m*/*z* 237 and *m*/*z* 211 resulting from multiple reaction steps including hydroxylation and the loss of carbon dioxide. The possible reaction pathway of the electrochemical oxidation of CIT is presented in Figure 5.

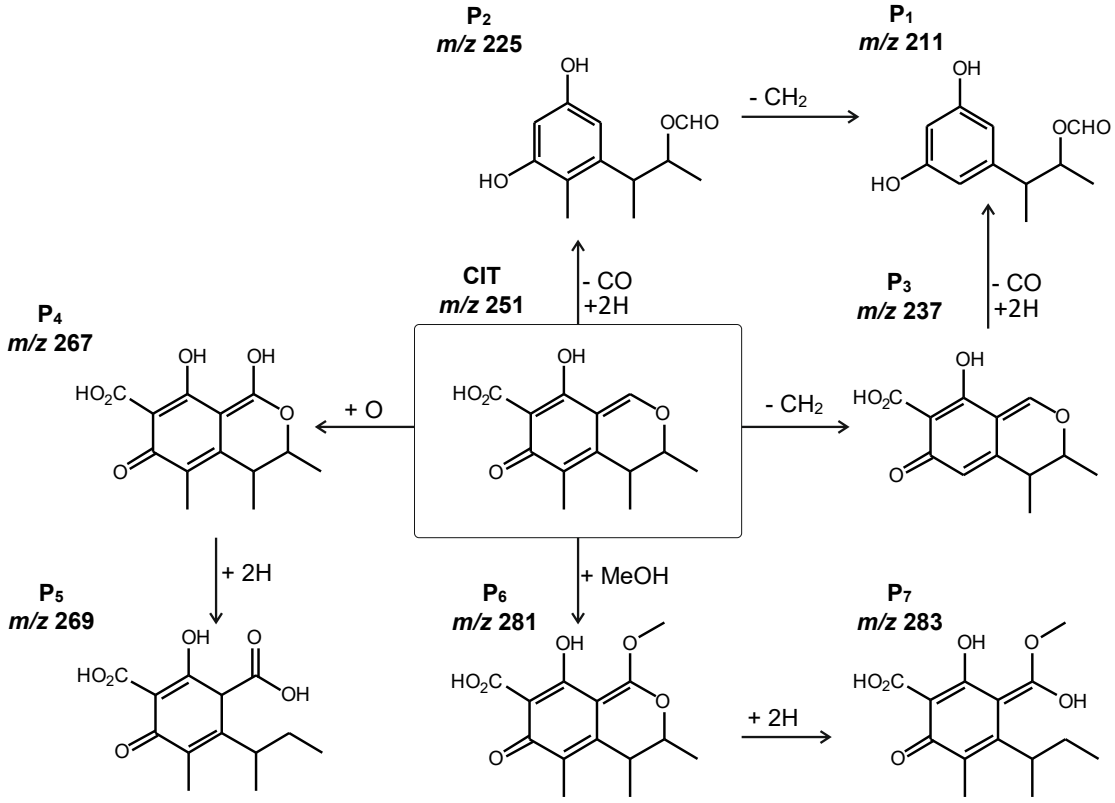


Figure 5. Reaction scheme of the electrochemical oxidation of CIT

CYP450 enzymes are capable of metabolizing dealkylation reactions. It is conceivable that the dealkylation achieved by EC may also take place in biological systems during the enzymatic oxidation of CIT and is of particular importance concerning the poor data conditions of CIT metabolites. Relatively well understood is the CIT derived metabolite dihydrocitrinone which has been found to be a major metabolite in the urine of rats [120] and humans [67]. Whether the *m/z* 267 detected by using EC/ESI-MS is dihydrocitrinone needs to be confirmed by structural elucidation. First results, by performing HPLC-MS/MS measurements of the EC eluate, revealed that no dihydrocitrinone was formed using EC but other hydroxylated species, as discussed in the following section.

Table 5 HRMS data of EC-modified protonated oxidation products of CIT and DHEC with the corresponding exact masses and deviations

| Compound | *m/z* determined | *m/z* calculated | Molecular formula | Suggested modification | δm/m |
|---|---|---|---|---|---|
| **CIT** | 251.0913 | 251.0919 | $C_{13}H_{15}O_5$ | - | 2.6 |
| **CIT-P$_1$** | 211.0963 | 211.0970 | $C_{11}H_{15}O_4$ | -CO, -$CH_2$, +2H | 3.5 |
| **CIT-P$_2$** | 225.1120 | 225.1127 | $C_{12}H_{17}O_4$ | -CO, +2H | 3.0 |
| **CIT-P$_3$** | 237.1120 | 237.1127 | $C_{12}H_{13}O_5$ | -$CH_2$ | 2.9 |
| **CIT-P$_4$** | 267.0862 | 267.0869 | $C_{13}H_{15}O_6$ | +O | 2.5 |
| **CIT-P$_5$** | 269.1019 | 269.1030 | $C_{13}H_{17}O_6$ | +O, +2H | 2.3 |
| **CIT-P$_6$** | 281.1017 | 281.1030 | $C_{14}H_{17}O_6$ | +$CH_2O$ | 2.9 |
| **CIT-P$_7$** | 283.1175 | 283.1182 | $C_{14}H_{19}O_6$ | +$CH_2O$, +2H | 2.3 |
| **DHEC** | 612.3193 | 612.3186 | $C_{35}H_{42}N_5O_5$ | - | 1.0 |
| **DHEC-P$_1$** | 626.2987 | 626.2979 | $C_{35}H_{40}N_5O_6$ | +O, –2H | 1.4 |
| **DHEC-P$_2$** | 626.3343 | 626.3342 | $C_{36}H_{44}N_5O_5$ | +$CH_2$ | 0.2 |
| **DHEC-P$_3$** | 628.3125 | 628.3135 | $C_{35}H_{42}N_5O_6$ | +O | 1.5 |
| **DHEC-P$_4$** | 642.2926 | 642.2928 | $C_{35}H_{40}N_5O_7$ | +2O, –2H | 0.3 |
| **DHEC-P$_5$** | 644.3082 | 644.3084 | $C_{35}H_{42}N_5O_7$ | +2O | 0.3 |
| **DHEC-P$_6$** | 660.3030 | 660.3033 | $C_{35}H_{42}N_5O_8$ | +3O | 0.4 |

*Investigation of hydroxylated citrinin by HPLC-MS/MS:*

Samples were measured during one HPLC/MS-MS run and screened for hydroxylated CIT species by using the mass transition *m/z* 265→221 and for CIT *m/z* 249→205 (Figure 6) which corresponds to the loss of carbon dioxide during fragmentation.

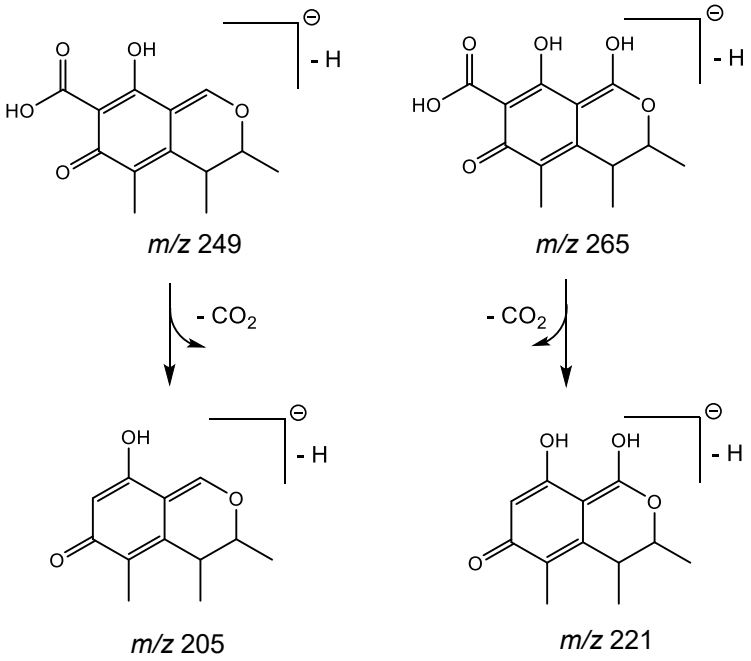


Figure 6. Fragmentation origin of CIT and OH-CIT with typical loss of 44 Da, caused by cleavage of the carboxylic acid

The combined results of all tested oxidation systems are presented in Figure 7. Every control contained a certain amount of hydroxylated CIT shown as a grey line from control measurements before oxidation started. This could be an artifact caused by storage and handling or comes directly from the standard obtained from *penicillium citrinum* as a biological source. It is known that this fungus also produces dihydrocitrinone, a hydroxylated form of CIT [121]. This important marker substance for CIT can be found after intake of the toxin by humans in both urine and blood plasma [122]. To our knowledge no microsomal incubation has been performed before with the focus on the production of metabolites. CIT was incubated with human and rat liver microsomes leading to the production of hydroxylated CIT. HPLC-MS/MS analysis of the collected EC fractions led to four different hydroxylation products all with earlier retention times compared to the CIT standard. Hydroxylated products are more polar than their mother compounds which led to shorter retention times on reversed-phase columns. Mass transition and retention time indicated the production of hydroxylated CIT, but obviously it needs to be confirmed by structural analysis techniques in future investigations. However, compared to biochemical oxidation by microsomes, the product pattern of EC is more divers, but no match was found comparing the EC and microsomal products (Figure 7). The reaction products $C_5$ and $C_6$ were only formed by using EC, indicating multiple reaction steps which led to two different reaction products with *m/z*

265→221. Fenton-like oxidation formed three hydroxylated species, $C_2$, $C_3$ and $C_4$. Reaction product $C_3$ was formed by HLM and RLM as well as by Fenton with higher signal intensities and $C_4$ was produced by Fenton-like reaction as a main product and in low yields by HLM and RLM. Both of the microsomal incubations tested have one reaction product in common eluting after CIT which indicates a metabolite more nonpolar than CIT itself. Hydroxylation normally leads to a shorter retention time; in this case the identification of this peak remained unanswered within the limits of that study. UV irradiation had no effect on the production of hydroxylated species.

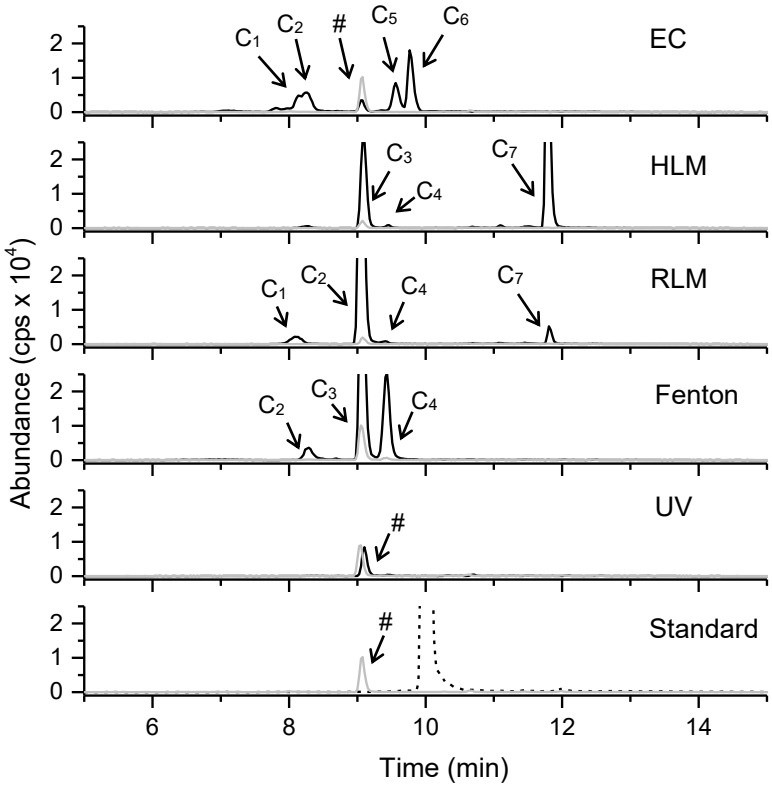


Figure 7. HPLC-MS/MS chromatograms of hydroxylated CIT after electrochemical oxidation (EC 1500 mV), human liver (HLM) and rat liver microsomal (RLM) incubation, Fenton-like reaction with $Fe^{3+}/H_2O_2$ (Fenton) and UV irradiation (UV) by using mass transitions *m*/*z* 265→221 of the control samples (grey, marked by #) and 265→221 after oxidation (black) (MRM negative). The control sample (Standard; *m*/*z* 249→205) indicates CIT without treatment

To sum up, it can be concluded that CIT was oxidized for the first time using Fenton, microsomes and EC successfully leading to hydroxylated species. EC was not suitable for mimicking phase I but provided a range of reaction products that could possibly be interesting compounds for future research. Fenton-like oxidation was the more appropriate method to predict phase I metabolites and it can be seen as a potential new tool to improve and support classical *in vitro* methods together with EC.

*Electrochemical oxidation of dihydroergocristine:*

Electrochemical conversion of the model mycotoxin DHEC with *m*/*z* 612 resulted in the production of mainly hydroxylated species as shown in Table 5, containing the HRMS data. Monohydroxylation was observed with *m*/*z* 628, dihydroxylation with *m*/*z* 644 and multiple hydroxylation with addition of three oxygen leading to *m*/*z* 660 could be observed after the application of a ramped voltage. From these three reaction products only the monohydroxylated form is already described in the literature as being found in human plasma and produced by rat liver microsomes [71]. From investigation of ergot alkaloids like ergotamine and bromocriptine it is known that monohydroxylation takes place at the C8′ position (Figure 7) of the condensed tripeptide [123]. Double and triple hydroxylated DHEC species (DHEC-$P_5$ and DHEC-$P_6$) are novel reaction products generated by electrochemical oxidation in low yields. Hydroxylation sites can differ between enzymatic and electrochemical reaction which leads to reaction products with the same mass-to-charge ratio but different structures. This can be seen in Table 5 in the case of DHEC-$P_1$ and DHEC-$P_2$ which have both *m*/*z* 626. Electrochemistry favors the hydroxylation of electron-rich regions like aromatic ring systems whereas CYP450 catalyze enzyme specific positions of the substrate like in the case of DHEC, hydroxylation of the condensed tripeptide [85]. Though mono- and dihydroxylation are typical CYP-derived reactions, to our knowledge a threefold hydroxylation has not yet been described in research reports for ergot alkaloids. New products also include the formation of the mono- and dihydroxylated DHEC species which were further dehydrogenated causing signals with *m*/*z* 626 (DHEC-$P_1$) and *m*/*z* 642 (DHEC-$P_3$) as shown in Table 5.

*Investigation of hydroxylated dihydroergocristine by HPLC-MS:*

Besides the monohydroxylated DHEC form with *m*/*z* 628 the dihydroxylated form with *m*/*z* 644 was also investigated within this study, observed already by EC/ESI-MS and ESI-HRMS. Dihydroxylation has been described for a few ergot alkaloids by introducing a second hydroxy group at the C9′ position of the tripeptide leading to four possible isomers (Figure 7), but is now described for DHEC as well. Due to various oxidation sites of DHEC in the cases of EC, Fenton and UV, a multiple ion scan was performed in positive ionization mode. All of the detected hydroxylated DHEC species eluted earlier than DHEC, as shown in Figure 8 and 9, because of their more polar nature. The two monohydroxylated species $MD_5$ and $MD_6$ were produced by EC and found also by using Fenton-like oxidation. In modest amounts $MD_5$ was formed by using RLM. Reaction product $MD_6$ was found after 60 minutes UV irradiation of DHEC. HLM metabolized DHEC to two monohydroxylated main products, $MD_4$ and $MD_7$ which were not produced and detected in EC, Fenton or UV samples and can be also found with smaller signal intensities in RLM samples (Figure 8).

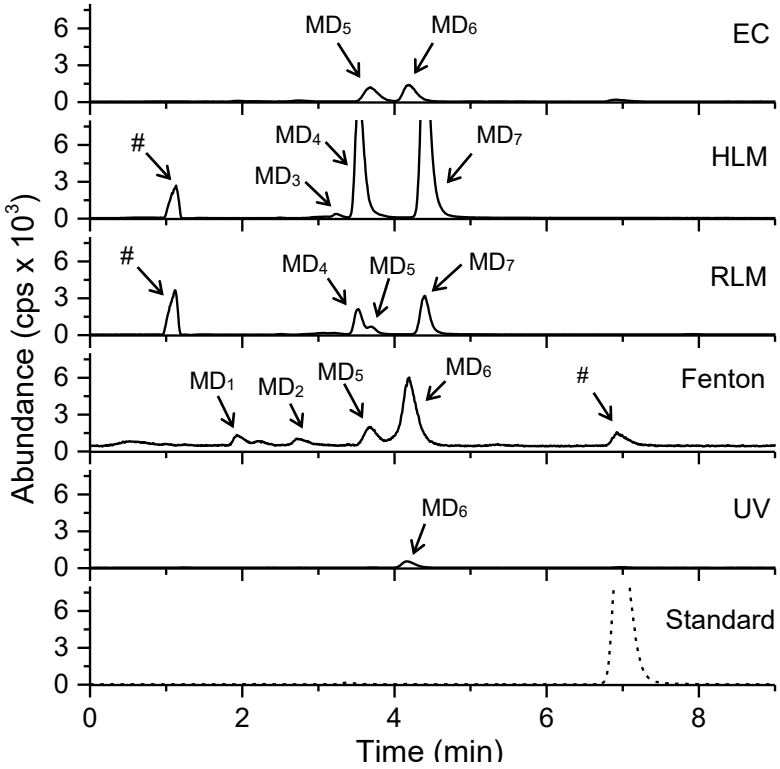


Figure 8 HPLC-MS/MS chromatograms of monohydroxylated DHEC after electrochemical oxidation (EC 1700 mV), human liver (HLM) and rat liver microsomal (RLM) incubation, Fenton-like reaction with $Fe^{3+}/H_2O_2$ (Fenton) and UV irradiation (UV) by using multiple ion scan with *m/z* 628 in positive ionization mode. The control sample (Standard; *m/z* 612) indicates DHEC without treatment. Peaks with *m/z* 628 occurred also in control samples are marked with #

EC and Fenton lead to nearly the same monohydroxylated reaction products of DHEC and were comparable to each other, but were not capable of mimicking or simulating phase I metabolism of DHEC one to one. Interestingly dihydroxylation for CIT was not observed using the different oxidation techniques, but in the case of DHEC dihydroxylation was achieved by using EC, microsomes, Fenton and UV (Figure 9). EC formed two dihydroxylated DHEC species, $DD_2$ and $DD_5$. $DD_5$ is generated in all of the tested systems in contrast to $DD_2$ which can only be found in the EC and Fenton samples. The reaction products $DD_4$ and $DD_6$ were only formed *in vitro* by HLM and RLM and could not be simulated by any of the tested instrumental techniques. Reactions mediated by enzymes are often highly stereo- and regio-selective and to obtain the same reaction products by EC is not always achievable [85]. DHEC has multiple oxidation sides and electron-rich ring systems favoring, in principle, several electrochemical oxidation products. Unfortunately, only low yields

of reaction products were achieved. The electrochemical degradation of DHEC of around three quarters (data not shown) may be leading to reaction products not detectable by the used analytical techniques. However, the low production level of mono- and dihydroxylated DHEC species is currently not high enough to obtain sufficient amounts for further structural elucidation. Yet, it would be conceivable to use EC in combination with Fenton-like reaction for the fast and affordable elucidation of other ergot alkaloids.

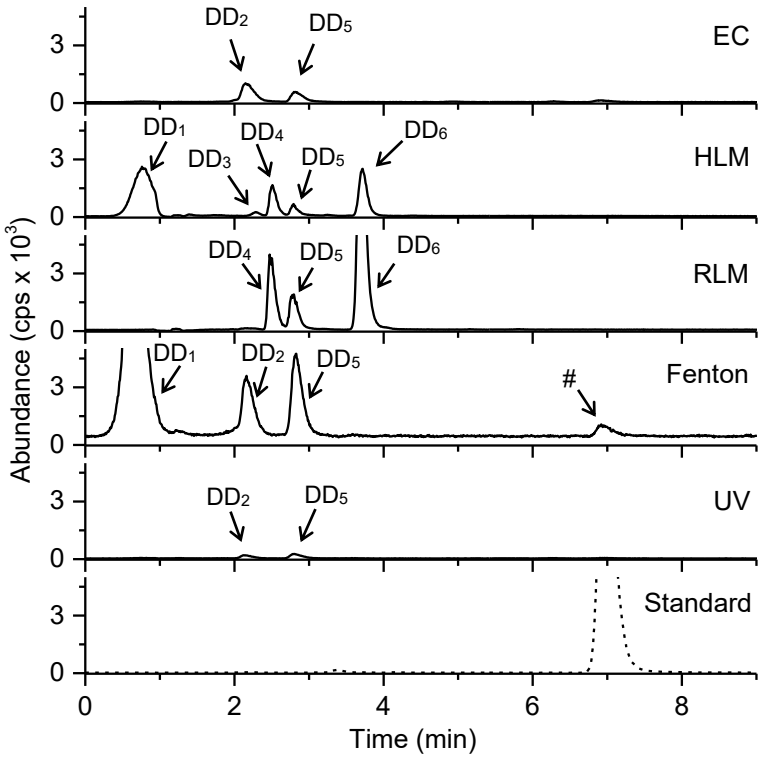


Figure 9. HPLC-MS/MS chromatograms of dihydroxylated DHEC after electrochemical oxidation (EC 1700 mV), human liver (HLM) and rat liver microsomal (RLM) incubation, Fenton-like reaction with $Fe^{3+}/H_2O_2$ (Fenton) and UV irradiation (UV) by using multiple ion scan with *m*/*z* 644 in positive ionization mode. The control sample (Standard; *m*/*z* 612) indicates DHEC without treatment. Peaks with *m*/*z* 644 occurred also in control and are marked with #

*Benefits and drawbacks of electrochemistry:*

EC coupled with ESI-MS provides a fast and affordable alternative in the investigation of mycotoxin metabolites without any biological matrices and a broad

reaction spectrum. Applying EC/ESI-MS in an early stage of metabolic studies may lead to a more efficient and economic procedure in mycotoxin research. Within this study, it has been shown that EC/ESI-MS provided a fast insight into the oxidation behavior of mycotoxins, but was not able to simulate all phase I products which have been found when performing microsomal experiments. Even if EC methods can be improved to a certain point by adjusting technical parameters like working electrode material, solvent or pH, the success of an electrochemical reaction is significantly influenced by the structural characteristics of the tested compound itself.

## 2.1.5 CONCLUSIONS

In this study, three different non-microsomal methods (EC, Fenton-like, and UV) were investigated to simulate oxidative phase I metabolism of selected mycotoxins and compared to results of *in vitro* assays. The electrochemical (EC) conversion method coupled online with ESI-MS proved as a fast and sensitive alternative method. More suitable for the simulation of phase I metabolites was the Fenton-like reaction. However, UV irradiation turned out to be impractical for phase I simulation of the two chosen mycotoxins. EC and Fenton offered the option of generating several oxidation products and in the case of EC it is possible to upscale the production quantities by using batch cells. Using the suitable equipment, conjugation experiments can be easily performed to mimic phase II reactions, which is also of major importance concerning the biotransformation of mycotoxins in living organisms. Furthermore, the system can reduce substances by applying a negative potential which highlights the wide range of electrochemical application in future mycotoxin research.

## 2.1.6 ACKNOWLEDGEMENT

The authors would like to thank Mr. Boris Neumann (Proteome Factory AG, Berlin, Germany) for the HRMS analyses.

# LICENSE

# 2.2 Hydroxylation and dimerization of zearalenone: Comparison of chemical, enzymatic and electrochemical oxidation methods

J. Keller, H. Haase, M. Koch*

Originally published in **World Mycotoxin Journal**
10(4): 297-307 (2017)
https://doi.org/10.3920/WMJ2017.2213


J. Keller, M. Koch
*Bundesanstalt für Materialforschung und -prüfung (BAM), Richard-Willstätter-Straße 11, 12489, Berlin, Germany. E-mail: Matthias.koch@bam.de*

H. Haase
*Berlin Institute of Technology, Gustav-Meyer-Allee 25, D-13355 Berlin, Germany. E-mail: Haase@TU-Berlin.de*
* *Corresponding author*

## 2.2.1 ABSTRACT

Investigations of the metabolic pathway of mycotoxins by microsomal techniques are often laborious, causing an increasing demand for easy and rapid simulation methods. Thus, the non-microsomal oxidation technique of electrochemistry coupled online to mass spectrometry (EC/MS) was applied to simulate phase I biotransformation of the *Fusarium* mycotoxin zearalenone (ZEN). The obtained transformation products were identified by high resolution mass spectrometry (FT-ICR) and HPLC-MS/MS. Transformation products (TPs) from EC/MS were compared to those of other oxidative methods such as Fenton-like and Ce(IV) reactions and metabolites derived from *in vitro* assays (human and rat liver microsomes). Electrochemical oxidization of ZEN was achieved by applying a potential between 0 and 2,500 mV vs. Pd/$H_2$ using a flow-through cell with a boron-doped diamond

working electrode. Several mono-hydroxylated TPs were generated by EC/MS and Fenton-like reaction, which could also be found in microsomal *in vitro* assays. EC and Ce(IV) led to the formation of structurally different ZEN dimers and dimeric quinones probably connected over covalent biaryl C-C and C-O-C bonds. Although the dimerization of phenolic compounds is often observed in natural processes, ZEN dimers have not yet been reported. This is the first report on the formation of stable ZEN dimers and their related quinones. The tested non-microsomal methods, in particular EC/MS, could be useful in order to predict the biotransformation products of mycotoxins, even in cases where one to one simulation is not always feasible.

## 2.2.2 INTRODUCTION

Zearalenone (ZEN) is produced by field fungi of the genus *Fusarium* that grow on grain cereals like maize and wheat [23]. As nonsteroidal estrogenic mycotoxin, ZEN causes various endocrine-disruptive effects related to its chemical structure consisting of a macrocyclic β-resorcyclic acid lactone [124]. Furthermore, it was shown to be hematotoxic, genotoxic, immunotoxic, hepatotoxic and carcinogenic [22]. Due to its worldwide occurrence in food and feed, maximum levels have been set by the European Commission. Because exposure of ZEN is almost inevitable, the understanding of harmful effects is crucial to secure food safety and protect consumer's health. During the metabolic phase I biotransformation ZEN is oxidized or reduced by cytochrome P450 enzymes, which have been identified in all kingdoms of life including animals, plants, fungi and bacteria [125]. Microsomal P450 systems transfer electrons from the cofactor NADPH via CYP450 reductase. This two-electron reaction causes oxidation of the organic substrate by simultaneous production of water [75]. ZEN was metabolized in cultured hepatocytes of pig, mouse and cattle to its reduced metabolites $\alpha$- and β-zearalenol and subsequently conjugated with glucuronic acid during phase II biotransformation [126, 127]. Besides reduction during phase I metabolism ZEN may undergo oxidation to monohydroxylated metabolites, discovered by using human and rat *in vitro* assays [128, 129] and in rat urine *in vivo* [63]. The preferred site for enzyme-catalyzed hydroxylation depends on the species and may be located either at the aromatic ring or the aliphatic macrocycle [130]. Phase I metabolites are also known to carry toxicological activities and are thereby of great interest for further investigations, mainly by using *in vitro* and *in vivo* approaches [113]. In contrast to these existing established techniques, the need for faster and cheaper alternative methods has been on the increase for years. One of the

most promising techniques is electrochemistry coupled to mass spectrometry (EC/MS), which is successfully used especially in drug and pharmaceutical research for the oxidation/reduction of substances without interfering matrices. Electrochemical oxidation is mediated by hydroxyl (OH•) radicals that are formed at the working electrode surface and is initiated through a one-electron loss of water [83]. EC offers a broad reaction spectrum like hydroxylation, dehydrogenation, dealkylation or dimerization [85, 131]. By using cyclic voltammetry Nasir and Pumera showed that ZEN is oxidized at a potential of 1.15 V vs. Ag/AgCl and was not reduced during reverse scan [132]. However, other studies focused mainly on detection of ZEN by using electrochemical detection techniques [133, 134]. Besides EC, classical non-microsomal methods are established for the oxidation of organic compounds: Fenton-like oxidation ($Fe^{3+}/H_2O_2$) is described as a method to destruct harmful organic pollutants in wastewater [90] but can be also used, in principle, as an oxidation method to generate transformation products (TPs). Chemical oxidation is achieved as well by using aqueous Ce(IV) solutions which are known for addition reactions of radicals to alkenes leading to carbon-carbon bonds (C-C) as well as carbon-heteroatom bonds. One case study dealt with the redox behavior of ZEN and used Ce(IV) and $H_2SO_4$ as powerful oxidant for the total destruction of the molecule at room temperature in the dark [104].

While data on the oxidative ZEN metabolism has already been achieved, a comparative study including both microsomal and non-microsomal techniques for ZEA is currently not available. Thus, the aim of the present study was to investigate the potential of non-microsomal methods, in particular, the online EC/MS system, to simulate phase I metabolism of ZEN and compare the results to those obtained by well-established microsomal *in vitro* assays. This study presents new possibilities to obtain phase I TPs and highlights the benefits and limits of EC/MS in mycotoxin research.

## 2.2.3 MATERIAL AND METHODS

*Chemicals*

Zearalenone (purity 98%) was purchased from Santa Cruz Biotechnology Inc. (Santa Cruz, CA). $FeCl_3 \cdot 6\ H_2O$ and $KH_2PO_4$ were obtained from Merck (Darmstadt, Germany) and $K_2HPO_4$ from Carl Roth (Karlsruhe, Germany). NADPH tetrasodium

salt was purchased from AppliChem GmbH (Darmstadt, Germany). Cerium(IV)sulfate and aqueous $H_2O_2$ (30%) were obtained from Sigma-Aldrich (Steinheim, Germany). Ultrapure water was produced by a Seralpur PRO 90 CN system (Ransbach-Baumbach, Germany). All standard chemicals were of p.a. grade, and all solvents, HPLC grade.

*Microsomal sources*

Human and rat liver microsomes (HLM and RLM) were purchased from Thermo Fisher *Scientific* (Pittsburgh, PA, US). RLM were prepared from Sprague-Dawley male rats. The protein concentration of 20 mg/mL and a CYP450 content of 319 pmol/mg protein was provided by the manufacturer. HLM were derived from a male-gender pool of 20 donors with a CYP450 content of 170 pmol/mg protein and a protein concentration of 20 mg/mL.

*Microsomal incubations*

Incubations with either HLM or RLM were carried out in a volume of 200 µL. The mixture contained 5 µM ZEN (2 µL) dissolved in acetonitrile (ACN), microsomes (10 µL), 0.1 mM $MgCl_2$ (20 µL) and 0.1 M potassium phosphate buffer (148 µL), pH 7.4. After preincubation for 5 minutes at 37°C, 20 µL of NADPH (6 mM) was added to the mixture to start the enzymatic reaction. After 90 min incubation at 37°C and 800 rpm the reaction was stopped by adding 150 µL of ice-cold ACN. The samples were mixed thoroughly for 20 seconds and centrifuged at 11,650g for 5 minutes to allow the precipitated proteins to settle on the ground. The supernatant was analyzed by HPLC-MS/MS. Reactions were performed in triplicate and control incubations were performed in duplicate without the co-factor NADPH.

*Online EC/ESI-MS*

ZEN was electrochemically oxidized by using an electrochemical flow-through cell (µPrepCell, Antec Leyden, Zoeterwoude, Netherlands) coupled to an electrospray

ionization source of a single quadrupole mass spectrometer (Agilent Technologies GmbH, Böblingen, Germany), shown in Figure 10. ZEN was dissolved in ACN and then further diluted with ammonium acetate (20 mM) and ACN (50/50, *v*/*v*) to a final concentration of 100 µM and was pumped through the µPrepCell by using a SP2 - ROXY dual piston syringe pump (Antec Leyden) and a flow rate of 80 µL/min. The µPrepCell was equipped with a boron-doped diamond (BDD) working electrode material, an auxiliary electrode consisting of a fully inert polymeric material containing conductive carbon and a $Pd/H_2$ reference electrode. The working and auxiliary electrodes were separated by two 100-µm spacers. A potentiostat (Antec Leyden) was used to apply a potential ramped between 0 and 2,500 mV versus $Pd/H_2$ (scan rate of 20 mV/s) in continuous scanning mode. Before starting the measurement, the working electrode was activated by using the pulse cleaning program provided by the manufacturer (50 µL/min solvent without analyte; potential be held for 100 ms at $E_1$=2V, $E_2$=-2V and $E_3$=0V, respectively for 5 min). Ionization of the electrochemically-generated TPs was achieved with nitrogen drying gas (12 L/min, 35 psi nebulizer pressure) of 350°C and 3,000 V on the capillary inlet. The ESI-MS was operated in positive ion mode and the scan range used was *m*/*z* = 100-700 with a threshold set to 2,000 counts/s. Each scan was recorded at least three times to ensure the reproducibility of the measurements. Aliquots were also collected from the electrochemical cell into HPLC vials offline and were used for HPLC-MS/MS and ESI-HRMS measurements by using the direct current mode with a constant potential of 1,200 mV vs. $Pd/H_2$.

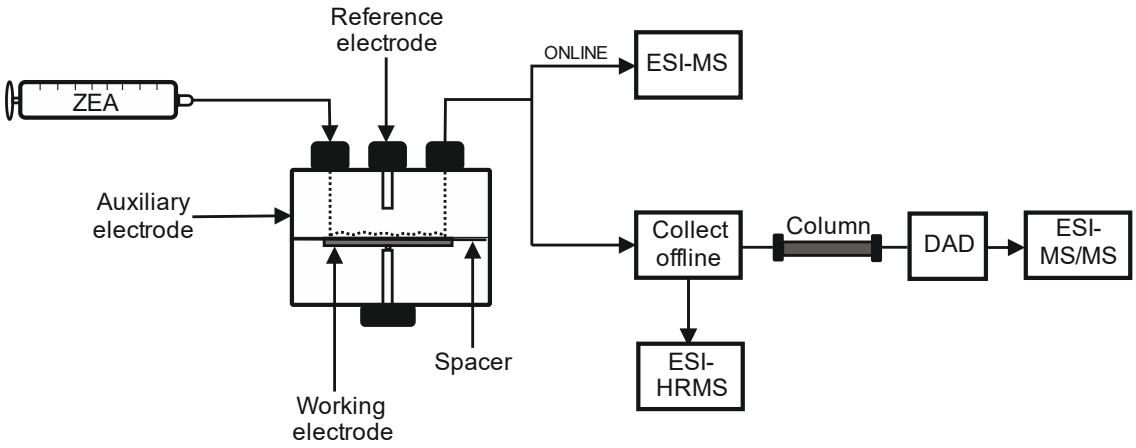


Figure 10. Instrumental set-up of electrochemical flow through cell and subsequent analysis tools.

*Fenton-like reaction*

The Fenton-like reaction ($Fe^{3+}/H_2O_2$) was carried out in a volume of 1 mL containing 100 µM of ZEN dissolved in ACN, 5 µM ferric (III) chloride and 100 µM of $H_2O_2$. The reaction proceeded at 30°C and 800 rpm in a thermoshaker and was stopped after different time points (t = 1, 3, 5, 7, 15 and 30 minutes) by adding a spatula tip full of manganese dioxide. Data presented within this study are from samples incubated for 15 minutes, due to the highest amount of TPs. For further HPLC-MS/MS analysis, samples were centrifuged (11,650g for 2 minutes) and the supernatant was used as it is. Control samples containing ZEN and manganese dioxide were performed in duplicate, all other reactions were performed in triplicate.

*Oxidation with Ce(IV)*

The reaction was carried out in a volume of 1 mL containing 100 µM of ZEN and 100 µM Ce(IV) dissolved in water ($H_2O$/ACN, 50/50, *v*/*v*). The samples were shaken in a thermoshaker for 30 min at 50°C using 800 rpm. For HPLC-DAD measurements the samples were used as they are. For HPLC-MS/MS analysis the samples were diluted to a final concentration of 10 µM with $H_2O$/ACN (50/50, *v*/*v*). Control samples containing only Ce(IV) or only ZEN in $H_2O$/ACN (50/50, *v*/*v*) were tested in duplicate and all other reactions were performed in triplicate.

*HPLC-DAD*

TPs of ZEN were analyzed by HPLC-DAD using an Agilent 1200 series HPLC (Agilent Technologies GmbH, Böblingen, Germany) consisting of an auto sampler, degasser, binary pump, column oven and diode array detector (DAD). The analytical column was a Gemini® NX-C18, particle size 3 µm, pore size 110 Å, 150 x 2 mm (Phenomenex, Torrance, CA) and the column oven was set to 40°C. For the separation of ZEN and its oxidation products a mobile phase consisting of $H_2O$ with 0.1 % formic acid (A) and ACN with 0.1 % formic acid (B) was used. The gradient used was as follows: 0-1 min 35% B, 1-30 min 35-90% B, 30-31 min 90-35% B and 31-35 min 35% B. The flow rate of the mobile phase was 250 µL/min and the injection volume was 20

μL. To determine the UV/VIS spectra of the TPs a DAD scan was performed in the range of $\lambda$ = 190–700 nm.

*HPLC-MS/MS*

Analyses were performed using the same instrument and conditions as described above. After the DAD, an API 4000 mass spectrometer (AB Sciex, MA) was coupled, operated in multiple reaction monitoring (MRM) mode with negative electrospray ionization (ESI). The following ion source parameters were used to analyze hydroxylated ZEN species: ion spray voltage, -4000 V; desolvation temperature, 450°C; ion source gas 1, 60 arbitrary units (a.u.); ion source gas 2, 20 a.u.; curtain gas, 20 a.u. The MRM compound-specific parameters were the following: declustering potential -65 V; entrance potential -10 V; collision energy -40 V; collision cell exit potential -9 V. The ion source and MRM compound-specific parameter for the dimeric species of ZEN were as follows: – 4500 V/450°C/40 a.u./30 a.u./14 a.u./-60 V/-8 V/-30 V/-6 V. For native ZEN the monitored transitions were (*m*/*z*) 317→131, for OH-ZEA 333→289 and 333→175 and for dimeric ZEN species 631→587, 631→473, 633→589, 633→565 and 633→315.

*High-resolution mass spectrometry (HRMS)*

Measurements were performed by using a hybrid linear quadrupole ion trap (LTQ) Fourier transform ion cyclotron resonance (FT-ICR) mass spectrometer (Thermo Finnigan Corp., Bremen Germany) with a magnetic field force of 7 Tesla. Samples were diluted with MeOH (0.1% formic acid) to a final concentration of 10 μM and pipetted into a static nano-ESI emitter. The ion spray voltage was set to 1,500 V and the detection was achieved by a Fourier transform mass spectrometry (FTMS) analyzer. Data were acquired in the negative and positive ionization mode within a range of *m*/*z* 100 to 800. The resolving power was set to 100,000 at *m*/*z* 400. Determination of the elemental composition of individual TPs was based on accurate masses, typically better than 5 ppm mass accuracy.

## 2.2.4 RESULTS AND DISCUSSION

The present study was dedicated to the investigation of the phase I metabolism of ZEN by performing different oxidative methods. Focus was on online EC/ESI-MS as a versatile technique for a fast prediction of metabolic pathways by elucidating biotransformation products.

*Online EC/ESI-MS*

One full scan cycle beginning at 0 mV and rising to 2,500 mV and back to 0 mV is shown in Figure 11. By applying the increasing oxidation potential signal, the intensity of ZEN (*m*/*z* 319) decreased eightfold within one minute. In parallel, several new signals could be recorded. In case of the traces with *m*/*z* 333, *m*/*z* 631, *m*/*z* 633 and *m*/*z* 635 a signal maximum at 5.4 min is observed at a potential of 1.1 to 1.2 V vs. Pd/$H_2$ matches the results from former studies [132]. This suggests that these three TPs are likely generated by direct electrochemical oxidation while the other observed TPs are formed by OH radicals at high potentials. The exact masses of numerous EC-derived TPs as well as the corresponding modifications of ZEN are listed in Table 6.

Table 6. HRMS data of EC-generated oxidation products of ZEN with the corresponding exact masses and deviations of protonated (ESI(+)) and deprotonated (ESI(-)) species

| **Molecular formula** | **calculated (*m*/*z*)** | **determined (*m*/*z*)** | **δm/m (ppm)** | **Suggested modification** |
|---|---|---|---|---|
| | | **ESI (+)** | | |
| **$C_{18}H_{23}O_5$** | 319.1545 | 319.1545 | 0.0 | - |
| **$C_{17}H_{23}O_4$** | 291.1596 | 291.1597 | 0.3 | +O, -$CO_2$ |
| **$C_{17}H_{25}O_4$** | 293.1753 | 293.1749 | -1.4 | +O, -$CO_2$, +2H |
| **$C_{17}H_{21}O_6$** | 321.1338 | 321.1333 | -1.6 | -$CH_2$, +O |
| **$C_{18}H_{21}O_6$** | 333.1338 | 333.1338 | 0.0 | +O, –2H |
| **$C_{18}H_{23}O_6$** | 335.1494 | 335.1495 | 0.3 | +O |
| **$C_{18}H_{25}O_6$** | 337.1651 | 337.1649 | -0.6 | +O, +2H |
| | | **ESI (-)** | | |
| **$C_{36}H_{39}O_{10}$** | 631.2543 | 631.2535 | -1.3 | Dimerization (i.e. -2H), –2H |
| **$C_{36}H_{41}O_{10}$** | 633.2700 | 633.2702 | 0.3 | Dimerization (i.e. -2H) |

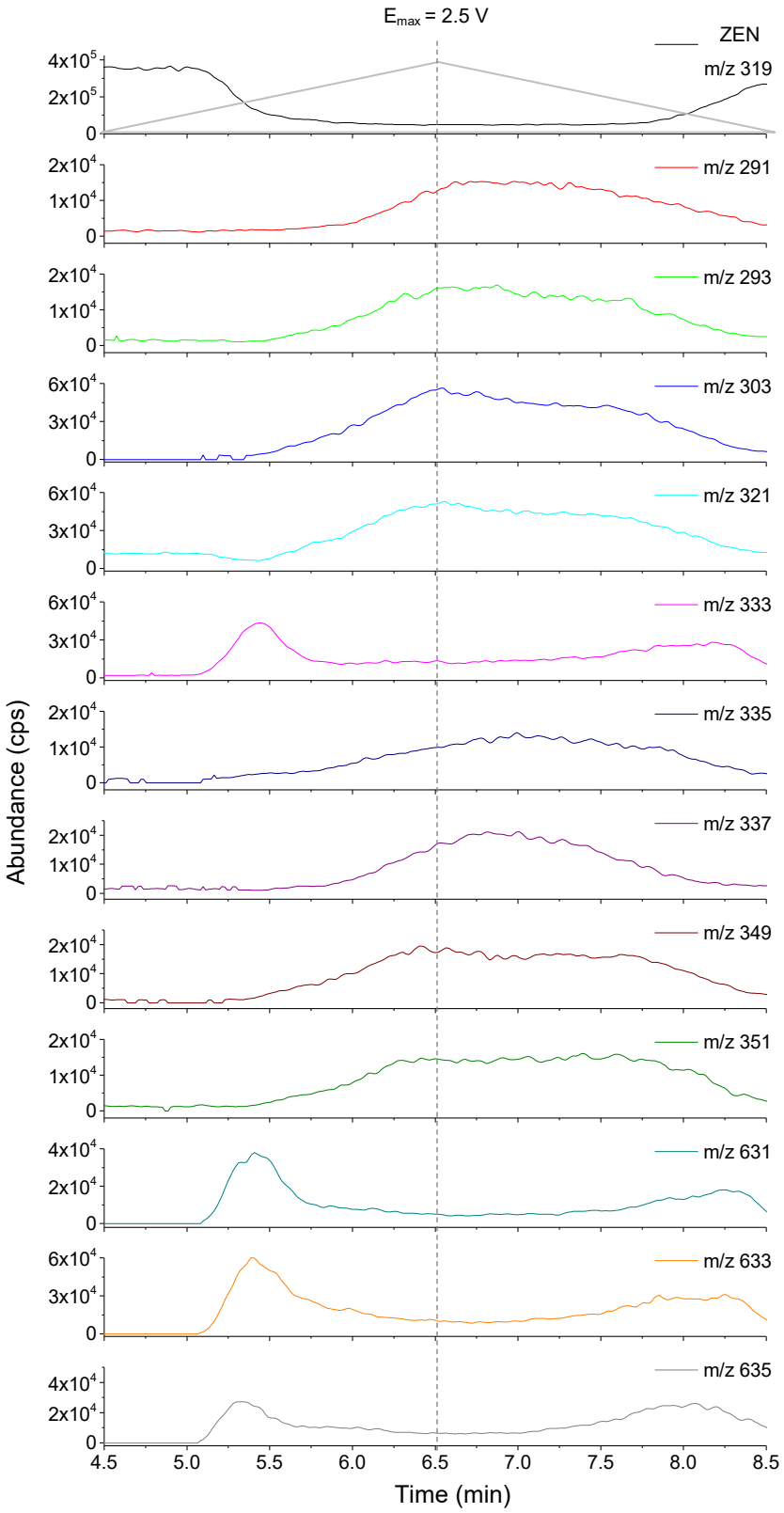


Figure 11. Ion/mass traces (ESI(+)) of ZEN and its oxidation products at increasing oxidation potentials. The full scan range from 0 to 2,500 mV vs Pd/$H_2$ is marked by the grey triangle (dashed line marks the potential maximum ($E_{max}$)).

The signal of *m/z* 335 is caused by the addition of one oxygen leading to the hydroxylation of ZEN. Hydroxylation of electron-rich systems like substituted aromatics are often observed as typical electrochemical reaction [79]. In case of ZEN mono-hydroxylation can principally be located at different aromatic and aliphatic positions. Hydroxylation of the aromatic ring would lead to the formation of a trihydroxybenzene moiety during a two-proton/two-electron process resulting in the formation of a quinone species at *m/z* 333 [135]. Furthermore, hydroxylation at the aliphatic position with subsequent dehydrogenation would lead to a ketone function. Due to the C14/C16 position of the two aromatic hydroxy groups of ZEN, a direct dehydrogenation leading to the formation of an electrophilic quinoid structure is not possible (for atom numbers see Figure 14). This allows the conclusion that a hydroxylation of the aromatic ring system takes place at first, introducing a hydroxy group at C13 or C15 position, followed by a further activation of the system and quickly leading to the formation of a quinoid structure. This is of high interest because of the very few data collected concerning the production and metabolic fate of quinoid ZEN species. It is known from the steroidal estrogens 17β-estradiol and estrone that they cause uterus, breast and prostate cancer by causing oxidative DNA damage due to the formation of reactive quinone species [136].
EC also generates oxidation products which cannot be formed by using *in vitro* or *in vivo* techniques and are very likely new TPs like an EC-product with *m/z* 321 which corresponds to a formal loss of $CH_2$ according to the obtained HRMS data in Table 7 and the addition of one oxygen atom. One out of these newly and, to the best of our knowledge, not described TPs are dimers of ZEN represented by a signal *m/z* 633 and *m/z* 635 in ESI(+) mode (Figure 11). Further elucidation of these new TPs is shown and discussed in the corresponding section Dimers of ZEN. Apart from the already presented ZEN-TPs resulting from electrochemical reaction there are yet several unidentified EC-products where no structural proposal can be drawn. Elucidation of structure remains unclear due to multiple reaction sides of the molecule. This also includes the signals with *m/z* 303, 349 and 351, which were unidentified together with TPs not shown in the data due to limited quantities.

*Hydroxylated ZEN*

In this comparative study including EC, Fenton-like reaction and liver cell microsomes about (at least) 18 different OH-ZEN peaks were detected. The distinct product patterns of the tested systems are shown in a combined HPLC-MS/MS

chromatogram (Figure 12). MRM(-) transitions of OH-ZEN derivatives were chosen from [85] and performed product ion scans by HPLC-MS/MS. The mass transition m/z 333→289 of OH-ZEN results from the loss of $CO_2$. All known OH-ZEN species have this fragment in common independent of their hydroxylation site. While this typical fragment is unaffected by the position of hydroxylation, the MRM transition m/z 333→175 is dependent on the hydroxylation site and resulted in a loss of C2 to C10 position followed by the formation of a new ring, containing C11 and C12 position from the former macro cyclic ring system (for atom numbers see Figure 14). This transition indicates the formation of hydroxylated ZEN at position C2 to C10 position which gets lost during fragmentation. Three hydroxylated ZEN species (during EC-ESI/MS detected as *m*/*z* 335 in positive ionization mode), were found by HPLC-MS/MS after electrochemical reaction. Reaction product $P_{15}$ with the highest signal intensity and $P_{18}$ were hydroxylated at the macrocyclic ring between C2′ and C10′position. The formation of OH-ZEN by microsomal incubation had to be expected due to former studies which have been performed [128, 129]. These results were reproduced within this work to have the direct comparison to the tested new oxidation techniques. Fenton-like reaction can be used to hydroxylate aromatic hydrocarbons by generating hydroxyl radicals, which abstract one hydrogen and induce the hydroxy group [137]. In this study, Fenton-like oxidation led to 11 hydroxylated species in total with 7 matches compared to the classically performed *in vitro* approach with human and rat liver microsomes shown in Figure 12.

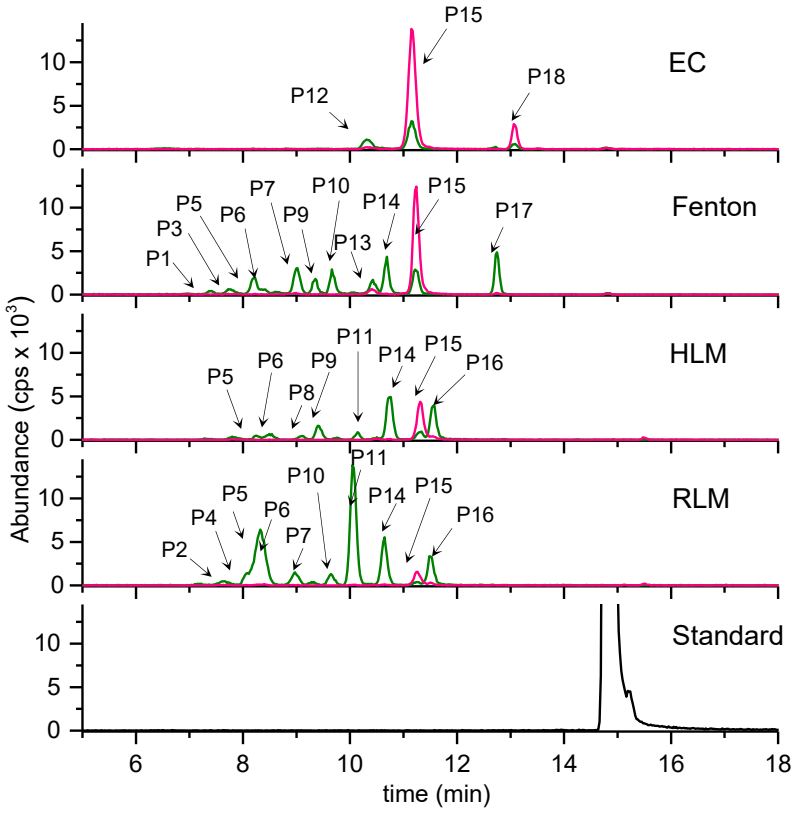


Figure 12. HPLC-MS/MS chromatograms MRM(-) of hydroxylated ZEN after electrochemical oxidation (EC 1,200 mV vs Pd/$H_2$), Fenton-like reaction with $Fe^{3+}/H_2O_2$ (Fenton), human liver (HLM) and rat liver (RLM) incubation by using mass transitions *m/z* 333→289 (green) and 333→175 (pink). The control sample (ZEA standard; *m/z* 317→131) indicates ZEN without treatment (black).

## Dimers of ZEN

*Oxidative production of dimeric ZEN derivatives*

Oxidation of ZEN by EC and Ce(IV) revealed several TPs. HPLC-MS analysis via Q1 scan showed that all the detected TPs had a signal with *m/z* 633 and *m/z* 631 in ESI negative mode and *m/z* 635 and m/z 633 in ESI positive mode. HRMS analyses of the offline-collected EC/MS aliquots (oxidation at a potential of 1,200 mV vs Pd/$H_2$) revealed a sum formula of dimers with $C_{36}H_{42}O_{10}$, as well as quinoid dimeric species

with $C_{36}H_{40}O_{10}$ shown in Table 7. The proceeded product ion scan performed in ESI (-) mode showed that all detected dimers as well as dimer quinones have one prominent fragmentation in common (Table 7). The transition detected for the dimeric ZEA derivatives are *m/z* 633→589 and *m/z* 631→587 for quinoid forms caused by the loss of carbon dioxide (- 44 amu) during fragmentation. This fragmentation is also found in the case of ZEN leading to a fragment with *m/z* 273.

The product pattern resulting from EC and Ce(IV) oxidation treatment of ZEN is nearly identical in the case of mass transition *m/z* 633→589 and about 10 TPs (ZEN dimers) were detected by HPLC-MS/MS (Figure 13, top) and HPLC-DAD (Figure 16). EC offers a wide range of reactions and especially dehydrogenation, leading to quinones which have been readily mimicked several times in drug and pharmaceutical research [83]. This could be observed in the present study, where EC probably led to the production of eight quinoid ZEN dimers (Figure 13, bottom). In contrast, Ce(IV) was not able to form dimeric quinones. This is surprising due to the fact that Ce(IV) is known for reactions promoting the formation of quinones [138].

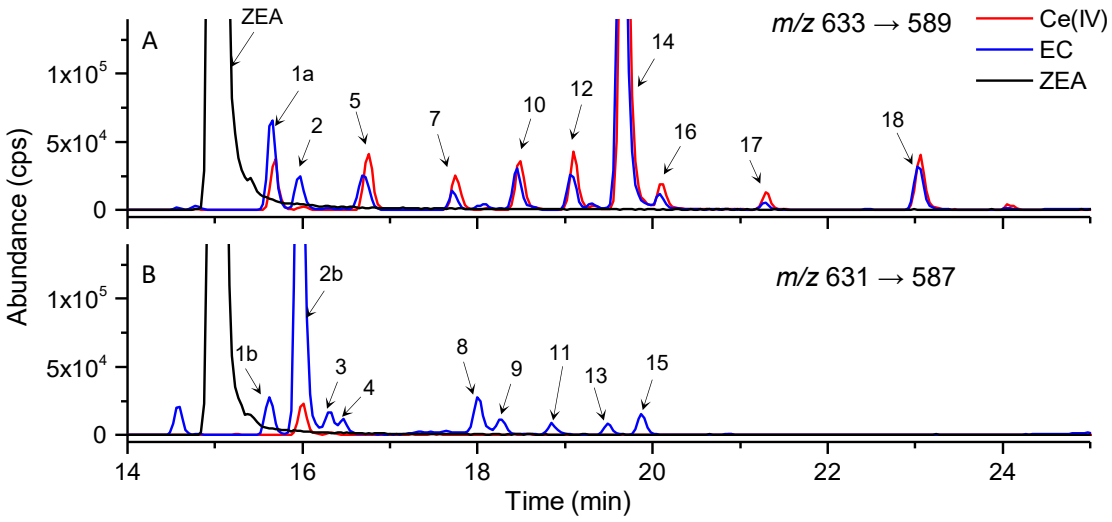


Figure 13. HPLC-MS/MS chromatograms (ESI(-)) of ZEN (black; *m/z* 317→131) and ZEN dimerization products after electrochemical treatment using 1,200 mV vs Pd/$H_2$ (blue) and oxidation by Ce(IV) (red). Top) ZEN dimers (*m/z* 633→589); Bottom) ZEN dimer quinones (*m/z* 631→587). Peak numbers are related to the listed data in Table 7.

Table 7. Adjusted retention time ($t_R'$), mass fragments and UV maxima of ZEN, its dimers and dimer quinones after oxidation by EC and Ce(IV) analyzed by HPLC-MS/MS

| TP | ESI(-) (*m*/*z*) | HPLC-MS/MS $t_R'$ (min) | UV maxima (nm) | Mass fragments (*m*/*z*) | Formed by |
|---|---|---|---|---|---|
| **ZEN** | 317 | 13.85 | 236, 274, 316 | 175, 273, 149, 161 | - |
| **1a** | 631 | 14.45 | 218, 258, 308 | 587, 445, 563 | EC |
| **1b** | 633 | 14.48 | 218, 258, 308 | 589, 565, 447 | EC, Ce(IV) |
| **2a** | 633 | 14.77 | 234, 268, 308 | 589 | EC, Ce(IV) |
| **2b** | 631 | 14.80 | 234, 268, 308 | 587 | EC |
| **3** | 631 | 15.12 | 234, 270, 306 | 587 | EC |
| **4** | 631 | 15.31 | 218, 266 | 587, 473, 445 | EC |
| **5** | 633 | 15.51 | 234, 322 | 589, 615, 577, 491 | Ce(IV), EC |
| **6** | n. d. | n. d. | 258, 292 | n. d. | EC |
| **7** | 633 | 16.54 | 234, 318 | 589, 357 | Ce(IV), EC |
| **8** | 631 | 16.82 | 224, 250, 290, 400 | 587 | EC |
| **9** | 631 | 17.11 | 224,266, 306 | 587, 473, 603, 447 | EC |
| **10** | 633 | 17.28 | 242, 274, 320 | 589, 357 | Ce(IV), EC |
| **11** | 631 | 17.67 | 254, 380, 496 | 587, 543, 445, 427 | EC |
| **12** | 633 | 17.89 | 244, 318 | 589 | Ce(IV), EC |
| **13** | 631 | 18.31 | 222, 262, 308 | 587 | EC |
| **14** | 633 | 18.49 | 234, 270, 314 | 589, 565, 605, 317 | Ce(IV), EC |
| **15** | 631 | 18.70 | 232, 282 | 587, 543, 563, 419 | EC |
| **16** | 633 | 18.91 | 246, 278, 322 | 589 | Ce(IV), EC |
| **17** | 633 | 20.12 | n. d. | 589 | Ce(IV), EC |
| **18** | 633 | 21.85 | 236, 270, 316 | 315, 589, 615, 491 | Ce(IV), EC |
| **19** | n. d. | n. d. | 250, 340 | n. d. | Ce(IV), EC |

In this study, three different molar ratios of ZEN to Ce(IV) were tested (Figure 21) to investigate the formation of TPs. However, the only quinoid product (product 2b) was obtained in low yields. The Fenton-like reaction ($Fe^{3+}/H_2O_2$) as well as microsomal incubations did not lead to ZEN dimers nor to quinoid dimers. It can be deduced that both techniques are too mild to produce dimers in comparison to oxidation by EC and Ce(IV). Dimers and dimer quinones still obtain UV absorption properties, so they can be easily analyzed by DAD detection after chromatographic separation. The UV maxima (Table 7) and spectra (Figures 17-20) of the TPs can be clearly distinguished from the UV spectrum of ZEN. Dimerization at different positions of the molecule lead to diverse UV spectra and in the case of six TPs (5,8,10,11,16 and 19) a bathochromic shift to longer wavelengths, probably due to the influence of the dimerization reaction, is observed. Because of the multiple ways of linkage between two ZEN molecules and low production yields, no further conclusion can be drawn at this point from the UV spectra but may be used together with retention time as specific characteristics for subsequent investigations.

*Structural elucidation of dimeric ZEN derivatives*

The obtained results for dimeric ZEN compounds (Figure 13) have shown, that there is a variety of possible ways in which monomeric ZEN can combine and yield dimers. The most common forms found in nature are a biaryl C-C bond or a biaryl ether C-O-C linkage. Especially in plants, bacteria, lichen and fungi regio- and stereo-selective biaryl linkages of phenolic compounds are known [139]. Dimers of mycotoxins are rare and the fungal red/yellow pigment aurofusarin is one of the very few examples [140] as well as the cytotoxic citrinin dimer, dicitrinin A [121]. Xanthone dimers, which are linked by biaryl bonding, are more prominent and well researched. The dimerization is mainly enzymatically-mediated but is probably induced as well by reaction with intracellular reactive oxygen species [141]. In the absence of structurally-influencing factors like enzymes the substrate dictates the available coupling products and a variety of compounds may result as shown for the ZEN dimers. Based on the detected peaks for ZEN dimers and ZEN dimer quinones (Figure 13) the number of the latter derivatives is rather limited. This could be explained by the proposed reaction mechanism for ZEN dimer quinones displayed in Figure 15. Although little is known from literature about quinoid dimeric species, e.g. perylene-quinones were found to be metabolized via dimerization of achiral naphtols [142]. In this context, it is surprising that nine *m*/*z* 631 species were found. Whether all of these species are quinones should be clarified in further studies by

structural elucidation. However, it is conceivable that ZEN dimers are metabolized during fungal metabolism and are further oxidized to their quinoid dimeric form.

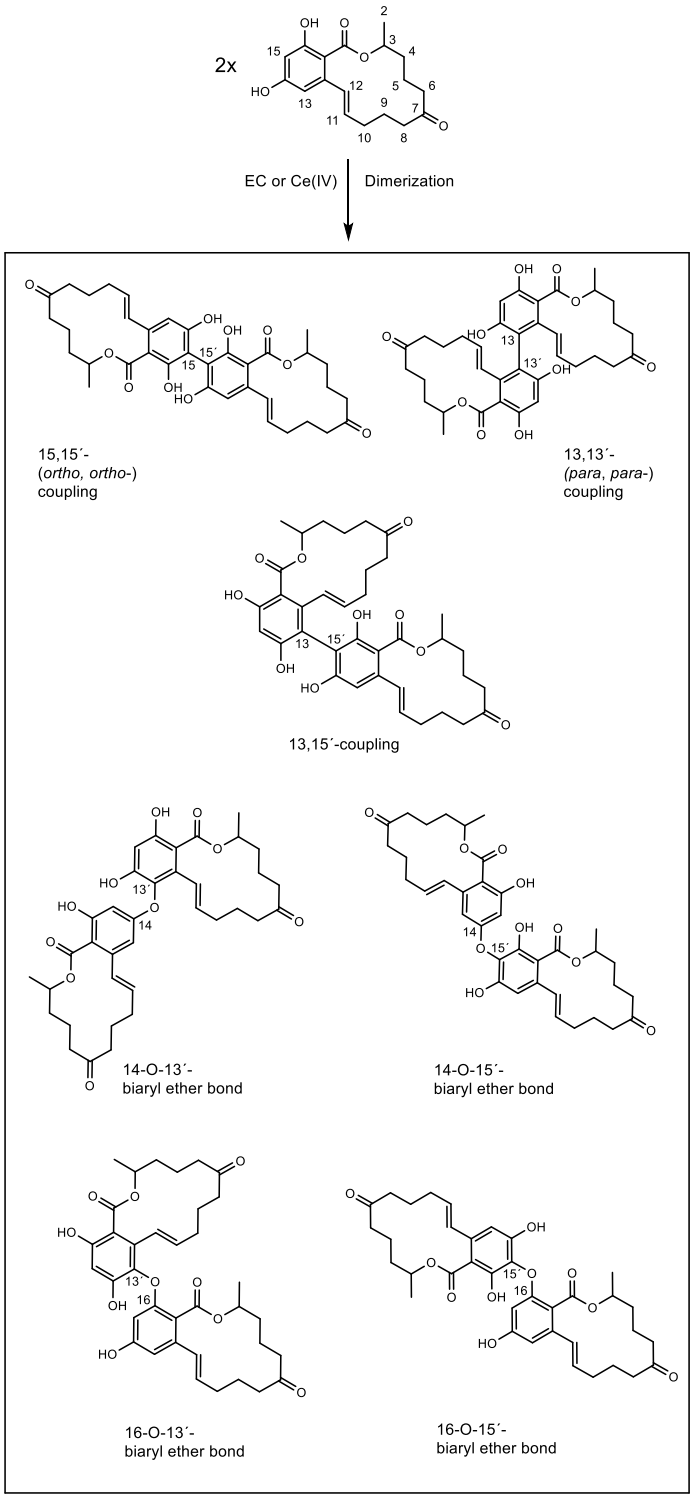


Figure 14. Postulated structures of ZEN dimers with C-C and C-O-C biaryl bonds after oxidative electrochemical treatment or oxidation by Ce(IV).

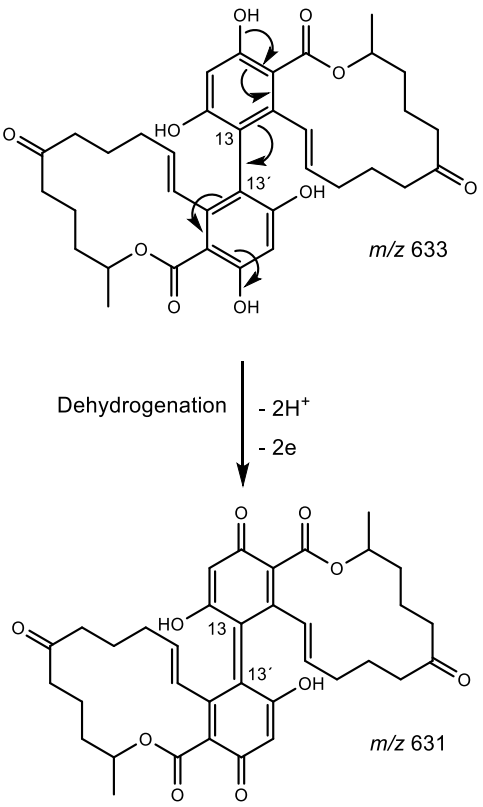


Figure 15. Postulated formation of 13,13′ ZEN dimer quinone after electrochemical treatment. Displayed masses (*m*/*z*) obtained in ESI(-) mode of HPLC-MS.

## 2.2.5 CONCLUSION

The results from using the non-microsomal oxidation techniques EC, Fenton-like reaction and Ce(IV) oxidation were compared with results obtained from *in vitro* assays. Several hydroxylated TPs found by Fenton-like reaction and EC are similar to biotransformation products of ZEN. These two systems could be easily applied in mycotoxin research to support metabolic investigations of new compounds. Additionally, EC offers the possibility of upscaling reaction product quantities, which is very useful due to the lack of available standards. One of the most interesting results of this study is to show that EC and Ce(IV) oxidation led to the formation of covalent dimeric ZEN derivatives, either with C-C or C-O-C biaryl bonds. Moreover, dimer quinones were detected as further oxidation products of the ZEN dimers. Performed product confirmation by applying high resolution mass spectrometry and investigating fragmentation pattern is the first essential step, but further structural

elucidation of dimeric ZEN compounds is necessary. Additionally, real samples should be analyzed for dimeric forms of ZEN because dimers of phenolic compounds might not be uncommon in nature.

## 2.2.6 ACKNOWLEDGEMENT

The authors would like to thank Mr. Boris Neumann (Proteome Factory AG, Berlin, Germany) for the HRMS analyses.

## LICENSE



## 2.2.7 SUPPLEMENTARY MATERIALS

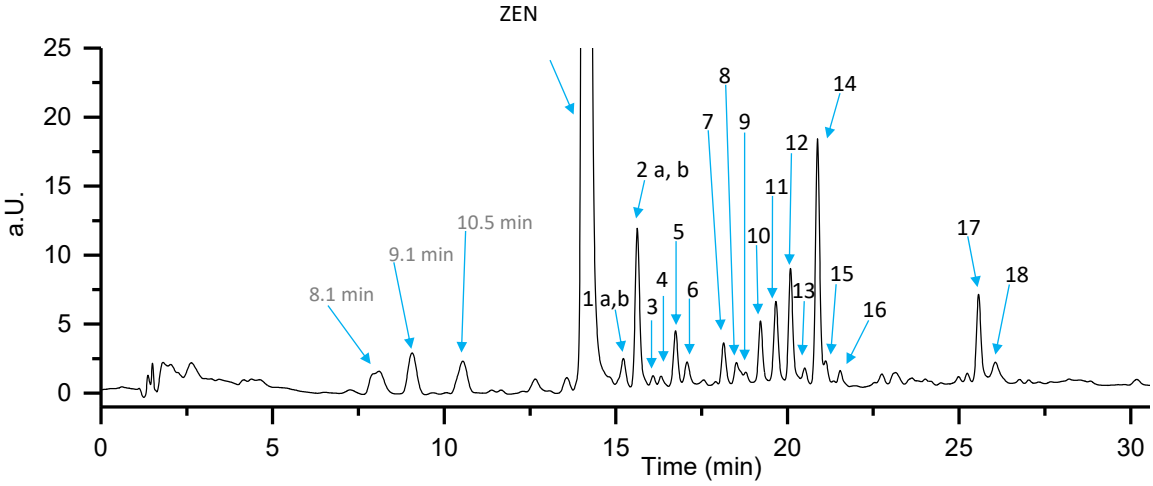


Figure 16. HPLC-DAD chromatogram of electrochemically oxidized ZEN (1,200 mV vs Pd/$H_2$)

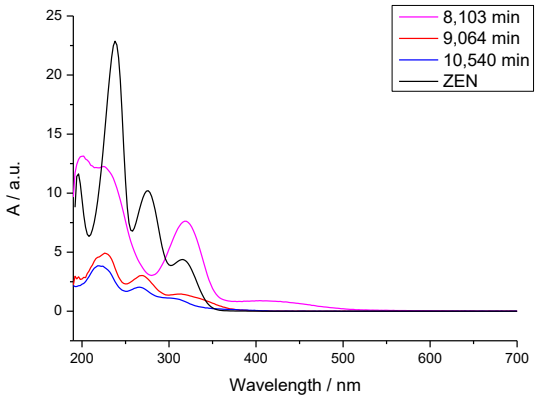


Figure 17. UV/VIS-absorbance spectra of ZEN and electrochemical generated reaction products of ZEN eluting after 8.10 min, 9.06 min and 10.54 min

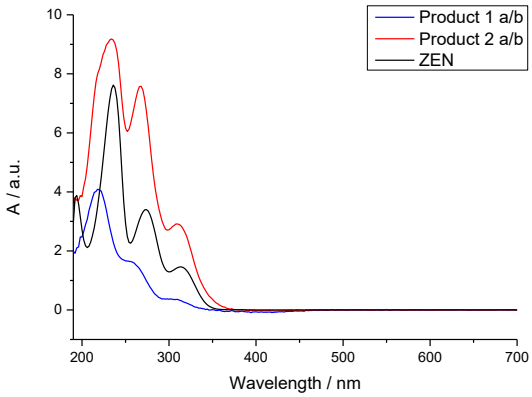


Figure 18. UV/VIS-absorbance spectra of ZEN and the electrochemical generated products 1 a/b and 2 a/b (both coeluting)

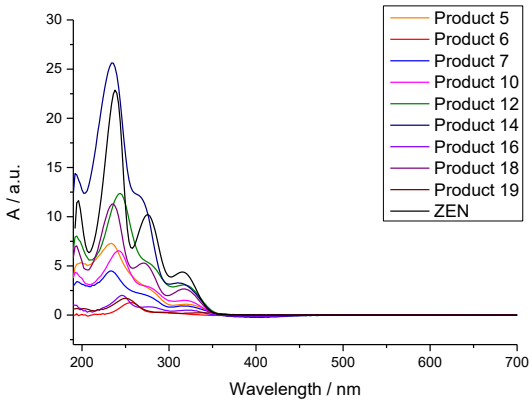

Figure 19. UV/VIS-absorbance spectra of ZEN and electrochemical ZEN dimers

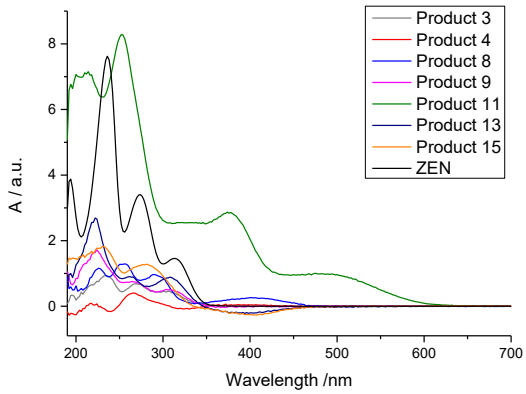


Figure 20. UV/VIS-absorbance spectra of ZEN and electrochemical generated ZEN dimer quinones

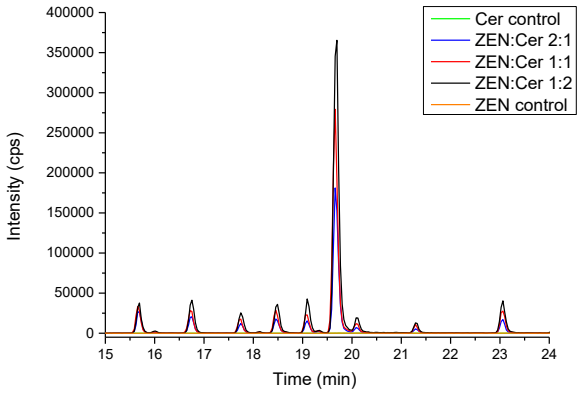


Figure 21. HPLC-MS/MS chromatogram of mixed ZEN: Ce(IV) (molar ratio: green Ce(IV) control, blue 2:1, red 1:1, black 1:2, orange ZEA control) leading to dimers of ZEN, MRM ESI (-); mass transition: 633 → 589

# 2.3 Synthesis and structural identification of a biaryl ether-linked zearalenone dimer

J. Keller[1], L. Hantschke[1], H. Haase[2], M. Koch[1,*]

Originally published in **Molecules**
23(10), 2624 (2018)
https://doi.org/10.3390/molecules23102624


[1] *Department 1, Division Organic Trace and Food Analysis, Federal Institute for Materials Research and Testing (BAM), Richard-Willstätter-Straße 11, D-12489 Berlin, Germany*
[2] *Department of Food Chemistry and Toxicology, Technische Universität Berlin, Gustav-Meyer-Allee 25, 13355 Berlin, Germany*

## 2.3.1 ABSTRACT

A new dimer of the food-relevant mycotoxin zearalenone was isolated after electrochemical and chemical oxidation. The structure was determined as a 16-O-15′-biaryl ether-linked dimer based on spectroscopic analyses (1H- and 13C-NMR, COSY, HMBC, and HSQCAD) and high-resolution mass spectrometry analysis (Q-TOF).

## 2.3.2 INTRODUCTION

The fungal secondary metabolite zearalenone (ZEN) is found worldwide and is primarily produced by *Fusarium* species [9, 17, 143]. Often found in common crops like corn, wheat, rice, soybeans, sorghum, spices or walnuts it poses a health risk to human and animals [19, 24, 103]. As mycoestrogen it causes swelling of the uterus and vulva, infertility and atrophy of ovaries reported in swine and cattle [20, 144]. Several metabolites derived from plants, fungi and mammalian metabolism are described so far and are part of ongoing research due to unknown toxic effects and occurrence [1, 29, 60, 145].
Oxidative reactions of ZEN lead to hydroxylated species obtained from in vitro assays with liver microsomes of rodent and non-rodent liver cells [63, 64]. A recent study

proposed the production of numerous hydroxylated as well as new dimeric species of ZEN using electrochemistry coupled to mass spectrometry [4]. The production, isolation and structural elucidation of the predominant dimeric species is now achieved.

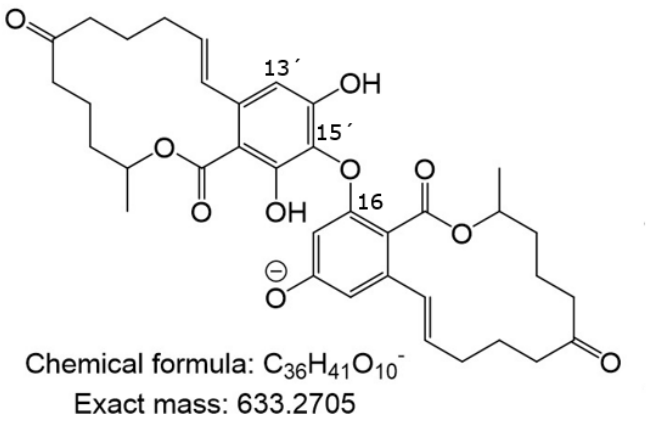


Figure 22. Structure of compound 1

## 2.3.3 RESULTS AND DISCUSSION

Compound 1 was obtained as pale orange solid substance with a molecular formula of $C_{36}H_{42}O_{10}$, measured by high-resolution mass spectrometry with *m/z* 633.2658 [M-H]- in ESI negative ionization mode (theoretical exact mass *m/z* 633.2702) as previously described [4]. The MS/MS measurements of compound 1 revealed a fragment with *m/z* 589.2756, which is due to the loss of $CO_2$, and a fragment with *m/z* 565.2746 because of a loss of $C_3O_2$. The signal with m/z 491.1658, corresponds to a loss of $C_8H_4O_2$, which led to the fragment m/z 447.1763 after the loss of $CO_2$ (Figure 23). The assumed fragments and their chemical formulas with theoretical exact masses are shown in Figure 24.

The $^1$H-NMR spectrum of compound 1 measured at 400 MHz in MeOH-*d4* gave the following information with 1.00-2.85 (m, H, J = 6.8 Hz); 1.34 (d, 3H, J =6.2 Hz); 1.39 (d, 3 H, J = 6.4 Hz); 5.06 – 5.16 (m, 1H); 5.20 – 5.36 (m, 1 H); 5.71 (ddd, 1H, J = 4.0, 9.8, 15.6 Hz); 5.77 (d, 1H, J = 2.1 Hz); 6.03 (ddd, 1H, J = 4.4, 9.6, 14.6 Hz); 6.34 – 6.41 (m, 2H); 6.42 (s, 1H); and 6.58 (d, 1H, J = 2.1 Hz). The $^{13}$C-NMR measurements with 100 MHz revealed the following chemical shifts with 20.2; 21.0; 22.1; 22.6; 23.4; 32.4; 35.9; 37.6; 38.3; 43.9; 44.7; 73.7; 74.3; 100.8; 104.3; 106.7; 126.4; 130.2; 134.4; 137.2; 139.4; 158.0;

161.0; 172.1; 213.8; and 214.1 (Figure 25 and 26). The assignments of the carbons and protons are summarized in Table 8.

Table 8 $^{1}$H-NMR and $^{13}$C-NMR data of **1** (400/100 MHz, Methanol-$d_4$).

| Position | $^{1}$H (ppm) | $^{13}$C (ppm) |
|---|---|---|
| 1, 1′ | - | 213.8, 214.1 |
| 2 | 1.39 (d, *J* = 6.4 Hz, 3H) | 35.9 |
| 3 | 5.20–5.36 (m, 1H) | 73.7 |
| 10, 10′ | - | 32.4, 32.4 |
| 11 | 6.03 (ddd, *J* = 4.4, 9.6, 14.6 Hz, 1H) | 134.4 |
| 12 | 6.38–6.41 (m, 1H) | 130.2 |
| 13 | 6.58 (d, *J* = 2.1 Hz, 1H) | 106.7 |
| 14 | - | 161.0 |
| 15 | 5.77 (d, *J* = 2.1 Hz, 1H) | 100.8 |
| 2′ | 1.34 (d, *J* = 6.2 Hz, 3H) | 35.9 |
| 3′ | 5.06–5.16 (m, 1H) | 74.3 |
| 11′ | 5.71 (ddd, *J* = 4.0, 9.8, 15.6 Hz, 1H) | 137.2 |
| 12′ | 6.34–6.37 (m, 1H) | 126.4 |
| 13′ | 6.42 (s, 1H) | 104.3 |

The $^{1}$H-NMR and COSY-spectra revealed two aromatic systems (Figure 25 and 27). One of these aromatic systems contained two protons (d 6.58 ppm, 1H, J = 2.1 Hz and d 5.77 ppm, 1H, J = 2.1 Hz), while the second aromatic system had only one proton (s 6.42 ppm, 1H). From this observation, the structures connected over the C-C linkages 15, 15′, 13, 13′, and 13, 15′ can be excluded since these dimers would have two aromatic systems with only one proton. Thus, only dimers having an C-O-C ether bridge between the monomers are possible. The COSY-spectrum showed nearly identical chemical structures for the spectral rest of the molecule (Figure 27). As a result, the dimerization of two ZEN molecules is only likely over an ether-link between 14-O-13′, 14-O-15′, 16-O-13′, or 16-O-15′. The HMBC spectrum (8 Hz) indicates a common coupling partner of the single aromatic proton and 12′-H, which is located in the aromatic-olefinic region (Figure 28, top). Due to the spatial proximity, it should be at the singlet (6.42 ppm) and, as a result, act around the 13′-H position. Consequently, an O-15′-linkage is conceivable.

The observed significant difference of the chemical shifts of 3-H and 3′-H indicated a different chemical environment. For a C-14 link, the closer chemical environment of 3-H and 3′-H would be very similar. A C-16 link, on the other hand, would be a greater steric influence and inductive effects would occur. Thus, the compound 16-O-15′-biaryl ether bond is the most likely structure, which is shown in Figure 22.

Whether this dimer can be found naturally in food or feed remains to be analyzed in detail. Especially in plants, lichen, bacteria, and fungi regio-selective and stereo-selective biaryl C C and biaryl ether C-O-C linkages are often found and it is conceivable that dimers of ZEN might not be uncommon in nature.

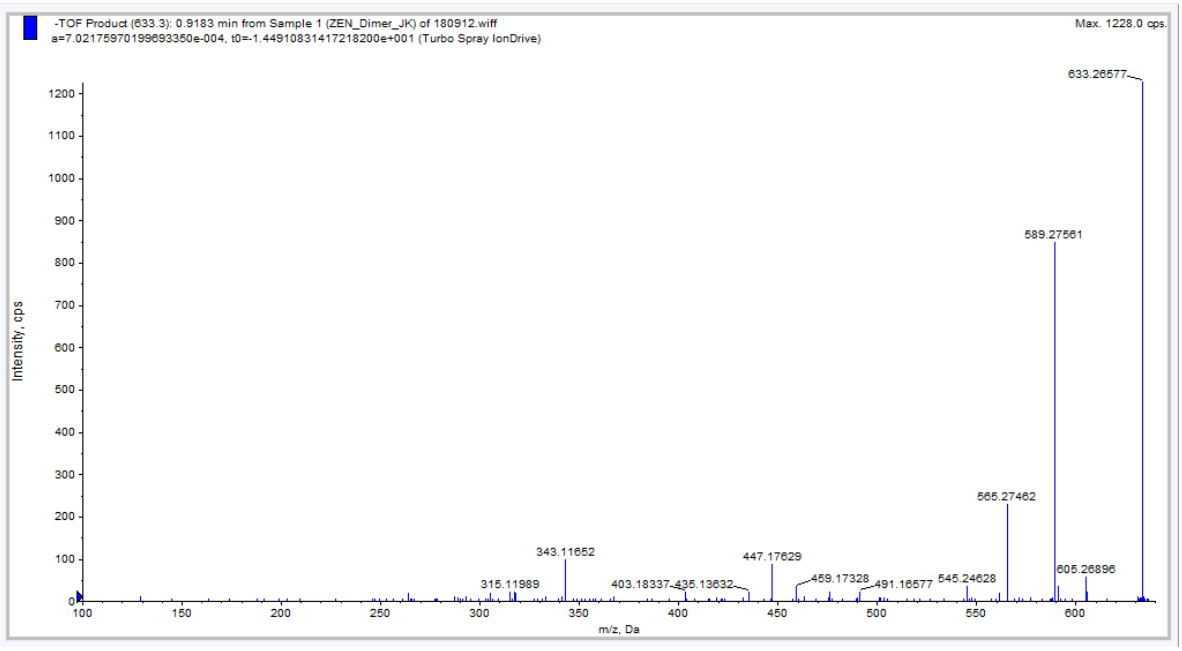


Figure 23. MS/MS fragmentation spectrum of the ZEN dimer obtained with Q-TOF in negative ionization mode

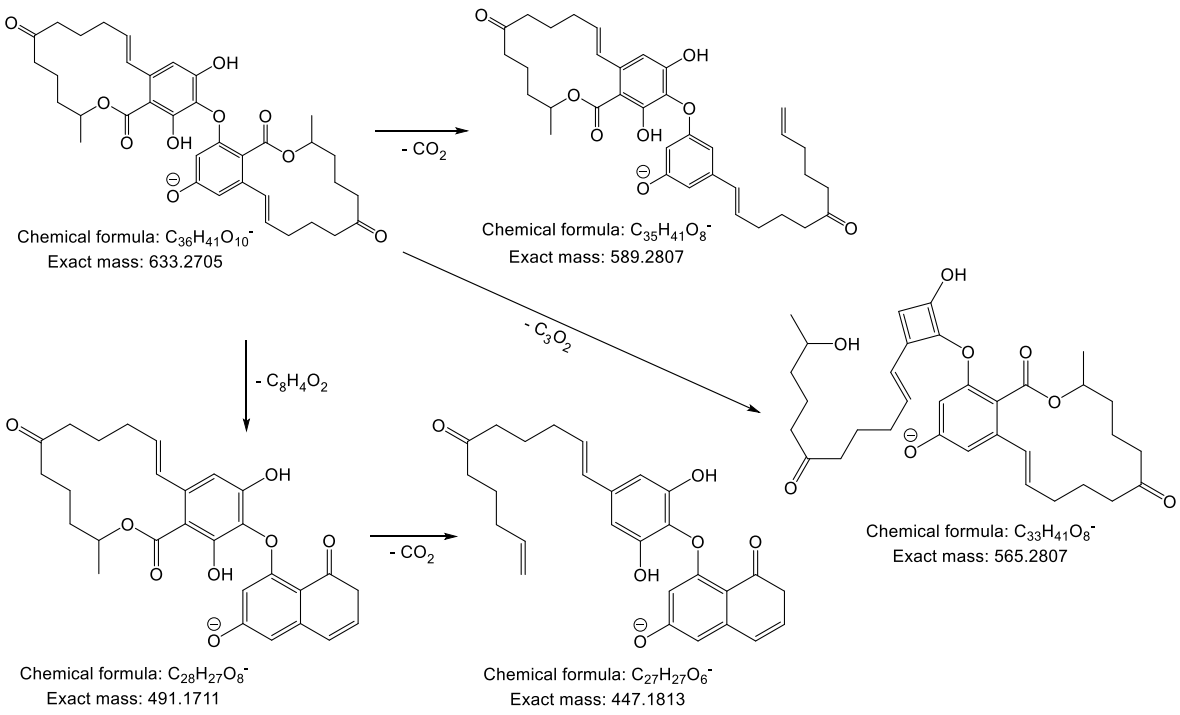


Figure 24. Postulated fragments of the ZEN dimer according to the MS/MS measurements with molecular structure and formula and the theoretical exact masses

## 2.3.4 MATERIALS AND METHODS

*Chemicals and General Experimental Procedures*

Zearalenone with a purity over 98% was obtained from Fermentek (Jerusalem, Israel) and Cerium(IV)sulfate was purchased from Sigma-Aldrich (Steinheim, Germany). Ultrapure water was generated by a Seralpur PRO 90 CN system (Ransbach-Baumbach, Germany). All standard chemicals were of p.a. grade and all solvents were of an HPLC grade. Electrochemical oxidation was achieved by using the Roxy® system synthesis cell (Antec, NV Zoeterwoude, the Netherlands) equipped with a platinum working electrode. The HPLC system used for fractionation consisted of an Agilent 1200 series autosampler, a 1260 series pump, a 1200 series diode array detector, and a column oven. A Macherey-Nagel Nucleosil C18 100-5 150 × 4.6 mm column (Düren, Germany) was used. The TripleTOF® 6600 Quadrupole Time-Of-

Flight (QTOF) mass analyzer (Sciex, Darmstadt, Germany) was operated in negative ionization mode and 10 μM of the dimer sample were dissolved in methanol with 0.1% of formic acid. The used parameters were as follows:
Gas temperature 350 °C, ion source gas 1 (nitrogen) 20 L/min, ion source gas 2 (nitrogen) 15 L/min, curtain gas (nitrogen) 20 L/min, and ion spray voltage floating −4500 V. The MS/MS-spectrum was recorded in the targeted MS/MS mode with the following parameters: De-clustering potential (−15 V), collision energy (−40 V), and TOF Masses 100–640 Da. Confirmation of the 16-O-15'-biaryl ether-linked dimer structure was conducted by nuclear magnetic resonance spectroscopy (NMR). The NMR spectra were recorded in methanol-d4 on an Agilent 400-MR NMR spectrometer (Agilent Technologies, Waldbronn, Germany) at 30 °C. For the measurements, the ATB 5mm-probe head was operated at 399.8 MHz for 1H and 100.5 MHz for 13C data.

*Electrochemical and chemical production of ZEN dimer*

*Electrochemical:* The optimal potential was tested by taking aliquots after different time points and using potentials of 0, 1.0, 1.4, and 1.8 V vs. Pd/H2. For the electrochemical oxidation, 80 mL of 250 μM ZEN in acetonitrile/water (50/50, v/v) was stirred for 48 h using 1.4 V vs. Pd/H2. The solution was subsequently evaporated to dryness by using a rotary evaporator and dissolved in water/acetonitrile (65/35, v/v) for HPLC fractionation.
*Chemical:* For the oxidative production of ZEN dimers, Ce(IV)sulfate was used. About 100 mg of ZEN and 350 mg of Ce(IV)sulfate were dissolved in 200 mL of acetonitrile/water (50/50, v/v) and stirred for two hours at 70 °C. Subsequently, the sample was stirred for 24 h at room temperature and a white precipitate was formed. The yellow solvent mixture was extracted three times with 20 mL of ethyl acetate. After the extraction, the ethyl acetate was colored yellow and the acetonitrile water mixture was colorless. After evaporation, a deep orange and highly viscous fluid was obtained. After freeze-drying, a pale orange solid was formed with a yield of 10%.

*Purification of ZEN dimer*

For the separation of ZEN dimers an already described HPLC method was adapted [4], using a flowrate of 1.2 mL/min and an isocratic eluent consisting of

(water/acetonitrile, 65/35, *v*/*v*) without modifiers. The ZEN dimer was isolated by collecting the fraction between 15.4 min and 16.2 min of the retention time using a Foxy® R1 fraction collector (Teledyne ISCO, Lincoln NE, USA). The purity of the dimer was determined to be 92% based on DAD spectra using a wavelength at $\lambda$=254 nm (Figure 29).

## 2.3.5 CONCLUSIONS

A new dimeric species of the food-relevant mycotoxin zearalenone was synthesized electrochemically and chemically with Ce(IV)sulfate and structurally identified. Among other possible dimers, the occurrence of the 16-O-15′-biaryl ether-linked dimer in food and feed is conceivable because the dimerization of phenolic compounds is often observed in plants, fungi, or lichen.

## LICENSE

## 2.3.6 SUPPLEMENTARY MATERIALS

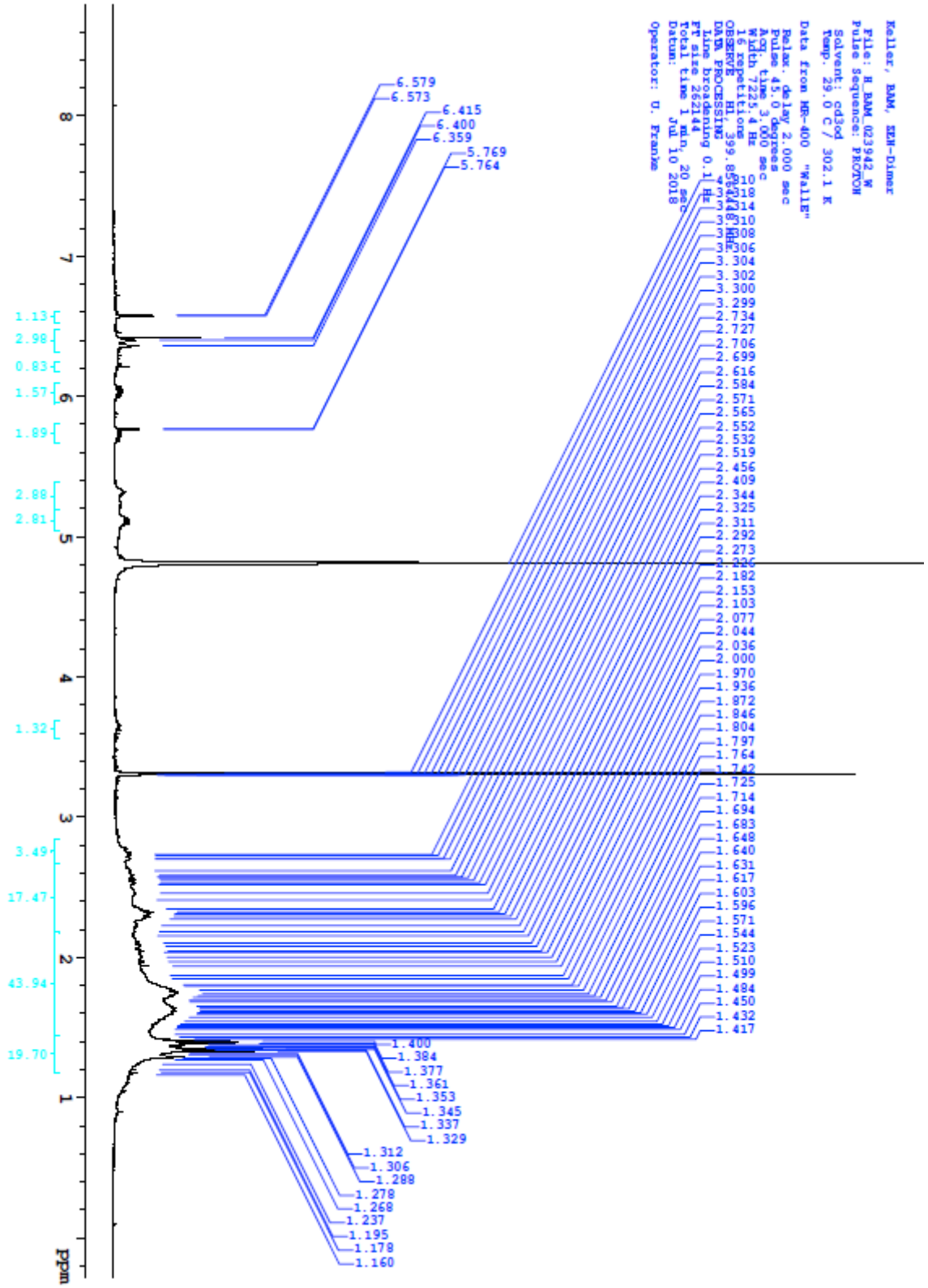


Figure 25. $^{1}$H-NMR spectrum of the 16-O-15′-biaryl ether-linked zearalenone dimer

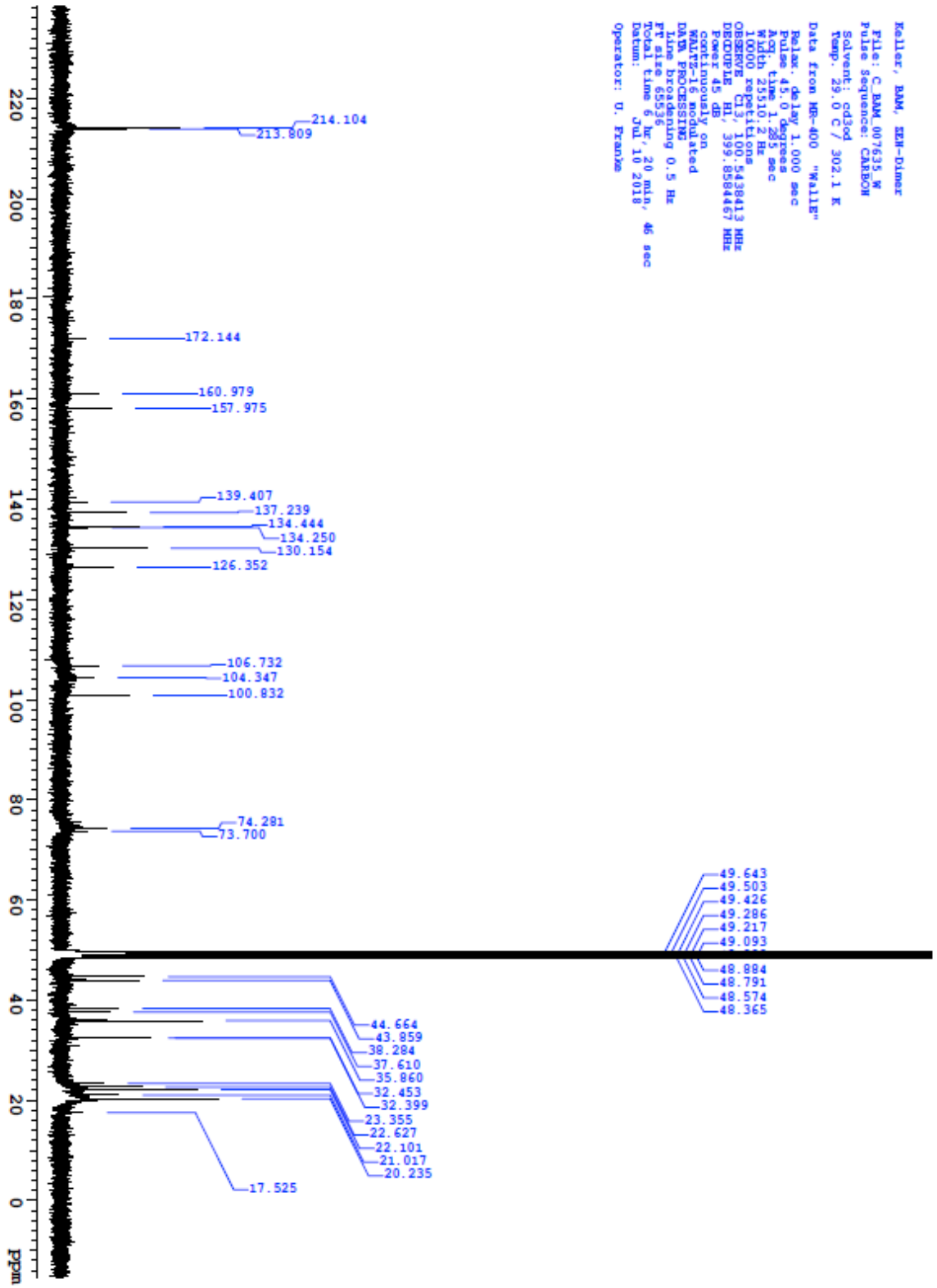


Figure 26. $^{13}$C-NMR spectrum of the 16-O-15′-biaryl ether-linked zearalenone dimer

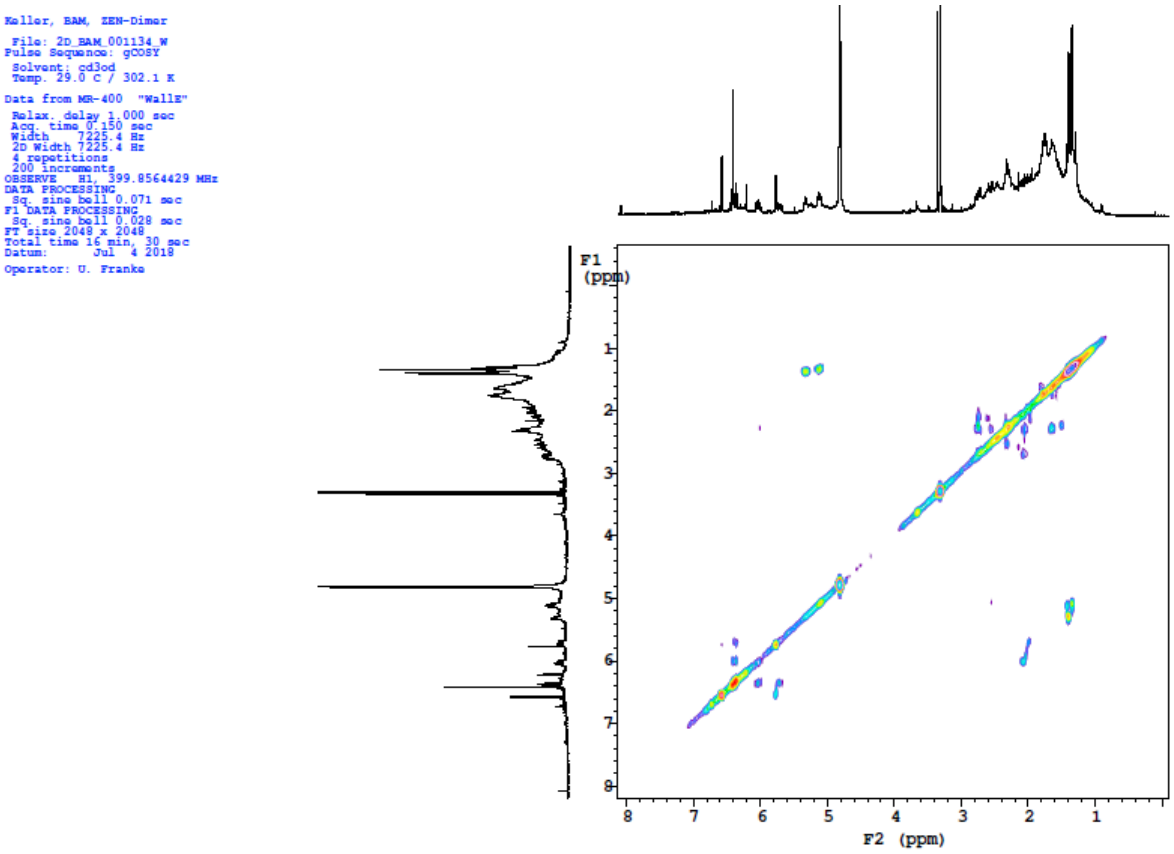


Figure 27. COSY spectrum of the 16-O-15′-biaryl ether-linked zearalenone dimer

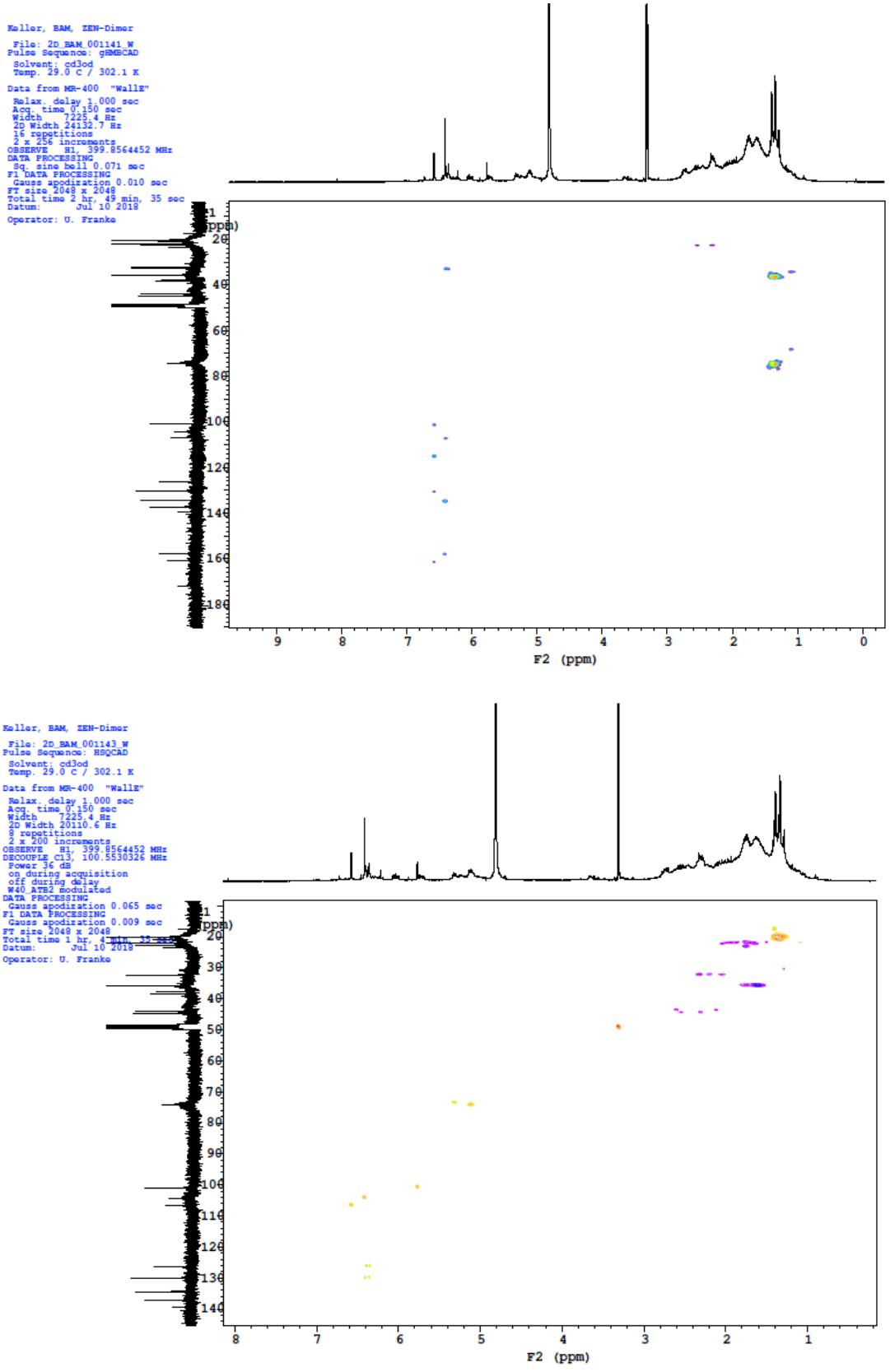


Figure 28. HMBC spectrum (top) and HSQC spectrum (bottom) of the 16-O-15′-biaryl ether-linked zearalenone dimer

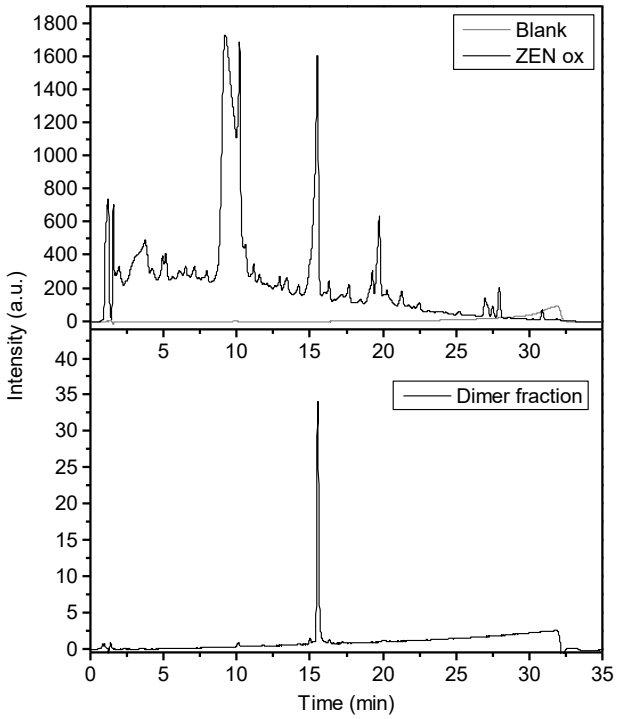


Figure 29. HPLC-DAD chromatograms (λ=254 nm) of the zearalenone dimer reaction mixture before fractionation (top) and after fractionation (bottom)

# 2.4 Biosynthesis and characterization of zearalenone-14-sulfate, zearalenone-14-glucoside and zearalenone-16-glucoside using common fungal strains

A. Borzekowski [1], T. Drewitz [1], J. Keller [1], D. Pfeiffer [1], H.-J. Kunte [2], M. Koch[1,*], S. Rohn[3] and R. Maul [3,4]

Originally published in **Toxins**
*10*(3), 104 (2017)
https://doi.org/10.3390/toxins10030104


[1] *Department Analytical Chemistry, Reference Materials, Bundesanstalt für Materialforschung und -prüfung (BAM), Richard-Willstätter-Straße 11, 12489, Berlin, Germany; antje.borzekowski@bam.de; tatjana.drewitz@bam.de; julia.keller@bam.de; dietmar.pfeiffer@bam.de*
[2] *Department Materials and the Environment, Bundesanstalt für Materialforschung und -prüfung (BAM), Unter den Eichen 87, 12205 Berlin, Germany; hans-joerg.kunte@bam.de*
[3] *Institute of Food Chemistry, Hamburg School of Food Science, University of Hamburg, Grindelallee 117, 20146 Hamburg, Germany; rohn@chemie.uni-hamburg.de; ronald.maul@chemie.uni-hamburg.de*
[4] *German Federal Institute for Risk Assessment (BfR), Max-Dohm-Str. 8-10, 10589 Berlin, Germany*
** Correspondence: Matthias.koch@bam.de; Tel.: +49-30-8104-1170*

## 2.4.1 ABSTRACT

Zearalenone (ZEN) and its phase II sulfate and glucoside metabolites have been detected in food and feed commodities. After consumption, the conjugates can be hydrolyzed by the human intestinal microbiota leading to a liberation of ZEN that implies an underestimation of the true ZEN exposure. To include ZEN conjugates in routine analysis, reliable standards are needed, which are currently not available.

Thus, the aim of the present study was to develop a facilitated biosynthesis of ZEN-14-sulfate, ZEN-14-glucoside and ZEN-16-glucoside. A metabolite screening was conducted by adding ZEN to liquid fungi cultures of known ZEN conjugating *Aspergillus* and *Rhizopus* strains. Cultivation conditions and ZEN incubation time were varied. All media samples were analyzed for metabolite formation by HPLC-MS/MS. In addition, a consecutive biosynthesis was developed by using *Fusarium graminearum* for ZEN biosynthesis with subsequent conjugation of the toxin by utilizing *Aspergillus* and *Rhizopus* species. ZEN-14-sulfate (yield: 49%) is exclusively formed by *A. oryzae*. ZEN-14-glucoside (yield: 67%) and ZEN-16-glucoside (yield: 39%) are formed by *R. oryzae* and *R. oligosporus*, respectively. Purities of ≥ 73% ZEN-14-sulfate, ≥ 82% ZEN-14-glucoside and ≥ 50% ZEN-16-glucoside were obtained by $^{1}$H-NMR. In total, under optimized cultivation conditions fungi can be easily utilized for a targeted and regioselective synthesis of ZEN conjugates.

## 2.4.2 INTRODUCTION

Zearalenone (ZEN) is a mycotoxin produced by *Fusarium* species, including *F. graminearum* [17, 146]. *Fusarium* spp. infest for instance wheat, maize and barley. Therefore, ZEN is a common contaminant in cereal based feed and food products [147, 148]. For many commodities, legal limits for ZEN have been established in various countries worldwide. In the metabolism of the infested plant and in fungal metabolism sulfate and glucoside conjugates of ZEN are formed. Kovalsky-Paris *et al*. [5] reported the conversion of ZEN to ZEN-14-glucoside (ZEN-14-G) and ZEN-16-glucoside (ZEN-16-G) in barley. Krenn *et al*. [6] described the production of ZEN-14-G by the model plant *Arabidopsis thaliana* after ZEN addition. ZEN-14-sulfate (ZEN-14-S) was found to be a natural fungal metabolite of *Fusarium*, *Rhizopus*, and *Aspergillus* species [146, 149, 150]. *R. oryzae*, *A. oryzae,* and *A. niger i*n particular convert ZEN very rapidly to ZEN-14-S. A study from De Boevre *et al.* [3] on the occurrence of ZEN and its metabolites showed that food and feed products can be highly contaminated with these compounds. One-hundred and seventy-four cereal-based food products and 67 compound feeds were analyzed for the occurrence of ZEN, the phase I metabolite zearalenol (ZEL) and the glucoside conjugates of ZEN and ZEL, and ZEN sulfate. For example, the cornflakes analyzed, contained ZEN-14-G and ZEN-14-S with average levels of 39 µg/kg and 23 µg/kg and maximum levels of 369 µg/kg and 417 µg/kg, respectively. Also, the sum of the ZEN metabolites in

cornflakes (144 μg/kg, mean value) exceeded the amount of the parent compound (76 μg/kg, mean value).

ZEN is regulated by the European Union (EU) with maximum levels from 20 – 400 μg/kg for cereals and cereal products [151], because of its estrogenic activity. ZEN is a mycroestrogen and can interact with the estrogen receptors ERα and ERβ and can cause hormonal disorder [152]. The most sensitive species for these effects are pigs, in which ZEN administration causes alteration of the reproductive tract and decreases fertility, for example [153]. The sensitivity can be attributed to the extensive reductive metabolism to α-ZEL which has a much higher binding affinity relative to ZEN and is the predominant contributor to total estrogen receptor ligand activity after oral dosing of juvenile female pigs with ZEN [154]. Formation of α-ZEL was also observed *in vitro* by investigation of ZEN metabolism in Caco-2 cells; β-ZEL and several glucuronides and sulfates were also formed [155]. Additionally, in epidemiological studies a chronically exposure of ZEN was associated with precocious development of children [156, 157]. Besides its estrogenic activity, ZEN is also an immunotoxic compound. In 2014 Hueza *et al*. showed that ZEN can modulate most aspects of immune response and impair lymphoid organs, resulting in thymus atrophy [21]. Additionally, ZEN can be considered as a clastogenic compound. The induction of chromosome aberrations was shown *in vitro* in HeLa cells and *in vivo* in mouse bone marrow cells. The proposed mechanism for the clastogenic effect is a CYP-mediated formation of catechols that can be oxidized to quinones that undergo redox cycling [17]. In human breast cancer cells (MCF-7 cells) ZEN stimulates cell proliferation and the authors conclude a possible contribution of ZEN to the increasing incidence rates of breast cancer. [18]. Nevertheless, the acute toxicity of ZEN is low and evidences for carcinogenic effects are not classifiable, because of inadequate evidence in human and limited evidence in experimental animals [19].

In present ZEN regulations, the conjugated metabolites as well as its reductive forms are not comprised. . *In vitro* analyses of the gastrointestinal digestive process showed no cleavage of ZEN conjugates, but in human microbiota fermentation the conjugates were cleaved by the microbial enzymes. [26, 158]. Thus, ZEN uptake might be underestimated, due to the release of absorbable ZEN. Recently, the EU-CONTAM Panel found it appropriate to set a group tolerable daily intake (TDI) for ZEN and its modified forms [159]. It must be considered that the estrogenic potency of ZEN derivatives differs. Potency factors assigned to these derivatives by EFSA CONTAM Panel are 0.2 for β-ZEL and 60 for α-ZEL relative to ZEN. Moreover, for sulfate and glucoside conjugates the same factors as for the free form are proposed. To obtain more data on the occurrence of ZEN metabolites in food and feed, standard substances are needed. Until now some synthetic and biosynthetic strategies were developed for production of ZEN glucosides and ZEN-14-S. Chemical synthesis of

ZEN-14-S and ZEN-16-G were conducted by Mikula *et al*. [160, 161]. A procedure for selective monosulfation of ZEN on position C-14 was established by applying a 2,2,2-trichloroethyl protection. Triisopropyl-protected ZEN was used as intermediate for subsequent regiocontrolled glucosylation of ZEN on position C-16.. ZEN-14-G was biosynthesized by a genetically modified yeast strain, expressing the *Arabidopsis thaliana* UDP-glucosyltransferase UGT73C6 [162]. A biosynthetic strategy for synthesis of mono- and di-glucosides of ZEN by recombinant barley glucosyltransferase HvUGT14077 was developed by Michlmayr *et al.* [163]. In sum, biotransformation of ZEN in plants is mainly catalyzed by UGTs and ZEN glucosides are formed. In phase II metabolism of fungi the biotransformation of ZEN to both, sulfate and glucoside conjugates, was observed. There is clear evidence that not only plant UGT can catalyze the conjugation of ZEN. Especially for fungi the ability to detoxify mycotoxins produced by co-occurring species is crucial for their survival. However, the full potential of microorganisms has not been elucidated. Thus, various species of the genera *Rhizopus* and *Aspergillus* which are known to glucosylate and or sulfatize ZEN are investigated in more detail. However, ZEN conjugates are either very expensive or not commercially available until now. Thus, the aim of the present study was to develop a simple and economic method for biosynthesis of ZEN conjugates without the need of special laboratory equipment. In 2014, *Rhizopus* and *Aspergillus* strains were already identified to be capable of ZEN conjugate formation after ZEN addition [149]. Based on that data, a consecutive biosynthesis was outlined for the current study (Figure 30). In a first step ZEN was supposed to be biosynthesized by *F. graminearum* and secondly the produced ZEN could be used for the formation of ZEN-14-S, ZEN-14-G and ZEN-16-G by selected *Rhizopus* and *Aspergillus* species under defined conditions.

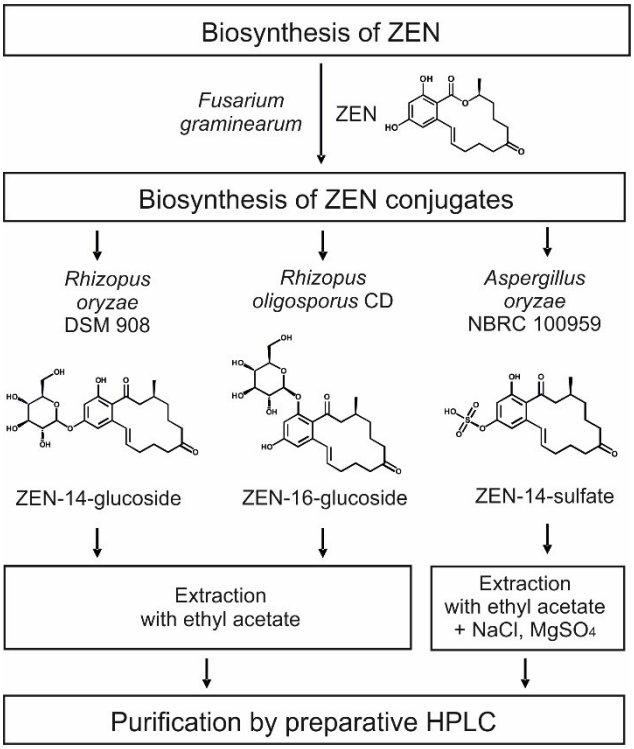


Figure 30. Chart of biosynthesis, isolation and purification of zearalenone(ZEN)-14-glucoside, ZEN-16-glucoside and ZEN-14-sulfate.

## 2.4.3 RESULTS

*In vitro-Screening of Conjugate Producing Aspergillus and Rhizopus Species*

As already reported, fungal strains which convert ZEN into its glucosides and sulfates show a heterogeneous product pattern [7]. Thus, such strains that conjugate ZEN most selectively into ZEN-14-S, ZEN-14-G or ZEN-16-G were characterized in the present study. Therefore, eight fungal strains (Table 9) of the genera *Rhizopus* and *Aspergillus* were screened for ZEN conjugate formation after ZEN addition to the liquid culture; time of harvest and ZEN addition to different fungal growth phases were varied. The analyzed strains showed a very diverse metabolite pattern. In particular, the formation of the conjugates strongly varied depending on the time of harvest (ZEN incubation time) and the growth phase of the fungus, in which ZEN was added. The vegetative and generative growth stages of the various fungi were reached by 24 h and 144 h cultivation in liquid media prior to ZEN addition. Four

representative fungal strains (*R. oryzae* DSM 906, *R. oryzae* DSM 908, *R. oligosporus* CD, and *A. oryzae* DSM 1864) with a diverse metabolite formation and pronounced change of the metabolite pattern dependent on different time of harvest and reproductive growth phase are shown in Figure 31. The metabolite pattern of *R. oryzae* DSM 907, *R. stolonifer* DSM 855, *R. microsporus* var. *chinensis* DSM 1834, and *A. oryzae* NBRC 100959 are shown in the supplementary material. To point out the effect of growth phase on the fungal metabolite pattern, in Figure 31, the metabolite formation after 24 h of ZEN incubation were compared for both phases. The importance of the ZEN incubation time was shown exemplarily for two time points (24 h, 144 h) after ZEN addition to the vegetative growth phase.

As described by Brodehl *et al.* [7] a response factor of 11 reflecting the significantly enhanced molar response in the detection for ZEN-14-S compared to ZEN was applied for better illustration of the metabolite formation obtained by HPLC-ESI-MS/MS measurements. Accordingly, for an approximate quantitative assessment of the $\alpha$-ZEL-sulfate ($\alpha$-ZEL-S) formation compared to ZEN, in Figure 31 a response factor of 2.3 was applied, which is derived from a factor of 16 for the $\alpha$-ZEL-sulfate ($\alpha$-ZEL-S) response compared to $\alpha$-ZEL [149] and a response factor of 1/7 for $\alpha$-ZEL compared to ZEN. The ZEL-S was identified as the isomer $\alpha$-ZEL-S by enzymatic hydrolysis conducted according to Brodehl *et al.* [149]. Qualitative identification of ZEN and the ZEN metabolites were conducted based on a comparison of the retention time of standard substances and self-synthesized standards.

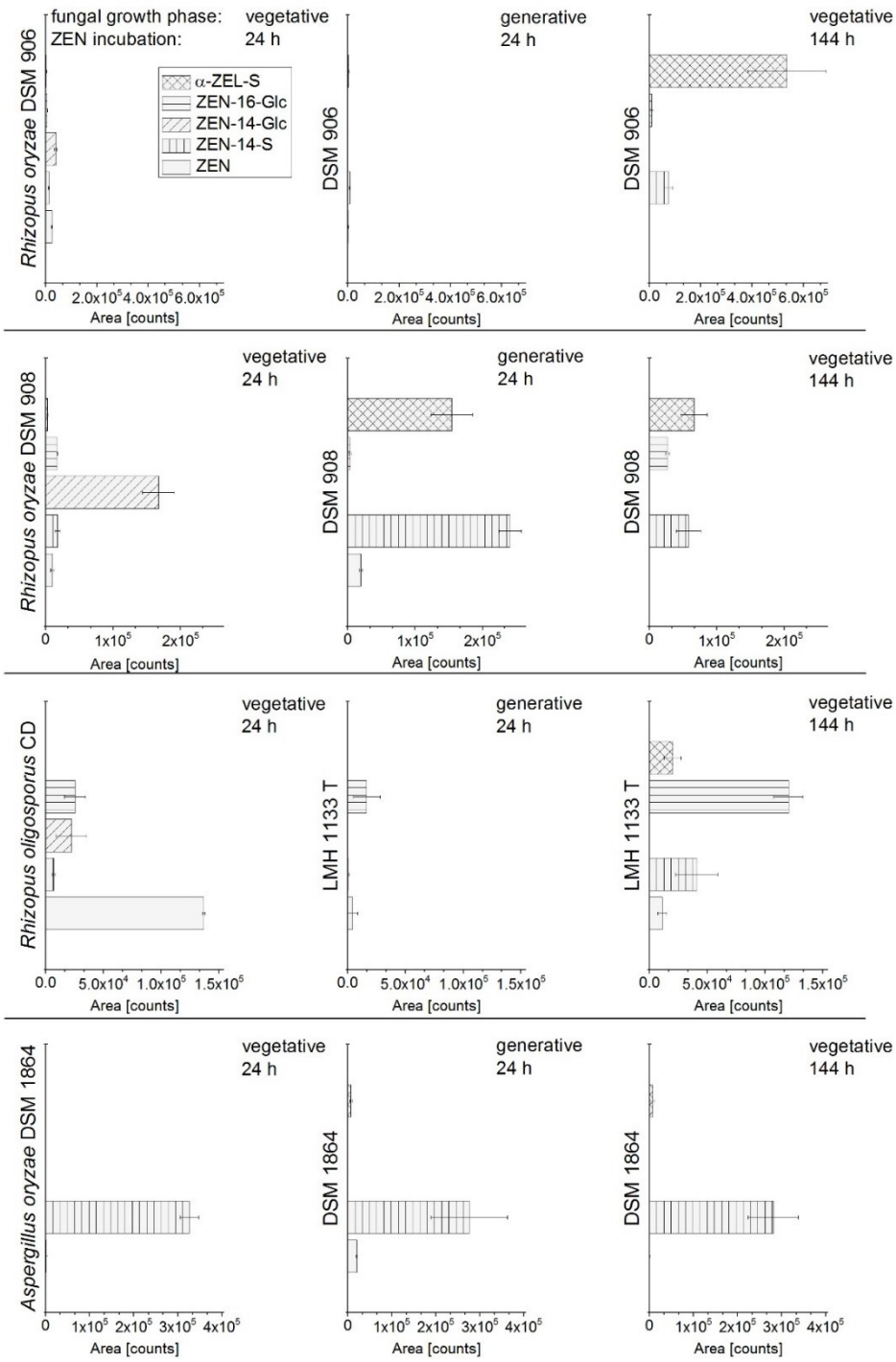


Figure 31. Formation of ZEN-14-sulfate (ZEN-14-S), ZEN-14-glucoside (ZEN-14-Glc), ZEN-16-glucoside (ZEN-16-Glc), and α-ZEL-sulfate (α-ZEL-S) by *R. oryzae* DSM 906, *R. oryzae* DSM 908, *R. oligosporus* CD, and *A. oryzae* DSM 1864 after ZEN addition to vegetative and generative fungal growth phase with subsequent ZEN incubation for 24 h (column 1 & 2) or 144 h (column 3); a response factor for ZEN-14-S/ZEN of 11 and for α-ZEL-S/ZEN of 2.3 was applied.

The analyzed *A. oryzae* strain DSM 1864 formed primarily the ZEN-14-S, and α-ZEL-S to a small extent; for *A. oryzae* NBRC 100959 the results were the same (Figure 32). Also, for *R. microsporus* var. *chinensis* DSM 1834 only the formation of ZEN-14-S and α-ZEL-S was shown. For all aforementioned strains, no glucoside conjugates were formed (supplementary material). The ZEN metabolite formation strongly differs between the closely related strains *R. oryzae* DSM 906 and DSM 908 depending on the time of harvest. After ZEN addition to the vegetative growth phase with subsequent incubation for 24 h, DSM 908 predominantly formed the ZEN-14-G; DSM 908 media sampled after 144 h contained ZEN-16-G, α-ZEL-S and ZEN-14-S, but no ZEN-14-G. In contrast, DSM 906 showed no considerable metabolite formation after 24 h of ZEN incubation in vegetative phase, but a strong formation of the α-ZEL-S after 144 h. The results of *R. oryzae* DSM 907 and *R. stolonifer* DSM 855 resemble to those detected for DSM 908 with only minor differences.

ZEN conjugate formation was analyzed for ZEN addition to the vegetative growth phase (fungal pre-cultivation: 24 h) and for ZEN addition to generative growth phase (fungal pre-cultivation: 144 h). Especially, *R. oryzae* DSM 908 showed a completely other metabolite spectrum, when ZEN was added to the fungal culture in the vegetative phase or in the generative growth phase. For both phases, the DSM 908 liquid culture was incubated for 24 h with ZEN (Figure 31. line 2, column 1 & 2). ZEN addition to the vegetative phase resulted in a formation of ZEN-14-G and the addition of ZEN to the generative phase showed a strong formation of sulfate conjugates. Interestingly, ZEN-16-G which is only a byproduct in the metabolite pattern of the other analyzed fungi was the major component following 144 h of ZEN incubation in the vegetative phase of *R. oligosporus* CD. For *R. oryzae* DSM 906, *R. oligosporus* CD and *A. oryzae* DSM 1864 comparison of metabolite formation in different growth phases of the fungi is shown in Figure 31 (column 1 & 2).

In sum, ZEN addition to different fungal growth phases had a strong impact on the conjugate formation of *Rhizopus* species, but no impact for *Aspergillus oryzae* incubations. Most of the analyzed *Rhizopus* strains formed sulfate conjugates as major metabolites, when ZEN was added to generative phase and further incubated for more than 6 h. Glucoside formation, especially ZEN-14-G, was predominantly observed in *Rhizopus* cultures in the first 24 h of incubation after ZEN addition to vegetative phase. However, metabolism of fungi is influenced by many external factors. Therefore, no predictions for conjugate formations of related fungal strains can be made.

The complete results of the eight fungal strains which include all points of harvest for ZEN addition to both growth phases are stated in the supplementary material.

**Consecutive Biosynthesis of ZEN Conjugates**

*Biosynthesis of ZEN*

First, the formation of ZEN by the *F. graminearum* strains F1, F2, and F3 was analyzed on autoclaved and, therefore, enzyme deactivated rice media. The strains analyzed, showed a strong variation in ZEN production. *F. graminearum* F3 showed the highest ZEN formation after 32 days of incubation with 19.5 ± 9.3 mg/kg dry mass, whereas *F. graminearum* F1 produced ZEN after 32 days with very high amounts of 3,005 ± 708 mg/kg dry mass. *F. graminearum* F2 had a maximum of ZEN formation after 20 days of incubation, but ZEN production was very inconsistent with ZEN amounts ranging from 34.6 up to 6,483 mg/kg dry mass. Thus, for the first step of the consecutive biosynthesis, *F. graminearum* F1 was chosen for ZEN production, because the data were consistent and ZEN was produced in high amounts. In addition to ZEN, ZEN-14-S was also formed by *F. graminearum* F1 in a ratio of ZEN to ZEN-14-S of 1:0.02 up to 1:0.2.

*Biosynthesis of ZEN Conjugates*

With a focus on conjugation products of unmodified ZEN as basic molecule, a consecutive biosynthesis was developed. Fungal strains with the best results for an exclusive formation of ZEN-14-S, ZEN-14-G, and ZEN-16-G were chosen: *A. oryzae* NBRC 100959, *R. oryzae* DSM 908, and *R. oligosporus* CD, respectively. ZEN biosynthesis and ZEN conjugate biosynthesis were combined by adding ZEN contaminated rice flour obtained from incubation with *F. graminearum* F1 into liquid media with subsequent fungal incubation. In Figure 32, the HPLC-MS/MS analysis of the ZEN-14-S formation by *A. oryzae* NBRC 100959 for five time points of media harvest is shown. Incubation from 6 h to 140 h with ZEN (80 mg/L) showed a decrease of the ZEN content and an increase of ZEN-14-S formation. After 72 h of incubation *A. oryzae* is in the generative growth phase and an exclusive formation of ZEN-14-S with a negligible residual content of ZEN was observed. ZEN incubation extended to 140 h did not result in an important increase of ZEN-14-S.

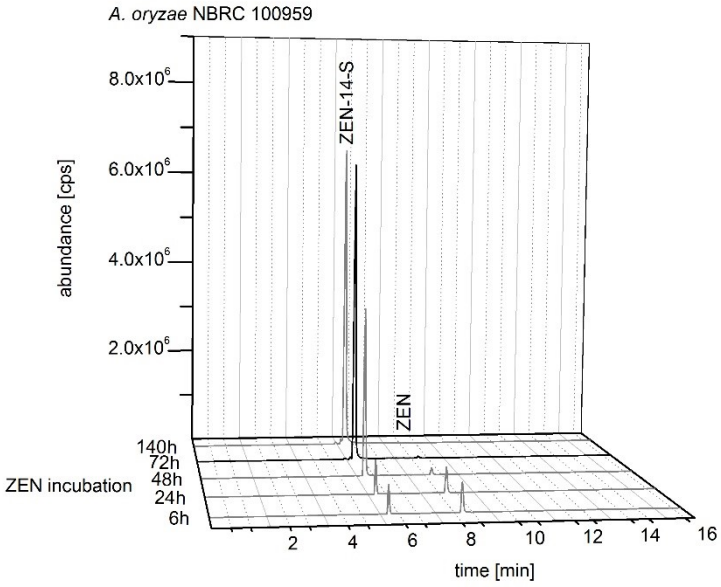


Figure 32. Reconstructed total ion chromatogram (TIC) with mass transitions of zearalenol (ZEL), ZEL-sulfate, ZEL-glucoside, zearalenone (ZEN), ZEN-14-sulfate (ZEN-14-S), and ZEN-glucoside analyzed in liquid media of *Aspergillus oryzae* NBRC 100959 incubated with ZEN.

As the ZEN conjugate formation of *R. oryzae* DSM 908 varied strongly depending on period of ZEN incubation, the most exclusive ZEN-14-G formation was achieved in the vegetative growth phase after 24 h of ZEN incubation (Figure 33). Besides to ZEN-14-G, also a marginal ZEN-16-G formation and a ZEN-14-S peak were detected after 24 h incubation with ZEN (80 mg/L). The impurity of the media with ZEN-14-S could be observed even in the beginning of the fungal incubation, because in ZEN biosynthesis by *F. graminearum* also ZEN-14-S was formed. Thus, the ZEN-14-S contamination in ZEN-14-G biosynthesis could not be avoided. However, ZEN-14-S and ZEN glucosides were separated in a subsequent cleanup step.

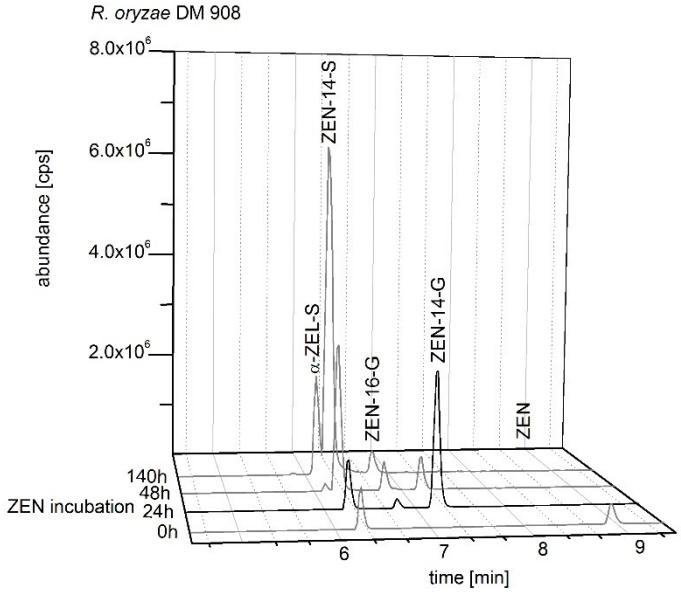


Figure 33. Reconstructed total ion chromatogram (TIC) with mass transitions of zearalenol (ZEL), $\alpha$-ZEL-sulfate ($\alpha$-ZEL-S), ZEL-glucoside, zearalenone (ZEN), ZEN-14-sulfate (ZEN-14-S), ZEN-14-glucoside (ZEN-14-G), and ZEN-16-glucoside (ZEN-16-G) analyzed in liquid media of *Rhizopus oryzae* DSM 908 incubated with ZEN.

*R. oligosporus* CD is an appropriate producer of ZEN-16-G. In Figure 34 several time points of ZEN incubation (80 mg/L) and the resulting ZEN metabolite formation are shown. After 144 h of ZEN incubation *R. oligosporus* is in the generative growth phase and ZEN-16-G is formed as the main metabolite; the by-products which were formed only in small amounts compared to ZEN-16-G are ZEN, $\alpha$-ZEL, ZEN-14-S, $\alpha$-ZEL-S, and ZEN-14-G. Next to the ZEN-14-S signal, a small peak which belongs to the mass transitions of a ZEL glucoside appeared. An earlier media harvest after 72 h resulted in a smaller amount of ZEN-16-G and a higher formation of ZEN-14-G. A media harvest at a later stage, after 194 h of incubation, showed a slightly higher ZEN-16-G formation compared to 144 h of incubation, but additional a higher formation of $\alpha$-ZEL-S and ZEN-14-S, and a small peak next to the ZEN-14-S signal which allocated to the mass transitions of a ZEL glucoside.

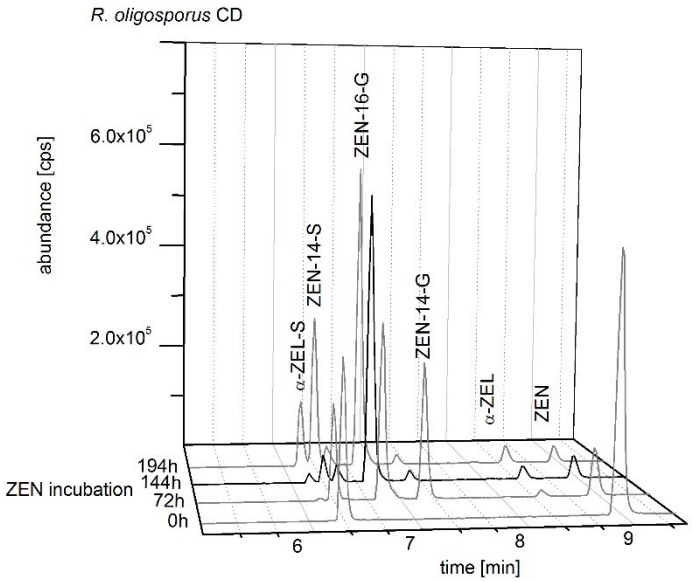


Figure 34. Reconstructed total ion chromatogram (TIC) with mass transitions of zearalenol (ZEL), $\alpha$-ZEL-sulfate ($\alpha$-ZEL-S), ZEL-glucoside, zearalenone (ZEN), ZEN-14-sulfate (ZEN-14-S), ZEN-14-glucoside (ZEN-14-G), and ZEN-16-glucoside (ZEN-16-G) analyzed in liquid media of *Rhizopus oligosporus* CD incubated with ZEN.

The reconstructed total ion chromatograms in Figures 32, 33, and 34 showed the conjugate formation of representative samples. The analyses were conducted in triplicate. The complete results are shown in the supplementary material.

*Cleanup by Liquid-Liquid-Extraction (LLE) and Preparative Chromatography*

For isolation of the ZEN conjugates the harvested media was first extracted by LLE with ethyl acetate. ZEN-14-G and ZEN-16-G were transferred into the organic phase with 99.8±0.1% and 87.2±0.3%, respectively. The extraction of ZEN-14-S was not sufficient with ethyl acetate (with only 50.1±0.5% recovery). Therefore, the efficiency of the extraction was optimized to 88.0±1.8% by adding $MgSO_4$ and NaCl.
In addition to the LLE, preparative chromatography was conducted as a further cleanup step. In Figure 35 the UV-chromatograms ($\lambda$ = 265 nm) of the extracted media of *A. oryzae* NBRC 100959, *R. oryzae* DSM 908, and *R. oligosporus* CD are shown. The peaks of ZEN-14-S, ZEN-14-G, and ZEN-16-G with retention times of 11.3 min, 16.5 min, and 7.7 min, respectively, are well separated and after fractionating the purity of each compound was improved. Especially, the preparative purification of ZEN-16-

G biosynthesis extract (Figure 35 (c)) led to the successful separation of the byproducts ZEN (RT 25.9 min), α-ZEL (RT 25.4 min), ZEN-14-S, α-ZEL-S (9.0 min), ZEN-14-G, and the possible ZEL glucoside (9.0 min) from the target compound.
The yields of the purified analytes were 49% ZEN-14-S, 67% ZEN-14-G and 39% ZEN-16-G.

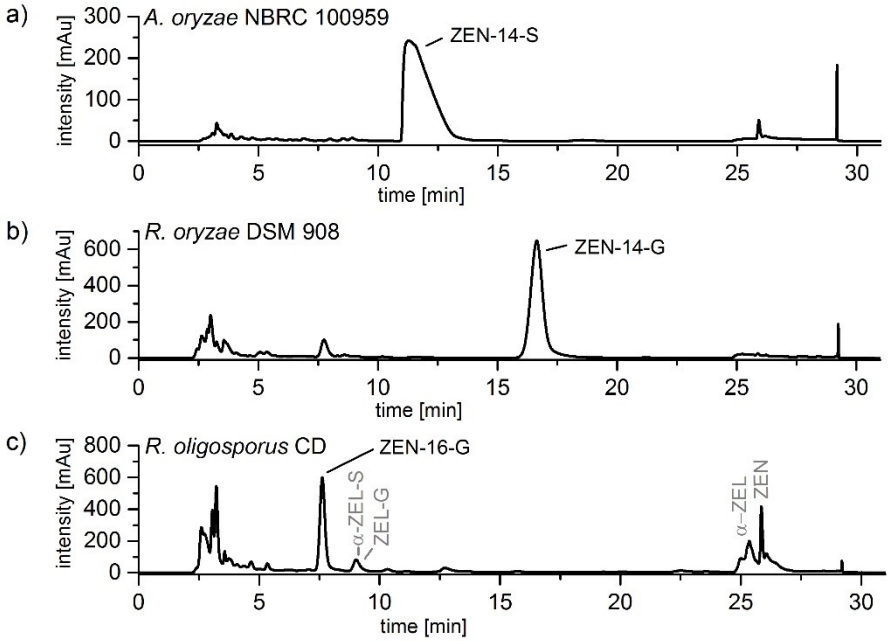


Figure 35. UV-chromatograms (λ = 265 nm) of the preparative separation (conducted on a Luna C18 reversed phase column; 250 mm x 21.2 mm; particle size 10 µm; pore size 100 Å) of extracted media from (a) *Aspergillus oryzae* NBRC 100959: Biosynthesis of zearalenone-14-sulfate (ZEN-14-S); (b) *Rhizopus oryzae* DSM 908: Biosynthesis of ZEN-14-glucoside (ZEN-14-G); (c) *Rhizopus oligosporus* CD: Biosynthesis of ZEN-16-glucoside (ZEN-16-G) with the byproducts ZEN, α-ZEL (α-zearalenol), α-ZEL-S (α-ZEL-sulfate), ZEL-G (ZEL glucoside).

*Structure Identification and Purity of ZEN-14-S, ZEN-14-G and ZEN-16-G*

Following the described biosynthesis with subsequent cleanup ZEN-14-S, ZEN-14-G, and ZEN-16-G were obtained as a slightly yellow solid. ZEN-14-S purity of ≥ 97% was determined by HPLC-UV at 227 nm by calculating the percentage of the peak area in relation to total area of peaks. The HPLC-UV purity at 227 nm of ZEN-14-G was ≥ 96%, and for ZEN-16-G a purity of ≥ 69% was measured. To evaluate purity, 1H-

NMR has also been used: purities of ≥ 73% ZEN-14-S, ≥ 82% ZEN-14-G, and ≥ 50% ZEN-16-G were obtained.
Structure identification was conducted by $^{1}H$ and $^{13}C$-NMR. For structure elucidation, spectra with the two-dimensional methods HH-COSY, HC-HMBC, and HC-HSQC were also recorded (supplementary material). Using these 2D methods the conjugation of ZEN on position 16 with the glucose molecule could be unambiguously proven by the HMBC crosspeak of the H-17/C-16 (H at the anomeric C of glucoside to the next bound phenoxy ring-C). The assignment of C-16 could been met by an HMBC crosspeak for H-15/C-16 and the lack of that for H-13/C-16. The assignment of C-14 in turn can be fixed by its strong HMBC-crosspeaks to both of the adjacent aromatic hydrogen atoms H-13 and H-15. Unambiguous assignment of ZEN-14-S was conducted by comparison of the $^{1}H$-spectrum with the spectrum of a ZEN-14-S standard (supplementary material) chemically synthesized with the method of Mikula *et al.* [22].

### 2.4.4 DISCUSSION

In this study an easy and cost-efficient biosynthesis for ZEN-14-S, ZEN-14-G, and ZEN-16-G was developed. Fungal strains with different ZEN formation and ZEN metabolization activities were used. In the first step, we searched for a strain producing consistent and high amounts of ZEN on a low cost solid medium. *F. graminearum* F1 was pointed out as a fungal strain which produces ZEN reproducible in a mg/g range on humid rice flour. In a straight forward approach, this biosynthesis was combined with the next biosynthetical step of conjugate formation. The ZEN contaminated flour can be directly used by adding the flour to the liquid media of conjugate biosynthesis.
For ZEN conjugate biosynthesis, fungal strains which convert ZEN to ZEN conjugates were used. In 2014, already eight fungal strains for ZEN metabolization were analyzed [149]. The results showed that the metabolite formation is very diverse even for closely related strains. In this study the *in vitro* screening was expanded. ZEN incubation time and ZEN addition to different growth phases of the fungi were varied. The data revealed for each ZEN conjugate one fungal strain which convert ZEN under defined conditions efficiently to ZEN-14-S, ZEN-14-G, and to ZEN-16-G (as major metabolite); yields of 49%, 67% and 39% could be achieved, respectively. Occurring losses are mainly caused by a saturation of the enzymatic reaction. The ZEN conversion rate decreases with higher initial ZEN amounts. However, there are

no relevant costs for ZEN in the developed consecutive biosynthesis. Further investigations should concentrate on upscaling the production on a biotechnological scale by increase of (flask) size and volume.
The purity of ZEN-14-G, ZEN-16-G, and ZEN-14-S was determined by HPLC-UV as 96%, 69%, and 97%, respectively. Purities additionally measured by $^{1}$H- and $^{13}$C-NMR were 82% for ZEN-14-G, 50% for ZEN-16-G and 73% for ZEN-14-S. As not only UV-active substances may represent impurities originating from fungal incubation samples, for the glucosides lower purity values are detected. Caused by the cleanup, the synthesized substances contain ammonium acetate, which is very hydrophilic. Therefore, the substances also contain residual $H_2O$. Additionally, the NMR spectra indicate impurities for ZEN-16-G and ZEN-14-S of small amounts (about 1-2%) of unknown substances which has a chemical structure containing a ZEN moiety.
For the very easy and fast cleanup of LLE with subsequent preparative chromatography, the results were very good. All the ZEN metabolites formed were well separated. Nevertheless, efficient strategies for chemical synthesis and biosynthesis of ZEN conjugates have already been developed. A chemical synthesis of ZEN-14-S and ZEN-16-G was conducted by Mikula *et al.* [22,23] and Michlmayr *et al.* [24] synthesized ZEN-14-G and ZEN-16-G in good purity. However, with the $^{1}$H-NMR purity of the conjugates known, also the standards obtained by our fungal biosynthesis can be used for accurate quantification or toxicological experiments.

One main advantage of this approach is the regio selctivity. Especially the 16-position of ZEN is difficult to conjugate in chemical synthesis, because the carbon atom is very inactive. Thus, biosynthesis is an appropriate alternative way for a targeted regioselective production of conjugated mycotoxins. While for plants it has been clarified which glucosyltransferases are responsible for the glucosylation of ZEN, the UGTs in *Rhizopus* or *Aspergillus* species are still unknown. As some *A. oryzae* species genomes have been sequenced, screening experiments could help to obtain information on which enzymes catalyze distinct conjugation reactions.
Additionally, the biosynthesis developed could be also used for biosynthesis of other metabolites like ZEL conjugates. The present results of the *in vitro* screening indicated the formation of a ZEL-glucoside by detection of the mass transitions and $\alpha$-ZEL-S was also formed as major metabolite by *Rhizopus oryzae* DSM 906. Nevertheless, more fungal strains should be screened for an exclusive formation and the cleanup must be optimized.

## 2.4.5 CONCLUSIONS

This study shows a new approach for the synthesis of ZEN conjugates. Fungal strains were successfully utilized for an economic targeted and regioselective biosynthesis of ZEN-14-S, ZEN-14-G and ZEN-16-G. No special laboratory equipment is needed. It is easy to handle and not cost intense. Additionally, costs for ZEN can be avoided, because ZEN biosynthesis by *F. graminearum* was combined with ZEN conjugate production by *Aspergillus* and *Rhizopus* species. Nevertheless, for the cleanup method the purities of the obtained standards are good, but especially for ZEN-16-G a further cleanup step should be conducted for improvement of its purity.

## 2.4.6 MATERIALS AND METHODS

*Chemicals and Media*

Potato dextrose agar (PDA) and potato dextrose broth (PDB) were purchased from Carl Roth GmbH + Co. KG (Karlsruhe, Germany). Rice flour was purchased from Biokorn GmbH + Co. KG (Aalen, Germany). ZEN was acquired from Tocris Bioscience (Bristol, England). A stock (1 mg $mL^{-1}$) and working (5 µg $mL^{-1}$) solution of ZEN was prepared as methanolic solution and stored at -20 °C. $\alpha$-ZEL was purchased from Sigma-Aldrich Chemie GmbH (Steinheim, Germany). ZEN-14-S, ZEN-14-G und ZEN-16-G as reference standard were kindly provided by Prof. Franz Berthiller (University of Natural Resources and Life Sciences, Vienna, Austria). Acetonitrile and methanol were of HPLC-grade and obtained from Th. Geyer (Renningen, Germany). Ethyl acetate p. a. and sodium chloride p. a. were also purchased from Th. Geyer (Renningen, Germany). Magnesium sulfate was acquired from Sigma Aldrich (Steinheim, Germany). Ammonium acetate was purchased from Mallinckrodt Baker Inc. (Griesheim, Germany). Ultrapure water was obtained from a Seralpur PRO 90 CN purification system by Seral (Ransbach-Baumbach, Germany). Deuterated dimethyl sulfoxide (99.8 atom-% D) was acquired from Merck Switzerland. Trimesic acid trimethyl ester were purchased from OrganoSpezialChemie GmbH Bitterfeld. It`s purity has been traced back to that of NIST standard MRM 350b by the inhouse $^{1}H$ qNMR method.

*HPLC-MS/MS Analysis*

HPLC-MS/MS (high-performance liquid chromatography hyphenated to tandem mass spectrometry) analysis was performed on a 1100 series HPLC system from Agilent Technologies (Waldbronn, Germany) connected to an API 4000 triple-quadrupole MS/MS system from Sciex (Framingham, MA, USA). The analytical column was a Synergi Polar-RP (150 mm x 3.0 mm, paricle size 4 µm, pore size 80 Å) in combination with a corresponding guard column (Phenomenex, Aschaffenburg, Germany). The column temperature was set to 30 °C. Solvent A was water with 5 mM ammonium acetate and solvent B acetonitrile/water (99:1; v/v) with 5 mM ammonium acetate. The gradient used was as follows: 0-2 min isocratic with 10% B, 2-4 min linear to 40% B, 4-10 min linear to 100% B, isocratic 10-13 min 100% B, shifting back to 10% B and reconditioning from 13-17 min. The flow rate of the mobile phase was 0.7 mL/min and 10 µL was used as standard injection volume. The ESI interface was operated in negative ionization mode at 450 °C with the following settings: curtain gas 20 psi, nebulizer gas 60 psi, heater gas 60 psi, ionization voltage -4500 V. MS/MS measurements were exclusively conducted in selected reaction monitoring (SRM) mode. Two mass transitions were recorded for each analyte: ZEN *m/z* 317.0 → 130.8 (declustering potential (DP) -15 V, collision energy (CE) -40 eV), *m/z* 317.0 → 174.8 (DP = -15 V, CE = -30 eV); ZEN-sulfate *m/z* 397.1 → 317.1 (DP = -65 V, CE = -30 eV), *m/z* 397.1 → 175.0 (DP = -65 V, CE = -50 eV); ZEN-glucoside *m/z* 479.1 → 317.0 (DP = -65 V, CE = -16 eV), *m/z* 479.1 → 130.8 (DP = -65 V, CE = -50 eV); ZEL *m/z* 319.2 → 174.0 (DP = -30 V, CE = -30 eV), *m/z* 319.2 → 160.0 (DP = -75 V, CE = -30 eV); ZEL-sulfate *m/z* 399.2 → 319.2 (DP = -30 V, CE = -30 eV), *m/z* 399.2 → 275.2 (DP = -30 V, CE = -40 eV); ZEL-glucoside *m/z* 481.2 → 319.2 (DP = -65 V, CE = -16 eV), *m/z* 481.2 → 275.2 (DP = -65 V, CE = -30 eV).

*In vitro-Screening of Aspergillus and Rhizopus Species*

Eight different fungal strains of the genera *Rhizopus* and *Aspergillus* (see Table 9) were screened for ZEN conjugate formation; ZEN addition to different fungal growth phases and time of harvest were varied.

Table 9. Fungal strains of *in vitro* screening.

| Species | Designation | Source |
|---|---|---|
| *Rhizopus oryzae* | DSM 906 | DSMZ * |
| *Rhizopus oryzae* | DSM 907 | DSMZ * |
| *Rhizopus oryzae* | DSM 908 | DSMZ * |
| *Rhizopus stolonifer* | DSM 855 | DSMZ * |
| *Rhizopus microsporus* var. *chinensis* | DSM 1834 | DSMZ * |
| *Rhizopus oligosporus* | CD (LMH 1133 T) | Hering *et al*. [25] |
| *Aspergillus oryzae* | DSM 1864 | DSMZ * |
| *Aspergillus oryzae* | NBRC 100959 | Nite Biological Resource Center (Tokio, Japan) |

* German Collection of Microorganisms and Cell Cultures (Braunschweig, Germany)

In the beginning of fungal growth only mycelia and no spores are produced (vegetative growth phase). Dependent on the fungal strains mycelia production stops after 2 - 4 days and the fungus starts sporulation (generative growth phase). Change of growth phase was detected by visual investigation of sporulation and detection of the pH value which changes from pH 3 (vegetative growth phase) to pH 7 (generative growth phase). ZEN conjugate formation was analyzed for ZEN addition to the vegetative growth phase (fungal incubation: 24 h) and for ZEN addition to generative growth phase (fungal incubation: 144 h).

Cultivation for biotransformation were conducted as follows: Liquid media (50 mL PDB) in 250-mL Erlenmeyer flasks were inoculated with pieces of mycelia. Fungal incubation was conducted for 24 h or 144 h at 30 °C in a New Brunswick Scientific Innova® 44 rotary shaker set to 150 rpm (Eppendorf AG, Hamburg, Germany). To each liquid culture 1 mL working solution of ZEN was added and incubation was continued for 6, 12, 24, 48, 72, 144 and 192 h. After incubation period, an aliquot of 1 mL was transferred to a 1.5-mL Eppendorf tube and centrifuged at 16 200 *g* for 10 min with an Eppendorf centrifuge 5415 R (Eppendorf AG, Hamburg, Germany). For protein precipitation, 500 µL ice-cold acetonitrile was added to 500 µL supernatant, stored over night at 4 °C and centrifuged at 11 500 *g* for 5 min with an Eppendorf MiniSpin Plus (Eppendorf AG, Hamburg, Germany). The supernatant was analyzed by HPLC-MS/MS.

*Biosynthesis of ZEN*

Three strains of *F. graminearum* were screened for ZEN production (see Table 10). Stock cultures were grown on potato dextrose agar (PDA) for 14 days at 23 °C. According to Plasencia and Mirocha which have shown a ZEN production by *F. graminearum* of 1.2 g/kg on rice, rice was chosen as incubation media in this study as well [146]. 30 g rice flour and 15 mL distilled water were added to 250-mL Erlenmeyer flask. The flask was closed with a cellulose plug and autoclaved for 20 min at 121 °C. The autoclaved media was inoculated with pieces of mycelia and incubated at 23 °C for 5, 10, 15, 20, 25 and 32 days. For 20, 25 and 32 days analyses in triplicate were conducted. ZEN biosynthesis was stopped by autoclaving the fungal incubation. Subsequently, the content of the flask was freeze dried and powdered. Analyzation of the ZEN amount was conducted by extraction of 2 g flour with 20 mL acetonitrile/water (80:20 v/v) for 3 h with 1/300 min at a horizontal shaker HS 501 digital (IKA®, Staufen, Germany). The supernatant was used for direct analysis by HPLC-MS/MS (see 5.2).

Table 10. *Fusarium graminearum* strains used for ZEN production screening [26]

| **Fungal strain** | **Isolate** | **Isolated by** |
|---|---|---|
| *F. graminearum* F1 | 37 | Gossmann, HU Berlin 1994 |
| *F. graminearum* F2 | 09-53b | Pogoda, Luxemburg 2009 |
| *F. graminearum* F3 | MUCL 11946 | Kinnard, Belgien 1969 |

As described by Brodehl *et al.* [7] ZEN-14-S was determined using relative response factor of 11 for ZEN-14-S to ZEN. Response factor was estimated by comparing the MS/MS peak area before and after quantitative sulfate ester cleavage. ZEN was determined by external calibration using the commercially available standard substances

*Biosynthesis of ZEN conjugates*

ZEN biosynthesis was coupled with ZEN conjugate biosynthesis by adding ZEN contaminated rice flour into liquid media with subsequent fungal incubation. *A. oryzae* NBRC 100959, *R. oryzae* DSM 908 and *R. oligosporus* CD were utilized for

biosynthesis of ZEN-14-S (incubation parameter: 72 h, 150 rpm, 30 °C), ZEN-14-G (incubation parameter: 24 h, 150 rpm, 30 °C) and ZEN-16-G (incubation parameter: 144 h, 150 rpm, 30 °C), respectively. ZEN contaminated rice flour produced by *F. graminearum* F1 (see 5.3.) with a total amount of 4 mg ZEN was added to 50 mL PDB in a 250-mL Erlenmeyer flask (c(ZEN) = 80 mg/L).
Prior to this, ZEN conversion in consecutive biosynthesis was analyzed by screening over a period of 9 days. The ZEN containing liquid media was autoclaved (120 °C, 20 min), inoculated with pieces of mycelia and incubated at 30 °C in a New Brunswick Scientific Innova® 44 rotary shaker set to 150 rpm Sampling was conducted after 0, 6, 24, 48 72, 140, 192 and 216 h. Analyzation of the media samples was conducted analogues to media samples of the *in vitro* screening.

*Liquid-Liquid-Extraction (LLE) and Preparartive Chromatography*

The liquid fungal culture of ZEN conjugate biosynthesis was centrifuged at 3101 *g* for 10 min with a Sigma 6K15 centrifuge (Sigma-Aldrich GmbH, Steinheim, Germany). The supernatant was extracted by LLE. 20 mL of liquid media were extracted three times was 20 mL ethyl acetate on a horizontal shaker with 1/300 min for 30 min. The extract was evaporated to dryness under a steam of nitrogen and subsequently dissolved in $H_2O$/ACN (70/30; v/v) and filtered with Chromavil® A-20/25 syringe filter (pore size 0.2 µm, diameter 25 mm) purchased from Macherey-Nagel (Düren, Germany). For ZEN-14-S the procedure of LLE was modified for improvement of extraction efficiency. Before ethyl acetate extraction 2 g of sodium chloride and 8 g of magnesium sulfate were added to the media and cooled in ice water for 2 min. Subsequently, media extraction is conducted as described above.
The concentrated extract was further purified by preparative chromatography. The HPLC was equipped with a fraction collector, a diode array detector (DAD) and a single quadrupole MS (Agilent Technologies 6130 Quadrupole LC/MS). HPLC-DAD analyses were conducted using an Agilent 1200 series HPLC (Agilent Technologies, Waldbronn, Germany). HPLC separation of ZEN and their metabolites was conducted on a Luna C18 (250 mm x 21.2 mm, particle size 10 µm, pore size 100 Å) reversed phase column (Phenomenex, Aschaffenburg, Germany) in combination with a corresponding guard column. The column temperature was set to 30 °C and the injection volume was 500 µL. The following gradient was applied with a flow rate of 20 mL/min: 0-22 min isocratic with 30% B, then from 22-22.5 min switched linear to 100% B, following by a wash out step of 2 min from 22.5-26 min and after shifting back to 30% B from 26-26.5 min a reconditioning step from 26.5-31 min followed.

Mobile phase A was water with 5 mM ammonium acetate and mobile phase B acetonitrile/water (99:1; v/v) with 5 mM ammonium acetate. The ESI interface was operated in negative-ionization mode at 250 °C with the following settings: nebulizer gas 35 psi, ionization voltage -3000 V. MS measurements were conducted in scan mode 100-700 *m/z*. The compounds were collected by mass-based fractionation set to *m/z* 397.1 for ZEN-14-S and *m/z* 479.1 for ZEN-14-G and ZEN-16-G.

*NMR Analysis*

Confirmation of ZEN-14-S, ZEN-14-G, and ZEN-16-G structure was conducted by nuclear magnetic resonance spectroscopy (NMR). NMR spectra were recorded in DMSO-$d_6$ on a Bruker Avance 600 MHz WB NMR spectrometer (Bruker BioSpin GmbH, Rheinstetten, Germany) equipped with a 5 mm BBI 600 MHz W2 (Z-gradient, BTO) probehead for $^{1}H$ and 2D measurements as well as a 5 mm BBO 600 MHz W2 (BTO) probehead for $^{13}C$ NMR, operating at 600.2 MHz for $^{1}H$ and 150.9 MHz for $^{13}C$. Data were recorded using TopSpin 2.1 and evaluated by means of TopSpin 3.1 software (Bruker BioSpin GmbH). Chemical shifts were established based on 1H and 13C signals of TMS = 0 ppm (tetramethylsilane). To evaluate the purities of the synthesized standards $^{1}H$-qNMR were conducted using trimesic acid trimethyl ester as standard.

*Purity of ZEN-14-S, ZEN-14-G and ZEN-16-G*

The purity was determined by HPLC-UV. The analyses were performed on a system from Agilent Technologies (Waldbronn, Germany) with a 1260 infinity quaternary pump, a 1100 series autosampler and a 1200 series column oven connected to a 1200 series DAD. The analytical column was a Gemini C18-NX (150 mm x 2.0 mm, paricle size 3 µm, pore size 110 Å) in combination with a corresponding guard column (Phenomenex, Aschaffenburg, Germany). The column temperature was set to 35 °C. Solvent A was water with 5 mM ammonium acetate and solvent B acetonitrile/water (99:1; v/v) with 5 mM ammonium acetate. The gradient used was as follows: 0-3 min isocratic with 10% B, switch from 3-3.1 min to 25% B, 3.1-16 min isocratic with 25% B, 16-25 min linear to 100% B, isocratic 25-29 min 100% B, shifting back to 10% B from 29-29.1 min and reconditioning from 29.1-36 min. The flow rate of the mobile phase was 0.25 mL/min and 20 µL was used as standard injection volume.

## LICENSE



## 2.4.7 SUPPLEMENTARY MATERIALS:

The following are available online at www.mdpi.com/link, Figure 36: Formation of ZEN-14-sulfate, ZEN-14-glucoside, ZEN-16-glucoside and $\alpha$-ZEL-sulfate by *Rhizopus oryzae* DSM 906, DSM 907 and DSM 908, *R. oligosporus* CD, *Aspergillus oryzae* DSM 1864, *A. oryzae* NBRC 100959, *R. microsporus* var. *chinensis* DSM 1834 and *R. stolonifer* DSM 855 after addition of 1 mL ZEN solution (c = 5 µg/mL) to 50 mL fungal culture in vegetative and generative growth phase and subsequent ZEN incubation over a period of 10 to 12 days, Figure 37: Formation of ZEN-14-sulfate, ZEN-14-glucoside, ZEN-16-glucoside and $\alpha$-ZEL-sulfate by *Aspergillus oryzae* NBRC 100959 after addition of ZEN contaminated rice flour (containing 4 mg ZEN) to 50 mL potato dextrose liquid media and subsequent fungal incubation over a period of 9 days, Figure 38: Formation of ZEN-14-sulfate, ZEN-14-glucoside, ZEN-16-glucoside and $\alpha$-ZEL-sulfate by *Rhizopus oryzae* DSM 908 after addition of ZEN contaminated rice flour (containing 4 mg ZEN) to 50 mL potato dextrose liquid media and subsequent fungal incubation over a period of 9 days, Figure 39: Formation of ZEN-14-sulfate, ZEN-14-glucoside, ZEN-16-glucoside and $\alpha$-ZEL-sulfate by *Rhizopus oligosporus* CD after addition of ZEN contaminated rice flour (containing 4 mg ZEN) to 50 mL potato dextrose liquid media and subsequent fungal incubation over a period of 9 days, Figure 40: $^{1}$H-qNMR spectrum of ZEN-14-G in DMSO-d6; standard: trimesic acid trimethyl ester, Figure 41: HH-COSY spectrum of ZEN-14-G, Figure 42: HC-HSQC spectrum of ZEN-14-G, Figure 43: HC-HMBC spectrum of ZEN-14-G, Figure 44: $^{1}$H-qNMR spectrum of ZEN-14-S in DMSO-d6; standard: trimesic acid trimethyl ester, Figure 45: HH-COSY spectrum of ZEN-14-S, Figure 46: HC-HSQC spectrum of ZEN-14-S, Figure 47: HC-HMBC spectrum of ZEN-14-S, Figure 48: $^{1}$H-qNMR spectrum of ZEN-16-G in DMSO-d6; standard: trimesic acid trimethyl ester, Figure 49: HH-COSY spectrum of ZEN-16-G, Figure 50: HC-HSQC spectrum of ZEN-16-G, Figure 51: HC-HMBC spectrum of ZEN-16-G, Table 11: $^{1}$H and $^{13}$C NMR shifts of ZEN-14-G, Table

12: $^{1}H$ and $^{13}C$ NMR shifts of ZEN-14-S, Table 13: $^{1}H$ and $^{13}C$ NMR shifts of ZEN-16-G, Figure 52: Comparison of the $^{1}H$-NMR spectra of the biosynthesized ZEN-14-S (above) and the chemically synthesized ZEN-14-S standard (below).

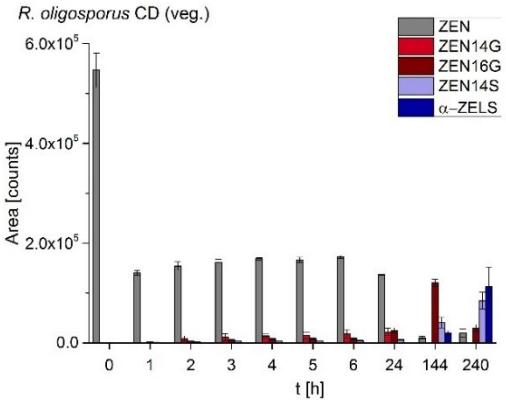
R. oligosporus CD (veg.)
ZEN
ZEN14G
ZEN16G
ZEN14S
α–ZELS
Area [counts]
6.0x10^5
4.0x10^5
2.0x10^5
0.0
0 1 2 3 4 5 6 24 144 240
t [h]

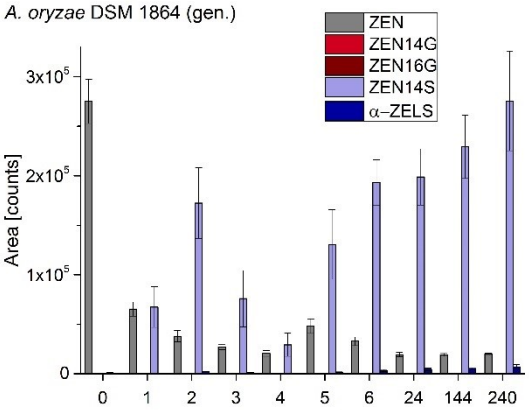
A. oryzae DSM 1864 (gen.)
ZEN
ZEN14G
ZEN16G
ZEN14S
α–ZELS
Area [counts]
3x10^5
2x10^5
1x10^5
0
0 1 2 3 4 5 6 24 144 240
t [h]

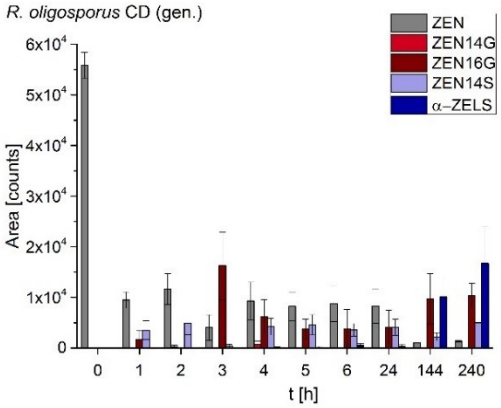
R. oligosporus CD (gen.)
ZEN
ZEN14G
ZEN16G
ZEN14S
α–ZELS
Area [counts]
6x10^4
5x10^4
4x10^4
3x10^4
2x10^4
1x10^4
0
0 1 2 3 4 5 6 24 144 240
t [h]

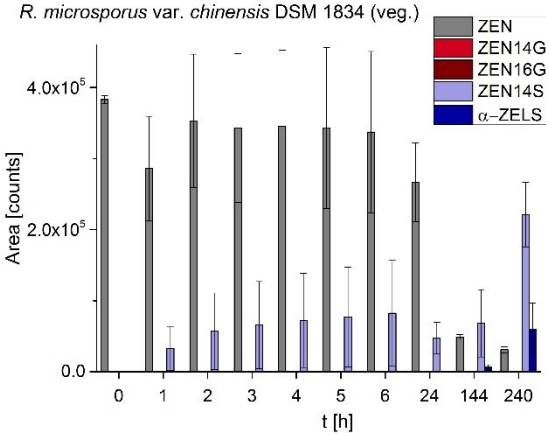
R. microsporus var. chinensis DSM 1834 (veg.)
ZEN
ZEN14G
ZEN16G
ZEN14S
α–ZELS
Area [counts]
4.0x10^5
2.0x10^5
0.0
0 1 2 3 4 5 6 24 144 240
t [h]

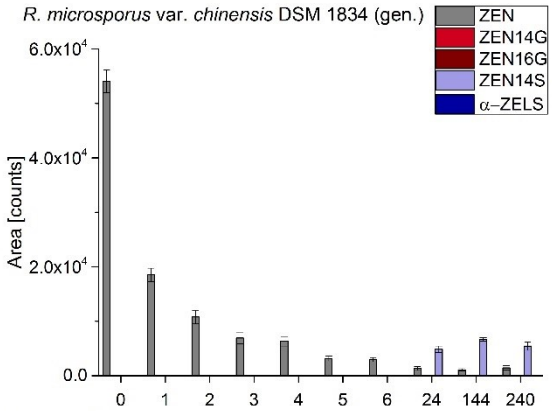
R. microsporus var. chinensis DSM 1834 (gen.)
ZEN
ZEN14G
ZEN16G
ZEN14S
α–ZELS
Area [counts]
6.0x10^4
4.0x10^4
2.0x10^4
0.0
0 1 2 3 4 5 6 24 144 240
t [h]

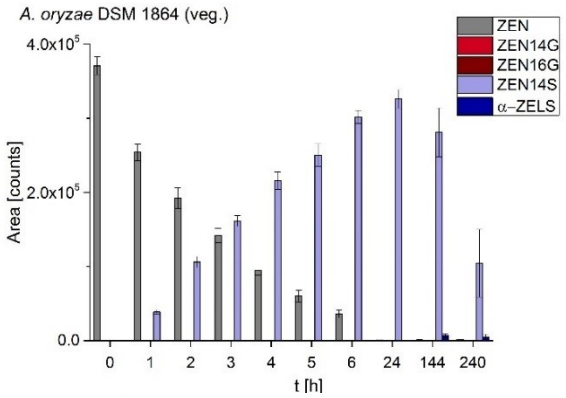
A. oryzae DSM 1864 (veg.)
ZEN
ZEN14G
ZEN16G
ZEN14S
α–ZELS
Area [counts]
4.0x10^5
2.0x10^5
0.0
0 1 2 3 4 5 6 24 144 240
t [h]

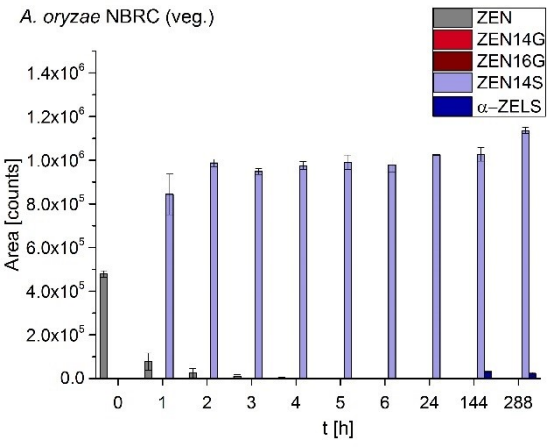
A. oryzae NBRC (veg.)
ZEN
ZEN14G
ZEN16G
ZEN14S
α–ZELS
Area [counts]
1.4x10^6
1.2x10^6
1.0x10^6
8.0x10^5
6.0x10^5
4.0x10^5
2.0x10^5
0.0
0 1 2 3 4 5 6 24 144 288
t [h]

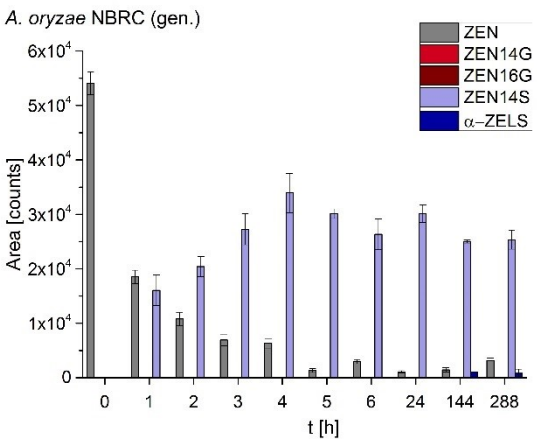
A. oryzae NBRC (gen.)
ZEN
ZEN14G
ZEN16G
ZEN14S
α–ZELS
Area [counts]
6x10^4
5x10^4
4x10^4
3x10^4
2x10^4
1x10^4
0
0 1 2 3 4 5 6 24 144 288
t [h]

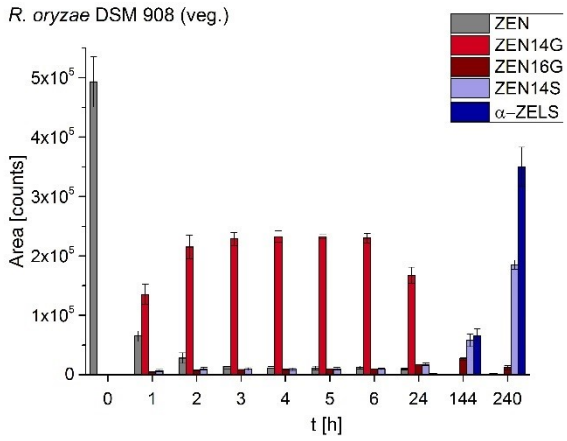
R. oryzae DSM 908 (veg.)
ZEN
ZEN14G
ZEN16G
ZEN14S
α–ZELS
Area [counts]
5x10^5
4x10^5
3x10^5
2x10^5
1x10^5
0
0 1 2 3 4 5 6 24 144 240
t [h]

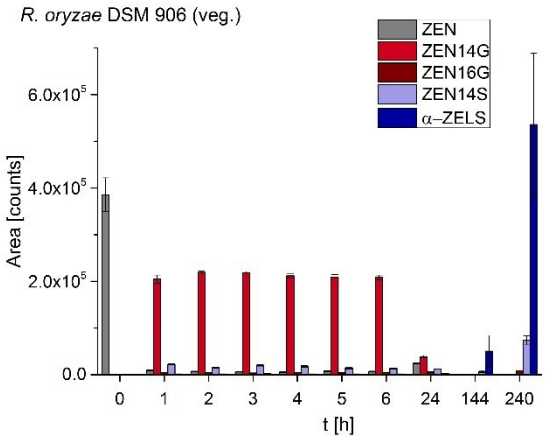
R. oryzae DSM 906 (veg.)
ZEN
ZEN14G
ZEN16G
ZEN14S
α–ZELS
Area [counts]
6.0x10^5
4.0x10^5
2.0x10^5
0.0
0 1 2 3 4 5 6 24 144 240
t [h]

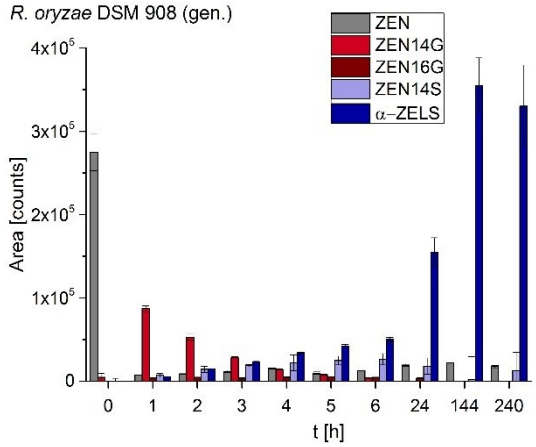
R. oryzae DSM 908 (gen.)
ZEN
ZEN14G
ZEN16G
ZEN14S
α–ZELS
Area [counts]
4x10^5
3x10^5
2x10^5
1x10^5
0
0 1 2 3 4 5 6 24 144 240
t [h]

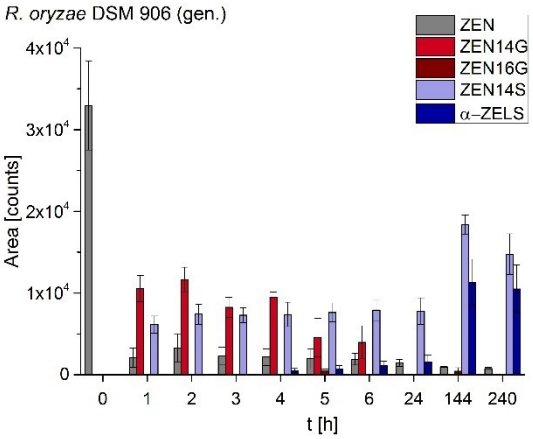
R. oryzae DSM 906 (gen.)
ZEN
ZEN14G
ZEN16G
ZEN14S
α–ZELS
Area [counts]
4x10^4
3x10^4
2x10^4
1x10^4
0
0 1 2 3 4 5 6 24 144 240
t [h]

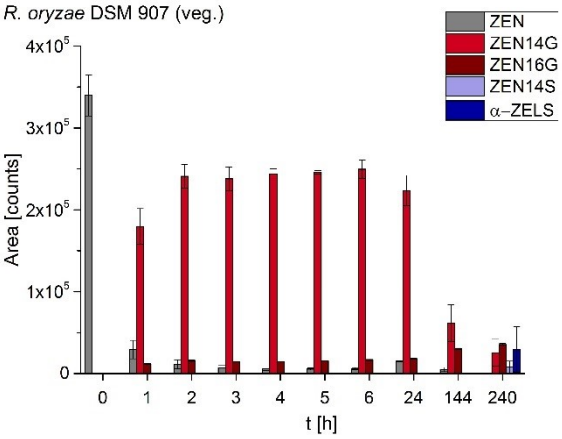
R. oryzae DSM 907 (veg.)
ZEN
ZEN14G
ZEN16G
ZEN14S
α–ZELS
Area [counts]
4x10^5
3x10^5
2x10^5
1x10^5
0
0 1 2 3 4 5 6 24 144 240
t [h]

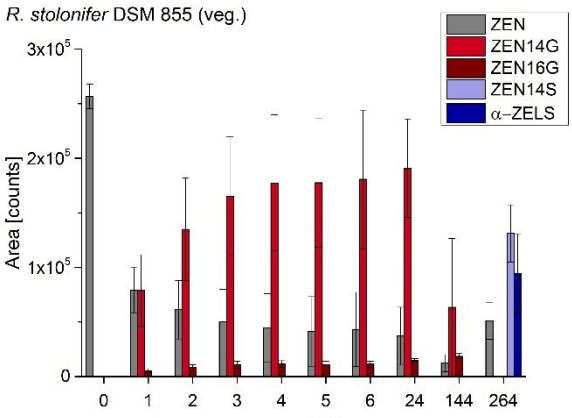
R. stolonifer DSM 855 (veg.)
ZEN
ZEN14G
ZEN16G
ZEN14S
α–ZELS
Area [counts]
3x10^5
2x10^5
1x10^5
0
0 1 2 3 4 5 6 24 144 264
t [h]

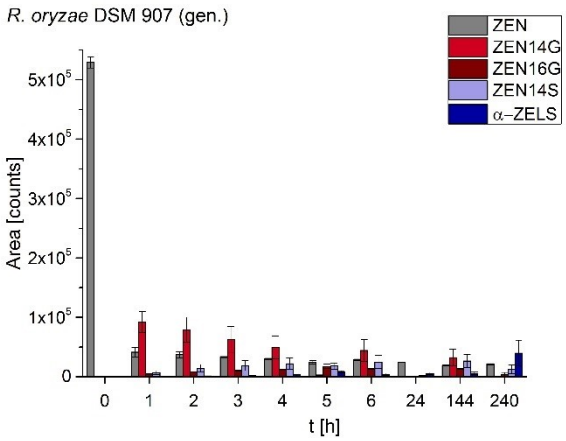
R. oryzae DSM 907 (gen.)
ZEN
ZEN14G
ZEN16G
ZEN14S
α–ZELS
Area [counts]
5x10^5
4x10^5
3x10^5
2x10^5
1x10^5
0
0 1 2 3 4 5 6 24 144 240
t [h]

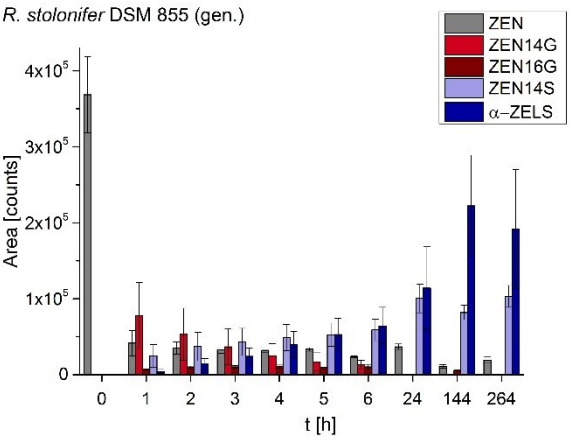
R. stolonifer DSM 855 (gen.)
ZEN
ZEN14G
ZEN16G
ZEN14S
α–ZELS
Area [counts]
4x10^5
3x10^5
2x10^5
1x10^5
0
0 1 2 3 4 5 6 24 144 264
t [h]

Figure 36. Formation of ZEN-14-sulfate (ZEN14S), ZEN-14-glucoside (ZEN14G), ZEN-16-glucoside (ZEN16G) and $\alpha$-ZEL-sulfate ($\alpha$-ZELS) by *Rhizopus oryzae* DSM 906, DSM 907 and DSM 908, *R. oligosporus* CD, *Aspergillus oryzae* DSM 1864, *A. oryzae* NBRC 100959, *R. microsporus* var. *chinensis* DSM 1834 and *R. stolonifer* DSM 855 after addition of 1 mL zearalenone (ZEN) solution (c = 5 µg/mL) to 50 mL fungal culture in vegetative (veg.) and generative (gen.) growth phase and subsequent ZEN incubation over a period of 10 to 12 days ; analyses were conducted in triplicate; a response factor for ZEN14S/ZEN of 11 and for $\alpha$-ZEL-S/ZEN of 2.3 was applied; bars represent mean values ± SEM (standard error of the mean).

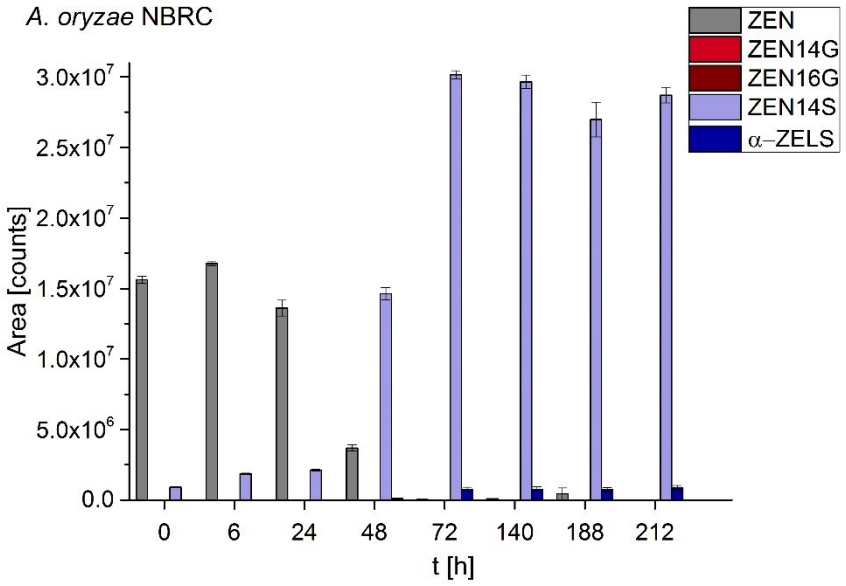


Figure 37. Formation of ZEN-14-sulfate (ZEN14S), ZEN-14-glucoside (ZEN14G), ZEN-16-glucoside (ZEN16G) and $\alpha$-ZEL-sulfate ($\alpha$-ZELS) by *Aspergillus oryzae* NBRC 100959 after addition of zearalenone (ZEN) contaminated rice flour (containing 4 mg ZEN) to 50 mL potato dextrose liquid media and subsequent fungal incubation over a period of 9 days; analyses were conducted in triplicate; a response factor for ZEN14S/ZEN of 11 was applied; bars represent mean values ± SEM (standard error of the mean).

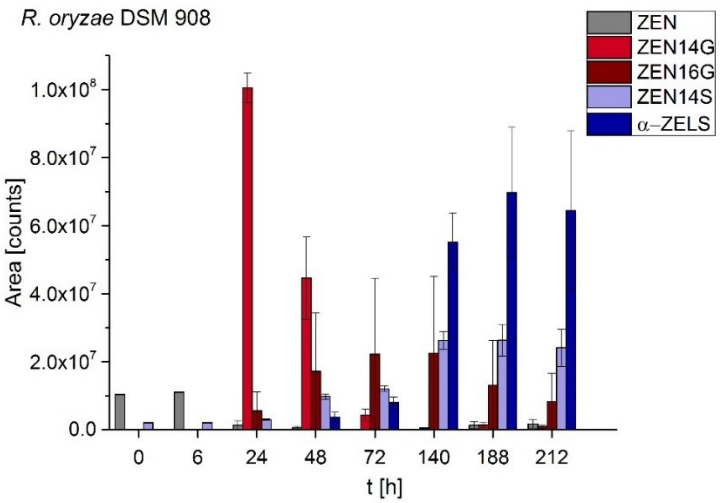


Figure 38. Formation of ZEN-14-sulfate (ZEN14S), ZEN-14-glucoside (ZEN14G), ZEN-16-glucoside (ZEN16G) and $\alpha$-ZEL-sulfate ($\alpha$-ZELS) by *Rhizopus oryzae* DSM 908 after addition of zearalenone (ZEN) contaminated rice flour (containing 4 mg ZEN) to 50 mL potato dextrose liquid media and subsequent fungal incubation over a period of 9 days; analyses were conducted in triplicate; a response factor for ZEN14S/ZEN of 11 was applied; bars represent mean values ± SEM (standard error of the mean).

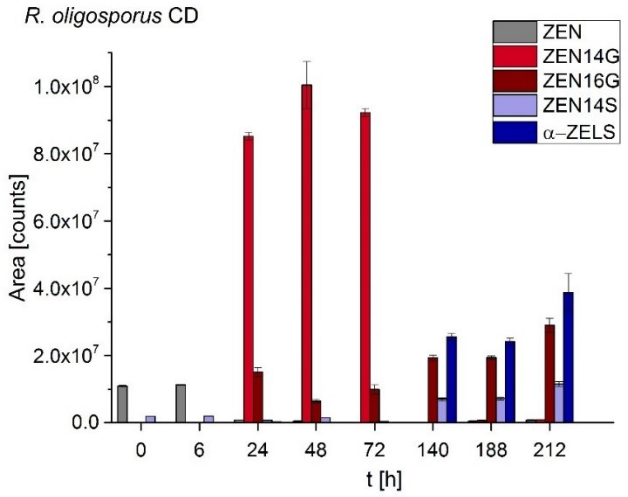


Figure 39. Formation of ZEN-14-sulfate (ZEN14S), ZEN-14-glucoside (ZEN14G), ZEN-16-glucoside (ZEN16G) and $\alpha$-ZEL-sulfate ($\alpha$-ZELS) by *Rhizopus oligosporus* CD after addition of zearalenone (ZEN) contaminated rice flour (containing 4 mg ZEN) to 50 mL potato dextrose liquid media and subsequent fungal incubation over a period of 9 days; analyses were conducted in triplicate; a response factor for ZEN14S/ZEN of 11 was applied; bars represent mean values ± SEM (standard error of the mean).

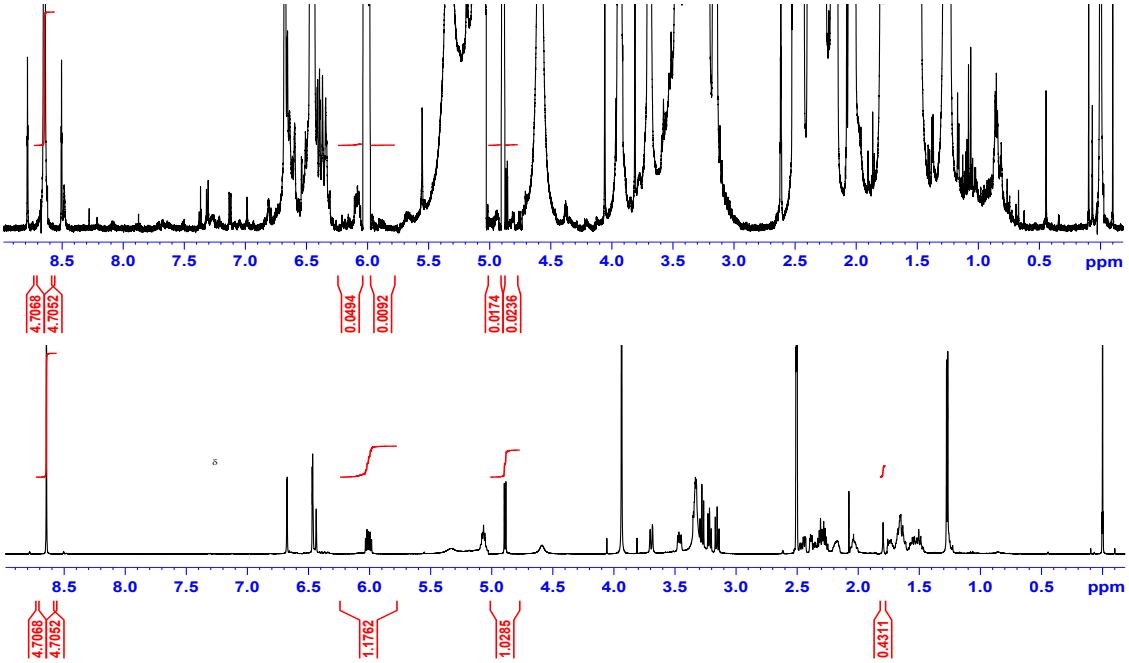


Figure 40. $^{1}$H-qNMR spectrum of ZEN-14-G in DMSO-d6; standard: trimesic acid trimethyl ester.

Table 11. $^{1}$H and $^{13}$C NMR shifts of ZEN-14-G.

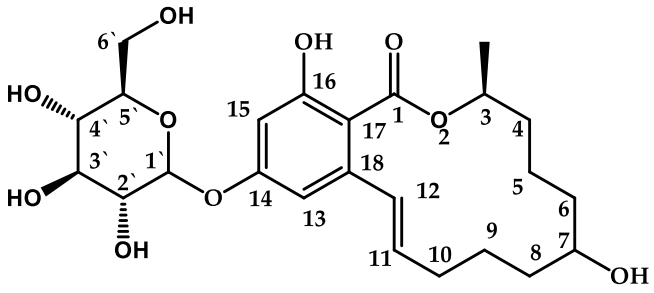


| position | $^{1}$H | mult | $^{13}$C |
|---|---|---|---|
| **1** | | | 168.3 |
| **3** | 5.07 | dqd, 8.7, | 71.5 |
| **3-CH$_3$** | 1.27 | d, 6.3 Hz | 19.8 |
| **4** | 1.51, | m | 34.2 |
| **5** | 1.60 | m | 20.9 |

| | | | |
|---|---|---|---|
| **6** | 2.28, | m | 42.9 |
| **7** | | | 210.5 |
| **8** | 2.37 | ddd, 17.7, | 36.5 |
| | 2.46 | ddd, 17.7, | |
| **9** | 1.67, | m | 20.9 |
| **10** | 2.03, | m | 30.9 |
| **11** | 6.01 | dt, 15.5, 7.3 | 132.8 |
| **12** | 6.45 | dt, 15.7, 1.5 | 133.4 |
| **13** | 6.68 | d, 2.3 Hz | 105.0 |
| **14** | | | 159.7 |
| **15** | 6.47 | d, 2.3 Hz | 102.6 |
| **16** | | | 158.5 |
| **17** | | | 111.5 |
| **18** | | | 138.3 |
| **1`** | 4.89 | d, 7.7 Hz | 100.1 |
| **2`** | 3.22 | t, 8.1 Hz | 73.1 |
| **3`** | 3.28 | t, 8.9 Hz | 76.5 |
| **4`** | 3.16 | t, 9.3 Hz | 69.7 |
| **5`** | 3.34 | m | 77.1 |
| **6`** | 3.46 | dd, 11.6, 5.8 | 60.6 |
| | 3.69 | dd, 11.6, 1.5 | |

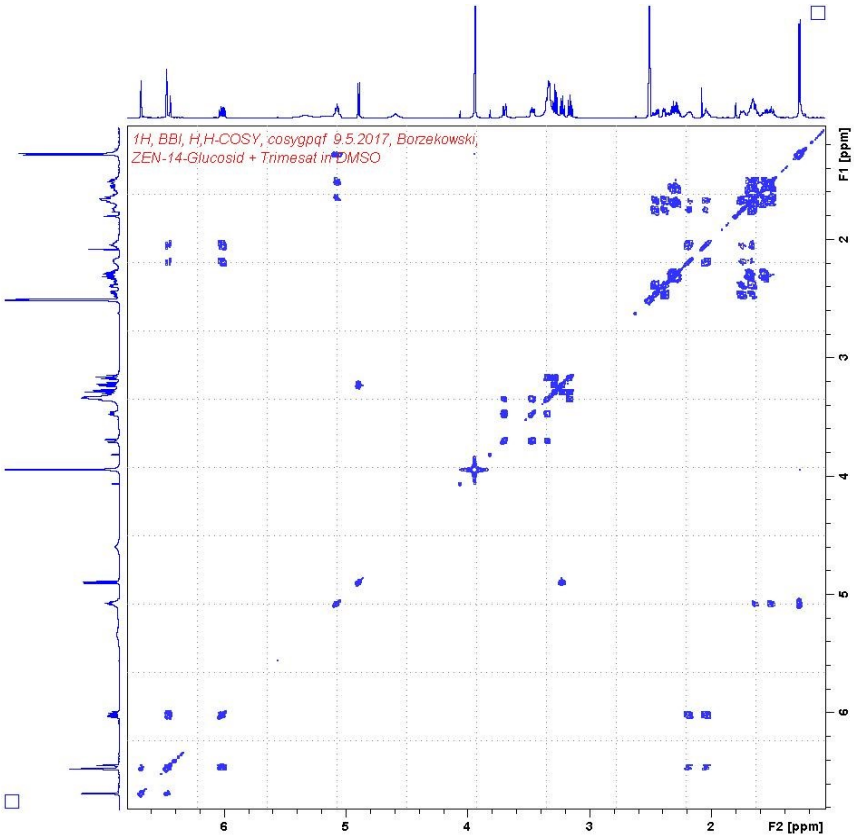


Figure 41. HH-COSY spectrum of ZEN-14-G.

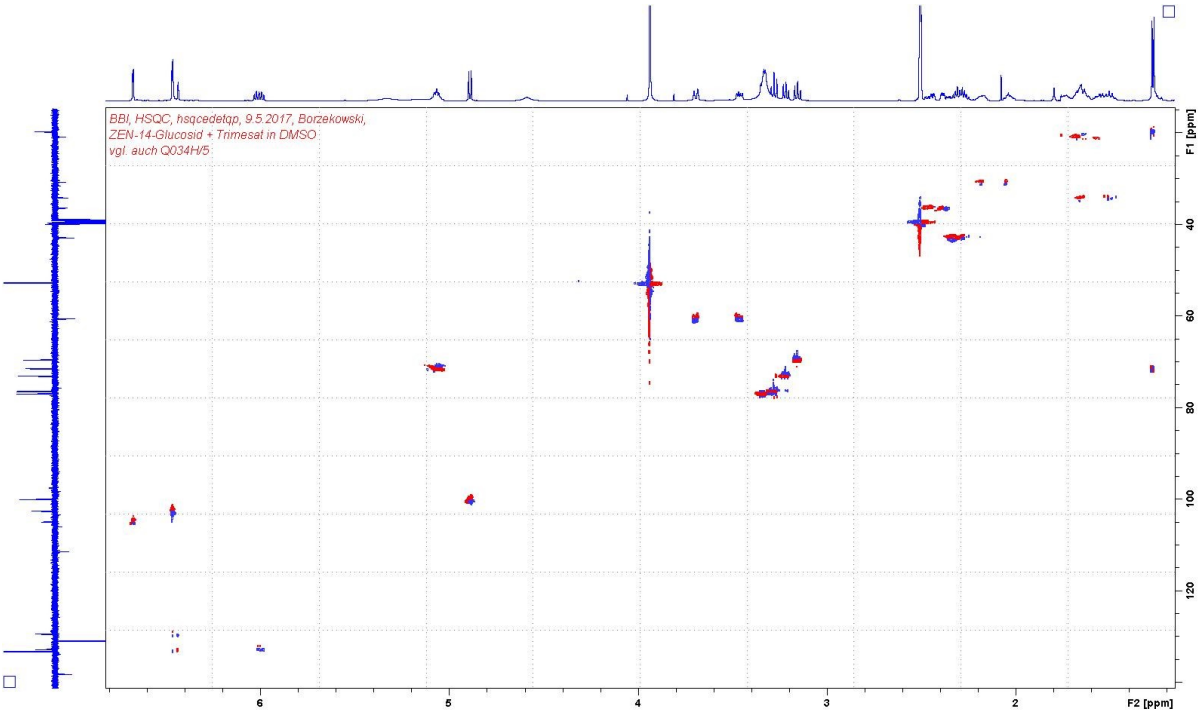


Figure 42. HC-HSQC spectrum of ZEN-14-G.

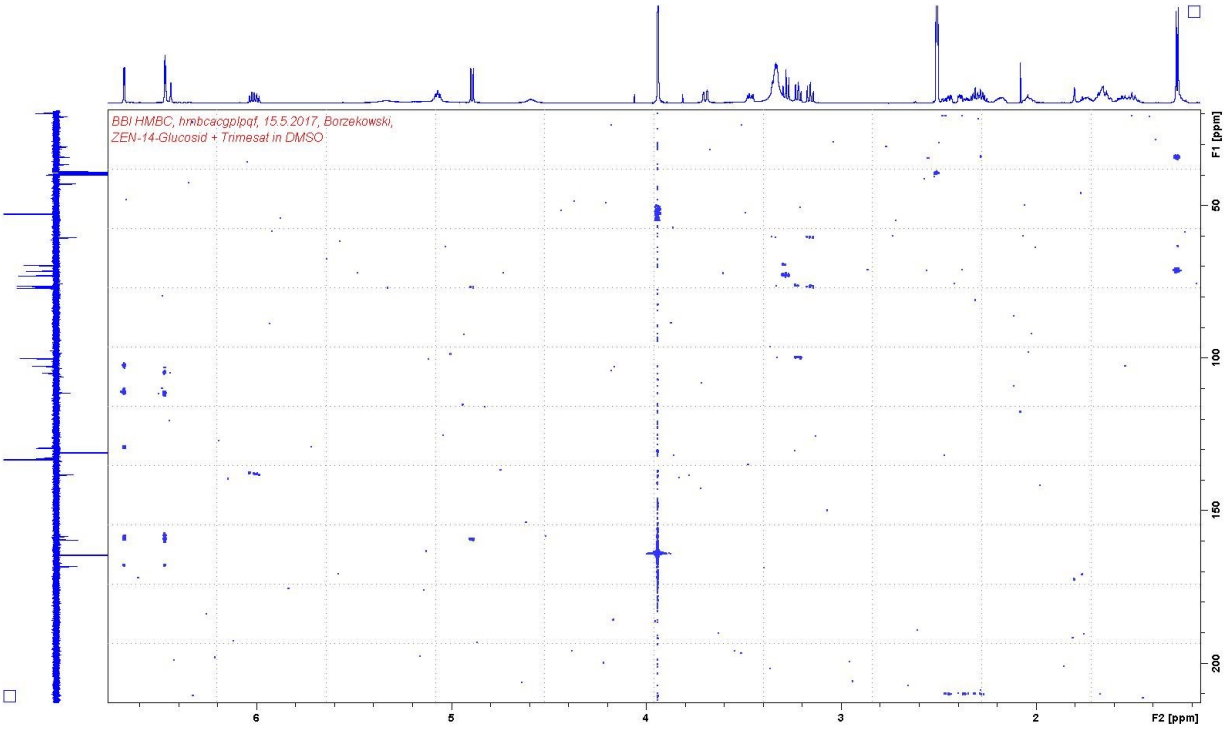


Figure 43. HC-HMBC spectrum of ZEN-14-G.

Table 12. $^{1}H$ and $^{13}C$ NMR shifts of ZEN-14-S.

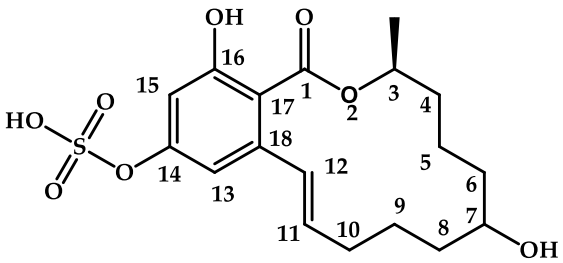


| position | $^{1}H$ | mult | $^{13}C$ |
|---|---|---|---|
| **1** | | | 167.9 |
| **3** | 5.01 | dqd, 8.7, | 71.1 |
| **3-CH$_3$** | 1.26 | d, 6.3 Hz | 19.7 |
| **4** | 1.50, | m | 34.2 |

| | | | |
|---|---|---|---|
| **5** | 1.54, | m | 20.8 |
| **6** | 2.26, | m | 43.1 |
| **7** | | | 210.6 |
| **8** | 2.30, | m | 35.6 |
| **9** | 1.61, | m | 20.9 |
| **10** | 1.99, | m | 30.7 |
| **11** | 5.93 | ddd, 15.6, | 132.3 |
| **12** | 6.35 | dd, 15.6, 3.1 | 129.0 |
| **13** | 6.77 | d, 2.1 Hz | 108.0 |
| **14** | | | 155.6 |
| **15** | 6.73 | d, 2.1 Hz | 106.2 |
| **16** | | | 156.7 |
| **17** | | | 113.7 |
| **18** | | | 136.6 |

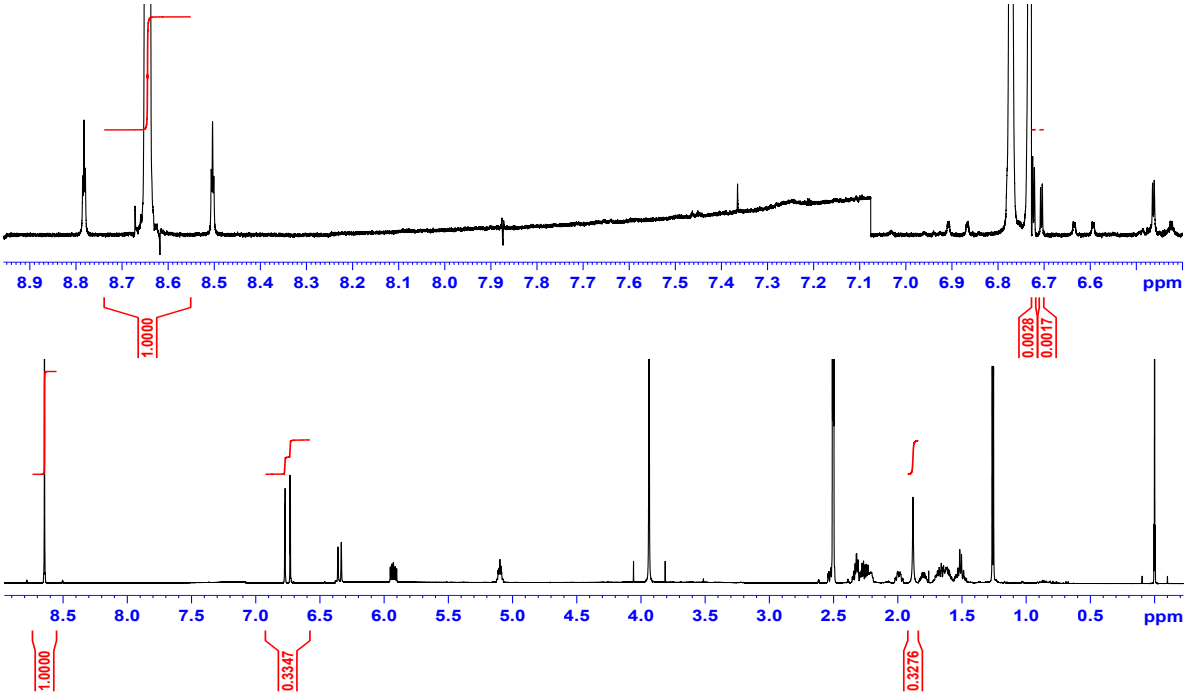


Figure 44. $^{1}$H-qNMR spectrum of ZEN-14-S in DMSO-d6; standard: trimesic acid trimethyl ester.

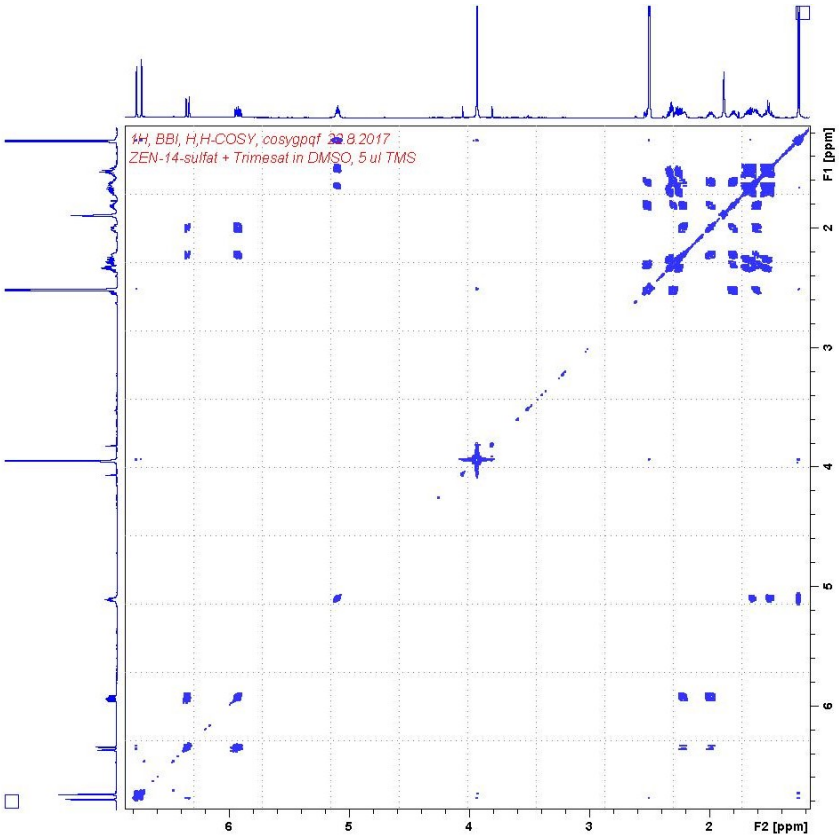


Figure 45. HH-COSY spectrum of ZEN-14-S.

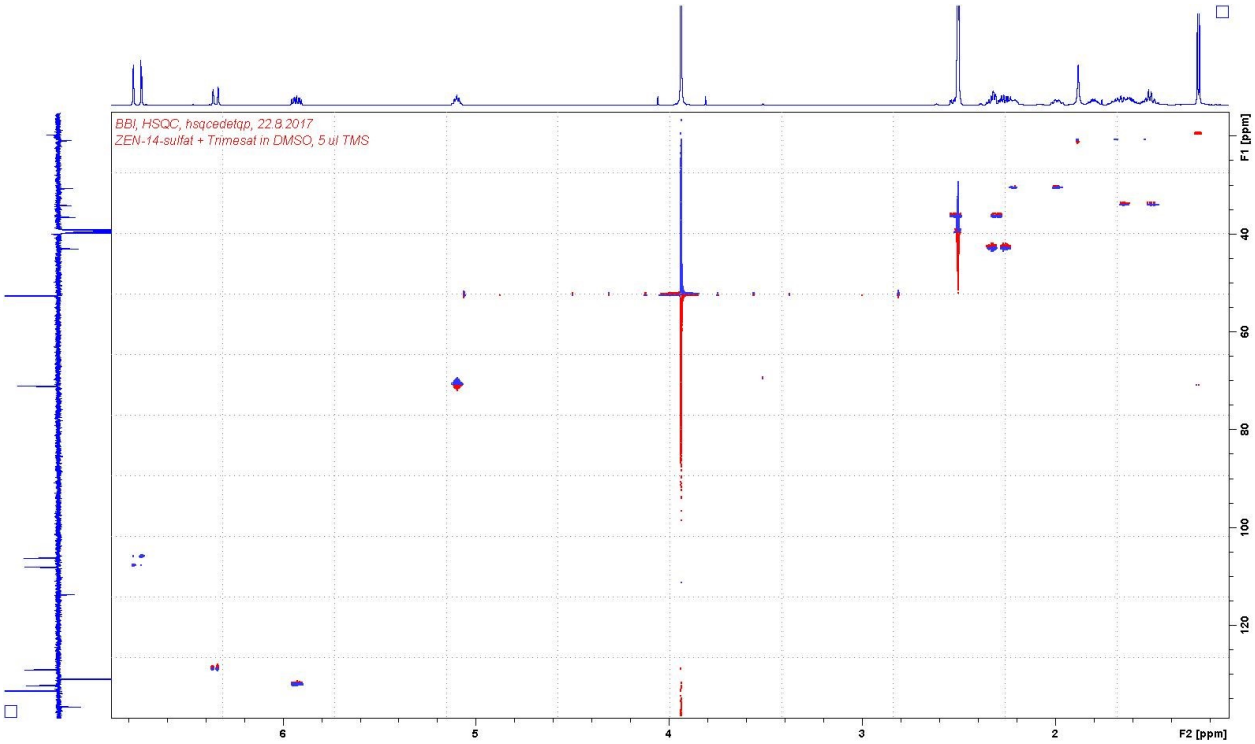


Figure 46. HC-HSQC spectrum of ZEN-14-S.

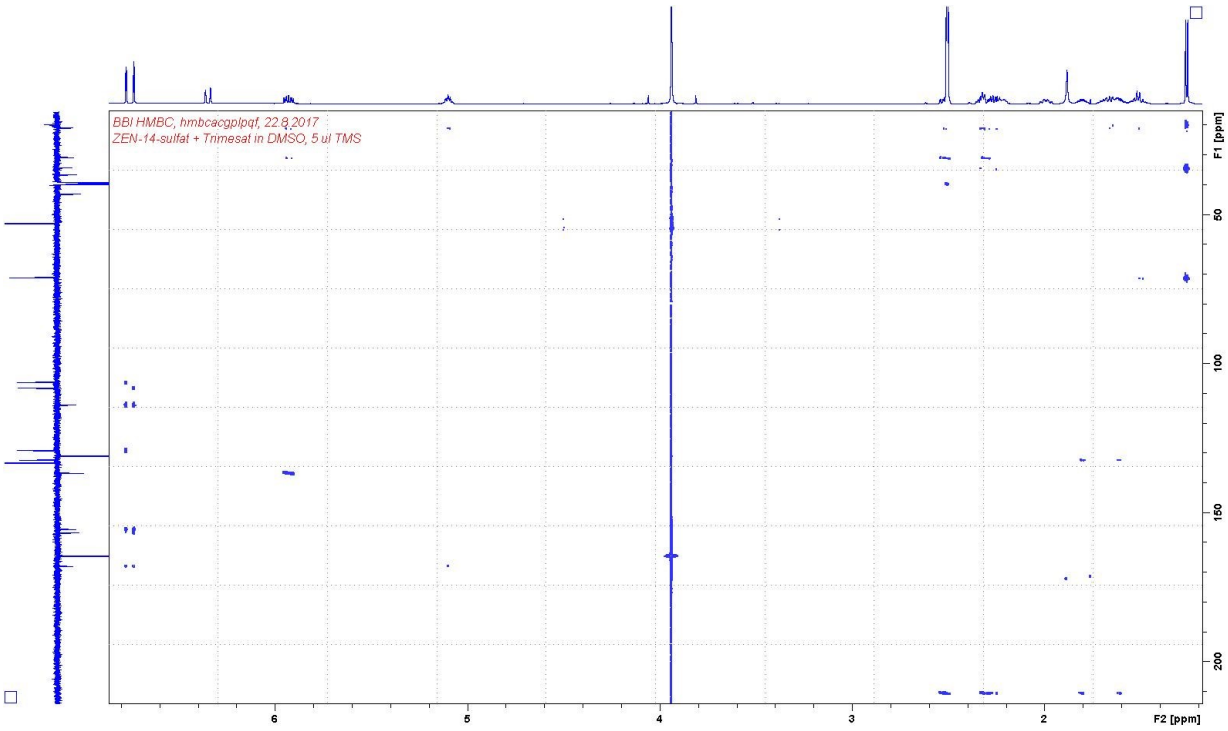


Figure 47. HC-HMBC spectrum of ZEN-14-S.

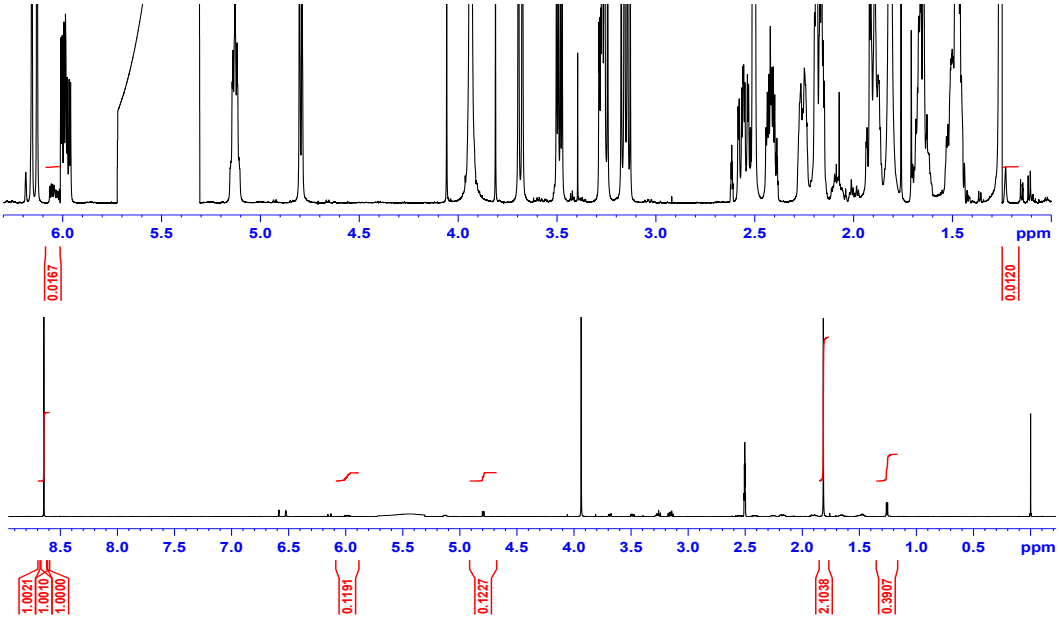


Figure 48. $^{1}$H-qNMR spectrum of ZEN-16-G in DMSO-d6; standard: trimesic acid trimethyl ester.

Table 13. $^{1}$H and $^{13}$C NMR shifts of ZEN-16-G.

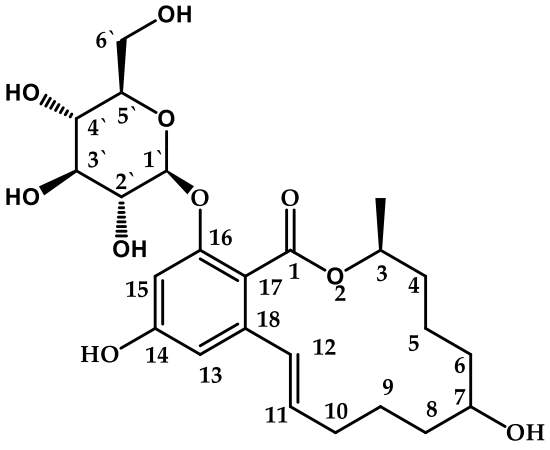


| position | $^{1}$H | mult | $^{13}$C |
|---|---|---|---|
| **1** | | | 166.8 |
| **3** | 5.13 | dqd, 8.4, 6.3, | 70.7 |
| **3-CH$_3$** | 1.26 | d, 6.4 Hz | 19.4 |
| **4** | 1.47, | m | 34.1 |

| | | | |
|---|---|---|---|
| **5** | 1.47, | m | 20.5 |
| **6** | 2.18 | m | 43.1 |
| | 2.42 | ddd, 13.2, 8.7, | |
| **7** | | | 210.5 |
| **8** | 2.18 | m | 36.9 |
| | 2.56 | ddd, 17.3, | |
| **9** | 1.50, | m | 20.8 |
| **10** | 1.90, | m | 30.7 |
| **11** | 5.99 | ddd, 15.6, 9.7, | 132.5 |
| **12** | 6.15 | dd, 15.6, 1.5 | 128.0 |
| **13** | 6.58 | d, 2.0 Hz | 104.5 |
| **14** | | | 159.1 |
| **15** | 6.51 | d, 2.0 Hz | 101.2 |
| **16** | | | 155.0 |
| **17** | | | 115.2 |
| **18** | | | 135.5 |
| **1`** | 4.80 | d, 7.7 Hz | 100.1 |
| **2`** | 3.14 | t, 8.9 Hz | 73.3 |
| **3`** | 3.26 | t, 8.9 Hz | 76.9 |
| **4`** | 3.16 | dd, 10.6, 9.0 | 69.5 |
| **5`** | 3.27 | ddd, 9.7, 5.4, | 77.0 |
| **6`** | 3.49 | dd, 11.9, 5.5 | 60.6 |
| | 3.69 | dd, 11.9, 2.1 | |

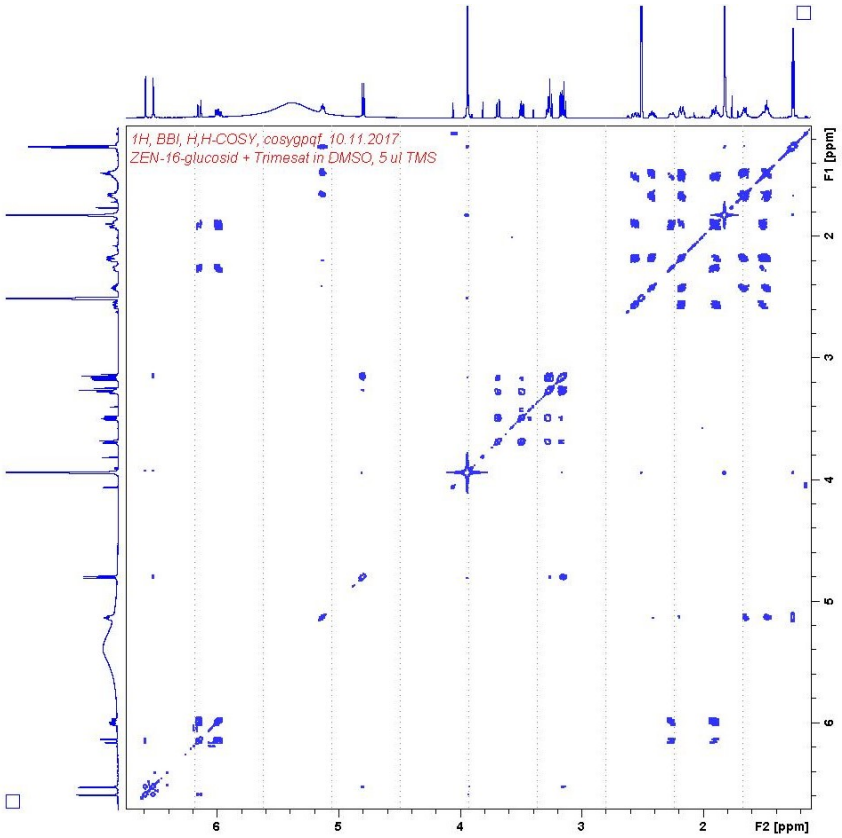


Figure 49. HH-COSY spectrum of ZEN-16-G.

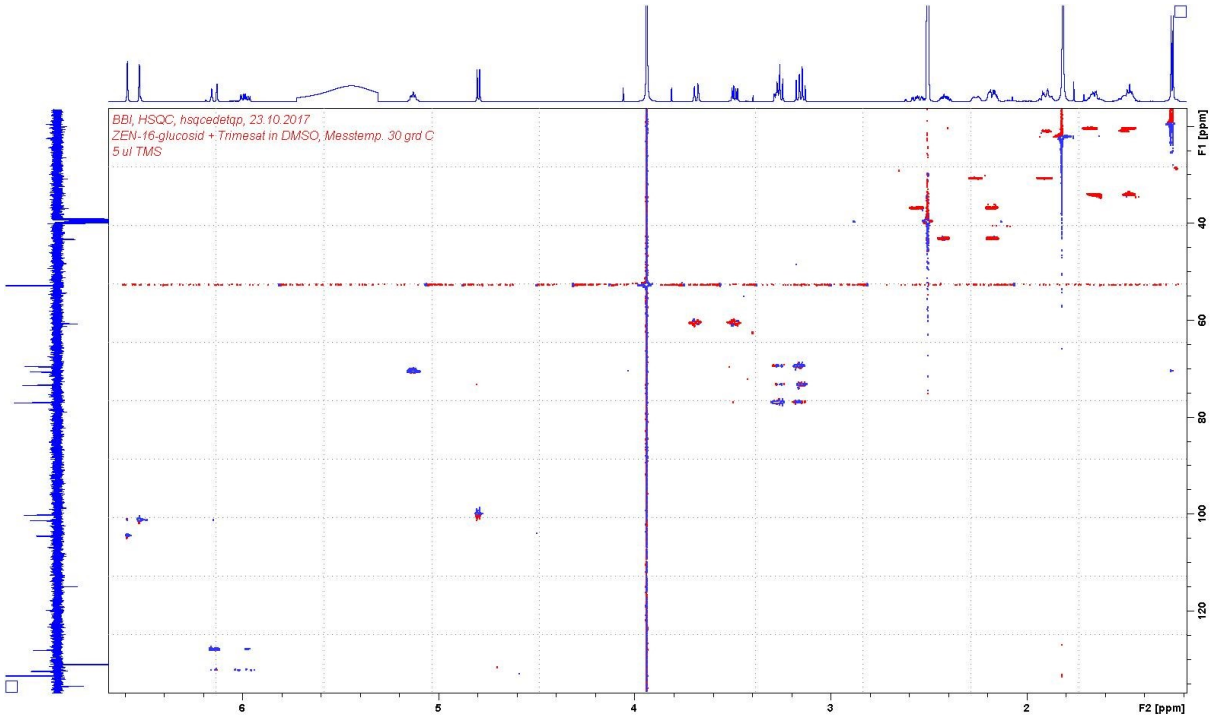


Figure 50. HC-HSQC spectrum of ZEN-16-G.

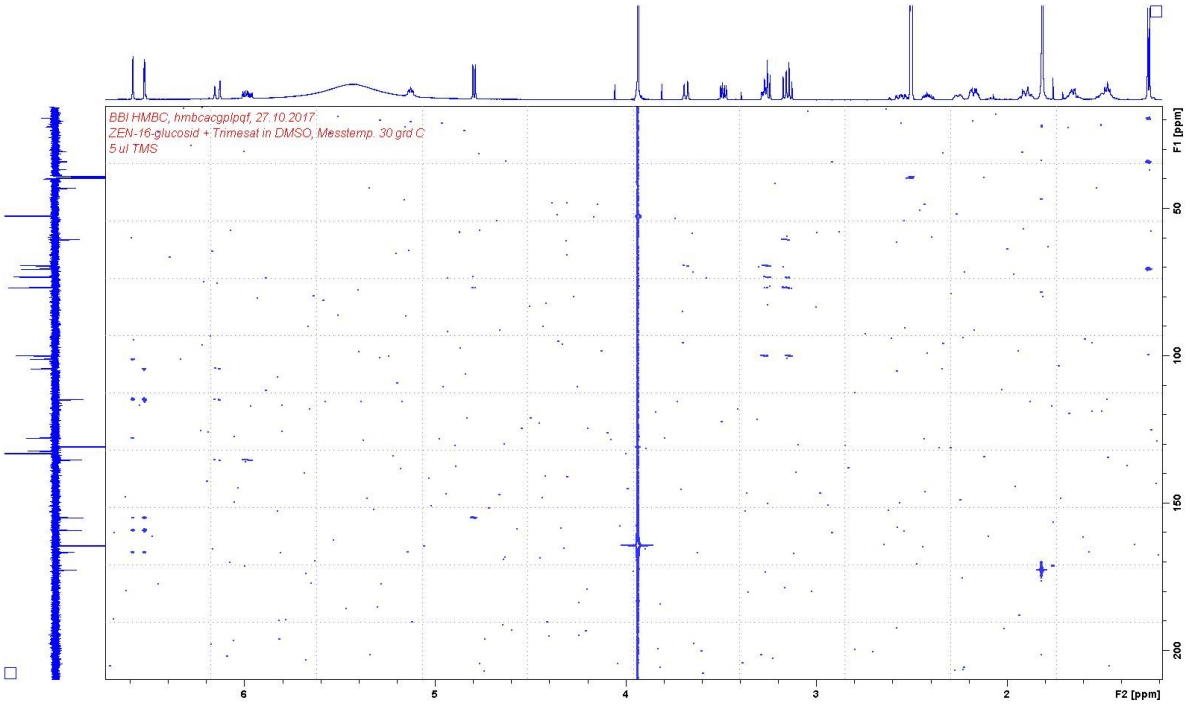


Figure 51. HC-HMBC spectrum of ZEN-16-G.

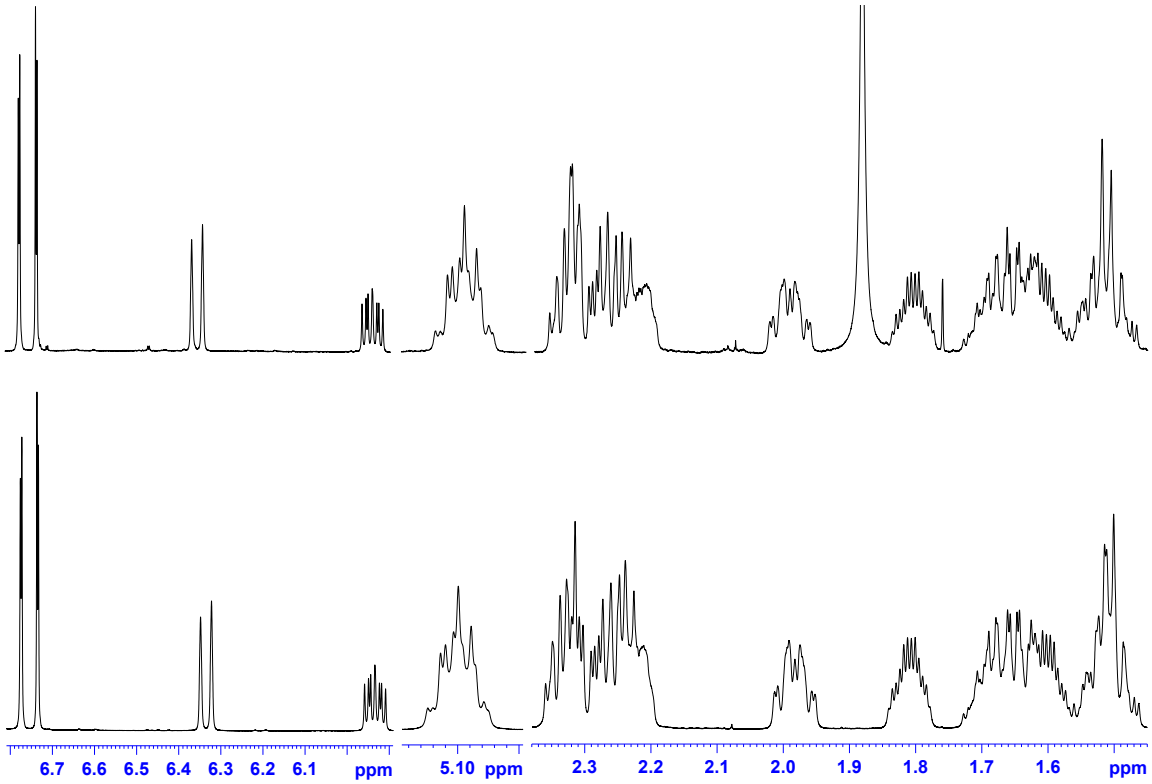


Figure 52. Comparison of the $^{1}$H-NMR spectra of the biosynthezied ZEN-14-S (above) and the the chemically synthesized ZEN-14-S standard (below).

# 2.5 Toxicity assay for citrinin, zearalenone and zearalenone-14-sulfate using the nematode *caenorhabditis elegans* as model organism

J. Keller [1], A. Borzekowski [1], H. Haase [2], R. Menzel [3], L. Rueß [3], M. Koch [1,*]

Originally published in **Toxins**
*10*(7), 284 (2018)
https://doi.org/10.3390/toxins10070284


[1] *Department Analytical Chemistry, Reference Materials, Bundesanstalt für Materialforschung und -prüfung (BAM), Richard-Willstätter-Straße 11, 12489, Berlin, Germany; julia.keller@bam.de; antje.borzekowski@bvl.bund.de*
[2] *Department of Food Chemistry and Toxicology, Technische Universität Berlin, Gustav-Meyer-Allee 25, 13355 Berlin, Germany; haase@tu-berlin.de*
[3] *Institute of Biology, Ecology, Humboldt-Universität zu Berlin, Philippstr. 13, 10115 Berlin, Germany; ralph.menzel@biologie.hu-berlin.de; Liliane.ruess@biologie.hu-berlin.de*
** Correspondence: Matthias.koch@bam.de; Tel.: +49-30-8104-1170*

## 2.5.1 ABSTRACT

To keep pace with the rising number of detected mycotoxins, there is a growing need for fast and reliable toxicity tests to assess the potential threat to food safety. Toxicity tests with the bacterial-feeding nematode *Caenorhabditis elegans* as model organism are well established. In this study the *C. elegans* wildtype strain N2 (var. Bristol) was used to investigate the toxic effects of the food relevant mycotoxins citrinin (CIT) and zearalenone-14-sulfate (ZEN-14-S) and zearalenone (ZEN) on different life cycle parameters including reproduction, thermal and oxidative stress resistance and lifespan. The metabolization of the mycotoxins by the nematodes *in vivo* was investigated using HPLC-MS/MS. ZEA was metabolized *in vivo* to the reduced isomers α-zearalenol (α-ZEL) and β-ZEL. ZEN 14-S was reduced to α-/β-ZEL 14-sulfate and CIT was metabolized to mono-hydroxylated CIT. All mycotoxins tested

led to a significant decrease in the number of nematode offspring produced. ZEN and CIT displayed negative effects on stress tolerance levels and for CIT an additional shortening of the mean lifespan was observed. In the case of ZEN-14-S, however, the mean lifespan was prolonged. The presented study shows the applicability of *C. elegans* for toxicity testing of emerging food mycotoxins for the purpose of assigning potential health threats.

## 2.5.2 INTRODUCTION

Mycotoxins are secondary metabolites produced by a variety of filamentous fungi from across the world, contaminating approximately 25% of all harvested crops [110]. The intake of contaminated food and feed may lead to different kinds of acute and chronic diseases in humans and animals [11]. From 400–500 already known mycotoxins only 11 are regulated and monitored by authorities within the EU [111, 112]. Maximum levels have been set for zearalenone (ZEN) (Figure 53), which is mainly found in cereal crops such as maize, barley, wheat and rice, and is produced by several molds of the genus *Fusarium* [17, 23]. ZEN induces estrogenic symptoms—such as uterine enlargement, vulvovaginitis or infertility—in higher animals such as rats, pigs or cows [22]. By causing DNA-adduct formation in *in vitro* cultures of bovine lymphocytes and in female mouse tissues ZEN has also been shown to act genotoxically [144, 164]. Further toxic effects of ZEN are lipid peroxidation, cell death and the inhibition of protein and DNA synthesis [165]. In cultured pig, mouse and cattle hepatocytes ZEN is metabolized by cytochrome P450 enzymes during phase I biotransformation to its reduced metabolites $\alpha$-zearalenol ($\alpha$-ZEL) and $\beta$-ZEL [127] (Figure 53). Using human and rat liver microsomes it has also been shown that ZEN may undergo oxidation to several mono-hydroxylated metabolites [114]. Furthermore, fungi and plants are able to modify ZEN by conjugation with sulfate or glucose at the aromatic OH-positions [145]. Mycotoxins and their modified forms are a cause of great concern for food safety and could pose a serious health risk due to their yet unknown toxic effects [19]. ZEN-14-sulfate (Figure 53) was originally found in cultures of *Fusarium graminearum* and is often detected in cereal-, soy- and corn-based products [30, 166]. The nephro-, hepato- and cytotoxic mycotoxin citrinin (CIT) (Figure 53) is mainly found in stored grains [167]. Produced by molds of the *Penicillium*, *Monascus* and *Aspergillus* genus, CIT often co-occurs with the highly nephrotoxic and carcinogenic mycotoxin ochratoxin A and can be found in foodstuffs like breakfast cereals or rice [34, 42, 43]. According to the European Food Safety

Authority (EFSA), there is still a substantial need for research to evaluate the occurrence and toxicity of CIT [36].

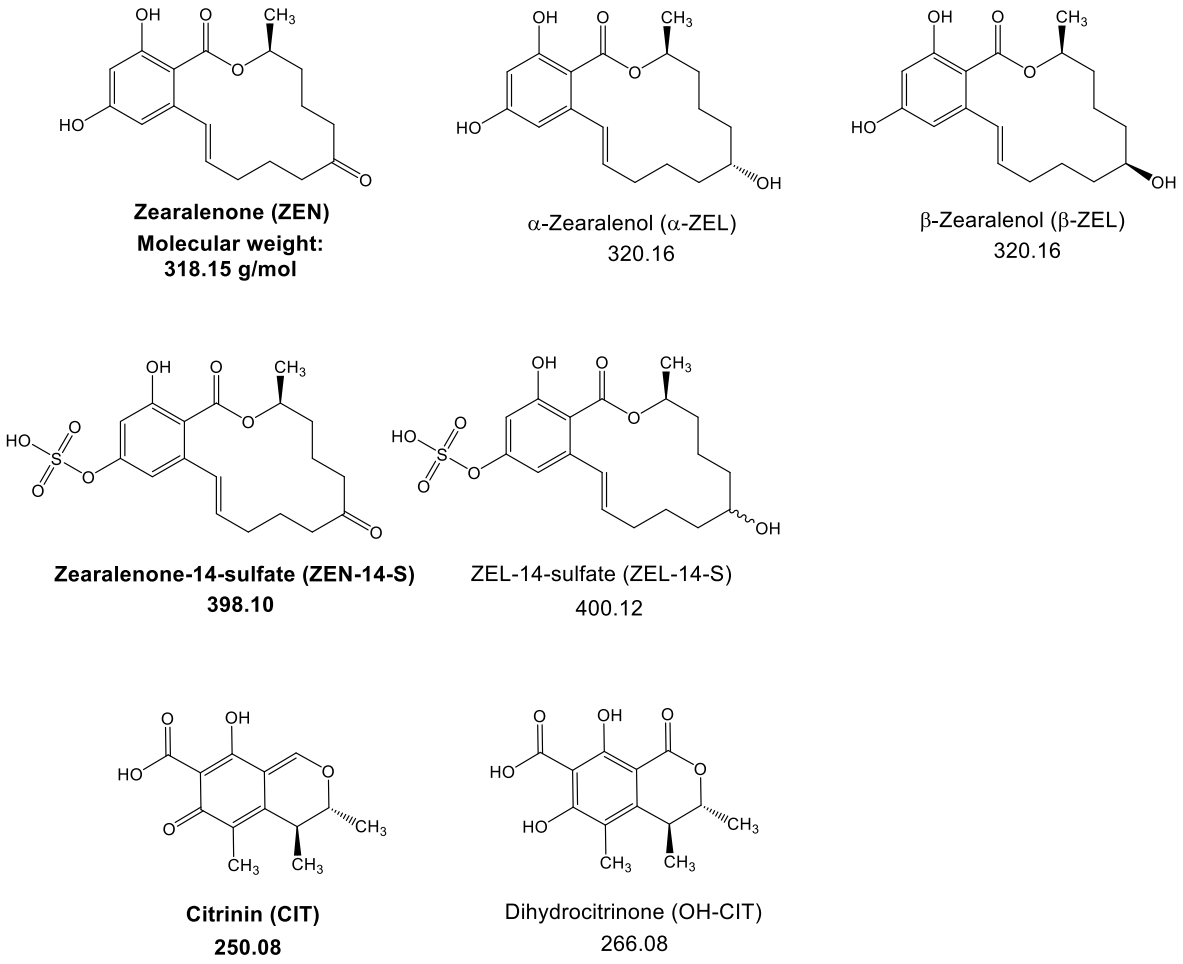


Figure 53. Chemical structures of the tested mycotoxins (shown in bold) and their related metabolites with their respective molecular weight

In order to evaluate the potential health risks posed by mycotoxins, in particular for emerging detected substances, reliable toxicity tests are necessary. Toxicity testing of mycotoxins is usually carried out by performing *in vitro* assays or alternatively it is evaluated by using laboratory animals like mice, rats or chickens in *in vivo* studies [9]. Since 1974 when Sydney Brenner described the cultivation and handling of *Caenorhabditis elegans*, this worm has been widely used as a model organism in developmental biology and neurology [105, 168]. Due to its many advantages—such as its easy and cost-effective cultivation, the fact that the nematodes genome is completely sequenced and its short generation time—it also plays an growing role in

toxicological research [107]. Finally, the high number of conserved genes between mammals and *C. elegans* make the worm an ideal candidate for toxicological investigations [169, 170].

Surprisingly, to date, only few studies are known to have used *C. elegans* to assess the toxic effects of mycotoxins. Yang *et al*. [171] described the multi-toxic endpoints of aflatoxin $B_1$, deoxynivalenol (DON), fumonisin $B_1$, T-2 toxin and ZEN using the *C. elegans* wildtype strain N2. They determined the lethality endpoint for ZEN with a $LC_{50}$ of 75.79 mg/L and investigated alterations in lifespan and reproduction as well as morphological changes. The nematodes were all negatively affected by ZEN and the other tested mycotoxins [171]. Gowrinathan *et al*. [106] evaluated the toxicity of DON by performing partial and complete brood size assays using the *C. elegans* wildtype strain and a mutant strain (AU1) that has enhanced susceptibility to pathogens. The toxic effects of aflatoxin $B_1$ in *C. elegans* were investigated by Feng *et al*. [172] by evaluating germline apoptosis, alteration of growth and reproduction. They found that the DNA damage response pathway was associated with the $AFB_1$-induced germline apoptosis, which is highly relevant to reproductive and growth dysfunction in the worms.

Scientific studies in toxicological fields have improved the current knowledge of mycotoxins in food and feed. However, most concerns are linked to potential health risks of mycotoxins and their modified forms. Beside established toxicity tests with cell cultures or using mammalian models the toxicity testing with *C. elegans* can be an additional and valuable tool in mycotoxin research. Compared to toxicological experiments with cell cultures, assays with *C. elegans* provide data from a whole organism with intact and metabolically active systems [107]. In the present study we used *C. elegans* to investigate the toxic effects of the food relevant mycotoxins CIT, ZEA and ZEN-14-S, on different life cycle parameters including reproduction, thermal and oxidative stress tolerance and lifespan. These are standard parameters in toxicological research with *C. elegans* and cover the most important toxic effects. Because no model is perfect, the assessment of multiple toxic endpoints could increase the sensitivity of the test and lead to more reliable results. Furthermore, for the first time, the metabolization of the mycotoxins in the worms was determined using HPLC-MS/MS to better understand the observed toxic effects in *C. elegans*.

## 2.5.3 RESULTS AND DISCUSSION

To determine the toxicological impact of ZEN, ZEN-14-S and CIT on *C. elegans* as model organism different concentrations were tested. In case of CIT concentrations of 2.5 mg/L (10 µM), 12.5 mg/L (50 µM) and 62.5 mg/L (250 µM) were used according to findings from other studies [37, 38]. For ZEN and ZEN-14-S concentrations of 7.5 mg/L (ZEN: 24 µM; ZEN-14-S: 19 µM) and 37.5 mg/L (ZEN:118 µM; ZEN-14-S: 95 µM) were used like described in Yang *et al.* [171] and adapted for the present study.

*Metabolization of Mycotoxins In Vivo*

After five days of cultivation on mycotoxin-enriched (CIT 62.5 mg/L, ZEN and ZEN-14-S 37.5 mg/L) and UV-inactivated feeding bacteria the worms were harvested, extracted and analyzed by HPLC-MS/MS in order to detect derived mycotoxin metabolites. The high conservation of genes and signaling pathways between mammals and *C. elegans* was shown in several studies and should result in the same or at least partially the same metabolic pattern of mycotoxins which have been found in mammalian models [107]. In the present study, ZEN was reduced *in vivo* by *C. elegans* to a lesser extent to $\alpha$-ZEL and $\beta$-ZEL (Figure 54A) confirmed using standard solutions of $\alpha$-ZEL and $\beta$-ZEL and the corresponding mass transitions (Figure 54B; residual ZEN not shown). The reduction of ZEN to its two stereoisomeric metabolites has already been widely described for mammals and is now shown in *C. elegans*, too [145, 173]. Beside reductive metabolic reactions, also the oxidation of ZEN to its mono-hydroxylated metabolites was described by Pfeiffer et al [63]. The formation of reduced and oxidized ZEN species is mainly catalyzed by several isoforms of cytochrome P450 enzymes. *C. elegans* has several CYP isoforms similar to those in higher animals and therefore the hydroxylation of ZEN is conceivable. However, during this study the analysis of extracted worms revealed no mono-hydroxylated ZEA metabolites or possible phase II metabolites like glucuronides.
Comparable to ZEN, the conjugated form ZEN-14-S was reduced to ZEL-14-S by *C. elegans* (Figure 54D). Due to the lack of a standard substance, currently no conclusion can be drawn about whether there are two stereoisomeric forms, and which stereoisomer it was that was metabolized. Surprisingly, in worms fed with ZEN-14-S no free ZEN was found, indicating that the worm is either not capable or only negligibly capable of deconjugating ZEN-14-S. In higher animals like pigs or in

the deconjugation of ZEN-14-S in humans, the main biotransformation reaction is caused by bacteria in the colon during digestion processes by hydrolysis [32, 145].
CIT was oxidized by *C. elegans* to its mono-hydroxylated form OH-CIT (Figure 54C). The major metabolite of CIT, OH-CIT, is found in human blood plasma and urine as a biomarker [122]. By testing the cytotoxic and genotoxic potential of OH-CIT compared to CIT, Föllman *et al*. [38] revealed that OH-CIT formation was a process of detoxification. It is conceivable that the key cellular metabolic pathways in *C. elegans* are to a certain extent conserved, leading to reduced and oxidized metabolites of mycotoxins which have been already described in mammalian models. Even if the metabolites are comparable, *C. elegans* lacks most mammalian organs and it would be not realistic to expect that *C. elegans* can be used to replace toxicological analyses in mammals. However, *C. elegans* as affordable and rapid model system could be a powerful tool in combination with other toxicity testing strategies and offers the opportunity to achieve relatively fast first toxicological data about emerging substances.
Beside the extracts derived from nematode biomass, the bacterial food solutions were extracted and measured with the same HPLC-MS/MS method. No metabolization of the added mycotoxin solution was detected (data not shown), indicating that the UV irradiation used effectively killed OP50 bacteria. This reveals UV irradiation to be an appropriate method for toxicity tests with bacterial consumers like *C. elegans*, as in contrast to killing using heat, UV light leaves the bacterial surface unaffected and unaltered. The use of heat to kill depresses the food quality of bacteria, potentially posing an additional stress to bacterial consumers, which can, as a consequence, distort toxicity testing.

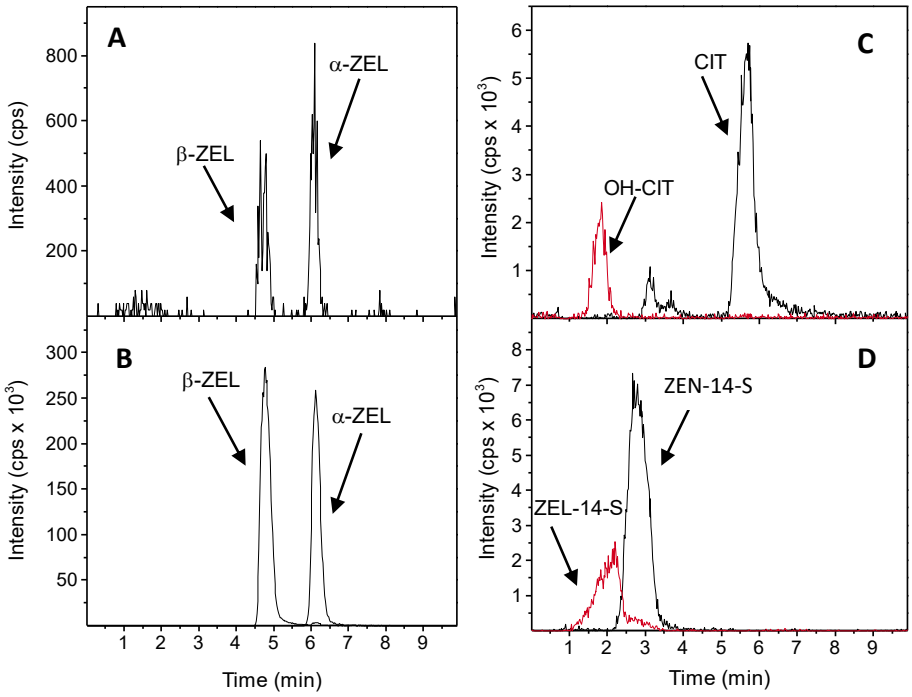


Figure 54. Worms fed for five days with mycotoxin containing OP50 bacteria were extracted and analyzed by HPLC-MS/MS in ESI negative mode using the multiple reaction mode with specific mass transitions given in material and methods. MRM chromatograms of worms treated with (A) zearalenone (37.5 mg/L) were compared with (B) a standard solution containing α-zearalenol and β-zearalenol. (C) citrinin (62.5 mg/L) and (D) zearalenone-14-sulfate (37.5 mg/L) are illustrated in black, whereas their metabolites are shown in red. Cps—counts per second.

*Lifespan Assay*

A preliminary conclusion about the negative or positive effects of exogenous substances can be drawn by performing lifespan assays. According to the log-rank test, which is used to determine whether experimental treatments significantly altered the lifespan or not, ZEN-14-S significantly prolonged lifespan compared to the control group treated with dimethyl sulfoxide (DMSO), as shown in Figure 55A. The mean lifespan was extended by up to 9.8 ± 4.4 % compared to the control group (Figure 55B). Several studies have described the life-prolonging effects of compounds in low doses that at higher concentrations induce toxic effects—the hormetic effect [174]. It is plausible that ZEN-14-S causes a mild stress in that low concentration

range, leading to a slightly increased mean lifespan. The increased occurrence of deaths in the ZEN-14-S-treated group starting after 18 days (Figure 55A) may be due to the accumulation of the mycotoxin itself in the worm or of the derived metabolization products such as ZEL-14-S.

In Yang *et al*.'s study [171] treatment with ZEN using 10 % of the estimated $LC_{50}$ of ZEN, in this case 7.6 mg/L caused strong toxic effects, leading to a significant decrease in lifespan. However, the nearly same concentration of ZEN used in the present study did not cause a significant change in the mean lifespan compared to the control group but did lead to a shortened maximum lifespan (Figure 55A, B). Toxic effects may have accumulated over its lifetime and thus caused increased mortality of the test group after a certain point of time, in this case after 17 days of adulthood. However, in the Yang *et al*. study [171] 5-fluorodeoxyuridine (5-FUdR) was used to simplify the lifespan assay process. As side effects, in adult worms, 5-FUdR slightly reduced the pharyngeal pumping rate, produced changes in body size and morphology, and increased superoxide dismutase levels [175]. The strong, toxic effects observed by Yang *et al*. [171] may have been caused by the simultaneous use of two substances, the toxin and the progeny blocker 5-FUdR.

Both concentrations of CIT tested had a significant negative effect on the lifespan of *C. elegans* (Figure 55A). The highest concentration of citrinin with 12.5 mg/L led to an increased mortality rate compared to the test group with 2.5 mg/L of citrinin. The mean lifespan was decreased to 11.5 ± 1.3 days (CIT 2.5 mg/L) and 11.0 ± 1.5 days (CIT 12.5 mg/L) which is a reduction of 17.1 ± 4.1 % and 20.8 ± 5.5 % compared to the control group (Figure 55B). The influence the CIT´s concentration has on the alteration of lifespan is greater during the first ten days of adulthood. This concentration dependence nearly vanished after 11 days and the lifespan curves ran similarly from that point on. It is conceivable, that it was the conversion of CIT to the less toxic mono-hydroxylated CIT, observed by HPLC-MS/MS measurements that caused this effect.

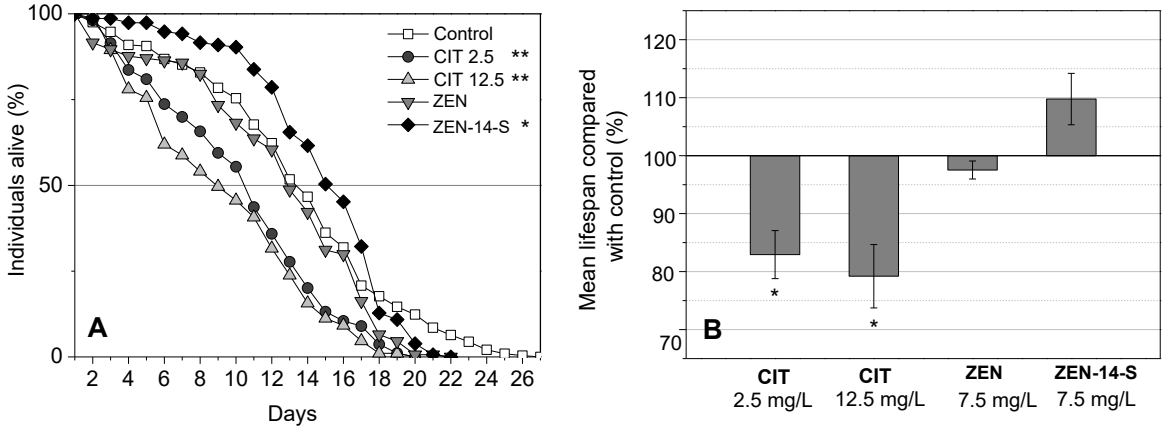


Figure 55. (A) Survival curves of *C. elegans* treated with single concentrations of citrinin (CIT 2.5 mg/L, 12.5 mg/L), zearalenone (ZEN 7.5 mg/L), zearalenone-14-sulfate (ZEN-14-S 7.5 mg/L) and untreated controls. Differences compared to the control were considered as significant with *p<0.05 and **p<0.001 and were determined using the log-rank test. (B) The percentage change of mean lifespan compared to the control group during exposure to CIT, ZEN and ZEN-14-S. Each bar represents the mean of two to four trials with a total of at least 154 nematodes per concentration. (A, B) Error bars represent the standard error of the mean. Differences compared to the control were considered as significant with *p<0.05.

*Brood Size Assay*

The average number of offspring after three days was significantly reduced at all tested concentrations (Figure 56). Compared to the number of offspring of the control group, with 72.2 ± 8.9 larvae, CIT decreased the number of nematode offspring produced significantly to 40.4 ± 9.6 (12.5 mg/L) and 23.1 ± 6.4 (62.5 mg/L). Among other toxic effects CIT has also been found to negatively affect the reproductive system. In Institute of Cancer Research (ICR) mice 2.5 and 5.0 µM of CIT reduced the oocyte maturation rate, as well as fertilization and embryo development [176]. Furthermore, female rats that were mated with CIT-treated males displayed a reduced pregnancy rate, as shown by Qingqing *et al*. [177].

Treatment with ZEN led to a reduction in the number of offspring to 39.0 ± 9.6 (7.5 mg/L) and 31.7 ± 6.1 by using 37.5 mg/L of ZEN, respectively. In laboratory and domestic animals ZEN is known to cause various estrogenic effects such as decreased fertility or alterations in the reproductive tract, whereby pigs and sheep appear to be more significantly affected by ZEN than rodents [173]. The influence of mycotoxins on reproductive fitness had also been previously shown by Yang *et al*. who observed

negative effects on the N2 nematode's reproduction in the case of fumonisin $B_1$, aflatoxin $B_1$, T-2 toxin and ZEN. Toxic effects on reproduction were more pronounced with higher concentration in all three tested mycotoxins, as shown in Figure 56. ZEN and ZEN-14-S had comparable toxic effects on reproduction. To date, only a few studies have investigated the toxic effects of conjugated mycotoxin forms, although modified toxins represent an emerging problem. Conjugation with glucose or sulfate is a known detoxification process in plants and it is supposed that conjugated mycotoxins possess a lower toxicity compared to their parental compounds. However, in this study, ZEN-14-S reduced the number of offspring to an average of 41.9 ± 9.4 (7.5 mg/L) and 36.3 ± 5.3 (37.5 mg/L) individuals.

The comparatively strong effect of ZEN-14-S in the reproduction assay is remarkable particularly in light of its dramatically decreased estrogenicity at the estrogen receptor level compared to ZEN (Figure 56) [20]. As an *r*-selected species *C. elegans* starts reproduction early, and a lowered progeny could result in the reduction or even the extinction of a population as reproductive fitness is a crucial factor for maintaining population size. To sum up, *C. elegans* appears to be an appropriate candidate for testing the reproductive toxicity of mycotoxins.

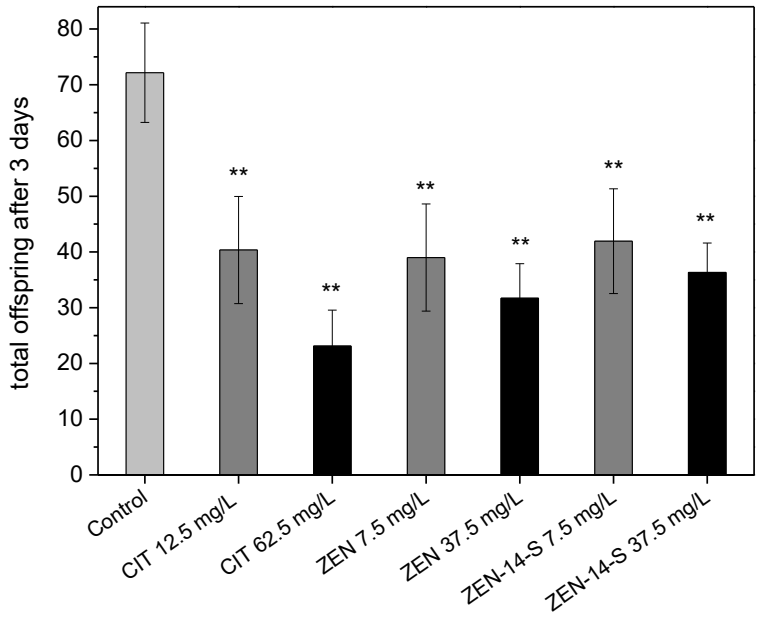


Figure 56. Effects of mycotoxins on the brood size of *C. elegans* after three days of reproduction, determined with at least 26 animals per concentration, displayed as the average of three trials; error bars represent the standard error of the mean. Differences compared to the control were considered as significant with **$p<0.001$.

*Oxidative and Thermal Stress Resistance Assay*

The treatment of *C. elegans* with CIT and ZEN led to a significantly increased mortality rate after 8 h of oxidative stress to 70.2 % ± 5.6 % (CIT) and 70.6 % ± 2.1 % (ZEN), compared to the control group with 53.7 % ± 1.8 %, as shown in Figure 57. Pascual-Ahuir *et al*. [178] investigated the mechanisms of CIT toxicity using the quantitative yeast model and observed the cellular defense mechanism in response to the mycotoxin. They concluded that CIT triggered the activation of stress responsive promoters like the glucocorticoid response element 2 (GRE2) and superoxide dismutase 2 (SOD2). Consequently, the induction of reactive oxygen species (ROS) could be the predominant toxicity mechanism of CIT. Hassen *et al*. [179] investigated the role of oxidative stress in ZEN-mediated toxicity by performing test assays with human HepG2 cells. This cell type responded to ZEN treatment with a loss of cell viability and the induction of oxidative DNA damage. Findings in the present study indicated that the ZEN-induced toxicity in *C. elegans* could be related to oxidative damage in the worms. For both mycotoxins there are indications that toxic effects in the worms could be probably driven by stress responsive factors. As a result, during this specific assay, these toxins perhaps negatively affected the stress resistance of *C. elegans* and thus led to enhanced mortality. Under thermal induced stress, N2 wildtype nematodes treated with CIT (62.5 mg/L) and ZEN (37.5 mg/L) showed higher mortality rates compared to the untreated control group (and ZEN-14-S). However, studies concerning the modes of toxicity caused by ZEN-14-S are still lacking. Several studies have found that in *C. elegans* longevity and stress resistance are linked [180]. Thus, it might be surprising that after having slightly positive effects on lifespan, ZEN-14-S failed to induce statistically significant changes in either the thermal stress assay or the oxidative stress assay. However, not all long-lived nematodes are more stress resistant and Cypser *et al*. [181] even proposed that thermal stress resistance and lifespan alteration were triggered by different molecular signals [182, 183].

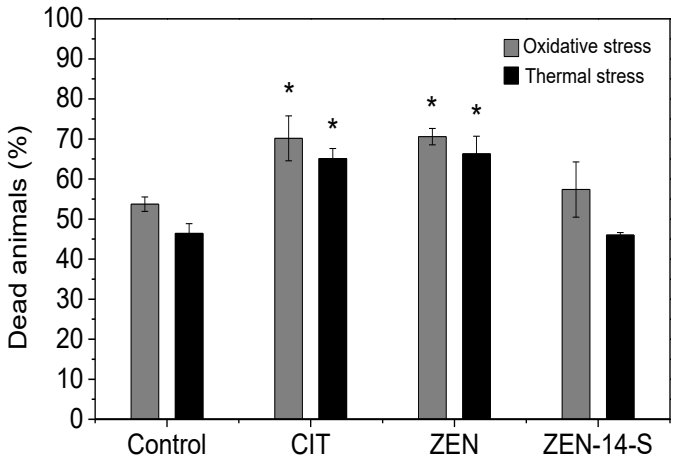


Figure 57. Effect of 62.5 mg/L citrinin (CIT), 37.5 mg/L zearalenone (ZEN) and 37.5 mg/L zearalenone-14-sulfate (ZEN-14-S) on the oxidative and thermal stress resistance of *C. elegans*. On the sixth day of adulthood, alive and dead animals were counted after a treatment of 8 h at 35°C for the thermal stress resistance assay (black bars) and after an 8 h exposure to 0.8 mM hydrogen peroxide for the oxidative stress resistance assay (grey bars). At least 174 nematodes per mycotoxin were scored for the thermal stress assay and 122 for the oxidative stress assay. Bars show the average of all three trials and the error bars represent the standard error of the mean. Differences compared to the control were considered as significant with *$p<0.05$.

## 2.5.4 CONCLUSIONS

To date, toxicological data for modified mycotoxins like ZEN-14-S or emerging mycotoxins like CIT are scarce or even non-existent. The model organism *C. elegans* that can provide a bridge between conventional *in vitro* and *in vivo* assays using mammalian models was used in this study as a simple, high throughput and cost-effective method to evaluate the toxicity of selected mycotoxins. Only a few toxicological studies on modified mycotoxins have already been carried out and reveal deconjugation to free mycotoxins as a preferred pathway of biotransformation. However, data obtained in this study showed the reduction of ZEN-14-S to ZEL-14-S in *C. elegans*. Probably due to the highly conserved genes and metabolic pathways between *C. elegans* and mammals, the metabolization of ZEN to its reduced and more estrogenic isomers $\alpha$-ZEL and $\beta$-ZEL was found, as well as the mono-hydroxylation of CIT. There is still a considerable need for further research concerning the metabolic fate and toxicity of food relevant mycotoxins. In combination with identification

techniques such as HPLC-MS/MS and high-resolution mass spectrometry or other toxicological model systems *C. elegans* is an ideal candidate for first toxicity screenings, not only in mycotoxin research.

## 2.5.5 MATERIALS AND METHODS

*Chemicals and Substances*

Citrinin was purchased from Fermentek (Jerusalem, Israel) with a purity of 98 %. Zearalenone was purchased from SantaCruz Biotechnology Inc. (Santa Cruz, CA, USA) with a purity of 99 %. Zearalenone-14-sulfate was produced by a double-staged biosynthesis and preparative fractionation as previously described [1]. $\alpha$-zearalenol ($\alpha$-ZEL), $\beta$-ZEL and dimethyl sulfoxide were purchased from Sigma-Aldrich Chemie GmbH (Steinheim, Germany). All standard chemicals were of p.a. grade, and all solvents of HPLC grade. Nematode growth media (NGM) powder was purchased from USBio (Salem, MA, USA) and lysogeny broth (LB) medium from Merck KGaA (Darmstadt, Germany). One liter of NGM medium was prepared as recommended by the manufacturer by adding 25 mL of 1M phosphate buffer (pH 6), 1 mL of 1M $CaCl_2$ and 1M $MgSO_4$ (both purchased from Merck KGaA; Darmstadt, Germany). Ultrapure water was produced using a Seralpur PRO 90 CN system.

*Strains and Conditions*

The *C. elegans* wildtype strain N2 was used and maintained at 20 °C on sterile NMG media. As a food source, *Escherichia coli* OP50 bacteria were used according to Brenner, 1974 [105]. The wildtype strain N2 and OP50 bacteria were kindly derived by the Caenorhabditis Genetics Center (University of Minnesota). For the cultivation of OP50 bacteria one colony was picked from an LB agar plate and brought in liquid LB medium and was shaken slightly over night at 37 °C. To kill the bacteria, sterilized quartz vessels were filled with 20 mL of the freshly prepared culture and irradiated by UV-C light at $\lambda$=254 nm for 2 h by gentle shaking. The inactivation of bacteria was tested by plating them on LB agar and incubating them overnight at 37 °C; no bacteria growth was observed. Mycotoxins were added to the UV-killed bacteria to obtain

final concentrations between 2.5 mg/L and 62.5 mg/L. Equal amounts of test solutions were used for all conditions (final concentration of 0.3 % [*v*/*v*] DMSO) and control solutions were mixed with DMSO.

*Lifespan Assay*

For each treatment 20–30 L4 larvae—easily distinguishable by the presence of a small, white half-circle patch in the worm midsection—were transferred with a small platinum wire to 70 x 15 mm petri dishes with 1 mL of mycotoxin containing bacteria and cultivated at 20 °C. From the following generation (F1), 150 L4 larvae were transferred to five small plates (35 x 12 mm) with 15 individuals per plate representing one trial. Two to four trials were performed per concentration. The number of surviving and dead animals were counted every day and the dead animals were removed from the plate. Individuals that died from internal hatching or that crawled out of the NMG medium were considered as being neither dead or alive and were excluded from the assay. Animals that failed to react after being gently touched with the platinum wire were rated as dead. During their reproductive phase (approx. 5 days) nematodes were transferred daily to avoid starvation or the mixing of generations and were fed with 150 μL of bacteria. After that, worms were transferred every two to three days. Plates contaminated with bacteria or molds were dismissed from the trial. Statistical significance for alteration of the mean lifespan was calculated using the log-rank test provided online by the Bioinformatics at the Walter and Eliza Hall Institute of Medical Research (http://bioinf.wehi.edu.au/software/russell/logrank).

*Brood Size Assay*

L4 larvae (F1) were separated on small petri dishes and the offspring of each worm was counted after three days of adulthood. The total number of offspring was determined and the statistical significance was calculated by using One-way ANOVA. Two to three trials per condition and control were performed, with at least 20 animals per trial.

*Thermal and Oxidative Stress Resistance Assay*

For every concentration and trial about 20–30 L4 larvae (F1) were used. On the sixth day of adulthood, untreated and treated animals were moved to 35 °C incubation for 8 h and the number of dead and surviving nematodes were counted for the thermal stress resistance assay. For the oxidative stress resistance assay nematodes were transferred to M9 buffer containing 0.8 mM hydrogen peroxide and were incubated at 20 °C for 8 h. Nematodes were gently touched with a platinum wire. If they failed to respond they were counted as dead. The statistical significance was calculated by using One-way ANOVA.

*Cultivation and Extraction of Nematodes for Metabolite Analysis*

*Cultivation* Mixed cultures were grown on NGM agar on 60 big petri dishes. To avoid starvation OP50 mixed with the test substances was provided during cultivation at 25 °C at least once a day. After five days of cultivation nematodes were rinsed from the plates using ice-cold M9 buffer, collected in 50 mL tubes and stored for the duration on ice. Worms were washed three times with 10 mL of M9 buffer to remove bacteria. In between, worms were allowed to settle to the bottom; afterwards the supernatant was always removed from the worm pellet. The final pellets were kept frozen at -80 °C for further extraction and analysis.
*Extraction* About 500 μL of worm pellet was dissolved with 4.5 mL of acetonitrile-water mixture (80:20 *v/v*) and treated for 10 min in an ultrasonic bath. After subsequent shaking with a horizontal shaker for 30 min at 330 $min^{-1}$, samples were centrifuged for 10 min at 2,931 × g at 20 °C. For further analysis 1 mL of the supernatant was evaporated under nitrogen at 40 °C and re-dissolved in HPLC eluent (65:35 *v/v* acetonitrile-water with 0.1% formic acid). For the extraction of OP50 bacteria an overnight culture was UV-killed and mixed with mycotoxin dissolved in DMSO (or only pure DMSO as control) and stored for 5 days at 4 °C to simulate the maximal usage time for a bacteria solution. About 10 mL of the bacteria culture was centrifuged for 10 min at 3,828 × g. The supernatant was kept and stored at -80 °C and the bacteria pellet was washed twice with M9 buffer. Th extraction of the supernatant and bacteria was performed in the same way as the extraction of the worms.

*HPLC–MS/MS Analysis*

HPLC–MS/MS measurements were performed using a 1100 series HPLC from Agilent Technologies (Waldbronn, Germany) coupled to an API 4000 triple-quadrupole MS/MS system (Sciex, Framingham, MA, USA). A Synergi Polar–RP column (150 mm x 3 mm; particle size: 4 μm; pore size: 80 Å) from Phenomenex (Torrance, CA, USA) was used. The column oven was set to 40 °C and the solvents used were water with 0.1% formic acid (solvent A) and acetonitrile with 0.1% formic acid (solvent B) using a flow rate of 800 μL/min. The gradient was as follows: 0–1 min isocratic with 35% B, 1–29 min linear to 100% B, isocratic 29–34 min 100% B, shifting back to 35% B and reconditioning from 35–40 min. The injection volume used was 20 μL and the ESI was operated in the negative ionization mode at 450 °C. The settings were as follows:
Curtain gas 20 psi, collision gas 8 psi, ion source gas 1 and 2 with 60 psi, respectively, and an ionization voltage of -4500 V. The MS/MS measurements were performed in the multiple reaction monitoring (MRM) mode. Mass transitions were recorded as follows for the investigated analytes by using a declustering potential of – 60 V and a collision energy of – 30 eV: ZEN *m*/*z* 317.1 → quantifier *m*/*z* 130.1/ qualifier *m*/*z* 174.8; ZEL *m*/*z* 319.2 → 174.0/160.0; ZEN-14-S *m*/*z* 397.1 → 317.1/175.0; ZEL-14-S *m*/*z* 399.2 → 319.2/275.2; CIT *m*/*z* 249.0 → 205.0, OH-CIT *m*/*z* 265.0→ 221.0.

## LICENSE

# 2.6 Complexes of the mycotoxins citrinin and ochratoxin A with aluminum ions and their spectroscopic properties

J. Keller[1], D. Moldenhauer[2], L. Byrne [1,3], H. Haase[4], U. Resch-Genger[2], M. Koch[1,*]

Originally published in **Toxins**
10(12), 538 (2018)
https://doi.org/10.3390/toxins10120538


*[1] Department 1, Division Organic Trace and Food Analysis, Federal Institute for Materials Research and Testing (BAM), Richard-Willstätter-Strasse 11, D-12489 Berlin, Germany*
*[2] Department 1, Division Biophotonics, Federal Institute for Materials Research and Testing (BAM), Richard-Willstätter-Strasse 11, D-12489 Berlin, Germany*
*[3] School of Chemical and Pharmaceutical Sciences, Dublin Institute of Technology (DIT), Kevin Street, Dublin 8, Ireland*
*[4] Department of Food Chemistry and Toxicology, Technische Universität Berlin, Gustav-Meyer-Allee 25, 13355 Berlin, Germany*

## 2.6.1 ABSTRACT:

The sensitive detection of the mycotoxin citrinin (CIT) utilizing its fluorescence requires approaches to enhance the emission. In this respect, we studied the complexation of CIT and ochratoxin A (OTA) with $Al^{3+}$ in methanol using absorption and fluorescence spectroscopy. In this context, an isocratic high performance liquid chromatography (HPLC) method using a polymer column and a fluorescence detector was also developed that enables the separation of the metal ion complexes from the free ligands and non-complexed $Al^{3+}$. CIT and OTA showed distinct changes in their absorption and fluorescence properties upon $Al^{3+}$-coordination, and the fluorescence of CIT was considerably enhanced. Analysis of the photometrically assessed titration of CIT and OTA with $Al^{3+}$ using the Job plot method revealed 1:2 and 1:1 stoichiometries for the $Al^{3+}$ complexes of CIT (Al:CIT) and OTA (Al:OTA),

respectively. In the case of CIT, only one β diketone moiety participates in $Al^{3+}$ coordination. These findings can be elegantly exploited for signal amplification and provide the base to reduce the limit of detection for CIT quantification by about an order of magnitude, as revealed by HPLC measurements using a fluorescence detector.

## 2.6.2 INTRODUCTION

The often co-occurring and nephrotoxic mycotoxins citrinin (CIT) and ochratoxin A (OTA) are produced by different fungi of the genera *Aspergillus*, *Monascus* and *Penicillium* [33, 184, 185]. CIT and OTA are frequently found in cereals, animal and plant products, food, and feed. They present a threat for human and animal health because of their chronic toxic effects [40, 42, 43]. For OTA, maximum levels are set by international legislation, whereas the CIT levels have not been regulated yet.. Both mycotoxins are fluorescent, which can be used for fluorescence-based trace analysis and quantification in real samples [186, 187, 188].

The absorption and fluorescence properties of almost every emissive species are responsive to its environment, including polarity, viscosity, pH, and the presence of additives like detergents or certain coordinating metal ions [189] and often lead to strong spectral shifts and changes particularly in fluorescence intensity/quantum yield and lifetime. This can be deleterious for their analytical determination, yet, it may also be beneficial when it is utilized as signal enhancement strategy. Common examples for the latter in environment and food analysis are post-column derivatization methods for high performance liquid chromatography (HPLC) exploiting cation coordination-induced fluorescence amplification [103, 190, 191]. Common metal ions used for signal enhancement are diamagnetic and light cations like magnesium or aluminum, thereby preventing possible fluorescence quenching by heavy atom effects [189]. This was exploited for example in a HPLC method with post-column derivatization for the mycoestrogen zearalenone chelated by $Al^{3+}$ [103] and the fluorescence of OTA could be enhanced by adding magnesium ions [101]. In another study, it was shown that OTA forms stable complexes with several alkaline earth ions, which were confirmed by X-ray analysis [100].

Common signal enhancing complexing agents in thin-layer and liquid chromatography are aluminum nitrate and chloride. $Al^{3+}$ is an octahedrally hexacoordinated ion that binds to one, two or three bidentate ligands, leading to the formation of 1:1, 1:2 or 1:3 complexes. Furthermore, it was demonstrated that small amounts of water in ethanol interfere with the complex formation and, as a result,

absolute methanol or ethanol are the most suitable solvents to investigate complexation reactions [192, 193]. The aim of the present study was to assess the capability of $Al^{3+}$ to form complexes with the mycotoxins CIT and OTA and whether the complexation is accompanied by a fluorescence enhancement. Here, we show a detailed spectroscopic analysis of the $Al^{3+}$ complexes of these two mycotoxins, including absorption and fluorescence spectra, fluorescence quantum yields, and fluorescence lifetimes. The complex stoichiometry was derived from the resulting absorption spectra using the method of continuous variation (Job plot) [194].

## 2.6.3 RESULTS AND DISCUSSION

*Coordination-induced changes in absorption and complex stoichiometry*

Adding $Al^{3+}$ to CIT and OTA in methanol led to a strong bathochromic shift in absorption (Figure 58, panels A1 and B1). The spectra of CIT shifted to longer wavelengths in the presence of $Al^{3+}$, and a new maximum appeared at $\lambda_{max}$ = 365 nm (Figure 58, panel A2). Analysis of the photometric data with the method of continuous variation (Job plot) indicated that a stoichiometry of the citrinin-aluminum complex (CIT-Al) of 2:1 (value of 0.66) (Figure 58, A2). A possible structure of the bidentate complex is given in Figure 59 on the left. In the case of CIT, it possesses two 1,3-dicarbonyl moieties that are capable to chelate $Al^{3+}$ and would lead to different complexes with the same metal to ligand ratio. The ratio depends on the nature of the central ion and its coordination number and the structure of the complex is also influenced by steric factors of the ligand itself. Furthermore, the formation is influenced by the used solvent system, too [193]. Adding $Al^{3+}$ to OTA led to a shift of the absorption maximum from 332 nm to $\lambda_{max}$ = 370 nm shown in Figure 58 (panel B1). The absorption spectra of OTA and $Al^{3+}$ cross at an isosbestic point at 350 nm. The observation of isosbestic points indicates that mainly two optically active species are involved, the free ligand and complex species. The Job plot of OTA and $Al^{3+}$ shown in Figure 58 B2 revealed a ratio of 1:1 (value 0.48) for the composition of the ochratoxin A-aluminum complex (OTA-Al). From other studies it is known that OTA chelates metal ions like $Zn^{2+}$ and $Mg^{2+}$ to 1:1 complexes with enhanced optical properties [101]. $Mg^{2+}$ interacted with three partially negatively charged oxygen atoms: the phenolic oxygen, the oxo group oxygen and the carboxylic group oxygen. $Zn^{2+}$ chelated close to the nitrogen atom of the amide group and the two partially negatively charged

oxygen atoms. These studies from Poor et al. demonstrated that the chelation occurred at different moieties of OTA and atoms that may interact with $Al^{3+}$ are highlighted in red in Figure 59.

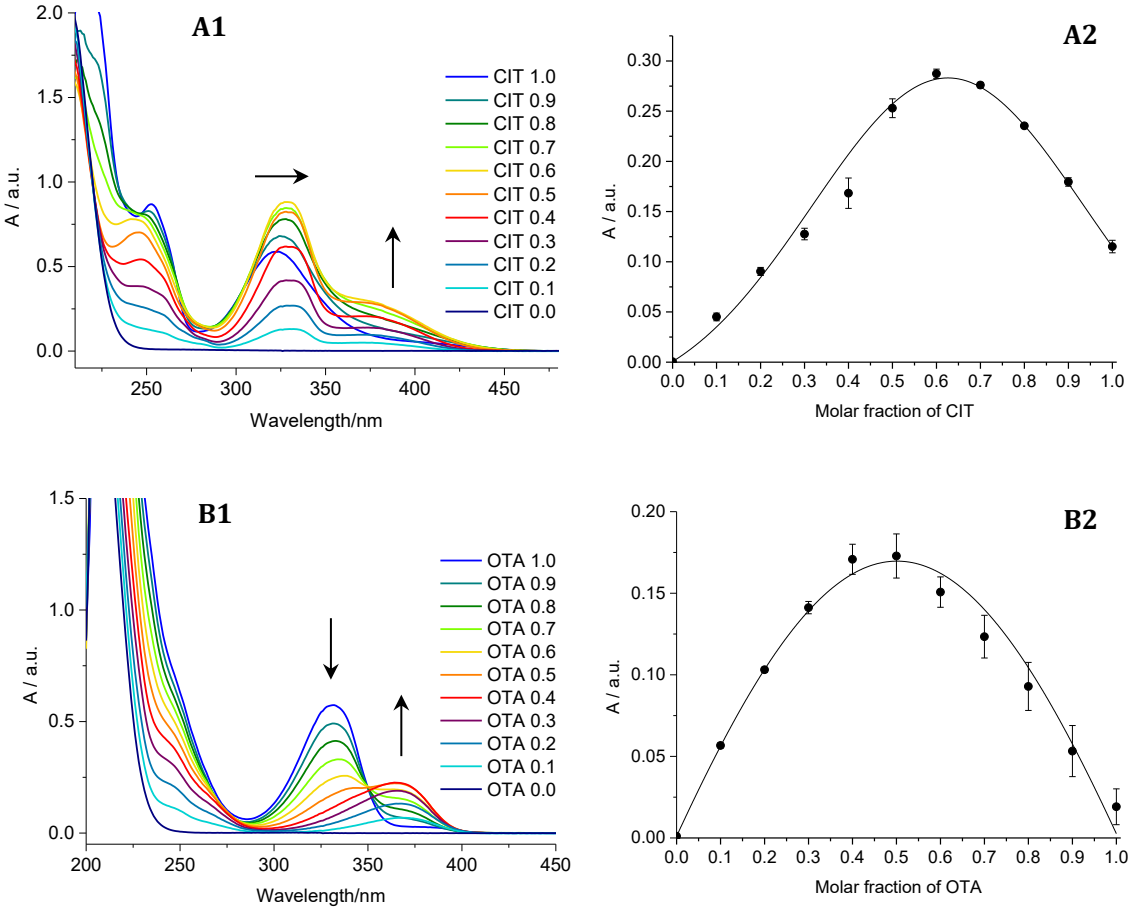


Figure 58. UV/VIS absorption spectra accompanying the complexation of citrinin (A1) and ochratoxin A (B1) with $Al^{3+}$ in methanol obtained with the method of continuous variation. Numbers in the spectra represent the molar fractions of citrinin and ochratoxin A after addition of $Al^{3+}$ and a total concentration of 100 µM per sample. Job plot curve and absorbance plot at $\lambda_{max}$ = 365 nm (A2 and B2). Black dots: observed absorbance and error bars representing the relative standard deviation; Black line: Gaussian fit of data points

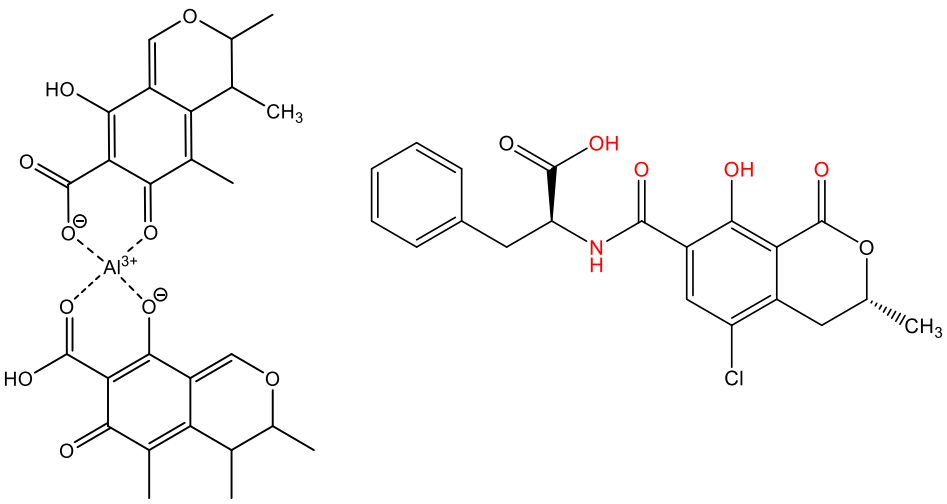


Figure 59. Structures of the citrinin-Al complex (left) and the ochratoxin A (right) with possible chelation sites shown in red

*Fluorescence characteristics*

The emission maxima of both complexes undergo a hypsochromic shift from 505 nm to 470 nm for CIT-Al and from 465 nm to 425 nm for OTA-Al (Figure 60, dashed lines). Overall, the fluorescence of CIT is very weak (Figure 61, photo), which is also reflected by a low fluorescence quantum yield of 0.6 % in Table 14, whereas CIT-Al showed an increased quantum yield of 29.5 % observable with a significant increase of fluorescence as also seen in the photo (Figure 61) by naked eye. The quantum yield represents the ratio of photons absorbed to photons emitted through fluorescence and is an important coefficient of performance for the optical quality of a fluorophore. This signal amplification could be used for a more sensitive detection using HPLC analysis with fluorescence detection (FLD) as previously described for zearalenone and flavonoids [103, 190]. For the OTA-Al-complex, however, a decrease in fluorescence quantum yield from 44.7 % to 34.2 % was observed in the presence of $Al^{3+}$ (Table 14) and the light blue fluorescence of OTA changed to deep blue/violet fluorescence as shown in Figure 61 on the right side.

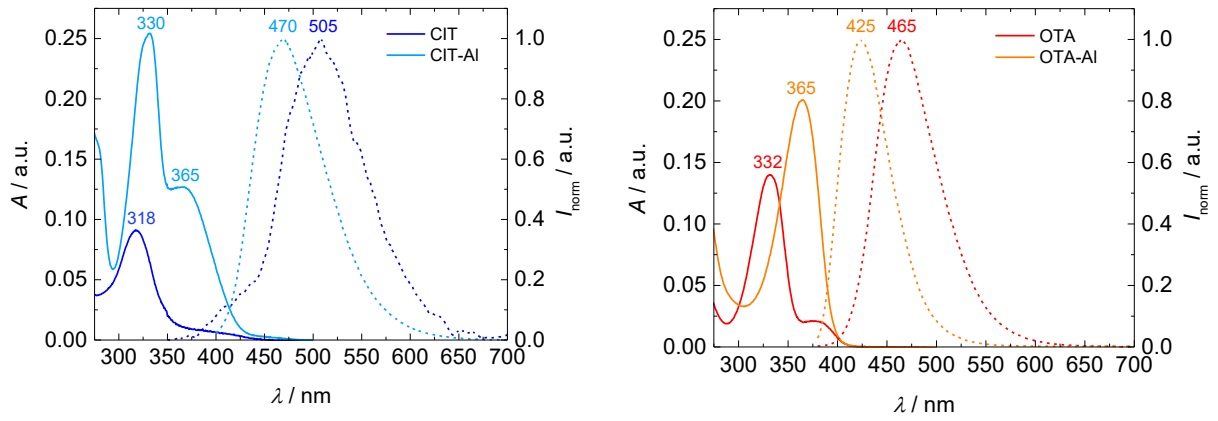


Figure 60. Absorption (solid lines) and normalized emission (dashed lines) spectra of citrinin and ochratoxin A and their $Al^{3+}$ complexes ($c$ = 30 µM).

Table 14. Spectroscopic properties of the mycotoxins CIT, OTA and their $Al^{3+}$ complexes in methanol.

| **Analyte** | **$\varepsilon(\lambda_{max})$ / L·mol$^{-1}$·cm$^{-1}$** | **$\lambda_{em}$ / nm** | **$\Phi$ / %** | **$\tau$ / ns** |
|---|---|---|---|---|
| **CIT** | 3030 (318) | 505 | 0.6 | 3.7 |
| **CIT-Al** | 8440 (330)<br>4220 (365) | 470 | 29.5 | 9.7 |
| **OTA** | 4650 (332) | 465 | 44.7 | 6.3 |
| **OTA-Al** | 6700 (365) | 425 | 34.2 | 5.5 |

$\varepsilon(\lambda_{max})$ = Molar extinction coefficient, $\lambda_{em}$ = wavelength of emission maximum, $\Phi$ =quantum yield, $\tau$ = fluorescence lifetime

The enhancement in emission resulting for CIT is ascribed to the enlarged quinoide system generated by connecting two CIT molecules by $Al^{3+}$ and leads to a much more pronounced red shift in the emission with 505 nm (Figure 60). This can also explain the small influence on the OTA fluorescence as in this case, only a 1:1 complex is formed and nearly no enlargement of the molecule takes place. The coordination-induced trends in fluorescence intensity are reflected by the fluorescence lifetime measurements. Measurements of fluorescence decay kinetics providing the fluorescence lifetimes ($\tau$) and has been widely used for the characterization of

fluorescent species. In the present study, a fluorescence lifetime elongation was observed for CIT-Al, whereas the complexation of OTA by $Al^{3+}$ changed only slightly the fluorescence lifetime of OTA (Figure 61, left and Table 14).

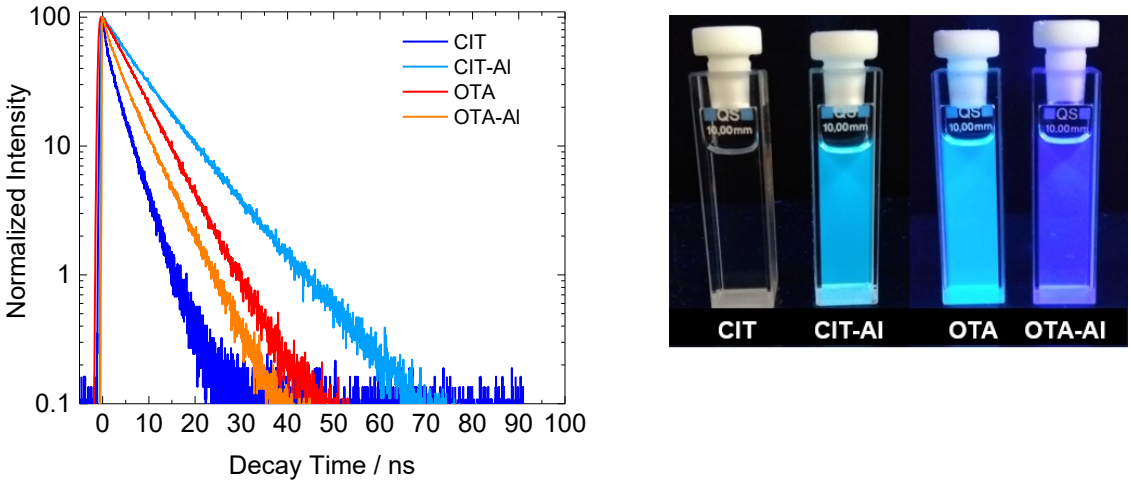


Figure 61. Left: Fluorescence decay curves of citrinin (CIT), citrinin-Al-complex (CIT-Al), ochratoxin A (OTA) and ochratoxin A- Al complex (OTA-Al) providing the fluorescence lifetimes ($\tau$); Right: Optical appearance of CIT, CIT-Al, OTA and OTA-Al ($c$ = 50 µM in MeOH) under UV light

*HPLC-FLD measurements*

Chromatographic separation of metal complexes comprises several obstacles. If the complexes are positively charged, they are may be adsorbed onto the unreacted silanols of reversed-phase material and the elution is consequently inhibited or delayed. Also, the disintegration of the complexes on a standard reversed-phase C18-HPLC column without endcapping reagents is possible. However, the use of a polystyrene/ divinylbenzene phase inhibits these effects and allows the separation of metal complexes from free ligands or metal ions [195]. In Figure 62 an eightfold enhancement of signal intensity of the CIT-Al complex compared to the free CIT was observed. Compared to the data obtained from fluorescence quantum yield measurements and the emission spectrum of CIT-Al complexes, the fluorescence enhancement is lower than expected. The fluorescence of the CIT-Al complex seems to be reduced in the water:acetonitrile solvent mixture used for the HPLC studies compared to that in methanol employed for the spectroscopic measurements.

Nevertheless, we still observe a considerable fluorescence enhancement also in the HPLC-FLD studies, which is analytically very promising. As the absorption spectra of the CIT-Al complex in acetonitrile/water and methanol are rather similar (Figure 62, right), we assume that the same complex is formed in both solvents as major species. As expected from the fluorescence spectroscopic studies no signal enhancement of OTA-Al was observable.

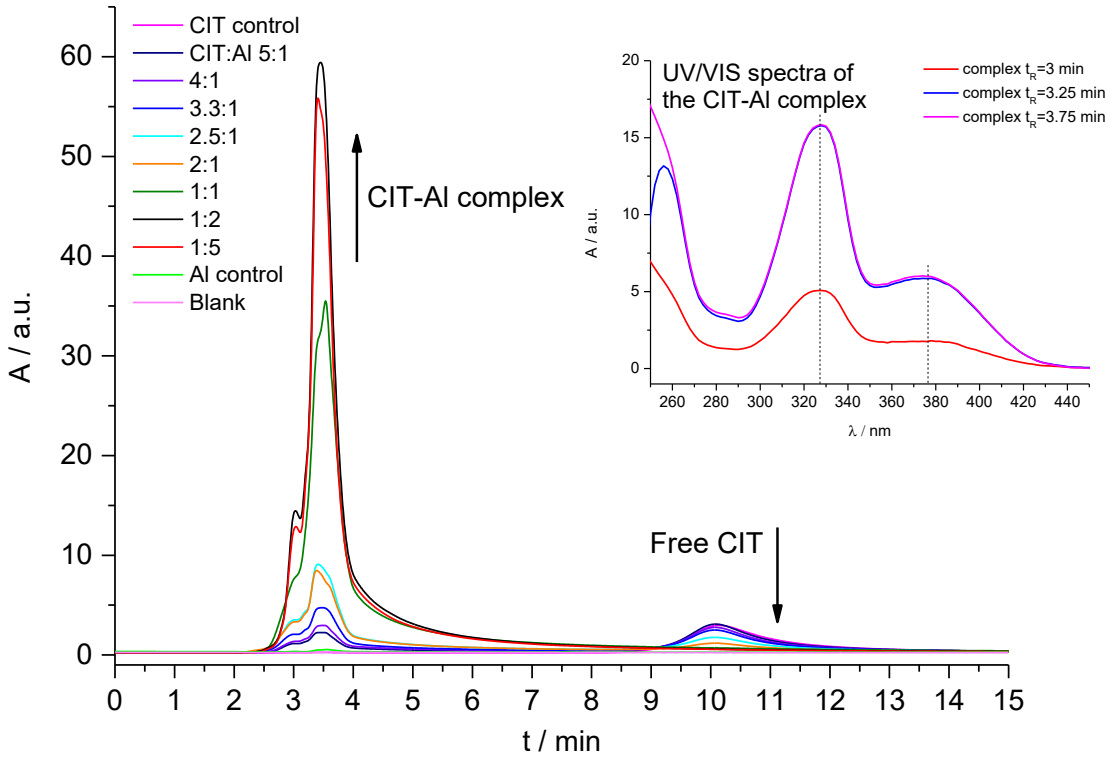


Figure 62. Overlayed HPLC-FLD chromatograms of citrinin ($c_{CIT}$ = 50 µM) with varying molar ratios of $Al^{3+}$ using a PolymerX column; UV/VIS spectra of CIT-Al in acetonitrile/water at different retention times measured by DAD scan from 190 to 800 nm

To conclude, the coordination of the mycotoxins citrinin and ochratoxin A to trivalent $Al^{3+}$ was studied photometrically and fluorometrically with special emphasis on chelation-induced fluorescence as tool for signal enhancement and decrease in detection limit. Citrinin-Al and Ochratoxin A-Al complexes were prepared and described for the first time. Analysis of the photometric data with Job´s method revealed the formation of a 1:1 complex of $Al^{3+}$ and OTA and a 1:2 complex stoichiometry for $Al^{3+}$ and CIT, with the participation of two CIT ligands causing a red shift in emission and a fluorescence enhancement factor of about 50 in methanol. A less pronounced signal enhancement in the order of a factor of eight was obtained

for HPLC with fluorescence detection (HPLC-FLD) using an acetonitrile-water solvent mixture. Thus, a possible application could be an improved CIT analysis by post-column derivatization with $Al^{3+}$, with enhanced fluorescence detection sensitivity.
Whether the mycotoxin-Al-complexes could also be found in fungi or food and feed, needs to be investigated in further studies, but it is conceivable that these complexes are easily formed if free $Al^{3+}$ is available and can react with the mycotoxin. However, nearly no data about the fate of metal complexes in biological systems or their degradation are present currently and there is still a need for further research.

## 2.6.4 MATERIAL AND METHODS

*Chemicals*

Citrinin (CIT) and Ochratoxin A (OTA) with purities over 98 % were obtained from Fermentek (Jerusalem, Israel). $Al(NO_3)_3 \cdot 9H_2O$ was obtained from Merck (Darmstadt, Germany) and HPLC grade methanol and acetonitrile from Chemsolute (Th. Geyer, Germany), respectively.

*Absorption and fluorescence spectroscopy*

Absorption spectra were recorded on a calibrated Varian Cary 5000 UV-/VIS-/NIR spectrometer with a scan rate of 300 nm/min and a slit width of 1 nm using a baseline correction (air/air) and a solvent sample (methanol) as reference. Fluorescence data were collected on a calibrated FluoroMax-4P fluorometer from HORIBA Jobin Yvon with an integration time of 0.1 s and slit widths of 2 nm for excitation and emission.

*Fluorescence quantum yields (Φ)*

$\Phi$ values, which represent the ratio of the number of emitted photons to absorbed photons, were determined absolutely with an integrating sphere setup from Hamamatsu (Quantaurus-QY C11347-11) as described previously [196]. All $\Phi$

measurements were performed at 25 °C using special 10 mm *x* 10 mm long neck quartz cuvettes from Hamamatsu.

*Time-correlated single photon counting (TCSPC)*

Fluorescence decay kinetics providing the fluorescence lifetimes ($\tau$) of the mycotoxins and aluminum-mycotoxin complexes, were recorded with a FLS 920 fluorometer from Edinburgh Instruments equipped with a 330 nm or 375 nm pulsed light-emitting diode of the EPLED series and a fast multichannel plate photomultiplier (MCP-PMT) as a detector. The samples of CIT and OTA were excited at 330 nm and the samples of CIT-AL and OTA-Al were excited at 375 nm, while the emission was detected at the respective emission maximum employing a spectral bandwidth of the excitation and emission monochromator of 15 nm, a 4096-channel setting, and time ranges of 100 ns and 200 ns, respectively. With this setup, $\tau$ values ≥ 0.2 ns can be reliably measured. The measured fluorescence decay kinetics were evaluated using the deconvolution procedure of the FAST program (Edinburgh Instruments). This procedure considers the measured instrument response function (IRF), which influences the fluorescence decays. All decay profiles could be analyzed with mono-exponential fits with reduced $\chi^2$ values between 0.8 and 1.2.
All spectroscopic measurements were performed with air saturated solutions at $T$ = 25 °C using 10 mm *x* 10 mm quartz cuvettes from Hellma GmbH filled with 3 mL of solvent or mycotoxin solution to be analyzed.

*Job plots*

For the application of the continuous variation method, also known as Job plot, citrinin, ochratoxin A and $Al(NO_3)_3$ were dissolved in methanol. A series of solutions were prepared in which the sum of the total concentration of mycotoxin and $Al^{3+}$ was constant (100 μM), but their proportions are continuously varied. Job plot working solutions of 2 mL were prepared and measured photometrically after 10 min of incubation at room temperature. All experiments were performed at least three times.

*HPLC-DAD/FLD measurements*

The mycotoxin-aluminum complexes were analyzed by HPLC using an Agilent 1200 series HPLC (Agilent Technologies GmbH) consisting of an auto sampler, a binary pump, a degasser, a column oven, a diode array (DAD) and fluorescence detector (FLD). The analytical column used was a PolymerX RP-1 with dimensions of 250 x 4.6 mm, a particle size of 5 µM and a pore size of 100 Å (Phenomenex, Torrance, CA, USA) and the column oven was set to 40 °C. The mobile phase consisted of 60% acetonitrile and 40% water without modifiers for the CIT-Al HPLC method and for the OTA-Al method 100 % of methanol were used. For both methods, the flow rate of the mobile phase was 800 µL/min, the injection volume was 20 µL and the isocratic run was held for 15 min. A DAD scan was performed in the wavelength range of $\lambda$ = 190-800 nm and the FLD was set to excitation and emission wavelengths as follows: CIT $\lambda_{Ex}$ = 331 nm and $\lambda_{Em}$ = 500 nm; CIT-Al complex $\lambda_{Ex}$ = 320 nm and $\lambda_{Em}$ = 474 nm; OTA $\lambda_{Ex}$ = 330 nm and $\lambda_{Em}$ =4 65 nm; OTA-Al complex $\lambda_{Ex}$ = 365 nm and $\lambda_{Em}$ = 425 nm.

## LICENSE

# 3 FINAL DISCUSSION

## 3.1 Establishment of simulation techniques to produce TPs from food relevant mycotoxins

Mycotoxins occurring worldwide and have been found to cause severe diseases in humans and animals. The consumption of these natural contaminants is almost unavoidable. Previous studies were focused on the degradation of mycotoxins with the goal to reduce the mycotoxin content in food and feed. Often-used techniques for the degradation of mycotoxin-contaminated material are the irradiation with UV-light, the microbial, chemical and biological detoxification [197, 198]. During these different processes of degradation, several new transformation products could be generated from the parental substance. As a result, several potentially harmful and highly toxic compounds in unknown quantities could occur. Surprisingly, only a hand full of studies concentrated on the investigation of TPs, which could be produced due to natural biotic and abiotic processes.

To understand main processes of metabolic reactions it is crucial to reduce the complexity of the system and as a result, *in vitro* and *in vivo* techniques were well-established in several decades of mycotoxin research. Since EC/MS is widely used in pharmaceutical and drug metabolism research, electrochemistry was only used as a pure detection method for mycotoxins, so far [199, 200]. Recently, the first description of EC/MS as a purely instrumental set-up to simulate biotransformation processes was applied to alternariol (AOH) and alternariol methyl ether (AME) [88]. This study revealed the applicability of EC/MS in mycotoxin research to simulate typical phase I reactions like hydroxylation or dehydrogenation for the first time. Unfortunately, the toxicologically relevant epoxide-formation from a double bound is not mimicked by EC. A prominent example of epoxide-derived toxicity is the strong genotoxic effect of Aflatoxin $B_1$ which is metabolized by CYP450 enzymes and causes severe damage of the DNA [201].
However, in the present thesis electrochemical oxidation reactions of the food relevant mycotoxins CIT, ZEN, DHEC (as member of the group of ergot alkaloids),

patulin and OTA have been intensively investigated. The method development during this thesis revealed that the reaction is depending on several parameters like analyte concentration, working electrode material, solvent and flow rate. Optimal and reproducible oxidation was ensured using the improved EC parameters shown in Table 15.

Table 15. Optimized parameters for electrochemical oxidation of mycotoxins using the μPrepCell; *unpublished

| Mycotoxin | *c* (μM) | Solvent | Flow rate (μL/min) | Working electrode |
|---|---|---|---|---|
| **Citrinin** | 100 | MeOH/$H_2O$ (50/50 *v*/*v*; 20 mM $NH_4Ac$) | 30 | Glassy Carbon |
| **Zearalenone** | 100 | ACN/$H_2O$ (50/50 *v*/*v*; 20 mM $NH_4Ac$) | 80 | Boron-doped diamond |
| **Dihydroergo-cristine** | 100 | ACN/$H_2O$ (80/20 *v*/*v*; 0.1 % FA) | 70 | Boron-doped diamond |
| **Patulin*** | 200 | ACN/$H_2O$ (85/15 *v*/*v*; 0.1 % FA) | 90 | Gold |
| **Ochratoxin A*** | 100 | ACN/$H_2O$ (50/50 *v*/*v*; 0.1 % acetic acid) | 50 | Platin |

Using these EC-parameters several mono-hydroxylated ZEN, DHEC and CIT species, and in the case of DHEC also di-hydroxylated species have been observed with MS detection. Also, dealkylation and dehydrogenation reactions lead to a broad spectrum of different reaction products. In order to evaluate the strength of EC/MS as suitable simulation technique for metabolic phase I reactions, *in vitro* microsomal assays with HLM and RLM were performed and the product patterns were compared to those from EC using increasing potentials from 0 to 2500 mV *vs*. Pd/$H_2$. It was shown that EC could mimic the oxidative phase I metabolism of the tested mycotoxins CIT, ZEN and DHEC to a certain extent, with mostly mono- and dihydroxylated mycotoxin species. Beside these typical oxidation products, also interesting and new reaction products like ZEN dimers were described for the first time during this thesis. Using 1.4 V *vs*. Pd/$H_2$ as oxidation potential 18 dimeric

species have been produced which were easily detectable using HPLC-DAD/FLD, as well as with MS detection.
Several maize germ oils, tempeh flours and fungal cultures have been screened for dimeric species of ZEN, but no positive match was found during the screening (unpublished, data not shown). Nevertheless, it is conceivable, that ZEN dimers could occur in food and feed, as a result of natural oxidation processes. Dimerization of phenolic compounds as products of metabolization is often observed especially in plants, bacteria, lichen and fungi [139]. However, dimers of mycotoxins are barely described and include the fungal red/yellow pigment aurofusarin or dicitrinin A, the dimeric form of CIT [202, 203]. Simon *et al*. also observed the dimerization of AME and AOH and Nieto *et al.* investigated the electrochemical reduction of sterigmatocystin to a dimeric species [88, 204]. In both cases, no structural elucidation was performed, and structures were proposed via HRMS fragments and retention times.

For the first time as a technique to produce TPs of mycotoxins, the Fenton-like reaction was tested. The Fenton-like reaction is driven by its two components: iron(III) and hydrogen peroxide and is often used to decompose harmful organic pollutants in wastewater by nonselective oxidation [89]. For CIT and DHEC, oxidation by EC and Fenton-like reaction was comparable and in both cases they could not mimic the phase I reaction pattern sufficiently. In the case of ZEN, Fenton-like reaction could mimic five metabolites found in microsomal incubations with HLM and RLM, whereas EC lead to one matching hydroxylated species. Due to a growing concern about mycotoxins and their derived TPs the trend of using new simulation methods in mycotoxin research is ongoing. UV irradiation over direct and indirect photolysis is known to destruct organic molecules. Until the complete degradation, stable oxidative reaction products are conceivable. A prominent example is the UV-induced *cis-trans* isomerization of ZEN. The *cis*-isomer could be potentially found in oils or other foodstuffs and is currently not included in routine analysis [24]. However, UV-studies conducted within this thesis did not show any generation of TPs, which allows the conclusion, that UV-irradiation is also strongly dependent on the analyte and the photon energy was not sufficient to break the chemical bonds of the mycotoxins.

Besides electrochemical, photochemical, Fenton-like and biochemical oxidation, Ce(IV)sulfate as strong oxidizing agent was tested in the case of ZEN. Reactions with Ce(IV) in water/acetonitrile produced dimeric species of ZEN comparable to the oxidation via EC and in a shorter period of time when compared to reactions

with the EC-synthesis cell. Hydroxylated species of ZEN were not found with Cer(IV), as well as the Fenton-like reaction did not lead to dimeric species. This emphasizes the diversity of oxidation reactions and the need to use more than one simulation technique. The tested simulation techniques alone are not capable to simulate, or mimic phase I biotransformation processes a hundred percent, but in combination they can be a useful and supportive tool in mycotoxin research with respect to the growing number of emerging mycotoxins.

Taken together, only a few studies are available yet describing alternative simulation methods and the present thesis provides information about new and straightforward oxidation techniques like the EC/MS and Fenton-like reaction, which could be easily applied to other mycotoxins and analytes in general.

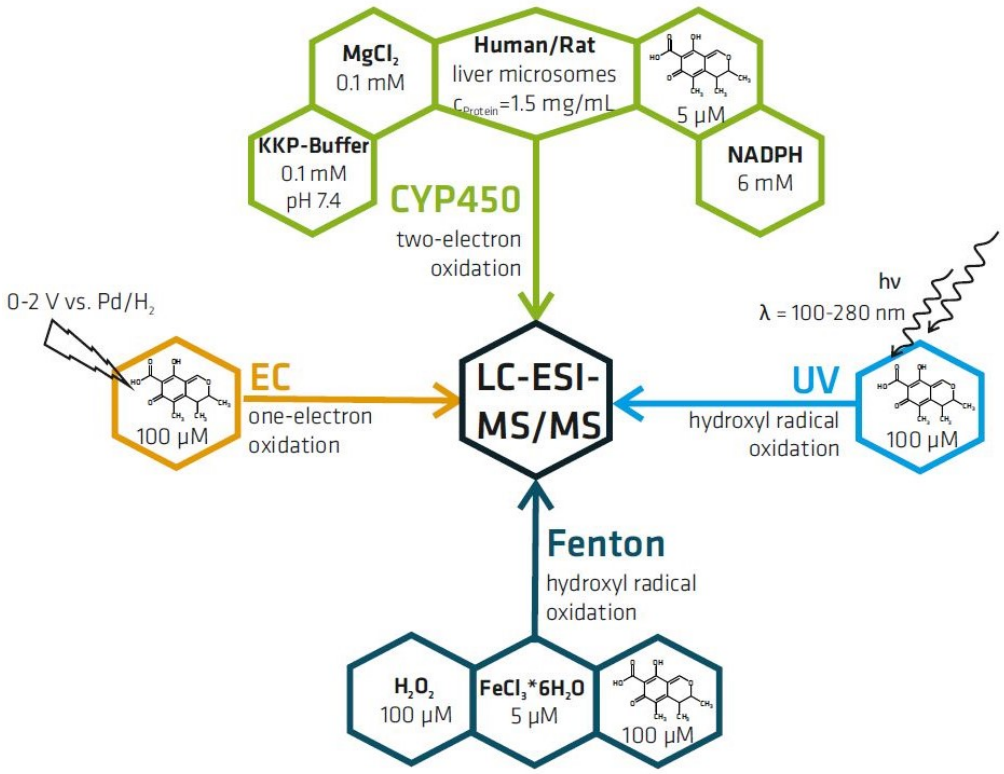


Figure 63. Overview about the tested simulation methods and the optimized parameters

## 3.2 Generation of pure substances of TPs for structural elucidation and toxicity testing

Currently, reference substances are scarce to even non-existent and impede the investigations of potentially harmful TPs. When it comes to structural elucidation or toxicity testing with distinct TPs the lack of a sufficient amount of initial substance is problematic. Pure mycotoxin standards for the quantities needed are simply too expensive. To overcome this problem, biosynthesis of mycotoxins using different fungal strains as affordable and easy technique was optimized during this thesis (Figure 64).

Masked mycotoxins like ZEN-14-S and ZEN-glucosides have been detected in food and feed and the consumption of these conjugates can cause an unknown exposure to ZEN, because the human intestinal biota deconjugates the masked mycotoxins [32, 148]. As a result, free ZEN poses a serious additional health risk especially for children, elderly people or persons with a low health status. ZEN is included in routine analysis but reference standards for its conjugated forms are still not available and hamper the current development of reliable detection methods. ZEN conjugating fungi like *Aspergillus* and *Rhizopus* are easily cultivated and can be used for a targeted synthesis of ZEN conjugates. In the developed biosynthesis, yields ranging from 39 % to 67 % were achieved with purities between 50 % and 82 %. A recent study showed that the content of ZEN metabolites exceeds the content of ZEN in cornflakes with 144 µg/kg compared to 76 µg/kg. Unfortunately, studies like this one are scarce, but emphasize the need for further investigations and improvements in this field of mycotoxin research.

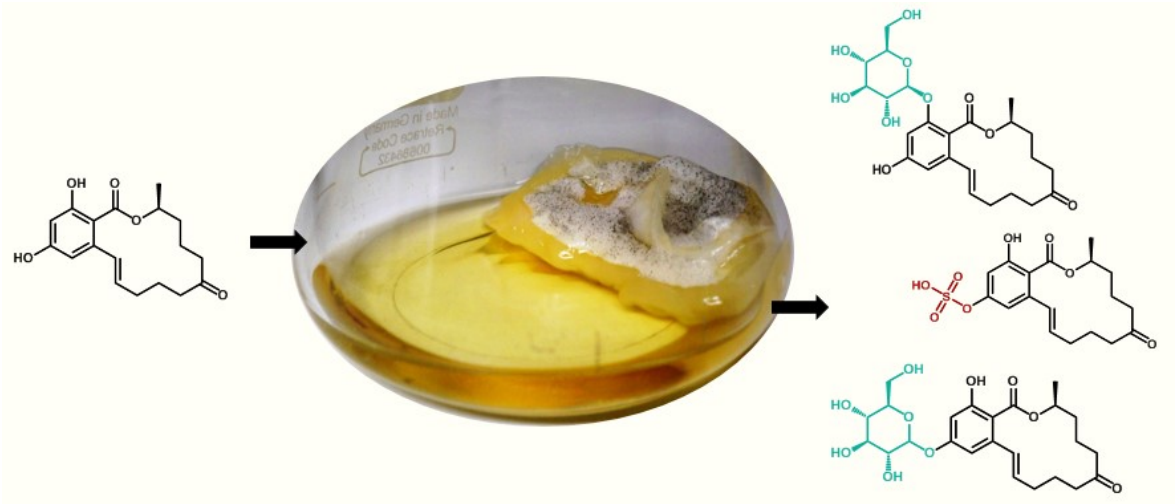

Figure 64. Illustration of the selective biosynthesis of zearalenone conjugates by *Rhizopus* or *Aspergillus* species (picture from Antje Borzekowski)

During the method development, a heterogenous metabolite pattern was observed and the strains with the highest selectivity towards ZEN-14-S, ZEN-14-G or ZEN-16-G were characterized and chosen. ZEN was added to the liquid culture and the time of harvest and addition of ZEN at different time points of fungal growth phases was tested. The resulting pattern of ZEN products varied depending on the time of harvest and fungal growth phase in *Rhizopus* species, but nearly no impact for *Aspergillus oryzae* cultures was observable. In the present thesis, ZEN was produced biosynthetically with *F. graminearum* strain F1 and after 32 days of cultivation about 3,005±708 mg ZEN per kg dry mass was formed and used for the conjugation experiments. The benefit was clearly, that the ZEN-containing flour is used directly as source for the cultivation of conjugate-producing fungi. Subsequently, the extraction of ZEN-14-G and ZEN-16-G from the harvested media was performed using LLE with ethyl acetate. For ZEN-14-S $MgSO_4$ and NaCl was added to the ethyl acetate to improve the extraction from 50.1±0.5 % recovery to 88.0±1.8 % and the preparative chromatography was applied as a final cleanup step. Finally, the structural elucidation was achieved with $^{1}H$ and $^{13}C$-NMR spectroscopy.

Chemical synthesis and biosynthesis have been described recently and ZEN conjugates were obtained in good purity [29, 163]. However, beside the cheap and easy approach the main advantage of the developed biosynthesis is the achieved regioselectivity. Especially ZEN-16-G is difficult to produce due to the inactive

carbon C16 atom. The biosynthetic production of mycotoxins is a valuable tool to produce high quantities of a needed compound.

The use of the electrochemical synthesis cell allows the oxidation of mg to g quantities of an analyte. The electrochemical production of standards offers the benefit, that no matrix must be removed during purification of the target product, like needed after the biosynthesis. However, one of the few drawbacks are that the target product is often co-occurring with many unwanted by-products which must be removed by chromatographic separation. In this thesis, the structural elucidation of the newly discovered ZEN dimers was given a high priority because other studies failed to generate a sufficient amount of dimeric species of mycotoxins electrochemically, so far. ZEN dimers were generated electrochemically using the synthesis cell equipped with the platinum working electrode and were as well chemically produced using Ce(IV)sulfate. Due to an unsatisfying yield (7 to 10%) with long reaction time (24 to 48 hours) and a concentration limit of 0.1 mg/mL, the chemical production of ZEN dimers with Ce(IV)sulfate was finally more successful. About 20 mg of ≥ 90 % pure dimeric substance was obtained with a pale-yellow color. NMR-analysis revealed a 16-O-15′-biaryl ether-linked ZEN dimer, which was described for the first time.

## 3.3 Assessment of the toxicity of mycotoxins and their TPs with reliable and effective toxicity tests

Metabolization of mycotoxins as a detoxification reaction by organisms could also result in more harmful substances. In the case of ZEN, it is known that the reduced form $\alpha$-ZEL is about 50-times more estrogenic than ZEN itself and poses a strong health risk to humans and animals after ingestion of ZEN contaminated food and feed [59]. To understand the toxicity and different modes of action, reliable and efficient test systems are needed. Toxicologically relevant data are obtained using several *in vivo* and *in vitro* model systems. Current gold standard in toxicology is the use of laboratory animals which share most organs with humans. The search for alternative cheap, reliable and high-throughput alternatives is on-going for the last decades. In mycotoxin research, standards are often barely available or are very expensive and as a result, feeding studies with animals are connected to high costs or cannot be performed, due to the lack of standards. Combination of

different animal models or using as well *in vitro* models can enhance the predictivity but increases costs and decreases the throughput. The model organism *C. elegans* can be handled using *in vitro* techniques and provides data from a whole and intact animal which possesses metabolically active digestive, endocrine, sensory, reproductive and neuromuscular systems [107]. The small size allows to test thousands of animals by only one technician and it offers several benefits, but also drawbacks, which are listed in Table 16.

Table 16. Overview of strengths and limitations of *C. elegans* as model organism in toxicity testing

| **Strengths** | **Limitations** |
|---|---|
| More than 40 years of genetics, cell signaling and neuroscience research | Lack of mammalian organs like lungs, heart, liver and kidney |
| Several key cellular signaling and metabolic pathways are conserved | Small changes in nutrient content, temperature, and salt concentration can alter the results of test assays |
| Homology to mammals at genetic level is relatively high | Lack of adaptive immunity |
| Good oral toxicity model due to conserved alimentary structures | Absorption is hampered due to the thick cuticle |
| Inexpensive and compact, allows multiple concentrations and substances at the same time | Altered gene expression patterns or the accumulation of males and dauers could result from incorrect handling of the culture |
| Multiple toxicity tests have shown good correlation in *C. elegans* to rat $LD_{50}$s | For liquid cultures test substances need to be soluble in water |

Biotests with *C. elegans* only need mg-quantities of the test substance; in this case the mycotoxins CIT, ZEN and ZEN-14-S were analyzed. With its rapid lifecycle and progeny with over 300 individuals per hermaphrodite, millions of worms are generated in a short period of time. This simple and fast cultivation allowed the

extraction of metabolized mycotoxins from the worms, giving a deeper insight into toxicologically relevant metabolic pathways. Within this thesis, the enzymatic reduction of ZEN to $\alpha$- and $\beta$-ZEL was observed using HPLC-MS/MS after extraction of the worms. Metabolization of ZEN-14-S *in vivo* led to the reduced form ZEL-14-S and no deconjugation of the sulfate was observed. As well, no hydroxylated or bioconjugated species could be found. As already described in the literature as typical detoxification reaction product, CIT was hydroxylated *in vivo*, leading to dihydrocitrinone.

Surprisingly, only a few studies were conducted with *C. elegans* to assess toxic endpoints of mycotoxins so far [106, 171, 172]. Testing the toxicity of CIT and ZEN-14-S with selected toxicologically relevant biotests was performed for the first time in the present thesis. Also, ZEN was tested to compare the obtained results to ZEN-14-S. As ZEN was already investigated currently, it was surprising that the toxicity of ZEN was not that high when compared to the already conducted study by Yang *et al*.[171]. In the present thesis, no FUdR was used to simplify the lifespan assay, which is the most time-consuming biotest. FUdR is used to suppress the fertility and allows to maintain *C. elegans* test animals on the same cultivation plate without interfering progeny or the risk of crowding. It is a contentious issue, whether FUdR should be used together with substances in toxicological research, because additive or antagonistic effects are to be expected. However, in this thesis due to these concerns, no FUdR was used.

It was shown, that especially the reproduction of *C. elegans* is strongly affected by all tested mycotoxins, which is in good correlation to other studies conducted with the nematodes and mycotoxins. For the first time, also the tolerance towards thermal and oxidative stress was assessed using short time cultivation at 35 °C or the addition of hydrogen peroxide to the liquid medium. After 8 hours of incubation, the stress tolerance assays showed a significantly increased death rate caused by CIT and ZEN. ZEN-14-S did not affect the stress tolerance. The lifespan assay revealed that CIT and ZEN caused a decrease of maximum and mean lifespan. Surprisingly, ZEN-14 led to an increase of mean lifespan. Often lifespan and thermal stress tolerance are linked, which was observed in the case of CIT and ZEN, but not when worms are treated with ZEN-14-S, were life-prolonging effects were observed. However, the reproductive and stress tolerance assays are realizable within one to two weeks and can be easily conducted by one technician even investigating different concentrations and substances in parallel, whereas the lifespan assay is the most time-consuming test.

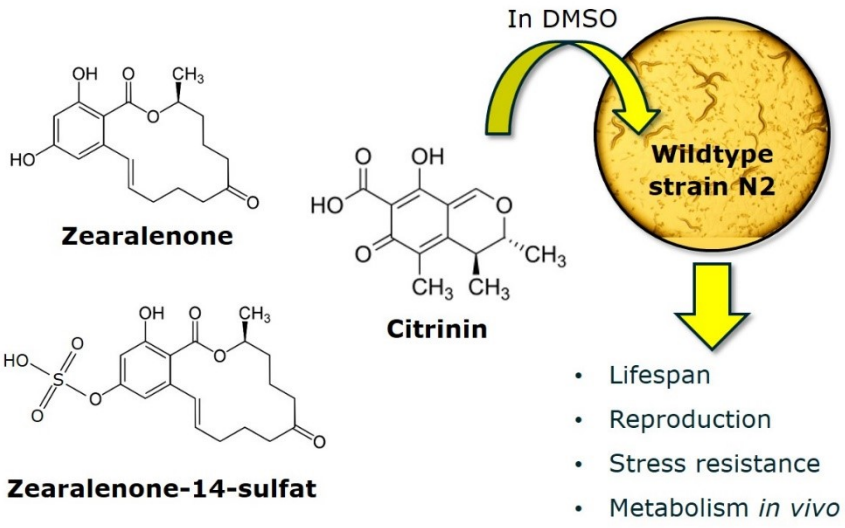


Figure 65. Experimental set-up for the toxicity testing of mycotoxins with *C. elegans*

A good cell culture practice is essential for reliable and consistent *in vitro* studies and *C. elegans* need to be maintained in a consistent manner with unaltered temperature and salt conditions as well as sufficient nutrient supply. To avoid the metabolization of the test substances by the feeding bacteria the biotests were conducted with UV-killed feeding bacteria. Even if heat inactivation is a common practice in *C. elegans* testing it should be mentioned, that this alters the bacterial surface and depresses food quality. The latter is essential for the optimal maintaining of the worm cultures. A hampered food quality could lead to a decreased intake of food, which could in turn cause a negative stress towards the worms and impedes the incorporation of the test substances. UV-killed bacteria have an unaltered bacterial surface and are an optimal food source with no metabolic activity and are clearly recommended as food source for toxicity tests.

To sum up, it can be said that *C. elegans* is easy to handle and can pose as a valuable additional tool in toxicity testing of mycotoxins offering the implementation of several standardized biotests with the simultaneous advantage of needing only mg quantities of test substance.

## 3.4 Identification of new application areas for mycotoxin-metal complexes

Metal ions like copper or iron oxidize organic compounds as well as form stable chelate complexes with ligands, whereas metal ions of the group 13 elements like aluminum, gallium or indium are known to form stable complexes with suitable ligands. This depends on the structural composition of a compound and mycotoxins possessing a 1,3-dicarbonyl function could easily act as a chelator for single or multiple charged metal ions. Complexation of organic molecules with lanthanide metals as an example, resulting in a significant enhancement of their luminescence [205].

In this thesis, the detailed investigation of the coordination of CIT and OTA with aluminum was made. Also tested was the complexation with gallium ions, which led to comparable results to aluminum complex formation (unpublished, data not shown). Maximum levels are set for OTA but not yet for CIT, which should be accomplished within the next years. As mentioned in the recent EFSA report, reliable methods for the detection of CIT as an emerging mycotoxin are strongly needed [41]. Several laboratories using HPLC-FLD/DAD systems instead of the cost expensive MS/MS systems, but non-MS techniques require laborious cleanup and pre-concentration steps before the analysis. Significant advances are made so far in CIT detection, but further improvements are needed and an enhancement of the limit of detection should be accomplished to even quantify low amounts of CIT in food and feed. One study used lanthanides as reagents to increase the fluorescence of OTA and CIT in a post-column set-up [205].

In the present thesis it was shown, that in the case of CIT the fluorescence of the Al complex is about 50 times higher (dissolved in pure methanol) when compared to CIT alone. The developed HPLC method led to an eightfold enhancement of the signal, which was probably caused by the HPLC eluent system, in this case an acetonitrile/water mixture (60/40 *v*/*v*). Water is known to quench the fluorescence of many fluorophores, but often a certain percentage of water is required for the HPLC separation of mycotoxin samples. However, the use of the acetonitrile/water solvent still allows an eightfold increase of the fluorescence signal.

For the first time the Job Plot method, also called method of continuous variation was applied to the complexation reactions of mycotoxins with metal cations and was used to assess the ratio of ligands and metal ions in a complex. The measurement of UV/Vis absorption revealed the formation of CIT-Al complexes with a ligand:metal ion ratio of 2:1, where CIT acted as bidentate chelator. The enlargement of the molecule led to the enhanced fluorescence intensity and lifetime as well as a strongly increased quantum yield, when compared to CIT alone. OTA and Al formed a 1:1 complex which showed a bathochromic shift and a change in fluorescence color from light blue to violet with only a small variation in quantum yield and fluorescence lifetime compared to the non-complexed OTA.

To profit from the benefits of aluminum complexation the use of a polymeric column is thinkable as described within this thesis. If a post-column system is available, also the derivatization with aluminum salts after separation of CIT on a regular C18 reversed-phase column could be easily included in routine analysis. Besides the application of a post-column derivatization step with aluminum salts also the occurrence of these complex species in food and feed is conceivable. Several flavonoid complex species have been found so far and it is thinkable, that mycotoxins could easily get in contact with free aluminum ions and form stable complexes [206]. This could occur during fungi or plant metabolism as well as during food processing and storage and could pose an unknown risk to humans and animals.

# 4 CONCLUSION AND PERSPECTIVES

Mycotoxins pose a serious food safety risk, due to their various harmful effects and ubiquitous presence in food and feed. While relevant food mycotoxins are well investigated, studies on transformations products are currently rare. Thus, the focus moves more and more towards natural occurring transformation products of mycotoxins, which could be even more dangerous as the parental compounds. This work implemented several alternative simulation methods to produce new and already known transformation products using electrochemical, chemical, photochemical and biochemical techniques. One simulation technique by itself does not mimic and characterize complete aspects of metabolism, unless combined with the concepts of other techniques. Each method has its own advantages and drawbacks and it is important to evaluate the strengths of a particular system. However, data obtained using simulation techniques are only one piece of a puzzle and it is essential to critically evaluate the obtained information in future research regarding mycotoxins.

Besides finding innovative simulation methods for the generation of transformation products, the complex formation of citrinin and ochratoxin A with aluminum ions were demonstrated. The enhancement of fluorescence after complexation could be easily included to routine analysis using a post column reactor, leading to a better sensitivity of citrinin analysis. Furthermore, the possibility of metal complexes in food and feed as natural, but unknown contaminants should be taken into account and further research need to be done.

Lastly, investigations on the toxicity of citrinin, zearalenone and zearalenone-14-sulfate with *C. elegans* showed that this model organism can be easily applied in mycotoxin research as an ideal complement to already existing *in vivo* and *in vitro* approaches. A necessary requirement for such studies is the availability of pure substances in a sufficient amount. The present study provided two innovative techniques, the electrochemical synthesis and a two-staged biosynthesis to produce transformation products meant for structural elucidation and toxicity assays.

To conclude, this thesis represents an important contribution to the knowledge on transformation products of food relevant mycotoxins and offers multiple start points for future research.

# 5 REFERENCES


1. Borzekowski, A., Drewitz, T., Keller, J., Pfeifer, D., Kunte, H.-J., Koch, M., Rohn, S., Maul, R. Biosynthesis and Characterization of Zearalenone-14-Sulfate, Zearalenone-14-Glucoside and Zearalenone-16-Glucoside Using Common Fungal Strains. *Toxins* **2018**, *10*, 104,
2. Keller, J., Borzekowski, A., Haase, H., Menzel, R., Rueß, L., Koch, M. Toxicity Assay for Citrinin, Zearalenone and Zearalenone-14-Sulfate Using the Nematode Caenorhabditis Elegans as Model Organism. *Toxins* **2018**, *10*,
3. Keller, J., Haase, H., Koch, M. Electrochemical Simulation of Biotransformation Reactions of Citrinin and Dihydroergocristine Compared to UV Irradiation and Fenton-Like Reaction. *Anal Bioanal Chem* **2017**, *409*, 4037-4045, 10.1007/s00216-017-0350-6.
4. Keller, J., Haase, H., Koch, M. Hydroxylation and Dimerization of Zearalenone: Comparison of Chemical, Enzymatic and Electrochemical Oxidation Methods. *World Mycotoxin J* **2017**, *10*, 297-307, 10.3920/wmj2017.2213.
5. Keller, J., Hantschke, L., Haase, H., Koch, M. Synthesis and Structural Identification of a Biaryl Ether-Linked Zearalenone Dimer *Molecules* **2018**, *23(10), 2624; 10.3390/molecules23102624*
6. Keller, J., Moldenhauer, D., Byrne, L., Haase, H., Resch-Genger, U., Koch, M. Complexes of the Mycotoxins Citrinin and Ochratoxin a with Aluminum Ions and Their Spectroscopic Properties. *Toxins* **2018**, *10(12), 538 10.3390/toxins10120538*
7. Bennett, J.W., Klich, M. Mycotoxins. *Clinical Microbiology Reviews* **2003**, *16*, 497-+, 10.1128/cmr.16.3.497-516.2003.
8. Boutrif, E., Canet, C. Mycotoxin Prevention and Control: Fao Programmes. *Revue De Medecine Veterinaire* **1998**, *149*, 681-694,
9. Fraeyman, S., Croubels, S., Devreese, M., Antonissen, G. Emerging Fusarium and Alternaria Mycotoxins: Occurrence, Toxicity and Toxicokinetics. *Toxins* **2017**, *9*, 10.3390/toxins9070228.
10. Frisvad, J.C., Thrane, U., Samson, R.A., Pitt, J.I. "Important Mycotoxins and the Fungi Which Produce Them." In *Advances in Food Mycology*, edited by A. D. Hocking, J. I. Pitt, R. A. Samson and U. Thrane, 3-31, 2006.
11. Marin, S., Ramos, A.J., Cano-Sancho, G., Sanchis, V. Mycotoxins: Occurrence, Toxicology, and Exposure Assessment. *Food Chem Toxicol* **2013**, *60*, 218-237, 10.1016/j.fct.2013.07.047.
12. Hussein, H.S., Brasel, J.M. Toxicity, Metabolism, and Impact of Mycotoxins on Humans and Animals. *Toxicology* **2001**, *167*, 101-134, 10.1016/s0300-483x(01)00471-1.
13. Zain, M.E. Impact of Mycotoxins on Humans and Animals. *Journal of Saudi Chemical Society* **2011**, *15*, 129-144, 10.1016/j.jscs.2010.06.006.

14. Van Dongen, P.W., De Groot, A.N. History of Ergot Alkaloids from Ergotism to Ergometrine. *European Journal of Obstetrics & Gynecology and Reproductive Biology* **1995**, *60*, 109-116,
15. Blount, W. Turkey "X" Disease. *Turkeys* **1961**, *9*, 52-55,
16. Park, D.L. Perspectives on Mycotoxin Decontamination Procedures. *Food Additives & Contaminants* **1993**, *10*, 49-60,
17. Caldwell, R.W., Tuite, J., Stob, M., Baldwin, R. Zearalenone Production by Fusarium Species. *Appl Microbiol* **1970**, *20*, 31-34,
18. Almeida, M., Almeida, N., Carvalho, K., Goncalves, G., Silva, C., Santos, E., Garcia, J., Vargas, E. Co-Occurrence of Aflatoxins B1, B2, G1 and G2, Ochratoxin a, Zearalenone, Deoxynivalenol, and Citreoviridin in Rice in Brazil. *Food Additives & Contaminants: Part A* **2012**, *29*, 694-703,
19. Alexander, J., Benford, D., Boobis, A., Ceccatelli, S., Cottrill, B., Cravedi, J.P., Di Domenico, A., Doerge, D., Dogliotti, E., Edler, L., Fanner, P., Filipic, M., Fink-Gremmels, J., Furst, P., Guerin, T., Knutsen, H.K., Machala, M., Mutti, A., Schlatter, J., Rose, M., Van Leeuwen, R., Chain, E.P.C.F. Scientific Opinion on the Risks for Public Health Related to the Presence of Zearalenone in Food Efsa Panel on Contaminants in the Food Chain. *Efsa Journal* **2011**, *9*, 10.2903/j.efsa.2011.2197.
20. Drzymala, S.S., Binder, J., Brodehl, A., Penkert, M., Rosowski, M., Garbe, L.-A., Koch, M. Estrogenicity of Novel Phase I and Phase Ii Metabolites of Zearalenone and Cis-Zearalenone. *Toxicon* **2015**, *105*, 10-12, https://doi.org/10.1016/j.toxicon.2015.08.027.
21. Hueza, I.M., Raspantini, P.C.F., Raspantini, L.E.R., Latorre, A.O., Gorniak, S.L. Zearalenone, an Estrogenic Mycotoxin, Is an Immunotoxic Compound. *Toxins* **2014**, *6*, 1080-1095, 10.3390/toxins6031080.
22. Zinedine, A., Soriano, J.M., Molto, J.C., Manes, J. Review on the Toxicity, Occurrence, Metabolism, Detoxification, Regulations and Intake of Zearalenone: An Oestrogenic Mycotoxin. *Food Chem Toxicol* **2007**, *45*, 1-18, 10.1016/j.fct.2006.07.030.
23. Schollenberger, M., Muller, H.M., Rufle, M., Suchy, S., Plank, S., Drochner, W. Natural Occurrence of 16 Fusarium Toxins in Grains and Feedstuffs of Plant Origin from Germany. *Mycopathologia* **2006**, *161*, 43-52, 10.1007/s11046-005-0199-7.
24. Koppen, R., Riedel, J., Proske, M., Drzymala, S., Rasenko, T., Durmaz, V., Weber, M., Koch, M. Photochemical Trans-/Cis-Isomerization and Quantitation of Zearalenone in Edible Oils. *J Agr Food Chem* **2012**, *60*, 11733-11740, 10.1021/jf3037775.
25. Berthiller, F., Crews, C., Dall'asta, C., De Saeger, S., Haesaert, G., Karlovsky, P., Oswald, I.P., Seefelder, W., Speijers, G., Stroka, J. Masked Mycotoxins: A Review. *Mol Nutr Food Res* **2013**, *57*, 165-186, 10.1002/mnfr.201100764.
26. Kovalsky Paris, M.P., Schweiger, W., Hametner, C., Stueckler, R., Muehlbauer, G.J., Varga, E., Krska, R., Berthiller, F., Adam, G. Zearalenone-16-O-Glucoside: A New Masked Mycotoxin. *J. Agric. Food. Chem.* **2014**, *62*, 1181-1189, 10.1021/jf405627d.

27. Kamimura, H. Conversion of Zearalenone to Zearalenone Glycoside by Rhizopus Sp. *Appl Environ Microb* **1986**, *52*, 515-519,
28. Elsharkawy, S. Microbial Transformation of Zearalenone. 3. Formation of 2, 4-O-Beta-Diglucoside. *Acta Pharmaceutica Jugoslavica* **1989**, *39*, 303-310,
29. Brodehl, A., Moller, A., Kunte, H.J., Koch, M., Maul, R. Biotransformation of the Mycotoxin Zearalenone by Fungi of the Genera Rhizopus and Aspergillus. *Fems Microbiology Letters* **2014**, *359*, 124-130, 10.1111/1574-6968.12586.
30. De Boevre, M., Di Mavungu, J.D., Landschoot, S., Audenaert, K., Eeckhout, M., Maene, P., Haesaert, G., De Saeger, S. Natural Occurrence of Mycotoxins and Their Masked Forms in Food and Feed Products. *World Mycotoxin J* **2012**, *5*, 207-219, 10.3920/wmj2012.1410.
31. Chancharoonpong, C., Hsieh, P.-C., Sheu, S.-C. Production of Enzyme and Growth of Aspergillus Oryzae S. On Soybean Koji. *International Journal of Bioscience, Biochemistry and Bioinformatics* **2012**, *2*, 228,
32. Dall'erta, A., Cirlini, M., Dall'asta, M., Del Rio, D., Galaverna, G., Dall'asta, C. Masked Mycotoxins Are Efficiently Hydrolyzed by Human Colonic Microbiota Releasing Their Aglycones. *Chem Res Toxicol* **2013**, *26*, 305-312,
33. Bragulat, M., Martínez, E., Castellá, G., Cabañes, F. Ochratoxin a and Citrinin Producing Species of the Genus Penicillium from Feedstuffs. *Int J Food Microbiol* **2008**, *126*, 43-48,
34. Scott, P.M., Vanwalbe.W, Kennedy, B., Anyeti, D. Mycotoxins (Ochratoxin-a, Citrinin, and Sterigmatocystin) and Toxigenic Fungi in Grains and Other Agricultural Products. *J Agr Food Chem* **1972**, *20*, 1103-+, 10.1021/jf60184a010.
35. Rodig, O., Ellis, L., Glover, I. The Biosynthesis of Citrinin in Penicillium Citrinum. I. Production and Degradation of Citrinin. *Biochemistry* **1966**, *5*, 2451-2458,
36. Böhm, J., De Saeger, S., Edler, L., Fink-Gremmels, J., Mantle, P., Peraica, M., Stetina, R., Vrabcheva, T. Scientific Opinion on the Risks for Public and Animal Health Related to the Presence of Citrinin in Food and Feed. *EFSA* **2012**, *10*, 1-82,
37. Flajs, D., Peraica, M. Toxicological Properties of Citrinin. *Arh Hig Rada Toksiko* **2009**, *60*, 457-464, 10.2478/10004-1254-60-2009-1992.
38. Follmann, W., Behm, C., Degen, G.H. Toxicity of the Mycotoxin Citrinin and Its Metabolite Dihydrocitrinone and of Mixtures of Citrinin and Ochratoxin a in Vitro. *Arch Toxicol* **2014**, *88*, 1097-1107, 10.1007/s00204-014-1216-8.
39. Ames, D., Wyatt, R., Marks, H.L., Washburn, K. Effect of Citrinin, a Mycotoxin Produced by Penicillium Citrinum, on Laying Hens and Young Broiler Chicks. *Poultry Science* **1976**, *55*, 1294-1301,
40. Vrabcheva, T., Usleber, E., Dietrich, R., Martlbauer, E. Co-Occurrence of Ochratoxin a and Citrinin in Cereals from Bulgarian Villages with a History of Balkan Endemic Nephropathy. *J Agr Food Chem* **2000**, *48*, 2483-2488, 10.1021/jf990891y.
41. Chain, E.P.O.C.I.T.F. Scientific Opinion on the Risks for Public and Animal Health Related to the Presence of Citrinin in Food and Feed. *EFSA Journal* **2012**, *10*, 2605,

42. Molinie, A., Faucet, V., Castegnaro, P., Pfohl-Leszkowicz, A. Analysis of Some Breakfast Cereals on the French Market for Their Contents of Ochratoxin a, Citrinin and Fumonisin B-1: Development of a Method for Simultaneous Extraction of Ochratoxin a and Citrinin. *Food Chemistry* **2005**, *92*, 391-400, 10.1016/j.foodchem.2004.06.035.
43. Nguyen, M.T., Tozovanu, M., Tran, T.L., Pfohl-Leszkowicz, A. Occurrence of Aflatoxin B1, Citrinin and Ochratoxin a in Rice in Five Provinces of the Central Region of Vietnam. *Food Chemistry* **2007**, *105*, 42-47, 10.1016/j.foodchem.2007.03.040.
44. Van Der Merwe, K., Steyn, P., Fourie, L., Scott, D.B., Theron, J. Ochratoxin a, a Toxic Metabolite Produced by Aspergillus Ochraceus Wilh. *Nature* **1965**, *205*, 1112,
45. Höhler, D. Ochratoxin a in Food and Feed: Occurrence, Legislation and Mode of Action. *Zeitschrift fur Ernahrungswissenschaft* **1998**, *37*, 2-12,
46. Peckham, J.C., Doupnik, B., Jones, O.H. Acute Toxicity of Ochratoxins a and B in Chicks. *Appl Microbiol* **1971**, *21*, 492-494,
47. Shreeve, B., Patterson, D., Roberts, B. The 'Carry-Over'of Aflatoxin, Ochratoxin and Zearalenone from Naturally Contaminated Feed to Tissues, Urine and Milk of Dairy Cows. *Food and cosmetics toxicology* **1979**, *17*, 151-152,
48. Kobel, H., Sanglier, J.-J. Ergot Alkaloids. *Biotechnology* **1986**, *4*, 569-609,
49. Monch, B., Kraus, W., Koppen, R., Emmerling, F. The Different Conformations and Crystal Structures of Dihydroergocristine. *J Mol Struct* **2016**, *1105*, 389-395, 10.1016/j.molstruc.2015.10.008.
50. Krska, R., Crews, C. Significance, Chemistry and Determination of Ergot Alkaloids: A Review. *Food Additives and Contaminants* **2008**, *25*, 722-731,
51. Shelby, R.A., Kelley, V.C. Detection of Ergot Alkaloids from Claviceps Species in Agricultural Products by Competitive Elisa Using a Monoclonal Antibody. *J Agr Food Chem* **1992**, *40*, 1090-1092,
52. Floss, H.G. Biosynthesis of Ergot Alkaloids and Related Compounds. *Tetrahedron* **1976**, *32*, 873-912,
53. Beuerle, T., Benford, D., Brimer, L., Cottrill, B., Doerge, D., Dusemund, B., Farmer, P., Fürst, P., Humpf, H., Mulder, P. Scientific Opinion on Ergot Alkaloids in Food and Feed. *EFSA Journal* **2012**, *10*, -,
54. Pierri, L., Pitman, I., Rae, I., Winkler, D., Andrews, P. Conformational Analysis of the Ergot Alkaloids Ergotamine and Ergotaminine. *Journal of medicinal chemistry* **1982**, *25*, 937-942,
55. Rogiers, V., Vandenberghe, Y., Callaerts, A., Verleye, G., Cornet, M., Mertens, K., Sonck, W., Vercruysse, A. Phase I and Phase Ii Xenobiotic Biotransformation in Cultures and Co-Cultures of Adult Rat Hepatocytes. *Biochemical pharmacology* **1990**, *40*, 1701-1706,
56. Rushmore, T.H., Kong, A.N.T. Pharmacogenomics, Regulation and Signaling Pathways of Phase I and Ii Drug Metabolizing Enzymes. *Current Drug Metabolism* **2002**, *3*, 481-490, 10.2174/1389200023337171.

57. Jancova, P., Anzenbacher, P., Anzenbacherova, E. Phase Ii Drug Metabolizing Enzymes. *Biomed Pap Med Fac Univ Palacky Olomouc Czech Repub* **2010**, *154*, 103-116,
58. Smith, G.S. Toxification and Detoxification of Plant Compounds by Ruminants: An Overview. *Journal of Range Management* **1992**, 25-30,
59. Olsen, M., Pettersson, H., Kiessling, K.H. Reduction of Zearalenone to Zearalenol in Female Rat Liver by 3α-Hydroxysteroid Dehydrogenase. *Acta pharmacologica et toxicologica* **1981**, *48*, 157-161,
60. Kiessling, K.H., Pettersson, H. Metabolism of Zearalenone in Rat Liver. *Acta pharmacologica et toxicologica* **1978**, *43*, 285-290,
61. Richardson, K.E., Hagler Jr, W.M., Mirocha, C.J. Production of Zearalenone,. Alpha.-And. Beta.-Zearalenol, And. Alpha.-And. Beta.-Zearalanol by Fusarium Spp. In Rice Culture. *J Agr Food Chem* **1985**, *33*, 862-866,
62. Miles, C.O., Erasmuson, A.F., Wilkins, A.L., Towers, N.R., Smith, B.L., Garthwaite, I., Scahill, B.G., Hansen, R.P. Ovine Metabolism of Zearalenone to A-Zearalanol (Zeranol). *J Agr Food Chem* **1996**, *44*, 3244-3250,
63. Hildebrand, A.A., Pfeiffer, E., Rapp, A., Metzler, M. Hydroxylation of the Mycotoxin Zearalenone at Aliphatic Positions: Novel Mammalian Metabolites. *Mycotoxin Res* **2012**, *28*, 1-8,
64. Bravin, F., Duca, R.C., Balaguer, P., Delaforge, M. In Vitro Cytochrome P450 Formation of a Mono-Hydroxylated Metabolite of Zearalenone Exhibiting Estrogenic Activities: Possible Occurrence of This Metabolite in Vivo. *Int J Mol Sci* **2009**, *10*, 1824-1837, 10.3390/ijms10041824.
65. Stevenson, D.E., Hansen, R.P., Loader, J.I., Jensen, D.J., Cooney, J.M., Wilkins, A.L., Miles, C.O. Preparative Enzymatic Synthesis of Glucuronides of Zearalenone and Five of Its Metabolites. *J Agr Food Chem* **2008**, *56*, 4032-4038,
66. Pfeiffer, E., Kommer, A., Dempe, J.S., Hildebrand, A.A., Metzler, M. Absorption and Metabolism of the Mycotoxin Zearalenone and the Growth Promotor Zeranol in Caco-2 Cells in Vitro. *Mol Nutr Food Res* **2011**, *55*, 560-567,
67. Ali, N., Blaszkewicz, M., Degen, G.H. Occurrence of the Mycotoxin Citrinin and Its Metabolite Dihydrocitrinone in Urines of German Adults. *Arch Toxicol* **2015**, *89*, 573-578, 10.1007/s00204-014-1363-y.
68. Fink-Gremmels, J., Jahn, A., Blom, M.J. Toxicity and Metabolism of Ochratoxin A. *Natural Toxins* **1995**, *3*, 214-220,
69. Ouethrani, M., Van De Wiele, T., Verbeke, E., Bruneau, A., Carvalho, M., Rabot, S., Camel, V. Metabolic Fate of Ochratoxin a as a Coffee Contaminant in a Dynamic Simulator of the Human Colon. *Food Chemistry* **2013**, *141*, 3291-3300,
70. Yang, S., Zhang, H., De Saeger, S., De Boevre, M., Sun, F., Zhang, S., Cao, X., Wang, Z. In Vitro and in Vivo Metabolism of Ochratoxin A: A Comparative Study Using Ultra-Performance Liquid Chromatography-Quadrupole/Time-of-Flight Hybrid Mass Spectrometry. *Anal Bioanal Chem* **2015**, *407*, 3579-3589,
71. Bicalho, B., Giolo, J.M., Lilla, S., De Nucci, G. Identification and Human Pharmacokinetics of Dihydroergotoxine Metabolites in Man: Preliminary Results. *Biopharm Drug Dispos* **2008**, *29*, 17-28, 10.1002/bdd.585.

72. Bicalho, B., Guzzo, G.C., Lilla, S., Santos, H.O.D., Mendes, G.D., Caliendo, G., Perissutti, E., Aiello, A., Luciano, P., Santagada, V. Pharmacokinetics of Dihydroergocristine and Its Major Metabolite 8'-Hydroxy-Dihydroergocristine in Human Plasma. *Current drug metabolism* **2005**, *6*, 519-529,
73. Lohmann, W., Karst, U. Biomimetic Modeling of Oxidative Drug Metabolism. *Anal Bioanal Chem* **2008**, *391*, 79-96, 10.1007/s00216-007-1794-x.
74. Remmel, R., Nagar, S., Argikar, U. Conjugative Metabolism of Drugs. *Drug Metabolism in Drug Design and Development: Basic Concepts and Practice* **2008**, 37-88,
75. Meunier, B., De Visser, S.P., Shaik, S. Mechanism of Oxidation Reactions Catalyzed by Cytochrome P450 Enzymes. *Chem Rev* **2004**, *104*, 3947-3980, 10.1021/cr020443g.
76. Bohnert, T., Gan, L.L. In Vitro Experimental Models for Studying Drug Biotransformation. *Handbook of Metabolic Pathways of Xenobiotics* **2014**, 1-61,
77. Dalvie, D., Obach, R.S., Kang, P., Prakash, C., Loi, C.-M., Hurst, S., Nedderman, A., Goulet, L., Smith, E., Bu, H.-Z. Assessment of Three Human in Vitro Systems in the Generation of Major Human Excretory and Circulating Metabolites. *Chem Res Toxicol* **2009**, *22*, 357-368,
78. Cheli, F., Fusi, E., Baldi, A. Cell-Based Models for Mycotoxin Screening and Toxicity Evaluation: An Update. *World Mycotoxin J* **2014**, *7*, 153-166,
79. Baumann, A., Karst, U. Online Electrochemistry/Mass Spectrometry in Drug Metabolism Studies: Principles and Applications. *Expert Opinion on Drug Metabolism & Toxicology* **2010**, *6*, 715-731, 10.1517/17425251003713527.
80. Karst, U. Electrochemistry/Mass Spectrometry (Eg/Ms) - a New Tool to Study Drug Metabolism and Reaction Mechanisms. *Angewandte Chemie-International Edition* **2004**, *43*, 2476-2478, 10.1002/anie.200301763.
81. Van Leeuwen, S.M., Blankert, B., Kauffmann, J.M., Karst, U. Prediction of Clozapine Metabolism by on-Line Electrochemistry/Liquid Chromatography/Mass Spectrometry. *Anal Bioanal Chem* **2005**, *382*, 742-750, 10.1007/s00216-005-3053-3.
82. Floyd, R.A., Watson, J.J., Wong, P.K., Altmiller, D.H., Rickard, R.C. Hydroxyl Free Radical Adduct of Deoxyguanosine: Sensitive Detection and Mechanisms of Formation. *Free radical research communications* **1986**, *1*, 163-172,
83. Jahn, S., Karst, U. Electrochemistry Coupled to (Liquid Chromatography/) Mass Spectrometry-Current State and Future Perspectives. *J Chromatogr A* **2012**, *1259*, 16-49, 10.1016/j.chroma.2012.05.066.
84. Marselli, B., Garcia-Gomez, J., Michaud, P.-A., Rodrigo, M., Comninellis, C. Electrogeneration of Hydroxyl Radicals on Boron-Doped Diamond Electrodes. *Journal of the Electrochemical Society* **2003**, *150*, D79-D83,
85. Jurva, U., Wikstrom, H.V., Weidolf, L., Bruins, A.P. Comparison between Electrochemistry/Mass Spectrometry and Cytochrome P450 Catalyzed Oxidation Reactions. *Rapid Commun Mass Sp* **2003**, *17*, 800-810, 10.1002/rcm.978.
86. Bussy, U., Chung-Davidson, Y.-W., Li, K., Li, W. Phase I and Phase Ii Reductive Metabolism Simulation of Nitro Aromatic Xenobiotics with Electrochemistry

Coupled with High Resolution Mass Spectrometry. *Anal Bioanal Chem* **2014**, *406*, 7253-7260,
87. Lohmann, W., Karst, U. Electrochemistry Meets Enzymes: Instrumental on-Line Simulation of Oxidative and Conjugative Metabolism Reactions of Toremifene. *Anal Bioanal Chem* **2009**, *394*, 1341-1348,
88. Simon, H., Hoffmann, G., Hubner, F., Humpf, H.U., Karst, U. Electrochemical Simulation of Metabolic Reactions of the Secondary Fungal Metabolites Alternariol and Alternariol Methyl Ether. *Anal Bioanal Chem* **2016**, *408*, 2471-2483, 10.1007/s00216-016-9344-z.
89. Ensing, B., Buda, F., Baerends, E.J. Fenton-Like Chemistry in Water: Oxidation Catalysis by Fe(Iii) and H2o2. *Journal of Physical Chemistry A* **2003**, *107*, 5722-5731, 10.1021/jp0267149.
90. Wang, S. A Comparative Study of Fenton and Fenton-Like Reaction Kinetics in Decolourisation of Wastewater. *Dyes Pigments* **2008**, *76*, 714-720, 10.1016/j.dyepig.2007.01.012.
91. Zepp, R., Erickson Iii, D., Paul, N., Sulzberger, B. Interactive Effects of Solar Uv Radiation and Climate Change on Biogeochemical Cycling. *Photochemical & Photobiological Sciences* **2007**, *6*, 286-300,
92. Moore, C., Carpi, A. Mechanisms of the Emission of Mercury from Soil: Role of Uv Radiation. *Journal of Geophysical Research: Atmospheres* **2005**, *110*,
93. Legrini, O., Oliveros, E., Braun, A.M. Photochemical Processes for Water-Treatment. *Chem Rev* **1993**, *93*, 671-698, 10.1021/cr00018a003.
94. Zepp, R.G., Cline, D.M. Rates of Direct Photolysis in Aquatic Environment. *Environmental Science & Technology* **1977**, *11*, 359-366,
95. Pereira, V.J., Weinberg, H.S., Linden, K.G., Singer, P.C. Uv Degradation Kinetics and Modeling of Pharmaceutical Compounds in Laboratory Grade and Surface Water Via Direct and Indirect Photolysis at 254 Nm. *Environmental science & technology* **2007**, *41*, 1682-1688,
96. Drzymala, S., Riedel, J., Köppen, R., Garbe, L.-A., Koch, M. Preparation of 13c-Labelled Cis-Zearalenone and Its Application as Internal Standard in Stable Isotope Dilution Analysis. *World Mycotoxin J* **2013**, *7*, 45-52,
97. Schmidt-Heydt, M., Cramer, B., Graf, I., Lerch, S., Humpf, H.-U., Geisen, R. Wavelength-Dependent Degradation of Ochratoxin and Citrinin by Light in Vitro and in Vivo and Its Implications on Penicillium. *Toxins* **2012**, *4*, 1535-1551,
98. Cheng, Z., Li, Y. What Is Responsible for the Initiating Chemistry of Iron-Mediated Lipid Peroxidation: An Update. *Chem Rev* **2007**, *107*, 748-766,
99. Nkhili, E., Loonis, M., Mihai, S., El Hajji, H., Dangles, O. Reactivity of Food Phenols with Iron and Copper Ions: Binding, Dioxygen Activation and Oxidation Mechanisms. *Food & function* **2014**, *5*, 1186-1202,
100. Poor, M., Kunsagi-Mate, S., Matisz, G., Li, Y., Czibulya, Z., Peles-Lemli, B., Koszegi, T. Interaction of Alkali and Alkaline Earth Ions with Ochratoxin A. *J Lumin* **2013**, *135*, 276-280, 10.1016/j.jlumin.2012.09.030.
101. Poor, M., Kuzma, M., Matisz, G., Li, Y., Perjesi, P., Kunsagi-Mate, S., Koszegi, T. Further Aspects of Ochratoxin a-Cation Interactions: Complex Formation with

Zinc Ions and a Novel Analytical Application of Ochratoxin a-Magnesium Interaction in the Hplc-Fld System. *Toxins* **2014**, *6*, 1295-1307, 10.3390/toxins6041295.

102. Lebrun, M.-H., Duvert, P., Gaudemer, F., Gaudemer, A., Deballon, C., Boucly, P. Complexation of the Fungal Metabolite Tenuazonic Acid with Copper (Ii), Iron (Iii), Nickel (Ii), and Magnesium (Ii) Ions. *Journal of inorganic biochemistry* **1985**, *24*, 167-181,
103. Hetmanski, M.T., Scudamore, K.A. Detection of Zearalenone in Cereal Extracts Using High-Performance Liquid Chromatography with Post-Column Derivatization. *J Chromatogr A* **1991**, *588*, 47-52,
104. Duca, R.C., Badea, I.A., David, I.G., Delaforge, M., Vladescu, L. Redox Behavior of Zearalenone in Various Solvents. *Analytical Letters* **2010**, *43*, 1287-1300, 10.1080/00032710903518708.
105. Brenner, S. The Genetics of Caenorhabditis Elegans. *Genetics* **1974**, *77*, 71-94,
106. Gowrinathan, Y., Pacan, J.C., Hawke, A., Zhou, T., Sabour, P.M. Toxicity Assay for Deoxynivalenol Using Caenorhabditis Elegans. *Food Addit Contam A* **2011**, *28*, 1235-1241, 10.1080/19440049.2011.587836.
107. Hunt, P.R. The C-Elegans Model in Toxicity Testing. *J Appl Toxicol* **2017**, *37*, 50-59, 10.1002/jat.3357.
108. Gruber-Dorninger, C., Novak, B., Nagl, V., Berthiller, F. Emerging Mycotoxins: Beyond Traditionally Determined Food Contaminants. *J Agr Food Chem* **2016**, *65*, 7052-7070,
109. Golden, J.W., Riddle, D.L. The Caenorhabditis Elegans Dauer Larva: Developmental Effects of Pheromone, Food, and Temperature. *Developmental biology* **1984**, *102*, 368-378,
110. Van Egmond, H.P., Jonker, M.A. Worldwide Regulations for Mycotoxins in Food and Feed in 2003. Rome, Italy. *FAO Food Nutr Pap* **2004**, *81*,
111. Petroczi, A., Nepusz, T., Taylor, G., Naughton, D.P. Network Analysis of the Rasff Database: A Mycotoxin Perspective. *World Mycotoxin J* **2011**, *4*, 329-338, 10.3920/wmj2010.1271.
112. Van Egmond, H.P., Schothorst, R.C., Jonker, M.A. Regulations Relating to Mycotoxins in Food. *Anal Bioanal Chem* **2007**, *389*, 147-157, 10.1007/s00216-007-1317-9.
113. Guengerich, F.P. Common and Uncommon Cytochrome P450 Reactions Related to Metabolism and Chemical Toxicity. *Chem Res Toxicol* **2001**, *14*, 611-650, 10.1021/tx0002583.
114. Pfeiffer, E., Schebb, N.H., Podlech, J., Metzler, M. Novel Oxidative in Vitro Metabolites of the Mycotoxins Alternariol and Alternariol Methyl Ether. *Mol Nutr Food Res* **2007**, *51*, 307-316, 10.1002/mnfr.200600237.
115. Dong, Q.F., Manns, D.C., Feng, G.P., Yue, T.L., Churey, J.J., Worobo, R.W. Reduction of Patulin in Apple Cider by Uv Radiation. *J Food Protect* **2010**, *73*, 69-74,

116. Espejo, F. Effect of Photo-Fenton Reaction on Physicochemical Parameters in White Wine and Its Influence on Ochratoxin a Contents Using Response Surface Methodology. *Eur Food Res Technol* **2016**, *242*, 91-106, 10.1007/s00217-015-2521-z.
117. Wadworth, A.N., Chrisp, P. Co-Dergocrine Mesylate – a Review of Its Pharmacodynamics and Pharmacokinetic Properties and Therapeutic Use in Age-Related Cognitive Decline *Drug Aging* **1992**, *2*, 153-173, 10.2165/00002512-199202030-00002.
118. Flieger, M., Wurst, M., Shelby, R. Ergot Alkaloids - Sources, Structures and Analytical Methods. *Folia Microbiol* **1997**, *42*, 3-29, 10.1007/bf02898641.
119. Bazin, I., Faucet-Marquis, V., Monje, M.C., El Khoury, M., Marty, J.L., Pfohl-Leszkowicz, A. Impact of Ph on the Stability and the Cross-Reactivity of Ochratoxin a and Citrinin. *Toxins* **2013**, *5*, 2324-2340, 10.3390/toxins5122324.
120. Dunn, B.B., Stack, M.E., Park, D.L., Joshi, A., Friedman, L., King, R.L. Isolation and Identification of Dihydrocitrinone, a Urinary Metabolite of Citrinin in Rats *J Toxicol Env Health* **1983**, *12*, 283-289,
121. Clark, B.R., Capon, R.J., Lacey, E., Tennant, S., Gill, J.H. Citrinin Revisited: From Monomers to Dimers and Beyond. *Org Biomol Chem* **2006**, *4*, 1520-1528, 10.1039/b600960c.
122. Blaszkewicz, M., Munoz, K., Degen, G.H. Methods for Analysis of Citrinin in Human Blood and Urine. *Arch Toxicol* **2013**, *87*, 1087-1094, 10.1007/s00204-013-1010-z.
123. Peyronneau, M.A., Delaforge, M., Riviere, R., Renaud, J.P., Mansuy, D. High-Affinity of Ergopeptides for Cytochromes P450 3a – Importance of Their Peptide Moiety for P450 Recognition and Hydroxylation of Bromocriptine *Eur J Biochem* **1994**, *223*, 947-956, 10.1111/j.1432-1033.1994.tb19072.x.
124. Panel, E.C. Scientific Opinion on the Risks for Public Health Related to the Presence of Zearalenone in Food. *EFSA J* **2011**, *9*,
125. Nelson, D.R., Koymans, L., Kamataki, T., Stegeman, J.J., Feyereisen, R., Waxman, D.J., Waterman, M.R., Gotoh, O., Coon, M.J., Estabrook, R.W., Gunsalus, I.C., Nebert, D.W. P450 Superfamily: Update on New Sequences, Gene Mapping, Accession Numbers and Nomenclature. *Pharmacogenetics* **1996**, *6*, 1-42, 10.1097/00008571-199602000-00002.
126. Ueno, Y., Tashiro, F., Kobayashi, T. Species-Differences in Zearalenone-Reductase Activity. *Food Chem Toxicol* **1983**, *21*, 167-173, 10.1016/0278-6915(83)90232-6.
127. Malekinejad, H., Maas-Bakker, R., Fink-Gremmels, J. Species Differences in the Hepatic Biotransformation of Zearalenone. *Vet J.* **2006**, *172*, 96-102, 10.1016/j.tvjl.2005.03.004.
128. Pfeiffer, E., Heyting, A., Metzler, M. Novel Oxidative Metabolites of the Mycoestrogen Zearallenone in Vitro. *Molecular Nutrition & Food Research* **2007**, *51*, 867-871, 10.1002/mnfr.200600295.
129. Pfeiffer, E., Hildebrand, A., Damm, G., Rapp, A., Cramer, B., Humpf, H.U., Metzler, M. Aromatic Hydroxylation Is a Major Metabolic Pathway of the

Mycotoxin Zearalenone in Vitro. *Molecular Nutrition & Food Research* **2009**, *53*, 1123-1133, 10.1002/mnfr.200800584.
130. Metzler, M. Proposal for a Uniform Designation of Zearalenone and Its Metabolites. *Mycotoxin Res* **2011**, *27*, 1-3,
131. Hambitzer, G., Heitbaum, J. Electrochemical Thermospray Mass-Spectrometry. *Anal Chem* **1986**, *58*, 1067-1070, 10.1021/ac00297a019.
132. Nasir, M.Z.M., Pumera, M. Mycotoxins: Simultaneous Detection of Zearalenone and Citrinin by Voltammetry on Edge Plane Pyrolytic Graphite Electrode. *Electroanalysis* **2014**, *26*, 1901-1904, 10.1002/elan.201400174.
133. De Andres, F., Zougagh, M., Castaneda, G., Rios, A. Determination of Zearalenone and Its Metabolites in Urine Samples by Liquid Chromatography with Electrochemical Detection Using a Carbon Nanotube-Modified Electrode. *J Chromatogr A* **2008**, *1212*, 54-60, 10.1016/j.chroma.2008.09.112.
134. Afzali, D., Padash, M., Mostafavi, A. Determination of Trace Amounts of Zearalenone in Beverage Samples with an Electrochemical Sensor. *Mycotoxin Res* **2015**, *31*, 203-208, 10.1007/s12550-015-0232-8.
135. Nasr, B., Abdellatif, G., Canizares, P., Saez, C., Lobato, J., Rodrigo, M.A. Electrochemical Oxidation of Hydroquinone, Resorcinol, and Catechol on Boron-Doped Diamond Anodes. *Environmental Science & Technology* **2005**, *39*, 7234-7239, 10.1021/es0500660.
136. Yager, J.D., Davidson, N.E. Mechanisms of Disease: Estrogen Carcinogenesis in Breast Cancer. *New England Journal of Medicine* **2006**, *354*, 270-282, 10.1056/NEJMra050776.
137. Bach, R.D., Dmitrenko, O. Transient Inverted Metastable Iron Hydroperoxides in Fenton Chemistry. A Nonenzymatic Model for Cytochrome P450 Hydroxylation. *Journal of Organic Chemistry* **2010**, *75*, 3705-3714, 10.1021/jo1004668.
138. Skarzewski, J. Cerium Catalyzed Persulfate Oxidation of Polycyclic Aromatic-Hydrocarbons to Quinones. *Tetrahedron* **1984**, *40*, 4997-5000, 10.1016/s0040-4020(01)91339-0.
139. Wezeman, T., Brase, S., Masters, K.S. Xanthone Dimers: A Compound Family Which Is Both Common and Privileged. *Natural Product Reports* **2015**, *32*, 6-28, 10.1039/c4np00050a.
140. Gray, J.S., Martin, G.C.J., Rigby, W. Aurofusarin. *Journal of the Chemical Society C-Organic* **1967**, 2580-&, 10.1039/j39670002580.
141. Fujisawa, S., Atsumi, T., Murakami, Y., Kadoma, Y. Dimerization, Ros Formation, and Biological Activity of O-Methoxyphenols. *Archivum Immunologiae Et Therapiae Experimentalis* **2005**, *53*, 28-38,
142. Morgan, B.J., Mulrooney, C.A., Kozlowski, M.C. Perylenequinone Natural Products: Evolution of the Total Synthesis of Cercosporin. *Journal of Organic Chemistry* **2010**, *75*, 44-56, 10.1021/jo9013854.
143. Placinta, C.M., D'mello, J.P.F., Macdonald, A.M.C. A Review of Worldwide Contamination of Cereal Grains and Animal Feed with Fusarium Mycotoxins. *Animal Feed Science and Technology* **1999**, *78*, 21-37, 10.1016/s0377-8401(98)00278-8.

144. Pfohlleszkowicz, A., Chekirghedira, L., Bacha, H. Genotoxicity of Zearalenone, an Estrogenic Mycotoxin - DNA Adduct Formation in Female Mouse-Tissues. *Carcinogenesis* **1995**, *16*, 2315-2320, 10.1093/carcin/16.10.2315.
145. Binder, S.B., Schwartz-Zimmermann, H.E., Varga, E., Bichl, G., Michlmayr, H., Adam, G., Berthiller, F. Metabolism of Zearalenone and Its Major Modified Forms in Pigs. *Toxins* **2017**, *9*, 10.3390/toxins9020056.
146. Plasencia, J., Mirocha, C.J. Isolation and Characterization of Zearalenone Sulfate Produced by Fusarium Spp. *Appl. Environ. Microbiol.* **1991**, *57*, 146-150,
147. De Boevre, M., Di Mavungu, J.D., Landschoot, S., Audenaert, K., Eeckhout, M., Maene, P., Haesaert, G., De Saeger, S. Natural Occurrence of Mycotoxins and Their Masked Forms in Food and Feed Products. *World Mycotoxin J* **2012**, *5*, 207-219, 10.3920/wmj2012.1410.
148. Vendl, O., Crews, C., Macdonald, S., Krska, R., Berthiller, F. Occurrence of Free and Conjugated Fusarium Mycotoxins in Cereal-Based Food. *Food Additives and Contaminants Part a-Chemistry Analysis Control Exposure & Risk Assessment* **2010**, *27*, 1148-1152, Pii 92247349910.1080/19440041003801166.
149. Brodehl, A., Moeller, A., Kunte, H.-J., Koch, M., Maul, R. Biotransformation of the Mycotoxin Zearalenone by Fungi of the Genera Rhizopus and Aspergillus. *FEMS Microbiol. Lett.* **2014**, *359*, 124-130, 10.1111/1574-6968.12586.
150. Jard, G., Liboz, T., Mathieu, F., Guyonvarc'h, A., Andre, F., Delaforge, M., Lebrihi, A. Transformation of Zearalenone to Zearalenone-Sulfate by *Aspergillus* Spp. *World Mycotoxin J* **2010**, *3*, 183-191, 10.3920/wmj2009.1184.
151. Commission Regulation (Ec) No 1126/2007 of 28 September 2007 Amending Regulation (Ec) No 1881/2006 Setting Maximum Levels for Certain Contaminants in Foodstuffs as Regards Fusarium Toxins in Maize and Maize Products. *Official Journal of the European Union* **2007**, *L 255/14*,
152. Kuiper, G.G.J.M., Lemmen, J.G., Carlsson, B., Corton, J.C., Safe, S.H., Van Der Saag, P.T., Van Der Burg, P., Gustafsson, J.A. Interaction of Estrogenic Chemicals and Phytoestrogens with Estrogen Receptor Beta. *Endocrinology* **1998**, *139*, 4252-4263, 10.1210/en.139.10.4252.
153. Zinedine, A., Soriano, J.M., Moltó, J.C., Mañes, J. Review on the Toxicity, Occurrence, Metabolism, Detoxification, Regulations and Intake of Zearalenone: An Oestrogenic Mycotoxin. *Food Chem. Toxicol.* **2007**, *45*, 1-18, http://dx.doi.org/10.1016/j.fct.2006.07.030.
154. Fleck, S.C., Churchwell, M.I., Doerge, D.R. Metabolism and Pharmacokinetics of Zearalenone Following Oral and Intravenous Administration in Juvenile Female Pigs. *Food Chem. Toxicol.* **2017**, *106*, 193-201, 10.1016/j.fct.2017.05.048.
155. Pfeiffer, E., Kommer, A., Dempe, J.S., Hildebrand, A.A., Metzler, M. Absorption and Metabolism of the Mycotoxin Zearalenone and the Growth Promotor Zeranol in Caco-2 Cells in Vitro. *Mol. Nutr. Food Res.* **2011**, *55*, 560-567, 10.1002/mnfr.201000381.
156. Massart, F., Saggese, G. Oestrogenic Mycotoxin Exposures and Precocious Pubertal Development. *Int. J. Androl.* **2010**, *33*, 369-376, 10.1111/j.1365-2605.2009.01009.x.

157. Sáenz De Rodriguez, C.A., Bongiovanni, A.M., Conde De Borrego, L. An Epidemic of Precocious Development in Puerto Rican Children. *The Journal of Pediatrics* **1985**, *107*, 393-396,
158. Dall'erta, A., Cirlini, M., Dall'asta, M., Del Rio, D., Galaverna, G., Dall'asta, C. Masked Mycotoxins Are Efficiently Hydrolyzed by Human Colonic Microbiota Releasing Their Aglycones. *Chem. Res. Toxicol.* **2013**, *26*, 305-312, 10.1021/tx300438c.
159. Efsa. Appropriateness to Set a Group Health-Based Guidance Value for Zearalenone and Its Modified Forms. *EFSA J* **2016**, *14*, 4425,
160. Mikula, H., Sohr, B., Skrinjar, P., Weber, J., Hametner, C., Berthiller, F., Krska, R., Adam, G., Froehlich, J. Sulfation of Beta-Resorcylic Acid Esters-First Synthesis of Zearalenone-14-Sulfate. *Tetrahedron Lett.* **2013**, *54*, 3290-3293, 10.1016/j.tetlet.2013.04.059.
161. Mikula, H., Weber, J., Svatunek, D., Skrinjar, P., Adam, G., Krska, R., Hametner, C., Froehlich, J. Synthesis of Zearalenone-16-Beta,D-Glucoside and Zearalenone-16-Sulfate: A Tale of Protecting Resorcylic Acid Lactones for Regiocontrolled Conjugation. *Beilstein Journal of Organic Chemistry* **2014**, *10*, 1129-1134, 10.3762/bjoc.10.112.
162. Krenn, P., Berthiller, F., Schweiger, W., Hametner, C., Ludwig, R., Adam, G., Krska, R., Schuhmacher, R. Production of Zearalenone-4-Glucoside, a-Zearalenol-4-Glucoside and Ss-Zearalenol-4-Glucoside. *Mycotoxin research* **2007**, *23*, 180-184, 10.1007/bf02946045.
163. Michlmayr, H., Varga, E., Lupi, F., Malachova, A., Hametner, C., Berthiller, F., Adam, G. Synthesis of Mono- and Di-Glucosides of Zearalenone and Alpha-/Beta-Zearalenol by Recombinant Barley Glucosyltransferase Hvugt14077. *Toxins* **2017**, *9*, 10.3390/toxins9020058.
164. Lioi, M.B., Santoro, A., Barbieri, R.B., Salzano, S.S., Ursini, M.V. Ochratoxin a and Zearalenone: A Comparative Study on Genotoxic Effects and Cell Death Induced in Bovine Lymphocytes. *Mutat Res-GenTox En.* **2004**, *557*, 19-27, 10.1016/j.mrgentox.2003.09.009.
165. Abid-Essefi, S., Ouanes, Z., Hassen, W., Baudrimont, I., Creppy, E., Bacha, H. Cytotoxicity, Inhibition of DNA and Protein Syntheses and Oxidative Damage in Cultured Cells Exposed to Zearalenone. *Toxicol In Vitro* **2004**, *18*, 467-474, 10.1016/j.tiv.2003.12.011.
166. Plasencia, J., Mirocha, C.J. Isolation and Characterization of Zearalenone Sulfate Produced by Fusarium Spp. *Appl Environ Microb* **1991**, *57*, 146-150,
167. Xu, B.J., Jia, X.Q., Gu, L.J., Sung, C.K. Review on the Qualitative and Quantitative Analysis of the Mycotoxin Citrinin. *Food Control* **2006**, *17*, 271-285, 10.1016/j.foodcont.2004.10.012.
168. Sengupta, P., Samuel, A.D.T. Caenorhabditis Elegans: A Model System for Systems Neuroscience. *Curr Opin Neurobiol* **2009**, *19*, 637-643, 10.1016/j.conb.2009.09.009.

169. Koelle, M.R., Horvitz, H.R. Egl-10 Regulates G Protein Signaling in the C-Elegans Nervous System and Shares a Conserved Domain with Many Mammalian Proteins. *Cell* **1996**, *84*, 115-125, 10.1016/s0092-8674(00)80998-8.
170. Brose, N., Hofmann, K., Hata, Y., Sudhof, T.C. Mammalian Homologs of Caenorhabditis-Elegans Unc-13 Gene Define Novel Family of C-2-Domain Proteins. *J Biol Chem* **1995**, *270*, 25273-25280, 10.1074/jbc.270.42.25273.
171. Yang, Z.D., Xue, K.S., Sun, X.L., Tang, L.L., Wang, J.S. Multi-Toxic Endpoints of the Foodborne Mycotoxins in Nematode Caenorhabditis Elegans. *Toxins* **2015**, *7*, 5224-5235, 10.3390/toxins7124876.
172. Feng, W.H., Xue, K.S., Tang, L.L., Williams, P.L., Wang, J.S. Aflatoxin B-1-Induced Developmental and DNA Damage in Caenorhabditis Elegans. *Toxins* **2017**, *9*, 10.3390/toxins9010009.
173. Minervini, F., Dell'aquila, M.E. Zearalenone and Reproductive Function in Farm Animals. *Int J Mol Sci* **2008**, *9*, 2570-2584,
174. Gems, D., Partridge, L. Stress-Response Hormesis and Aging:"That Which Does Not Kill Us Makes Us Stronger". *Cell Metab* **2008**, *7*, 200-203,
175. Gruber, J., Ng, L.F., Poovathingal, S.K., Halliwell, B. Deceptively Simple but Simply Deceptive–Caenorhabditis Elegans Lifespan Studies: Considerations for Aging and Antioxidant Effects. *FEBS Lett* **2009**, *583*, 3377-3387,
176. Chan, W.-H. Effects of Citrinin on Maturation of Mouse Oocytes, Fertilization, and Fetal Development in Vitro and in Vivo. *Toxicol Lett* **2008**, *180*, 28-32,
177. Qingqing, H., Linbo, Y., Yunqian, G., Shuqiang, L. Toxic Effects of Citrinin on the Male Reproductive System in Mice. *Exp Toxicol Pathol* **2012**, *64*, 465-469,
178. Pascual-Ahuir, A., Vanacloig-Pedros, E., Proft, M. Toxicity Mechanisms of the Food Contaminant Citrinin: Application of a Quantitative Yeast Model. *Nutrients* **2014**, *6*, 2077-2087, 10.3390/nu6052077.
179. Hassen, W., Ayed-Boussema, I., Oscoz, A.A., Lopez, A.D.C., Bacha, H. The Role of Oxidative Stress in Zearalenone-Mediated Toxicity in Hep G2 Cells: Oxidative DNA Damage, Gluthatione Depletion and Stress Proteins Induction. *Toxicology* **2007**, *232*, 294-302, 10.1016/j.tox.2007.01.015.
180. Johnson, T., Henderson, S., Murakami, S., De Castro, E., De Castro, S.H., Cypser, J., Rikke, B., Tedesco, P., Link, C. Longevity Genes in the Nematode Caenorhabditis Elegans Also Mediate Increased Resistance to Stress and Prevent Disease. *J Inherit Metab Dis* **2002**, *25*, 197-206,
181. Cypser, J.R., Tedesco, P., Johnson, T.E. Hormesis and Aging in Caenorhabditis Elegans. *Exp Gerontol* **2006**, *41*, 935-939, 10.1016/j.exger.2006.09.004.
182. Munoz, M.J., Riddle, D.L. Positive Selection of Caenorhabditis Elegans Mutants with Increased Stress Resistance and Longevity. *Genetics* **2003**, *163*, 171-180,
183. Doonan, R., Mcelwee, J.J., Matthijssens, F., Walker, G.A., Houthoofd, K., Back, P., Matscheski, A., Vanfleteren, J.R., Gems, D. Against the Oxidative Damage Theory of Aging: Superoxide Dismutases Protect against Oxidative Stress but Have Little or No Effect on Life Span in Caenorhabditis Elegans. *Gene Dev* **2008**, *22*, 3236-3241,

184. Ostry, V., Malir, F., Ruprich, J. Producers and Important Dietary Sources of Ochratoxin a and Citrinin. *Toxins* **2013**, *5*, 1574-1586,
185. Wang, Y.-Z., Ju, X.-L., Zhou, Y.-G. The Variability of Citrinin Production in Monascus Type Cultures. *Food Microbiol* **2005**, *22*, 145-148,
186. Commission, E. "Commission Regulation (Ec) No 123/2005 of 26 January 2005 Amending Regulation (Ec) No 466/2001 as Regards Ochratoxin A." In *Off J Eur Union*, 3-5, 2005.
187. Dall'asta, C., Galaverna, G., Dossena, A., Marchelli, R. Reversed-Phase Liquid Chromatographic Method for the Determination of Ochratoxin a in Wine. *J Chromatogr A* **2004**, *1024*, 275-279,
188. Dohnal, V., Pavlikova, L., Kuča, K. Rapid and Sensitive Method for Citrinin Determination Using High-Performance Liquid Chromatography with Fluorescence Detection. *Analytical Letters* **2010**, *43*, 786-792,
189. Lakowicz, J.R. "Principles of Fluorescence Spectroscopy, (1999)." Kluwer Academic/Plenum Publishers, New York, 2004.
190. Hollman, P.C., Van Trijp, J.M., Buysman, M.N. Fluorescence Detection of Flavonols in Hplc by Postcolumn Chelation with Aluminum. *Anal Chem* **1996**, *68*, 3511-3515,
191. Saito, A., Sugisawa, A., Umegaki, K. Comparison of Photometric, Electrochemical and Post-Column Fluorescence Detection for the Determination of Flavonoids by Hplc. *J Food Hyg Soc Jpn* **2001**, *42*, 174-178, 10.3358/shokueishi.42.174.
192. Cornard, J., Boudet, A., Merlin, J. Complexes of Al (Iii) with 3′ 4′-Dihydroxy-Flavone: Characterization, Theoretical and Spectroscopic Study. *Spectrochimica Acta Part A: Molecular and Biomolecular Spectroscopy* **2001**, *57*, 591-602,
193. Porter, L., Markham, K. The Unsuitability of Ethanol as a Solvent for the Spectroscopic Detection of Functional Groups in Hydroxyflavones with Aluminium Chloride. *Phytochemistry* **1970**, *9*, 1363-1365,
194. Renny, J.S., Tomasevich, L.L., Tallmadge, E.H., Collum, D.B. Method of Continuous Variations: Applications of Job Plots to the Study of Molecular Associations in Organometallic Chemistry. *Angewandte Chemie-International Edition* **2013**, *52*, 11998-12013, 10.1002/anie.201304157.
195. Langseth, W. Separation of Inorganic and Organomercury Chelates on a Polystyrene—Divinylbenzene Copolymer Column. *J Chromatogr A* **1988**, *438*, 414-418,
196. Würth, C., Lochmann, C., Spieles, M., Pauli, J., Hoffmann, K., Schüttrigkeit, T., Franzl, T., Resch-Genger, U. Evaluation of a Commercial Integrating Sphere Setup for the Determination of Absolute Photoluminescence Quantum Yields of Dilute Dye Solutions. *Appl Spectrosc* **2010**, *64*, 733-741,
197. Kabak, B., Dobson, A.D., Var, I.L. Strategies to Prevent Mycotoxin Contamination of Food and Animal Feed: A Review. *Critical reviews in food science and nutrition* **2006**, *46*, 593-619,
198. Mccormick, S.P. Microbial Detoxification of Mycotoxins. *Journal of chemical ecology* **2013**, *39*, 907-918,

199. Catanante, G., Rhouati, A., Hayat, A., Marty, J.L. An Overview of Recent Electrochemical Immunosensing Strategies for Mycotoxins Detection. *Electroanalysis* **2016**, *28*, 1750-1763,
200. Vidal, J.C., Bonel, L., Ezquerra, A., Hernandez, S., Bertolin, J.R., Cubel, C., Castillo, J.R. Electrochemical Affinity Biosensors for Detection of Mycotoxins: A Review. *Biosensors & Bioelectronics* **2013**, *49*, 146-158, 10.1016/j.bios.2013.05.008.
201. Eaton, D.L., Groopman, J.D. *The Toxicology of Aflatoxins: Human Health, Veterinary, and Agricultural Significance*: Elsevier, 2013.
202. Neuhof, T., Koch, M., Rasenko, T., Nehls, I. Occurrence of Zearalenone in Wheat Kernels Infected with Fusarium Culmorum. *World Mycotoxin J* **2008**, *1*, 429-435,
203. Lu, Z.-Y., Lin, Z.-J., Wang, W.-L., Du, L., Zhu, T.-J., Fang, Y.-C., Gu, Q.-Q., Zhu, W.-M. Citrinin Dimers from the Halotolerant Fungus Penicillium Citrinum B-57. *Journal of natural products* **2008**, *71*, 543-546,
204. Nieto, C.H.D., Granero, A.M., Zon, M.A., Fernández, H. Novel Electrochemical Properties of an Emergent Mycotoxin: Sterigmatocystin. *Journal of electroanalytical chemistry* **2016**, *765*, 155-167,
205. Vazquez, B., Fente, C., Franco, C., Cepeda, A., Prognon, P., Mahuzier, G. Simultaneous High-Performance Liquid Chromatographic Determination of Ochratoxin a and Citrinin in Cheese by Time-Resolved Luminescence Using Terbium. *J Chromatogr A* **1996**, *727*, 185-193,
206. Selvaraj, S., Krishnaswamy, S., Devashya, V., Sethuraman, S., Krishnan, U.M. Flavonoid–Metal Ion Complexes: A Novel Class of Therapeutic Agents. *Medicinal research reviews* **2014**, *34*, 677-702,

# 6 EIDESSTATTLICHE ERKLÄRUNG

Hiermit versichere ich, dass ich die vorliegende Arbeit selbstständig und nur unter der Verwendung der angegebenen Quellen, Hilfen und Hilfsmittel angefertigt habe. Ich erkläre, dass ich mich nicht bereits woanders um einen Doktorgrad beworben habe bzw. einen entsprechenden Doktorgrad besitze und diese Arbeit in dieser oder anderer Form noch keiner Prüfungsbehörde vorgelegt wurde. Der Inhalt der im angestrebten Verfahren zugrunde liegenden aktuellen Promotionsordnung der Fakultät III - Prozesswissenschaften der Technischen Universität Berlin ist mir bekannt.

Berlin, den 28.09.2018

_____

Julia Keller

# 7 DANKSAGUNG

Die vorliegende Arbeit wäre ohne die Unterstützung und Motivation zahlreicher Personen nicht zustande gekommen. Für die vielfältig erfahrene Hilfe möchte ich mich an dieser Stelle sehr herzlich bedanken.

Mein außerordentlicher Dank gilt zunächst meinem Doktorvater Prof. Dr. Hajo Haase, für die Betreuung dieser Arbeit mit viel Verständnis und konstruktiven Anregungen, sowie für die mir überlassene Freiheit bei der Durchführung. Weiterhin geht mein besonderer Dank an Dr. Matthias Koch, welcher mir die Arbeit an diesem Thema ermöglicht hat und mir die Chance gab, als Biologin in der Lebensmittelanalytik erfolgreich Fuß zu fassen. Für sein Vertrauen, seine Geduld und die zahlreichen produktiven Diskussionen möchte ich meinen tiefen Dank aussprechen. Weiterhin möchte ich Dr. Rudolf Schneider für den engagierten Einsatz als Drittgutachter danken und Prof. Dr. Lothar W. Kroh für die Übernahme des Vorsitzes der Kommission.

Des Weiteren danke ich allen Kollegen des FB 1.7 „Organische Spuren- und Lebensmittelanalytik“. Ganz besonders möchte ich mich bei Antje Borzekowski, Dominique Lörchner, Lisa Kotthoff und Maike Makowski für die etlichen fachlichen Diskussionen bedanken, welche mich aus so mancher wissenschaftlichen und emotionalen Krise herausgeführt haben. Weiterhin danke ich Dr. Robert Köppen für seine wertvolle Hilfe in allen messtechnischen Notlagen. Für ihre außerordentliche Unterstützung möchte ich ebenfalls Luisa Hantschke (Masterarbeit) und Liam Byrne (Erasmus Student) danken.

Diese Arbeit wäre ohne das Knowhow vieler Experten nicht möglich gewesen. Daher danke ich Dr. habil. Ralph Menzel und Prof. Dr. Liliane Rueß für die Möglichkeit mein Forschungsprojekt mit *C. elegans* als Testorganismus in Ihren Laboren an der HU Berlin unkompliziert umsetzen zu dürfen. Für die erfolgreiche Kooperation innerhalb der BAM möchte ich mich ausdrücklich bei Dr. Ute Resch-Genger und Dr. Daniel Moldenhauer vom FB 1.2 „Biophotonik“ für die vielfältigen Fluoreszenz-Messungen bedanken und die gewährten Einblicke in dieses spannende Feld. Weiterhin danke ich Boris Neumann (Proteome Factory AG, Berlin) für die Aufnahme hochaufgelöster Massenspektren, Dr. René Kudick (ASCA GmbH, Berlin) für die Aufnahme und Auswertung der ZEN-Dimer NMR-Spektren und der AG Schunck (Max-Delbrück-Zentrum) für die Möglichkeit, die Aktivität von Lebermikrosomen in ihrem Labor bestimmen zu können. Dr. Daniel Vetter (Fa. Antec, Niederlanden) danke ich für die etlichen Hilfestellungen und Anwendungstipps rund um das Thema Elektrochemie. Weiterhin danke ich Dr. Jan Lisec für die Hilfestellung bei der Strukturaufklärung der ZEN-Dimer Fragmente mittels hochaufgelöster Masse. Zuletzt danke ich Dr. Ulrike Mülow-Stollin und Dr. Caroline Goedecke vom FB 1.8 „Umweltanalytik“ für Ihre wertvollen fachlichen Anmerkungen und die kollegiale und gute Zusammenarbeit.

Zu allerletzt geht mein großer Dank an meine Eltern und Großeltern für ihre stete Unterstützung, ihre Liebe und Motivation.